

NESTLE to ORIGAMI Coupling: A Nuclear Non-proliferation Tool for
LWR Fuel Assembly Isotope Analysis

A Dissertation Presented for the
Doctor of Philosophy
Degree

The University of Tennessee, Knoxville

Margaret Alva Kurtts

December 2017

Copyright © 2017 by Margaret Alva Kurttis

All rights reserved

Acknowledgements

A number of individuals provided support and encouragement to me during the course of my research. I would like to thank Dr. Steven Skutnik for his guidance, expertise, and patience as my advisor. Dr. Skutnik provided me the flexibility to freely explore my research all the while offering guidance that kept me focused on a definitive outcome. I would also like to thank my committee members Dr. Ivan Maldonado, Dr. Howard Hall, and Dr. Vasileios Maroulas for their time and support during this project. I would like to acknowledge the contributions of a number of students and faculty who worked tirelessly to improve NESTLE and keep the NE Cluster operational in support of student research. Dr. Nicholas Luciano and Dr. Keith Ottinger provided me exceptional support with NESTLE and answered my questions in patient detail. Dr. Ondrej Chvala and Troy Eckleberry worked tirelessly to keep the NE Cluster functioning without interruption and always answered my questions. I would also like to thank my Master's degree advisor Dr. Lawrence Miller who first sparked the atoms of nuclear creativity in me and encouraged me to follow my research goals.

I would also like to thank my family for their love and encouragement. My mother, Dr. Sara York Kenny, has always been an inspiration to me as an intellectual leader, strong professional, and loving mother. My father provided me encouragement, wisdom, and kindness though both his words and actions. My parents have supported my research goals in an immeasurable way and I will be forever grateful.

Finally I want to thank my husband Robert who has never let me lose track of my professional goals and encourages me daily to be better. He is a loving father to our children and my best friend. Robert is my copilot in all things and I am grateful for his support on this journey.

Abstract

NESTLE to ORIGAMI coupling is a versatile nuclear modeling tool that allows researchers to directly observe the impact of operator induced changes on LWR assembly isotope production. The paper presents an experimental method by which to test the ability of an operator to manipulate the core neutron spectrum in order to produce higher quality plutonium for weapons use. The paper presents two plutonium production scenarios and evaluates their feasibility based on potential for detection and production capacity. Reactor modeling of a VVER-1000 uses NESTLE core simulation software. NESTLE outputs burnup and relative power information for all nodes in the core. Burnup-weighted relative power serves as a conduit for assessing the impact of core environment changes to be captured during ORIGAMI depletion analysis. When used in a nonproliferation capacity, this tool gives safeguards professionals a method by which to verify the burnup declarations of an operator for spent nuclear fuel. This tool is useful for verifying irradiation history in the case of an undeclared operator action such as the scenarios presented in this paper. NESTLE to ORIGAMI coupling is used to model the axial distribution of plutonium isotopes in the affected assembly so as to determine the suitability of the material for direct weapons use. Spent nuclear fuel isotope signatures commonly used in safeguards determine if the scenario would be detectable. Using NESTLE to ORIGAMI coupling it is determined that attempts to manipulate the neutron spectrum for producing illicit weapons useable plutonium in a LWR would be unfeasible due to the material being undesirable for weapons use, inefficient production rates, and the potential for detection.

Table of Contents

CHAPTER 1: INTRODUCTION	1
1.1 MOTIVATION	4
1.2 INFLUENCING PLUTONIUM PRODUCTION	7
1.3 REACTOR SELECTION--WHY A VVER?	9
1.4 PAPER STRUCTURE	12
CHAPTER 2: LITERATURE REVIEW	14
2.1 PLUTONIUM AND SAFEGUARDS	14
2.2 SCALE SUITE OF MODELING SOFTWARE	17
2.3 NESTLE 6.2 DEVELOPMENTAL	18
CHAPTER 3: MODEL DEVELOPMENT	20
3.1 MODEL DEVELOPMENT OVERVIEW	20
3.2 LATTICE PHYSICS MODELING	20
3.2.1: <i>13AU</i>	22
3.2.2: <i>30AV5</i>	22
3.2.3: <i>39AWU</i>	24
3.2.4: <i>390GO</i>	24
3.2.5: <i>Branches and Data Processing</i>	24
3.2.6: <i>VVER 1000 Reflectors</i>	26
3.3 NESTLE VVER 1000 BENCHMARK MODEL	27
3.4 DEVELOPING A TESTING FRAMEWORK	31
3.5 NESTLE TO ORIGAMI COUPLING	34
3.5.1: <i>Burnup Weighted Relative Power</i>	35
3.6 PLUTONIUM PRODUCTION AND SAFEGUARDS	38
CHAPTER 4: PLUTONIUM PRODUCTION SCENARIO: CONTROL ROD INSERTION	40
4.1 INTRODUCTION	40
4.2 MODELING	40
4.3 RESULTS	45
4.3.1: <i>CRO-CRI boundary</i>	50
4.3.2: <i>Plutonium Production Pathway</i>	50
4.4 CONCLUSION	56

CHAPTER 5: PLUTONIUM PRODUCTION SCENARIO: SS316 “DUMMY”	
MATERIAL	59
5.1 INTRODUCTION	59
5.2 2-D FLUX SPECTRUM ANALYSIS	59
5.2.1: <i>Fast Flux Spectrum Shift</i>	59
5.2.2: <i>Thermal Flux Spectrum Shift</i>	61
5.3 SS316 MODIFICATION RESULTS.....	62
5.3.1: <i>NESTLE VVER-1000 SS Model Results</i>	62
5.3.2: PLUTONIUM PRODUCTION PATHWAY	67
5.4 CONCLUSION	69
CHAPTER 6: SCENARIO FEASIBILITY ASSESSMENT	70
6.1 INTRODUCTION	70
6.2 DETECTION ASSESSMENT.....	71
6.2.1: <i>Spent Nuclear Fuel Signatures</i>	71
6.2.2: <i>Detection Analysis</i>	74
6.2.3: <i>Detection Summary</i>	80
6.3 PRODUCTION ASSESSMENT	80
6.3.1: <i>Scenario-Control Rod Insertion</i>	81
6.3.2: <i>Scenario-Stainless Steel Modification</i>	82
6.4 FEASIBILITY ASSESSMENT	84
CHAPTER 7: CONCLUSION AND FUTURE WORK.....	87
LIST OF REFERENCES.....	90
APPENDICES.....	97
APPENDIX A SCALE 6.2.1 ASSEMBLY MODELING AND CROSS-SECTION LIBRARY	
GENERATION	98
A.1: <i>Introduction</i>	98
A.2: <i>SCALE 6.2.1 Settings</i>	98
A.3: <i>Model Assumptions</i>	100
A.4: <i>Burndata</i>	101
A.5: <i>Branches</i>	102
A.6: <i>Material Depletion</i>	103
A.7: <i>VVER Assembly Origami Material Libraries</i>	113
A.8: <i>VVER Reflector Cross-Sections</i>	114

APPENDIX B NESTLE VVER-1000 MODEL BENCHMARK COMPARISON.....	118
<i>B.1: VVER-1000 Benchmark Reactor</i>	118
<i>B.2: NESTLE VVER-1000 Benchmark Model</i>	121
<i>B.3: NESTLE VVER-1000 Benchmark Results</i>	125
<i>B.4: Error Analysis and Bias Assessment</i>	129
<i>B.5: Conclusion</i>	130
APPENDIX C TESTING FRAMEWORK.....	131
<i>C.1: VVER-1000 Test Reactor</i>	131
<i>C.2: Assembly Identification</i>	132
APPENDIX D BURNUP WEIGHTED RELATIVE POWER.....	140
<i>D.1: Axial Power Distribution and Isotope Production</i>	140
<i>D.2: Relative Power Weighting</i>	143
<i>D.3: Weighted PRELZ and Origami Modeling</i>	146
<i>D.4: Plutonium Production and Safeguards</i>	152
<i>D.5: Conclusion</i>	156
APPENDIX E SELECT INPUT FILES.....	157
<i>E.1: Introduction</i>	157
<i>E.2: SCALE Triton Input Files</i>	157
<i>E.3: Nestle Input Files</i>	206
<i>E.4: Origami Input Files</i>	259
APPENDIX F LINUX AND PYTHON SCRIPTS.....	263
<i>F.1: Introduction</i>	263
<i>F.2: NESTLE VVER-1000 Benchmark Flux Extraction and Calculation</i>	263
<i>F.3: NESTLE VVER-1000 Benchmark PREL Linux</i>	272
<i>F.4: NESTLE VVER-1000 Test Flux Extraction and Calculation</i>	273
<i>F.5: NESTLE VVER-1000 Test PREL No Weighting</i>	282
<i>F.6: NESTLE VVER-1000 Test PREL Weighting Linux</i>	286
<i>F.7: NESTLE VVER-1000 Test PREL Python Calculations</i>	294
VITA	299

List of Tables

Table 1: Nuclear Reactors of the World July 2017[[20]]	11
Table 2: World VVER Distribution Dec 2016[7].....	11
Table 3: Plutonium Production Safeguards ([24, 26, 27]).....	15
Table 4: VVER 1000 First Cycle Fuel Assembly Distribution (adapted from Table 7, [16]).....	21
Table 5: VVER-1000 Benchmark Core Characteristics	28
Table 6: VVER-1000 Coolant Properties	29
Table 7: Control Rod Depth and Burnup	44
Table 8: Pu Mass and Pu Fissile Content Comparision	48
Table 9: Assembly Total ²³⁹ Pu Change	49
Table 10: Nodal Assembly Analysis Control Rod Depth Node 4	52
Table 11: Flux Spectrum Hardening and Assembly Burnup	65
Table 12: Assembly Selection	70
Table 13: Detection Tools and Isotope Signatures ([56, 57, 59, 60]).....	73
Table 14: ²⁴⁴ Cm Activity Predicted and Modeled for Proliferation Scenarios.....	77
Table 15: Production Statistics Control Rod Insertion Model.....	81
Table 16: Rate of Production Control Rod Insertion Model.....	82
Table 17: Production Statistics SS316 Model	83
Table 18: Rate of Production SS316 Model	84
Table 19: Branch Conditions	102
Table 20: VVER Reflector Material Composition	117
Table 21: VVER Reflector Model Dimensions	117
Table 22: VVER-1000 Core Characteristics.....	119
Table 23: VVER-1000 Benchmark Coolant Properties.....	124

Table 24: Weighted PRELZ and Burnup..... 149

List of Figures

Figure 1: Coal Plant Beijing China (Kevin Frayer /Getty Images [5]).....	2
Figure 2: Inspectors Training With CVD (Source: IAEA Calma, D. [11]).....	5
Figure 3: Modeling Methodology.....	8
Figure 4: ^{239}Pu Neutron Capture Cross-Section([19])	10
Figure 5: ^{239}Pu Fission Cross-Section([19])	10
Figure 6: VVER Fuel Assembly Designs (Figure 1, [50])	21
Figure 7: Stiffening Angle Modeled in T-Newt	22
Figure 8: FA 13AU T-Newt Model	23
Figure 9: FA 30AV5 T-Newt Model	23
Figure 10: FA 39AWU T-Newt Model	24
Figure 11: FA 390GO T-Newt Model	25
Figure 12: Radial Reflector 1D Newt Model.....	26
Figure 13: VVER-1000 Core Map First Cycle (Adapted from Figure 16 in [16]).....	28
Figure 14: Boron Letdown Modeling	30
Figure 15: VVER-1000 Benchmark Flux Spectrum Hardness.....	32
Figure 16: Assembly #139 Flux Spectrum Hardness in VVER-1000 Benchmark.....	33
Figure 17: Assembly #139 Flux Spectrum Hardness in VVER-100 Test	33
Figure 18: Model Design Sequence.....	34
Figure 19: VVER-1000 Test Nodal PRELZ.....	35
Figure 20: PRELZ for Target Assembly EOC vs. Weighted.....	36
Figure 21: Weighted PRELZ vs Non-Weighted PRELZ Axial Burnup.....	37
Figure 22: Pu Fissile Content Using Burnup Weighted PRELZ NESTLE to ORIGAMI Coupling.....	39

Figure 23: NESTLE VVER-1000 Relative Power with Target Control Rod Fully Inserted	41
Figure 24: NESTLE VVER-1000 Relative Power with Target Control Rod Fully Inserted, Top View, Mid-Core.....	41
Figure 25: NESTLE VVER-1000 Thermal Flux with Target Control Rod Fully Inserted	42
Figure 26: NESTLE VVER-1000 Thermal Flux with Target Control Rod Fully Inserted, Top View, Mid-Core.....	42
Figure 27: Control Rod Insertion Model	43
Figure 28: ORIGAMI Assembly XY Model Format.....	45
Figure 29: Nodal Impact of Control Rod Insertion on ²³⁹ Pu mass and Pu Fissile Fraction (MATLAB).....	46
Figure 30: Observations of Nodal Impact of Control Rod Insertion on ²³⁹ Pu mass and Pu Fissile Fraction (MATLAB).....	47
Figure 31: CRO-CRI Boundary	51
Figure 32: CRI-CRO Boundary Node Isotope Difference	51
Figure 33: ²³⁹ Pu (g) Control Rod Depth Node 4.....	53
Figure 34: ²³⁹ Pu (g) No Control Rod	54
Figure 35: Pu Fissile Content Control Rod Depth Node 4	54
Figure 36: Pu Fissile Content No Control Rod.....	55
Figure 37: Burnup Control Rod Depth Node 4.....	57
Figure 38: Burnup No Control Rod	57
Figure 39: FA13AU Fast Flux Normal Assembly T-NEWT.....	60
Figure 40: FA13AU Fast Flux SS316 Assembly T-NEWT	60
Figure 41: FA13AU Thermal Flux Normal Assembly T-NEWT.....	61
Figure 42: FA13AU Thermal Flux SS316 Assembly T-NEWT	62
Figure 43: Flux Spectrum Hardness (G1/G2) Comparison between Reference Assembly (left) and an Assembly Modified with SS316 in the Control Rod Guide Channels (right)	64

Figure 44: Axial Model of Change in Flux Spectrum Hardness (G1/G2) to the Assembly with the Insertion of SS316 into the Control Rod Guide Tubes	64
Figure 45: Axial Power Shape Factor Comparison between Reference Assembly (left) and the Assembly with SS316 Insertion into the Control Rod Guide Tubes (right)	65
Figure 46: ²³⁵ U Comparison between Reference Assembly (left) and the Assembly with SS316 Insertion into the Control Rod Guide Tubes (right)	66
Figure 47: ²³⁸ U Comparison between Reference Assembly (left) and the Assembly with SS316 Insertion into the Control Rod Guide Tubes (right)	66
Figure 48: ²³⁹ Pu Comparison between Reference Assembly (left) and the Assembly with SS316 Insertion into the Control Rod Guide Tubes (right)	67
Figure 49: Pu Fissile Fraction Comparison between Reference Assembly (left) and the Assembly with SS316 Insertion into the Control Rod Guide Tubes (right)	68
Figure 50: Relative Increase in Fissile Pu Fissile Fraction Resulting from SS316 Modification.....	68
Figure 51: Pathway Gross Isotope Signature Percent Difference from Reference Assembly.....	74
Figure 52: Axial Distribution of ¹³⁴ Cs/ ¹³⁷ Cs for Test Assemblies.....	76
Figure 53: Axial Distribution ²⁴⁴ Cm for Test Assemblies.....	78
Figure 54: Axial Distribution ¹⁵⁴ Eu for Test Assemblies	79
Figure 55: 2 Group Flux Spectrum FA 39AWU modeled with T-Newt	103
Figure 56: FA 13AU T-Newt Model	106
Figure 57: FA 13AU Thermal Flux Profile With Material Regions Defined.....	106
Figure 58: FA 30AV5 Modeled in T-Newt	107
Figure 59: FA 30AV5 Thermal Flux Profile With Material Regions Defined.....	108
Figure 60: FA 39AWU Model t-newt.....	109
Figure 61: FA 39AWU Thermal Flux Profile With Material Regions Defined	110
Figure 62: FA 390GO T-Newt Module	111
Figure 63: FA 390GO Thermal Flux Profile With Material Regions Defined.....	112
Figure 64: Radial Reflector 1D Newt Model.....	117

Figure 65: VVER Core Load Map First Cycle (Adapted from Figure 16 taken from [16])	119
Figure 66: Control Rod Working Groups First Core Load (Adapted from Figure 5 in [16])	120
Figure 67: NESTLE Input File Control Rod Array	120
Figure 68: First Cycle Power History	121
Figure 69: NESTLE Core Input.....	122
Figure 70: B ₄ C and Dy ₂ TiO ₅ Rod Example taken from Figure 10 in [68]	123
Figure 71: NESTLE k-eff VVER-1000 Model 323 Data Points	126
Figure 72: NESTLE k-eff VVER-1000 Model 63 Data Points	126
Figure 73: PCM from Critical (k-eff 1.0) 63-Point Model	127
Figure 74: Boron Letdown Modeling	128
Figure 75: VVER-1000 Operational Data Flux Spectrum Hardness.....	134
Figure 76: FA13AU Core Load	134
Figure 77: FA13AU VVER-1000 Locations	135
Figure 78: VVER-1000 Operating Data Flux Spectrum Hardness.....	135
Figure 79: VVER-1000 Operating Data Flux Spectrum Hardness (2).....	136
Figure 80: Assembly ID using Flux Spectrum Hardness.....	136
Figure 81: Assembly ID using Flux Spectrum Hardness (top view)	137
Figure 82: FA13AU #139 Flux Spectrum Hardness.....	138
Figure 83: VVER-1000 Test Model Flux Spectrum Hardness.....	139
Figure 84: Assembly #139 VVER-1000 Benchmark Model Flux Spectrum Hardness .	141
Figure 85: Assembly #139 VVER-1000 Benchmark PRELZ	141
Figure 86: ²³⁹ Pu (g) Flat PRELZ VVER-1000 Benchmark	142
Figure 87: ²³⁹ Pu using PRELZ EOC VVER-1000 Benchmark	143
Figure 88: VVER-1000 Test Nodal PRELZ.....	144

Figure 89: Axial Relative Power Distribution PRELZ Weighting	146
Figure 90: PRELZ for Target Assembly EOC (left) vs. Weighted (right)	147
Figure 91: ORIGAMI Power History Block VVER-1000 Test Assembly #139.....	148
Figure 92: Weighted vs. EOC PRELZ Comparison	149
Figure 93: ²³⁵ U Mass EOC (left) vs PRELZ Weighted (right) Comparison.....	150
Figure 94: ²³⁵ U Mass Distribution Weighted vs. EOC PRELZ Comparison	150
Figure 95: ²³⁸ U Mass EOC (left) vs PRELZ Weighted (right) Comparison.....	151
Figure 96: ²³⁸ U Mass Distribution Weighted vs. EOC PRELZ Comparison	151
Figure 97: ²³⁹ Pu Mass EOC (left) PRELZ Weighted (right) Comparison.....	152
Figure 98: ²³⁹ Pu Mass Distribution Weighted vs EOC PRELZ Comparison	153
Figure 99: Pu Fissile Content Weighted vs. EOC PRELZ Comparison.....	154
Figure 100: Pu Fissile Content Weighted vs EOC PRELZ Comparison.....	155

Chapter 1: Introduction

“[...] fear of nuclear energy, a technology introduced in connection with a powerful weapon, has forestalled the development of this energy source. The economic and ecological consequences of that circumstance are still in the future”

-Edward Teller, *Memoirs*, 2001[1]

Taken from the epilogue of his memoirs, Edward Teller describes the undeserved bridling of nuclear energy through its association to weapons. He observed, at the turn of the century, rapid increases in world energy demand could not be sustained by current energy sources nor relieved by renewable technology. He argued that nuclear energy, with some modifications, was the most viable solution to rising energy demands. Yet due to fear caused by association with weapons and ignorance of the fundamental technology, the use of nuclear energy would face significant obstacles.[1]

In May of 2016, the U.S. Energy Information Administration (EIA), an office within the U.S. Department of Energy, published its annual International Energy Outlook for the years 2012 to 2040. The assessment ascertains that worldwide energy demand will increase by 48% over the next three decades with the largest demand growth occurring in Asia[2]. The IAEA estimates the Middle East, South Asia, and the Far East currently have some of world’s highest populations but have energy generation rates similar to countries with much lower populations. Over the next 40 years, the IAEA expects the energy per capita in these regions to drastically increase.

Currently the Middle East, South Asia, and the Far East get the majority of their energy from coal, oil, and natural gas (Figure 1).[3] Lower prices and additional access has increased the attractiveness of natural gas yet the total energy deficient in these regions can only be addressed by a multi-fuel solution. While nuclear power plants have high initial costs, once built they offer a state a source of reliable, baseload power with low operating costs. [4]



Figure 1: Coal Plant Beijing China (Kevin Frayer /Getty Images [5])

The year 2016 added 9 GWe of new nuclear energy to the grid and a net nuclear capacity increase of 8 GWe.[6] China contributed greatly to this increase by adding 4.6 GWe.[6] As of December 2016, China operated 36 power reactors that supplied only 3.6% of its total electricity. China is growing its nuclear capacity at an incredible rate with 21 reactors under construction as of the end of 2016.[7] China is leading a cohort of developing nations planning or activity working to add nuclear to their energy portfolio. In 2015, the IAEA reported that 27 countries were in some stage of planning for an initial nuclear power plant. Of the 27, the majority was in the initial stage of consideration and working to build the supporting infrastructure. Two countries, Belarus and the United Arab Emirates (UAE) had begun construction on their first nuclear plant at the time of this report. [8]

Nation states that at one time were leading consumers of nuclear energy, such as Germany, are making plans to decommission power plants and fill their energy gaps with renewables.[9] Many of these nations have well established energy programs with the high per capita electrical output.[3] These nations do not face the same impending energy crisis of nations coping with both large populations and low electrical capacity. For developing countries, where the energy deficient between production and demand is high, nuclear power offers a robust long-term base load solution from which to grow capacity.

As nuclear energy spreads to new nations, the questions raised by Teller will surely be discussed in forums ranging from the halls of policy to the kitchen dinner table. This paper offers a response about the potential for misuse of peaceful nuclear technology by examining the proliferation potential of LWRs. The paper presents an experimental method by which to test the ability of an operator to manipulate core neutron spectrums in order to produce higher quality plutonium for weapons use. The paper presents and models two possible scenarios by which an operator could utilize reactor controls to locally modify the neutron spectrum within a single core assembly in an effort to improve plutonium quality in the assembly. After modeling, the paper assesses the production scenarios for feasibility based on detectability and production capacity.

The work of this research provides a modeling tool and two tangible examples from which to draw upon when discussing the usefulness of LWR technology for illicit use. Teller pointed out that fear and ignorance of nuclear technology cause it to be off-putting, forcing many people to make rash, emotional conclusions as to its usefulness. The results of this work provide a platform from which to reduce nuclear unawareness through informed discussion and perhaps even provide enough distance between LWR technology and nuclear weapons to reduce individual fears.

1.1 Motivation

As new countries incorporate nuclear into their energy portfolio, the IAEA works with them to develop the nuclear infrastructure necessary for supporting the safe, secure, and peaceful use of nuclear technology. In 2016, the IAEA published a best practices infrastructure road map to aid nation states when standing up a nuclear power program. The IAEA framework helps the state to address a series of infrastructure issues across three developmental milestones to foster growth and the capacity to deal with the complexities of nuclear power.[10] In this publication, the IAEA advises,

“[...]a nuclear power programme involves a commitment of at least 100 years to maintain sustainable national infrastructure throughout construction, operation, decommissioning, and waste disposal”[10]

Not specifically addressed in the report is the capacity of safeguards professionals to keep pace with the changing nuclear energy market. As new nuclear programs build infrastructure capacity, safeguards professionals will be needed to offer guidance and training while still maintaining rigorous inspection standards for existing states. Though some nations are planning to phase nuclear out of their energy portfolio, reductions are not swift. Decommissioning a single facility and establishing a waste management plan can take many decades during which material is still subject to safeguards.

The safeguards community faces a challenging situation in the coming decades as its workforce establishes programs to meet the needs of new, existing, and retiring operators. Nations new to nuclear safeguards will likely find developing a regulatory framework a challenging task but with the help of trained safeguards professionals, a state can

cultivate a system that ensures the safe and peaceful use of nuclear energy. Existing operators will continue to expect the same level of cooperation they received in past years despite changing demands on the safeguards community (Figure 2). Finally, retiring operators will need to work with the safeguards community to adjust their regulatory framework to support the long-term safety and security of decommissioned material.

The dynamic changes facing the safeguards community call for new tools to reduce inspector and operator burden. This paper puts forth a modeling methodology that improves the ability of safeguards professionals to predict the impact operator actions have on assembly isotopic content. Improvements in modeling, detection, and monitoring all help to reduce the burden on the safeguards professional. Pre-inspection modeling tools, such as the one proposed in this paper, reduce the workload on team of individuals while still ensuring safe, secure operating practices. The model proposed will help the members of the safeguards community address the suite of challenges it faces in the coming decades.



Figure 2: Inspectors Training With CVD (Source: IAEA Calma, D. [11])

The method developed couples a nodal core simulator, NESTLE, to the LWR assembly depletion software ORIGAMI. By coupling a core simulator to depletion software, it becomes possible for safeguards professionals to determine the impact of unexpected operator behavior such as emergency shutdowns, power reductions, and control rod adjustments on individual assembly isotopic content. The nodal core simulator NESTLE allows for modeling changes in the reactor environment throughout the core fuel cycle. Typical deterministic neutron transport or Monte Carlo tools require some reactor environment variables to remain fixed during depletion intervals. By accurately capturing the impact of unexpected changes to the reactor environment on individual assembly isotope content, it is possible to assist safeguards professionals in confirming adjusted burnup declarations.

Generating isotope results using the NESTLE to ORIGAMI coupling method proposed is relatively quick as compared to using deterministic or Monte Carlo neutron transport modeling platforms. While a significant amount of time is required to develop a single full core model in NESTLE, once developed the model is versatile and runs quickly. Coupling to ORIGAMI requires the use of a NESTLE output parsing code which this paper developed using a simple Linux-Python script. Once parsed, input into ORIGAMI is straightforward and isotope results are easily observed via SCALE 6.2.1 GUI Fulcrum.[12] ORIGAMI requires the use of unique ORIGEN libraries that match the libraries used by NESTLE.[13] Therefore, as part of NESTLE model development, a researcher also creates ORIGEN libraries for use later with ORIGAMI.

This paper contends that the misuse of LWR technology within a civilian power production center is not a useful means for producing nuclear material for a weapons program. Yet as Edward Teller made clear, the historical underpinnings of nuclear technology make divesting reactors from weapons applications incredibly difficult. This paper contributes to scientific efforts supporting the peaceful application of LWR technology and counters the negative association to weapons programs.

LWRs do produce plutonium during the fuel cycle. At the end of a reactor fuel cycle, a significant portion of the fission energy is actually derived from plutonium. As such,

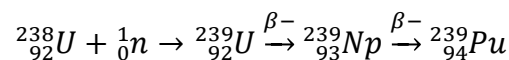
reactors and irradiated fuel are subject to safeguards. With the market for nuclear reactors expanding to new nations and it being well known that reactors make plutonium, questions can arise from a concerned public about if these reactors can be used for weapons. Rather than dismiss this question or ask the public to place complete trust in a safeguards program it does not fully understand, this paper demonstrates the challenge of making weapons-grade plutonium in a LWR through an operator misuse scenario.

This project demonstrates the nuclear nonproliferation capabilities of the NESTLE to ORIGAMI coupling by assessing two potential plutonium production scenarios using LWR technology. Both pathways attempt to manipulate the axial isotope content of a single assembly by altering the local neutron flux spectrum of the assembly. The first pathway attempts to reduce ^{239}Pu losses from thermal fission by increasing thermal flux absorption through the adjustment of control rods. The second pathway models operator efforts to harden the assembly flux spectrum by inserting dummy material, SS316, into the control rod guide tubes.

Figure 3 illustrates the modeling methodology used in this paper. A full description of the methodology is found in Chapter 3. Highlighted in Figure 3 are the four NESTLE models created for this project. The models used for testing plutonium production pathways are the VVER-1000 Control Rod Test and the VVER-1000 Stainless Steel Test. These models replicate actions that could potentially be taken by an operator to illicitly produced plutonium in a LWR. By coupling the NESTLE simulation to the ORIGAMI depletion interface, this paper test the feasibility of both pathways.

1.2 Influencing Plutonium Production

Plutonium production in a LWR is closely related to neutron flux. ^{239}Pu is produced during ^{238}U neutron capture and β^- decay.



^{238}U has a capture cross-section for thermal neutrons of 2.68 bn [14] and less than 1 bn for neutrons with an energy of 1 MeV[15].

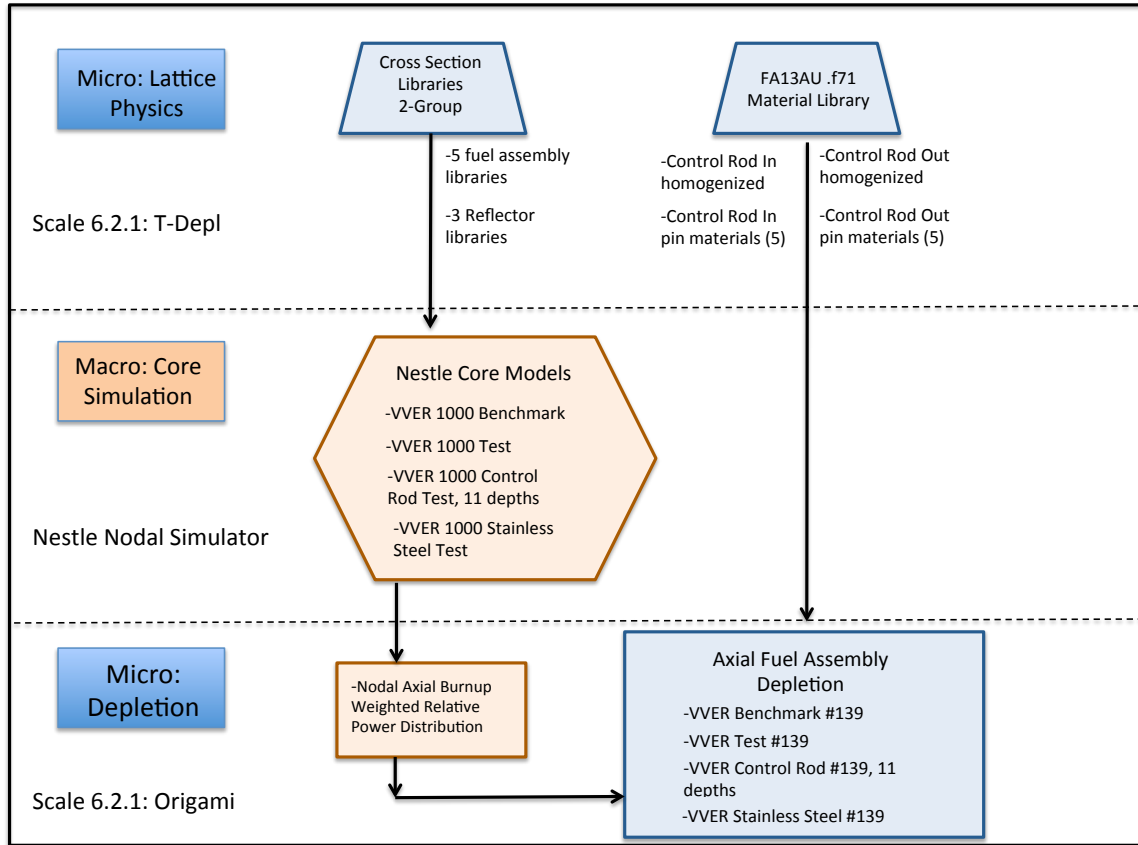
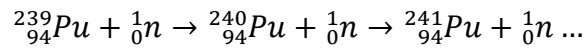


Figure 3: Modeling Methodology

^{239}U decays to ^{239}Np with half-life of 23.45 min. ^{239}Np subsequently decays to ^{239}Pu with a 2.36 d half-life.[14, 15]



Plutonium losses are greatly impacted by neutron flux. ^{239}Pu transmutes to additional plutonium isotopes primarily through neutron capture. Figure 4 shows that ^{239}Pu has a thermal neutron capture cross section of 271 bn.[14] At 1 MeV, the capture cross section is 0.04 bn.[15]

While ^{239}Pu undergoes fission at thermal and fast energies, thermal fission is the greatest source of ^{239}Pu loss in a reactor. Figure 5 shows that ^{239}Pu has a thermal fission cross-section of 748 bn [14] and a fast fission cross-section of 1.74 bn at 1 MeV. [15]

The scenarios modeled using NESTLE to ORIGAMI coupling attempt to use a LWR to produce plutonium for weapons use. The scenarios modeled seek to reduce ^{239}Pu inventory losses from thermal fission and neutron capture. In the case of the control rod scenario, the assembly local thermal utilization factor is reduced due to the presence of a strongly absorbing control rod. Less thermal neutrons are absorbed in the fuel and therefore less fissions will occur. In the case of the stainless steel test, the effective moderator content within the assembly is reduced. Fewer neutrons are slowed to thermal energies by the stainless steel and thus the number of thermal fissions inside the assembly is also reduced.

1.3 Reactor Selection--Why a VVER?

The LWR modeled for this project is a VVER-1000 and is based on a series of benchmark publications from (Lotsch T., et al., 2009-2011) presented from 2009-2011 in the *Symposium of Atomic Energy Research on WWER Physics and Reactor Safety*. [16-18] The benchmark documents offer information from four operating cycles but this paper only uses the core configuration from the first cycle.

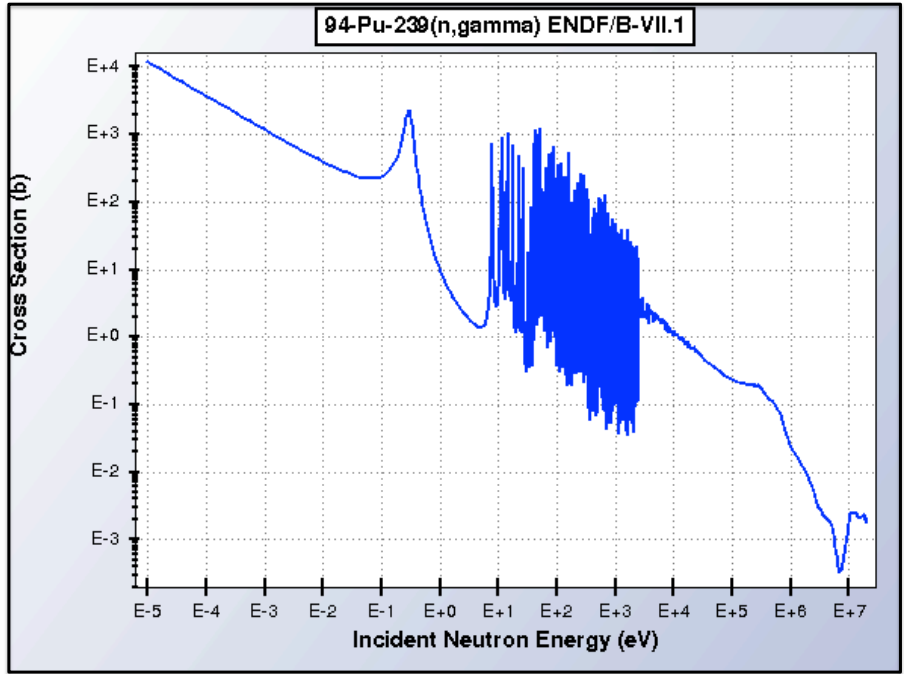


Figure 4: ^{239}Pu Neutron Capture Cross-Section([19])

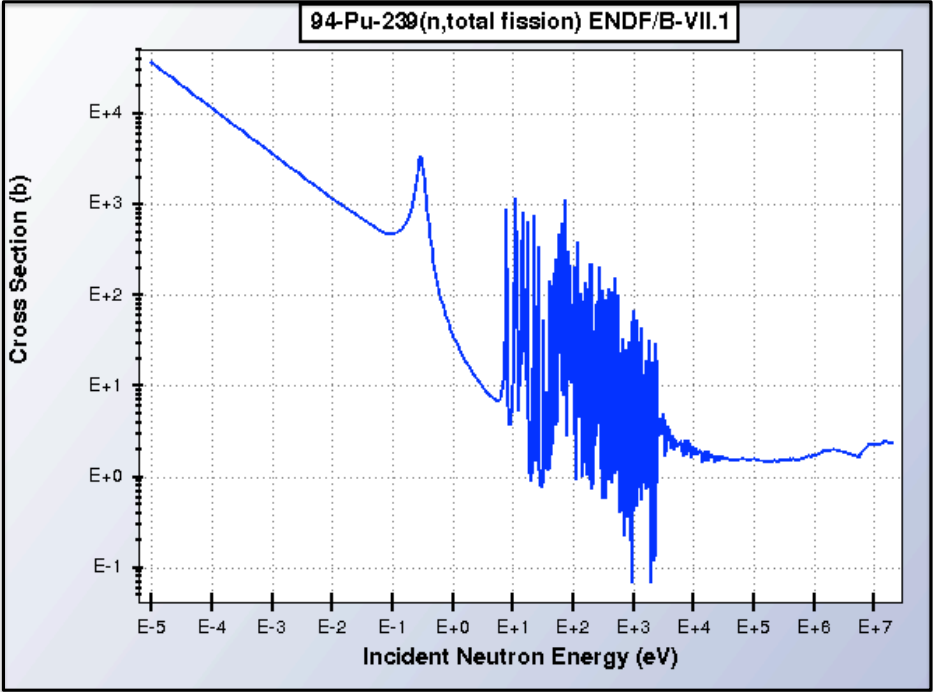


Figure 5: ^{239}Pu Fission Cross-Section([19])

The VVER-1000 is a Russian PWR used commonly around the world. PWRs are the most abundant reactor used in the world today. Table 1 illustrates the current number of reactors in operation throughout the world by reactor type and capacity. Table 2 illustrates the nations constructing or using VVERs as part of their civil power program as of December 2016.

Table 1: Nuclear Reactors of the World July 2017[[20]]

Reactor Type	Number	Total Net Electrical Capacity (GWe)
PWR	289	272.28
BWR	77	74.85
PHWR	49	24.63
LWGR	15	10.22
GCR	14	7.72
FBR	3	1.37
Total	447	391.07

Table 2: World VVER Distribution Dec 2016[7]

VVER Distribution By Country			
Operating		Under Construction	
Armenia	1	Belarus	2
Bulgaria	2	China	2
China	2	Russia	5
Czech Republic	6	Slovakia	2
Finland	2	Ukraine	2
Hungary	4	World Total	21.31%
India	2		
Iran	1		
Russia	18		
Slovakia	4		
Ukraine	15		
World Total	12.72%		

There are 57 VVERs in operation in the world.[7] VVERs are a popular reactor for emerging civil nuclear programs. The Russian government actively exports VVER reactors and markets specifically to emerging nuclear nations by offering an attractive support package called a “build, own, operate” (BOO) model[21]. Russia and Turkey are

using a BOO agreement for the construction of the Akkuyu NPP.[8, 22] A BOO structure agreement divides risk, responsibly, and revenue between a developer and the host country.[23] This model is attractive to a country with limited financial options and a nascent nuclear infrastructure. Thus a VVER was chosen as an LWR model over a more standard US reactor design due to the proclivity for the VVER outside the United States and in areas which may experience nuclear infrastructure growth in the future. The modeling methodology presented in the document is not unique to the VVER however, and could be applied to any NESTLE-supported reactor design.

1.4 Paper Structure

The paper begins by reviewing plutonium nonproliferation research and modeling software in a Literature Review found in Chapter 2. Chapter 3 offers an overview of the model development steps needed to couple NESTLE to ORIGAMI. Chapter 3 is a summary of four appendixes. Appendix A provides a description of the SCALE lattice physics simulations needed to generate NESTLE and ORIGAMI libraries. Appendix B describes the development of the VVER-1000 model and the verification of that model using benchmark data. Appendix C describes the testing framework developed to support conducting two nonproliferation test cases. Appendix D describes the burnup weighted relative power coupling method used for linking NESTLE to ORIGAMI.

Chapter 4 describes the model development, testing, and results of the control rod induced proliferation scenario. Chapter 5 provides the model, testing, and results of the SS316 dummy material scenario. Chapter 6 offers a feasibility assessment of both scenarios by assessing the detection signatures and production results of the pathways. Chapter 7 concludes the assessment and provides suggestions for future work. Additional appendixes include Appendix E: Input Files, and Appendix F: Linux and Python scripts.

The coupling of NESTLE to ORIGAMI makes it possible to quickly explore the impact of core operations on axial isotope distribution of a single LWR assembly. The expansion of LWR technology into new, undeveloped markets will increase pressure on safeguards professionals to reaffirm confidence in the peaceful nature of LWR technology. This paper demonstrates (through the use of a versatile modeling tool) two potential

proliferation scenarios involving operator misuse of LWR technology and provides an assessment of pathway feasibility.

Chapter 2: Literature Review

2.1 Plutonium and Safeguards

^{239}Pu in spent nuclear fuel is a concern for safeguards professionals. Boyer and Schanfein present an excellent study in practical safeguards as part of the book by James Doyle, *Nuclear Safeguards, Security, and Nonproliferation; Achieving Security with Technology and Policy*. [24, 25] The IAEA requires that irradiated fuel be inspected with a frequency that would allow for the timely detection of material diversion. The interval is based on what the IAEA assesses is the time it could take to convert from its original form to a weapons useable form. [24] In the case of irradiated LWR fuel, the IAEA assesses conversion could occur in 1-3 months. [26] The IAEA views practically all plutonium in LWR fuel as necessitating safeguards by defining a significant quantity of plutonium to be 8 kg for any plutonium containing less than 80% ^{238}Pu . [26] As part of an ongoing effort to reduce plutonium stockpiles and mitigate the production of weapons usable plutonium in civil technology, a great deal of research has gone toward studying the relationship between plutonium isotopes and proliferation.

B. Pellaud, who served as the head of safeguards for the IAEA from 1993-1999, provides in *Proliferation Aspects of Plutonium Recycling*, an overview of both the challenge and the contentious debate within the scientific community when characterizing the weapon suitability of plutonium. Pellaud contends that the suitability of plutonium must depend on its handling characteristics as well as its ability to produce a yield. [27] The distribution of plutonium and non-plutonium isotopes in spent fuel and the impact of that distribution on weapons functionality is a source of much debate. Pellaud argues that many researchers weight heavily the yield production of an isotope distribution while neglecting or simply mentioning challenges associated with material handling and engineering. [27]

There seems to be agreement that any material capable of producing yields greater than conventional devices, even if that yield is only a fraction of the nominal yield, is a threat. There is great divergence in opinion, however, as to the significance of non-yield related

characteristics such as radiation hazards, decay heat, and handling challenges. (Mark J., et al., 2009) and (Kessler G., et al., 2008) explore the feasibility of using reactor grade plutonium for weapons material. Both Mark and Kessler conclude that a hypothetical nuclear explosive device using reactor-grade plutonium will result in a nuclear yield however the researchers have different conclusions as to the magnitude of the yield[28, 29]. In later research, (Kessler G., et al., 2008) concludes that while from a physics perspective reactor-grade plutonium can produce a nuclear yield, the thermal properties of the fuel can be prohibitive to weapon functionality.[30] (Permana S., et al., 2013) and (Kimura, Y., et al., 2011), offers insights into the impact of even-numbered Pu isotopes (e.g., ^{238}Pu , ^{240}Pu , ^{242}Pu) on weapon performance. Both researchers note that the high decay heat emitted from ^{238}Pu would present a serious challenge for weapon functionality and Kimura attempts to quantify the impact of decay heat on the material attractiveness using a variable of technical difficulty. [31, 32] Many of these researchers went on to propose fuel cycle methods that increase the production of isotopes that would reduce the suitability of material for weapons use and thus enhance the proliferation resistance of LWR fuel.[30, 33-36]

Table 3: Plutonium Production Safeguards (I24, 26, 27)

Plutonium and Safeguards	
Plutonium Grades	
Grade	Content ¹
Super	$\leq 3\% \text{ Pu240}$
Weapons	$3\% < \text{Pu240} < 7\%$
Fuel	$7\% < \text{Pu240} < 18\%$
Reactor	$18\% < \text{Pu240} < 30\%$
Mox	$\text{Pu240} > 30\%$
IAEA Significant Quantity	8 kg
	$< 80\% \text{ Pu238}^2$
1. All even number Pu isotopes (puEven) considered in this paper, not just Pu240	
2: The IAEA does not differentiate between Pu isotope grades, greater than 80% Pu238 viewed unusable for weapons	

As part of his previously mentioned work, Pellaud presents what he considers is the currently agreed upon understanding of plutonium grades (Table 3). Pellaud notes that most debate involving weapon suitability deals primarily with “fuel” and “reactor” grade plutonium. The grades found in Table 3 will be used throughout this project to define the

isotope content of the fuel modeled understanding that there are many differences of opinion about the suitability of plutonium with a ^{240}Pu content between 7% and 30%.

Pellaud argues for a more rigorous method of assessing the weapon suitability of plutonium beyond the IAEA's broad, all-inclusive definition and the simple isotope distribution of Table 3. By monitoring virtually all plutonium, Pellaud argues that safeguards professionals cannot prioritize limited resources resulting in monitoring practices that are excessive for some cases and potential vulnerabilities in others.[27] (Bathke, C, et al., 2009) developed a more comprehensive suitability test than Table 3 using a figure of merit (FOM) system that evaluated material based on bare critical mass, heat content, and dose rate. Bathke's assessment differentiated between state and non-state actors by including an additional variable for state actor evaluations, spontaneous neutron generation rate, which reflects an assumption that a state would place more emphasis on weapon effectiveness than a non-state actor.[37] Pellaud argues that the assessment must go further than even Bathke's work and include for consideration burnup, reactor type, cooling time, and engineering considerations that may impact the timeliness of the diversion.

Rather than address the weapon suitability of plutonium by isotope content as described in the work of previous researchers, this research seeks to further reduce the scope of the plutonium safeguards challenge by identifying assemblies within a core that are most attractive for proliferation. This project presents a modeling capability that allows safeguards professionals to quickly determine the impact of core operator inputs on LWR assembly axial isotope content. By quickly delivering an axial isotope profile for a LWR assembly, this tool allows safeguards professionals to fully understand and prioritize locations within a core where illicit plutonium production is most likely occur while deemphasizing portions of the core with highly undesirable plutonium. In the event of unexpected changes to the reactor environment, this model allows the safeguards professional to quickly determine the impact of that change on assembly isotope content and determine if additional safeguards measures are needed.

2.2 SCALE Suite of Modeling Software

SCALE code system is a collection of nuclear modeling and simulation programs maintained by Oak Ridge National Laboratory. SCALE software platforms offer the user a wide array of tools for many different nuclear applications to include criticality analysis, cross-section processing, lattice physics modeling, and depletion analysis. SCALE offers both deterministic and Monte Carlo transport solvers that when coupled with the depletion capabilities of ORIGEN, provides the user a full suite of versatile, highly accurate nuclear modeling tools.[12]

SCALE excels at modeling reactor and lattice physics simulations. Earlier versions of SCALE gave the user integrated reactor modeling and depletion capabilities through a selection of TRITON depletion sequences.[38] With the release of SCALE 6.2, additional reactor modeling capabilities were added with the inclusion of Polaris, a 2D lattice physics simulation specifically designed for LWRs. Polaris includes design-specific features allowing the user to transfer few-group cross sections from SCALE modeling to a nodal core simulator, thus streamline a feature already present in TRITON.[39] Unfortunately for this project, Polaris is only capable of modeling square lattices so the hexagonal lattice of the VVER required the use of TRITON.

When building reactor assembly models in SCALE, either using the 2D discrete ordinate solver NEWT or KENO for 3D Monte Carlo analysis, the user must define a number of material properties.[12, 38] While there are limited tools for modifying these properties throughout the simulation, the breadth of material property fluctuations within the entire core cannot be capture with a Monte Carlo or discrete ordinates solution. The inability of lattice physics simulation to capture changes in material properties caused by the reactor environment necessitates the use of a nodal core simulator. A nodal core simulator can simulate changes in moderator properties, fuel properties, control rod position, boron levels, and core power. The nodal simulator requires a wide library of cross-sections to query and that library is built using lattice physic programs such as Polaris or TRITON.[40] Due to the complexity of lattice physics calculations and the wide variety of cross-sections needed for a nodal simulator, some TRITON simulations can run for

extended periods of time. While this could be considered a drawback, once the cross-section library is created, it should not require modification unless new assembly types are added to the core.

2.3 NESTLE 6.2 Developmental

This project uses a nodal core simulator, NESTLE, to model a VVER reactor. NESTLE, Nodal Eigenvalue Steady-State, Transient, Le core Evaluator, was developed originally by N.C. State, in partnership with ORNL, and version 5.2.1 was released in 2004.[41] Since that time, modernizing and improving NESTLE has become a major research effort within the Department of Nuclear Engineering at the University of Tennessee. In 2010, J. Galloway updated the thermal hydraulic modeling capability of NESTLE to model BWRs and proposed an initial isotope inventory tracking system as part of his doctoral research.[42] Since his update, a number of University of Tennessee students worked to modernize NESTLE. K. Ottinger enhanced the plotting and visualization features of NESTLE while demonstrating in his doctoral work the full capabilities of NESTLE by developing a reactor fuel cycle optimization algorithm.[43] N. Luciano further improved NESTLE by being the first student to successfully model a VVER-1000.[44, 45] C. Gentry demonstrated through his doctoral research, which modeled the Advanced High Temperature Reactor (AHTR), the visual and modeling enhancements of NESTLE and its versatile capabilities.[46] The work of this project built upon the lessons learned by Luciano and his success modernizing the hexagonal modeling capabilities of NESTLE.

Unlike TRITON, which uses a “predictor-corrector depletion process” to update cross-sections and isotope inventories, NESTLE queries a pre-generated library of cross-sections in order to generate a flux solution.[41] [47] This means that while the NESTLE provides burnup data, it is not actually performing depletion and updating isotopic inventories. (Collins E.P., et al., 2014) attempted to directly couple NESTLE generated flux solutions to the SCALE depletion code ORIGEN but found as ORIGEN modernized, coupling the two programs, while generating valid results, proved to be challenging and unsustainable.[44] A nascent algorithm built into the original NESTLE program included the capability to track a limited number of isotopes. N. Luciano resurrected this micro-

depletion capability that allows the software to track a limited number of isotopes as part of his doctoral work and built a pin-power reconstruction capability into NESTLE for hexagonal lattices.[48]

At the time of this project, the micro-depletion and pin-power reconstruction work of Luciano, N was still in progress.[48] Therefore, this project sought an alternate method to link the NESTLE core simulation results to depletion analysis. With the release of SCALE 6.2 and ORIGAMI, a new coupling approach became apparent. ORIGAMI is a new interface to the well-established Origen depletion code specifically designed for 3-D depletion modeling of LWR fuel assemblies.[13] As such, ORIGAMI includes a feature that allows the user to specify the power distribution of the assembly. NESTLE provides a relative power distribution for all nodes in the model. Through use relative assembly power provided by NESTLE, ORIGAMI can model axial isotope distributions directly correlated to the reactor environment.

Chapter 3: Model Development

3.1 Model Development Overview

Lattice physics modeling of a reactor fuel assembly only captures a snapshot of the conditions to which the assembly is subject within the core. This project addresses that limitation by coupling a core VVER-1000 model to individual assembly depletion using burnup weighted axial relative power (PRELZ). The project required the use of three distinct sets of models: SCALE lattice physics simulations, NESTLE VVER-1000 nodal core models, and ORIGAMI assembly depletion modeling. Figure 3 shows an overview of the nuclear software codes used in this project and the models created with those codes.

The LWR modeled for this project is a VVER-1000 and is based on a series of benchmark publications from Lotsch T., et., al. presented from 2009-2011 in the *Symposium of Atomic energy Research on WWER Physics and Reactor Safety*. [16-18] The documents offer information from four operating cycles but this paper only uses the core configuration from the first cycle. The next sections provide a summary of the model architecture described by Figure 3 and found in detail in Appendix A through Appendix D. The final section is a description of how this model architecture relates directly to plutonium production and safeguards.

3.2 Lattice Physics Modeling

Nodal core simulators require a wide range of cross-section data be built into a single cross-section library. Rather than calculating the cross-sections for each change in model state, nodal simulators interpolate the cross-section library. It is important for the cross-section library generated to bound as many possible model states that the nodal simulator may encounter. If the nodal simulator requires a cross-section that is outside the range of the cross-section library, it will extrapolate the cross-section. Extrapolated cross sections are less accurate than those that are interpolated. [12, 38, 49]

The cross-section library created for the NESTLE VVER-1000 core consisted of five fuel assembly cross-sections and three reflector cross-sections. The benchmark cycle data provided realistic information from which to create a VVER 1000 core model and verify its behavior. This section will provide a general description of the fuel assemblies and reflector materials in the VVER-1000. Appendix A contains a complete description of the assumptions, parameters, and branches used for lattice physics modeling. Appendix E contains select SCALE 6.2.1 input files.

Table 4: VVER 1000 First Cycle Fuel Assembly Distribution (adapted from Table 7, [16])

VVER 1000 Fuel Assembly Types							
Fuel Assembly	Enrichment	UO ₂ Pins		Gd-UO ₂ Pins			Number of Assemblies
		Number	Enrichment	Number	Gd ₂ O ₃ Enrichment	U235 Enrichment	
13AU	1.30%	312	1.30%	n/a			48
22AU	2.20%	312	2.20%	n/a			42
30AV5	2.99%	303	3.00%	9	5.00%	2.40%	37
39AWU	3.90%	243	4.00%	9	5.00%	3.30%	24
		60	3.60%				
390GO	3.90%	240	4.00%	6	5.00%	3.30%	12
		66	3.60%				

Table 4 shows the number and type of each fuel assembly in the core for the first cycle. Figure 6, taken from a publication created by scientists employed at TVEL’s JSC NCCP (Novosibirsk Chemical Concentrates Plant), illustrates a number of different VVER fuel assembly designs.[50] The VVER1000 core modeled uses the TVSA fuel assembly design.

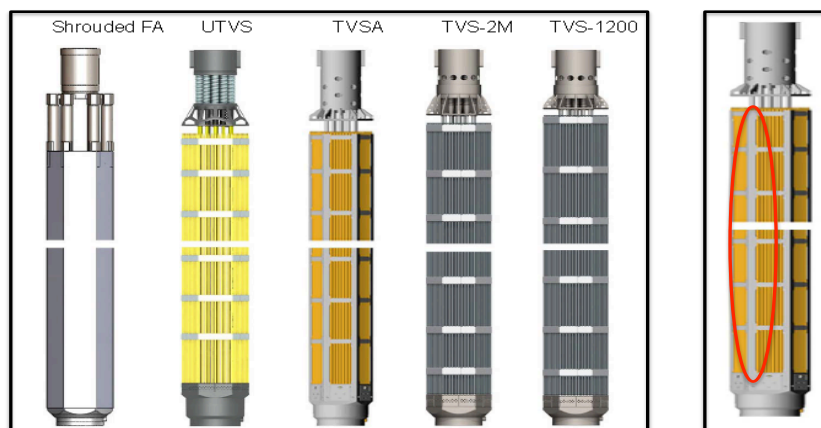


Figure 6: VVER Fuel Assembly Designs (Figure 1, [50])

The TVSA fuel assembly is notably different from the other assemblies due to the presence of a vertical stiffening plate. The image on the right in Figure 6 highlights the stiffening plate. The stiffening plate reinforces the assembly at each corner of the hexagon as seen in radial view in Figure 7. The image in Figure 7 is a close-up snapshot of the TVSA stiffening angle from an FA 13AU fuel assembly. The model was created using SCALE 6.2.1 T-Newt. Figure 7 also shows the fuel pin cladding (yellow) and the central hole of the VVER annular fuel pin (green).

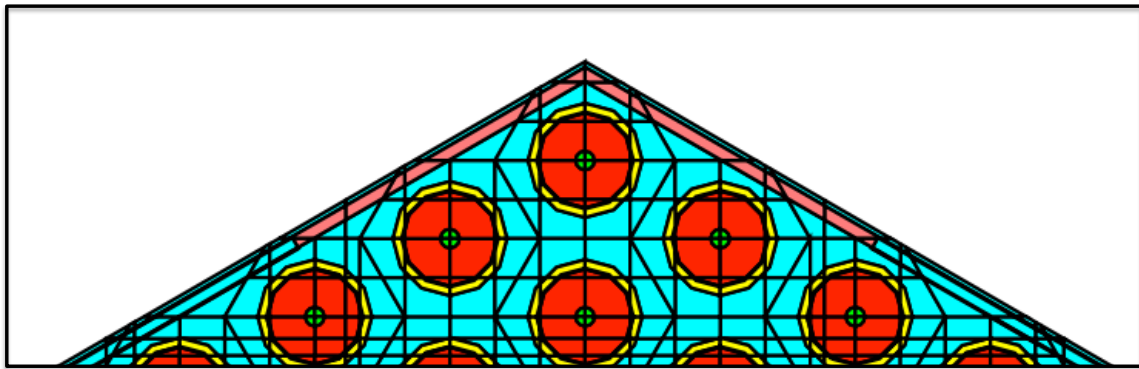


Figure 7: Stiffening Angle Modeled in T-Newt

3.2.1: 13AU

Figure 8 shows FA 13AU modeled in T-Newt. All 312 fuel pins in FA 13AU are 1.3% enriched ^{235}U . The pin map is identical for 22AU assembly however the enrichment is slightly higher at 2.2% ^{235}U . The fuel pins are in red. The moderator is in blue. The control rod guide channels are filled with moderator and are colored light green. The central guide tube is filled with moderator and is purple. The stiffening plate is in place on each corner (red).

3.2.2: 30AV5

Figure 9 illustrates TVSA FA 30AV5 which consists of 303 fuel pins (red) enriched at 3.00% ^{235}U and 9 burnable absorber (BA) pins (dark). The BA pins are 5% Gd_2O_3 and 95% UO_2 . The UO_2 in the BA pins has a ^{235}U enrichment of 2.40%. Structural features of the assembly, such as the position of the control rod guide tubes, central guide tube, and stiffening angle remain the same for all the fuel assemblies modeled.

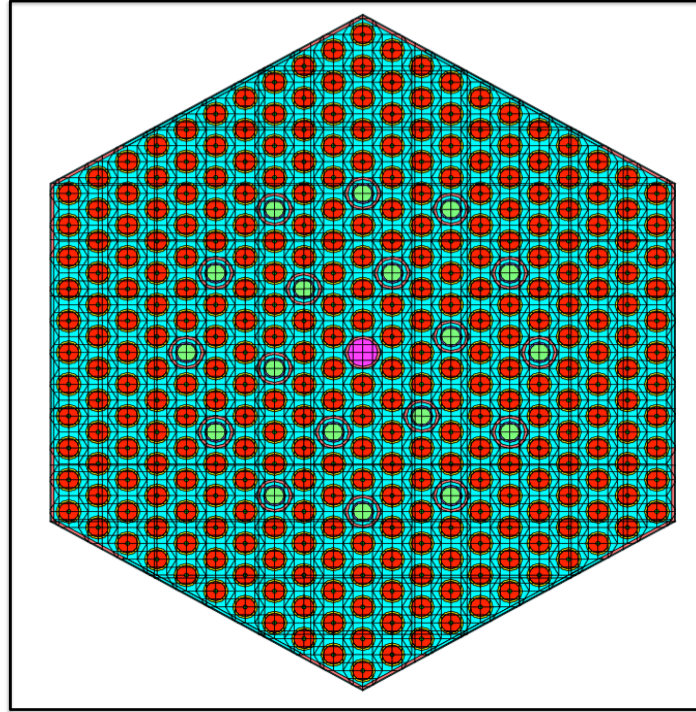


Figure 8: FA 13AU T-Newt Model

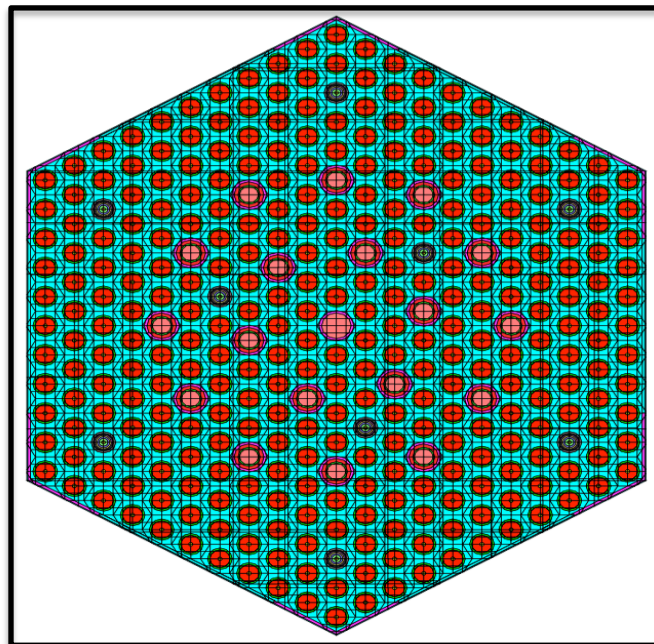


Figure 9: FA 30AV5 T-Newt Model

3.2.3: 39AWU

Figure 10 illustrates TVSA FA 39AWU which consists of 243 fuel pins (red) enriched at 4.00% ^{235}U , 60 fuel pins (purple) enriched at 3.60% ^{235}U , and 9 burnable absorber pins (dark). All BA pins consist of 5% Gd_2O_3 and 95% UO_2 . The UO_2 in the BA pins has a ^{235}U enrichment of 3.3%.

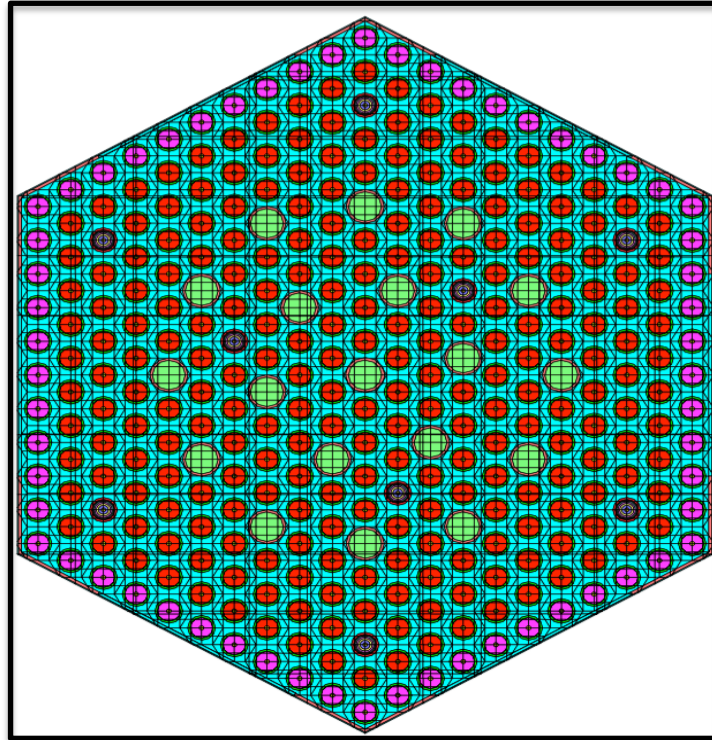


Figure 10: FA 39AWU T-Newton Model

3.2.4: 390GO

Figure 11 illustrates the TVSA FA 390GO which consists of 240 fuel pins (red) enriched at 4.00% ^{235}U , 66 fuel pins (purple) enriched at 3.60% ^{235}U , and 6 centrally located burnable absorber pins (dark/black). The BA pins consist of 5% Gd_2O_3 and 95% UO_2 . The UO_2 in the BA pins is 3.3% ^{235}U enriched.

3.2.5: Branches and Data Processing

The T-Depl branch feature allows the user to specify a variety of core conditions such that the nodal simulator has a wide number of model states from which to interpolate.

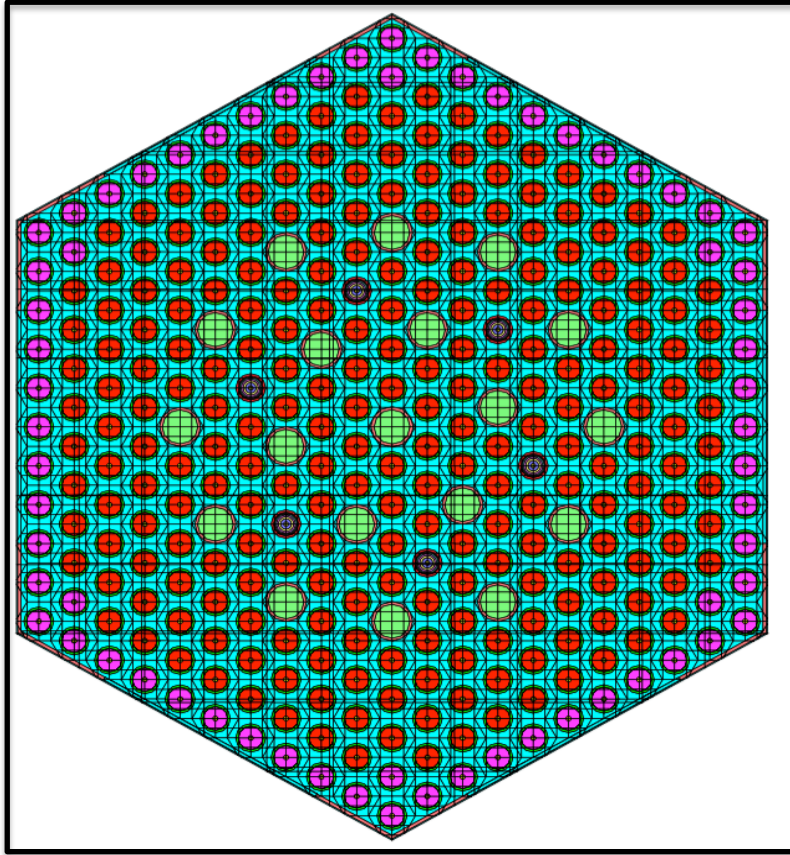


Figure 11: FA 390GO T-Newt Model

The cross-section library in this project incorporated 18 different branch simulations, which included variations in moderator density, control rod presence, boron concentration, and fuel temperature. Due to the complexity of cross-section modeling, some SCALE 6.2.1 T-Depl simulations ran for as 16 days. Appendix A provides a list of model branches. SCALE 6.2.1 outputs cross-section data for all branches to a file named xfile016. Also included on the xfile016 are assembly discontinuity factors (ADFs). Nodal simulators use ADFs to force continuity of flux between assembly boundaries.[12, 51] A more detailed discussion of ADFs is found in Appendix A when discussing reflector modeling. A local University of Tennessee program called Triton2Nestle (T2N) converts the xfile016 into a format usable in NESTLE. T2N requires the use of a program specific input file to convert the xfile016 into a NESTLE cross-section file. Each assembly has a unique NESTLE cross-section file. The individual files must be manually constructed into a master cross-section file (cross-section library) for VVER-1000 core modeling.

3.2.6: VVER 1000 Reflectors

The VVER-1000 has both radial and axial reflectors. Reflectors must be included in the NESTLE VVER-1000 model in order to ensure the core model has the correct boundary conditions. NESTLE has the capability to differentiate between reflector material and fuel material however it requires reflector cross-sections be included in the cross-section library. VVER-1000 reflectors are not homogenous and consist of multiple sections, of differing dimensions and materials. Figure 12 is a NEWT 1D representation of the core and radial reflector.

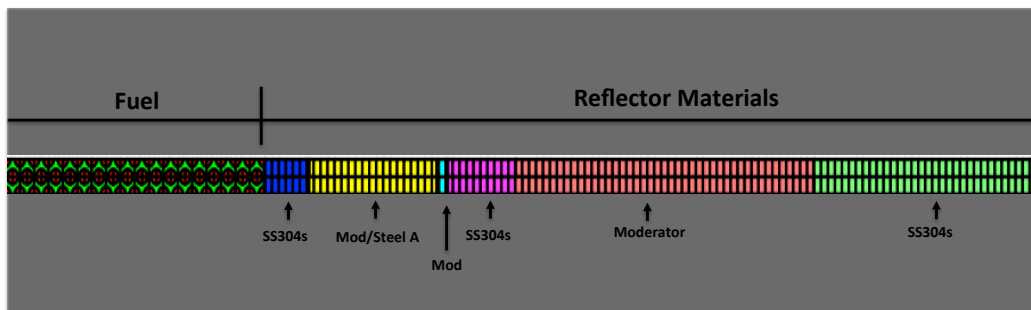


Figure 12: Radial Reflector 1D Newt Model

Figure 12 is not to scale. The radial reflector is modeled as a series of material segments. Axial reflectors were modeled using this approach as well. SCALE T-Newt homogenizes the fuel and reflector region separately and outputs two sets of cross-sections to the xfile016. The reflector cross-sections must be manually added to the master VVER-1000 cross-section library. The reflector ADFs are approximated as 1.0 meaning that the heterogeneous and homogenous flux at the fuel-reflector boundary is the same. While not physically correct, calculating hexagonal reflector ADFs is quite complicated. A complete discussion of the reflector cross-section models and the hexagonal ADF challenge can be found in Appendix A.

3.3 Nestle VVER 1000 Benchmark Model

This project uses a NESTLE VVER-1000 model built using information from the previously stated benchmark documents. Table 5 provides a list of general reactor characteristics for the VVER-1000 from the benchmark documents. The core of a VVER consists of 163 hexagonal fuel assemblies. The reactor uses borated water as both a coolant and a moderator. There are 61 RCCAs that insert 18 $\text{Dy}_2\text{O}_3 \cdot \text{TiO}_3$ and B_4C control rods. The reactor modeled for this project assumes the control rods to be comprised entirely of B_4C . Reactivity is also controlled early in the cycle through the presence of burnable absorber pins that contain a mixture of 5.00% Gd_2O_3 and 95% UO_2 (differing levels of uranium enrichment).

Figure 13 shows the core map for the VVER-1000 first cycle taken directly from the benchmark document.[16] The thermodynamic properties of the core are found in Table 6. The core coolant flow rate, provided in the benchmark study, is 88,000 m^3/hr .[17] The core coolant is borated water. The core power density in NESTLE is in units of kW/l and is calculated to be 111.68 kW/l . The calculated core power density is higher than the IAEA defined core power density for a VVER-1000, which is 108 kW/l and is suspected to be a source of model of error.[52] A complete discussion of this error source is found Appendix B.

Table 5: VVER-1000 Benchmark Core Characteristics

VVER1000 Benchmark	
Core	
Power (MWth)	3000
Average Moderator Temperature (K)	578
Coolant Outlet Pressure (Mpa)	15.7
Average Power density (W/gU)	42.5
Average Boron Concentration (ppm)	525
Number of Cycles	4
Fuel Assemblies	
Number	163
Height (cm)	355
Active fuel height (cm)	352
Average fuel temp (K)	1005
Number of fuel pins	312
Fuel assemblies with control rod clusters	61
Fuel	UO2
Burnable Absorber Pin	Gd2O3
Control Rod Material (lower)	Dy2O3 TiO3
Control Rod Material (Upper)	B4C

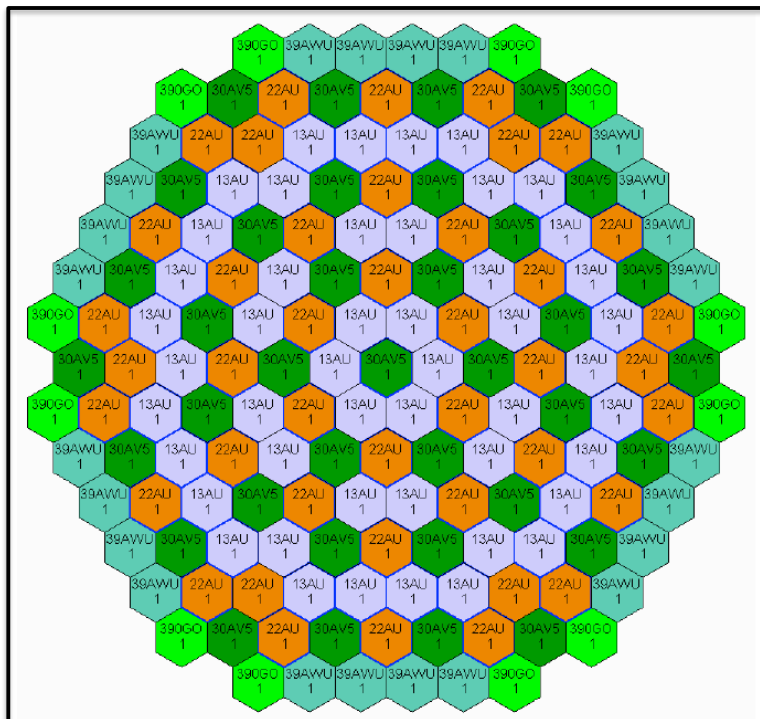


Figure 13: VVER-1000 Core Map First Cycle (Adapted from Figure 16 in [16])

Table 6: VVER-1000 Coolant Properties

VVER-1000 Benchmark	
Core Thermodynamic Properties	
Power (MWth)	3000
Average Moderator Temperature (K)	578
Coolant Outlet Pressure (MPa)	15.7
Coolant Flow Rate (m ³ /hr)	88000
Coolant Temp at Core Inlet (K)	563.15
Coolant Temp at Core Outlet (K)	592.75

Cycle-1 operating information was used to verify the accuracy of the NESTLE VVER-1000 model and determine model bias. Two models were created using 323 operational data points and 63 operational data points. Figure 14 illustrates the boron letdown curve of the 63-point model as compared to the data provided by the reactor operator. The NESTLE VVER-1000 model requires less boron to maintain criticality implying that the core is less reactive.

The benchmark comparisons and boron modeling reveal that the NESTLE VVER-1000 model is negatively biased meaning that there is less reactivity in the system than expected. The bias is acceptable for the purposes of this research, which focuses primarily on using core coupled isotope modeling for nonproliferation analysis. Steps to reduce the bias and improve model accuracy could be part of future work. A complete analysis of the NESTLE VVER-1000 model including comparisons to the benchmark information and potential sources of modeling error can be found in Appendix B.

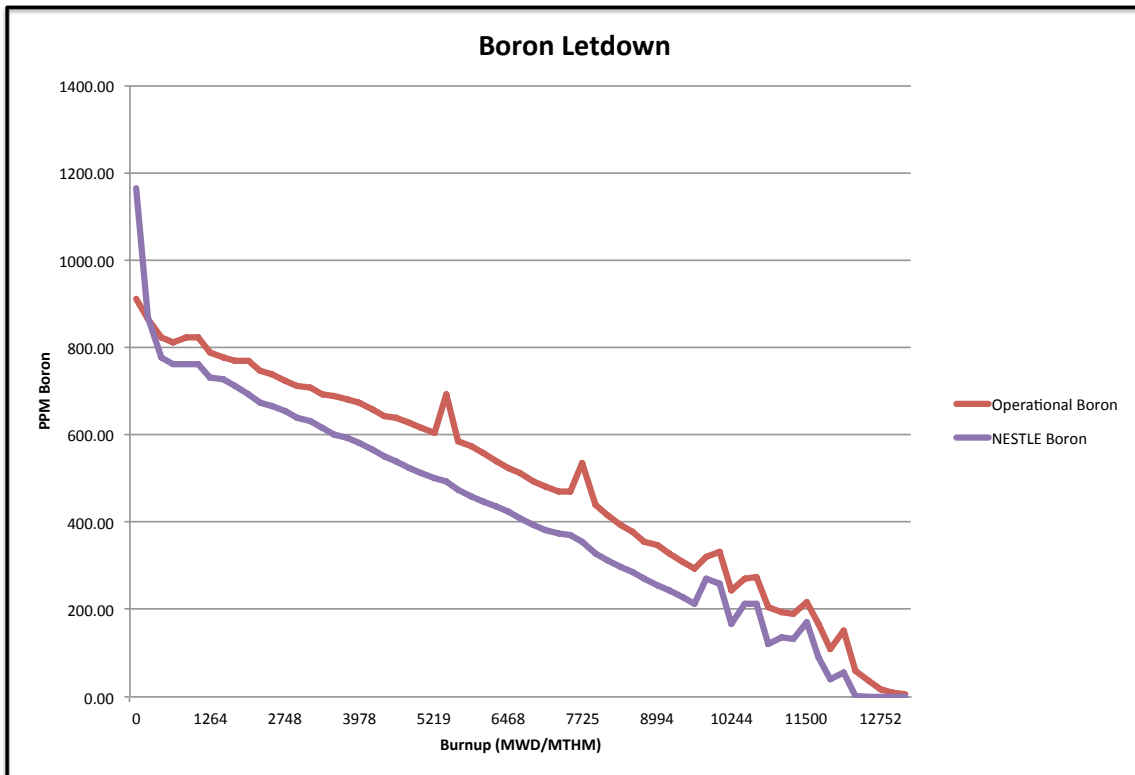


Figure 14: Boron Letdown Modeling

3.4 Developing a Testing Framework

A framework was needed to identify and test the impact of core changes on assembly axial isotope distribution. The VVER-1000 Test model was created in order to provide a framework in which to isolate the impact of a core level change on a single assembly. The VVER-1000 Test model described in Appendix C uses the same core design characteristics as the VVER-1000 Benchmark model. The VVER-1000 Test model has different operational inputs. The Test model uses burnup steps of 1000 MWD/MTHM to step through the core fuel cycle. The VVER-1000 Test model has a 13000 MWD/MTHM core burnup but all data analysis is conducted at a core burnup of 12000 MWD/MTHM. The power and control rod positions are kept constant throughout the core fuel cycle with the exception of the last step, which exhibits a power coast down. The boron levels are set to critical by NESTLE. Appendix C describes the VVER-1000 Test model and the input file can be found in Appendix E.

This project tested the capability of an operator to influence plutonium isotope production in a single fuel assembly. Assembly selection was determined by prospect for generating maximum plutonium mass. FA 13AU assemblies were selected as they had the highest weight percent of ^{238}U . A Linux-Python script was used to extract and calculate the ratio of fast to thermal nodal fluxes (G1/G2 flux). The script found the axial nodes with the highest G1/G2 flux. The FA 13AU assembly with the highest G1/G2 flux was selected for targeted ^{239}Pu production modeling. Appendix C describes the assembly selection process using both the VVER-1000 Benchmark model and the VVER-1000 Test model. In both cases, assembly #139 had the most axial nodes with a high G1/G2 flux. The G1/G2 flux is also at times in this product referred to as the flux spectrum hardness.

Figure 15, created using Paraview Visualization Software[53], shows the location of the FA 13AU fuel assemblies in the VVER-1000 Benchmark core model and their flux spectrum hardness. The FA13AU assemblies have been increased in size for ease of identification but they clearly have lower flux spectrum hardness than surrounding nodes. This is likely due to both their low level of enrichment and the absence of burnable absorbers.

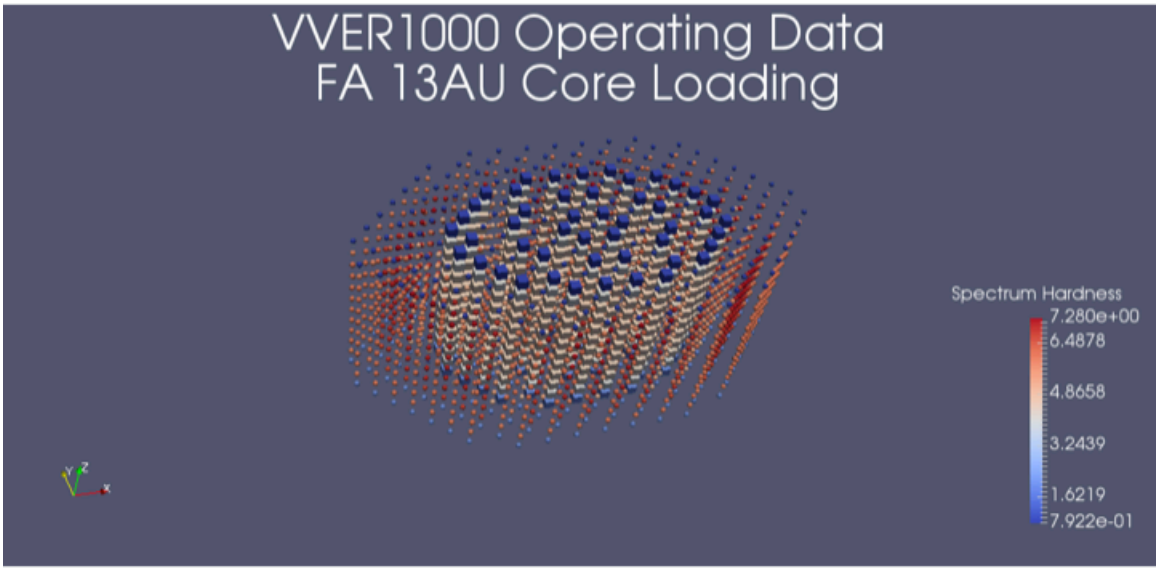


Figure 15: VVER-1000 Benchmark Flux Spectrum Hardness

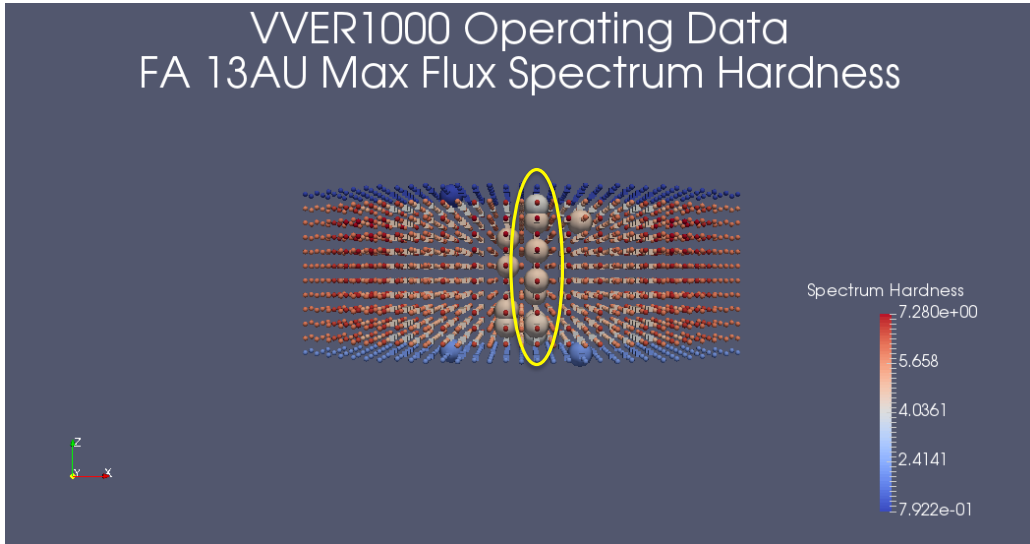


Figure 16 illustrates assembly #139 and illustrates the nodes with a high G1/G2 ratio. Figure 17 illustrates assembly #139 in the VVER-1000 Test model. Once again, assembly #139 had the most nodes with a high G1/G2 flux ratio. Assembly #139 was selected to be the target production assembly for this project. As the project target assembly, all single assembly models are that of Assembly #139.

Figure 16: Assembly #139 Flux Spectrum Hardness in VVER-1000 Benchmark

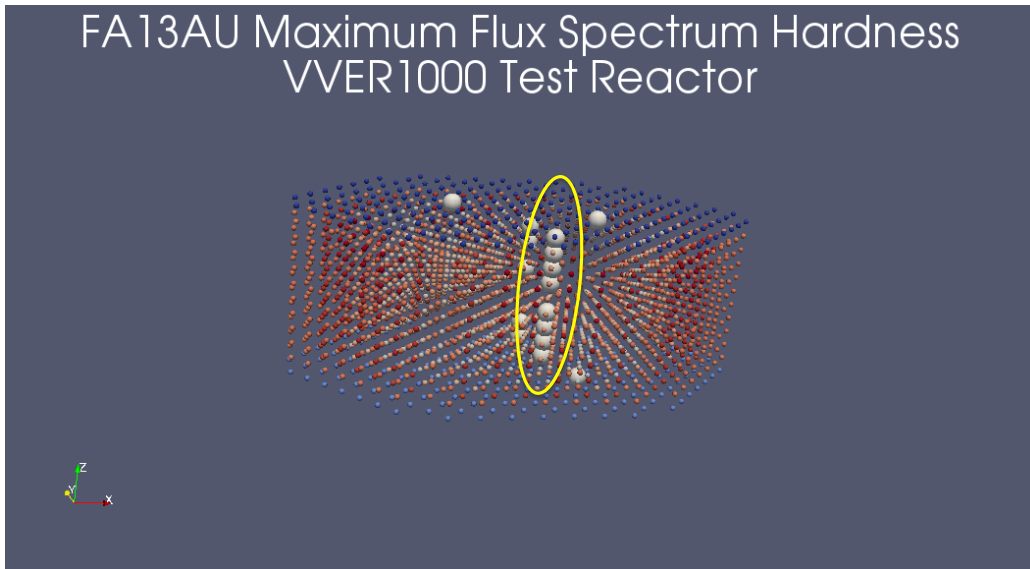


Figure 17: Assembly #139 Flux Spectrum Hardness in VVER-100 Test

3.5 NESTLE to ORIGAMI Coupling

Depletion calculations are computationally intensive requiring the software platform to combine subroutines that execute cross-section processing, material inventory, neutron transport, and depletion. Coupling a full core simulator to depletion software adds another layer of complexity in that the homogenized inputs used in the core simulator must somehow be made useful in the depletion software. Figure 18 provides a general overview of the modeling challenge described.

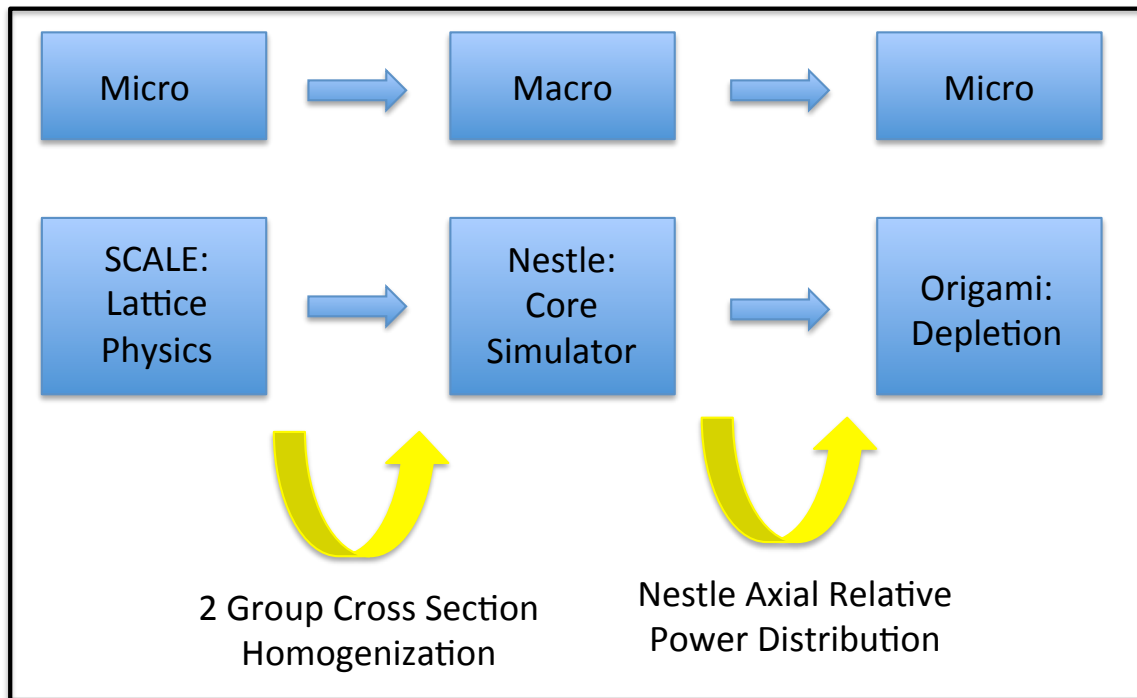


Figure 18: Model Design Sequence

ORIGAMI allows the user to specify variations in the assembly power by defining both an axial power distribution for an assembly or a radial, pin-by-pin power distribution.[13]. NESTLE outputs relative power for each node of the core at all burnup steps. The burnup weighted axial relative power (PRELZ) output by NESTLE provides a variable through which the impact of the reactor environment is transferred to depletion analysis. Appendix D provides a detailed overview of NESTLE to ORIGAMI coupling using burnup weighted axial relative power.

3.5.1: Burnup Weighted Relative Power

Appendix D also shows that the axial power distribution of an assembly changes throughout the fuel cycle. Figure 19 illustrates the relative power of each node in the VVER-1000 Test model target assembly from BOC to EOC. Central nodes peak in power early in the cycle and then steadily decrease. Axial fuel nodes steadily increase in relative power from BOC to EOC. Thus, at EOC the axial relative power is not reflective of nodal power changes throughout the cycle.

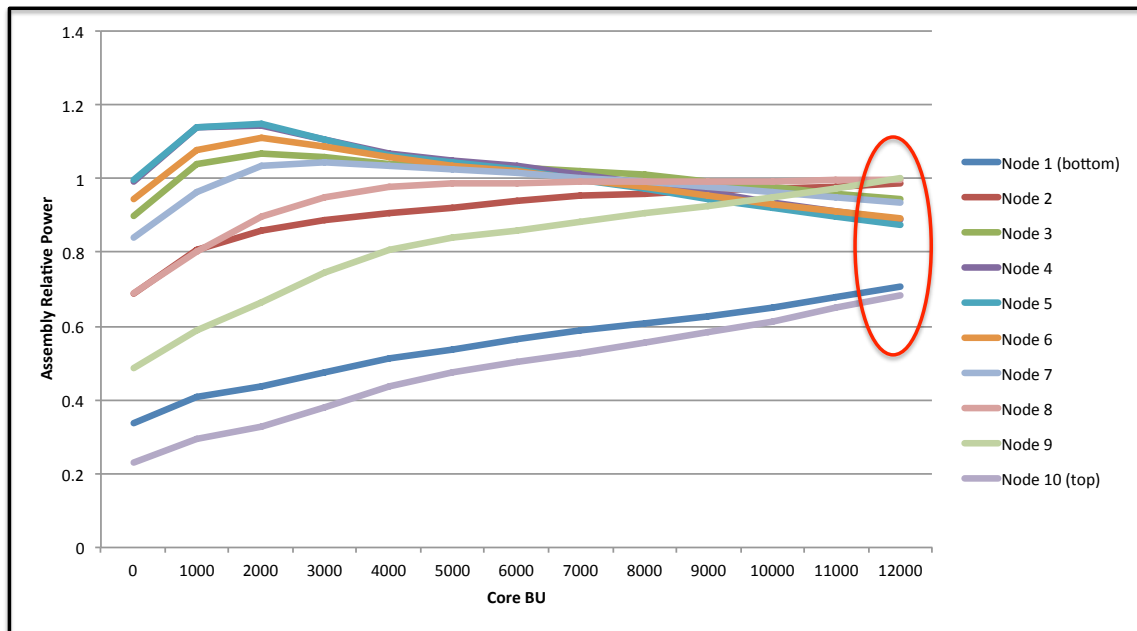


Figure 19: VVER-1000 Test Nodal PRELZ

ORIGAMI only allows the user to define a single axial power distribution for each model. To capture the changes in PRELZ with respect to core burnup, a PRELZ weighting method was developed. The axial power from each burnup step was incorporated in the final PRELZ solution and had a weight equivalent to the size of the burnup step. Eq. 1 through Eq. 6 provides the weighting formula and inputs for axial relative power weighting with burnup.

$$i = \text{nestle calculation iteration } [0,1,2 \dots 12] \quad \text{Eq. 1}$$

$$\text{step} = i + 1 [1,2,3 \dots 12] \quad \text{Eq. 2}$$

$$n = \text{nestle axial node } [0,1,2, \dots 12] \quad \text{Eq. 3}$$

$$\Delta BU_{n,step} = BU_{n,i+1} - BU_{n,i} \quad \text{Eq. 4}$$

$$\overline{PREL}_{n,step} = \frac{(PREL_{n,i} - PREL_{n,i+1})}{2} \quad \text{Eq. 5}$$

$$PREL_n = \frac{\sum_1^{12} [(\Delta BU_{n,step})(\overline{PREL}_{n,step})]}{\sum_1^{12} \Delta BU_{n,step}} \quad \text{Eq. 6}$$

To facilitate calculation of the burnup weighted relative power, a Linux script extracted the nodal burnup and PREL for each core burnup step as well as the final assembly burnup. The Linux script then used a python program to calculate the burnup weighted PRELZ using Eq. 6 for use in ORIGAMI. All Linux and python scripts can be found in Appendix F.

Figure 20 illustrates the impact of using burnup weighting on PRELZ distribution. As seen in Figure 19, PRELZ at EOC is not reflective of the assembly power throughout the cycle.

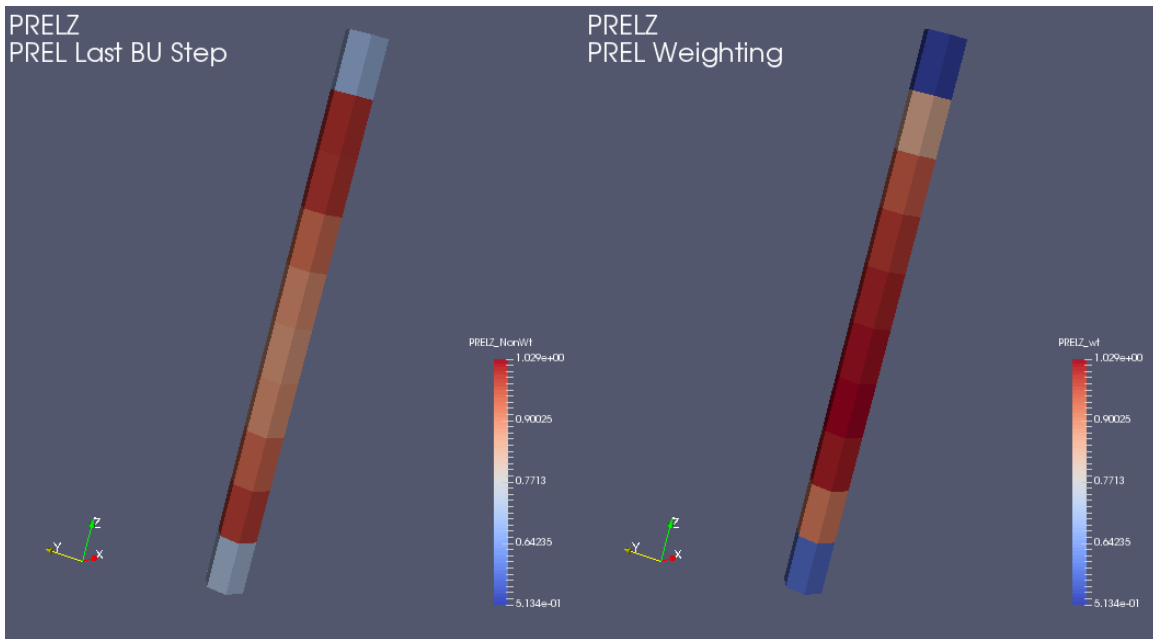


Figure 20: PRELZ for Target Assembly EOC vs. Weighted

Figure 20 reveals a noticeable shift in assembly power in to fuel nodes centrally located in the core. This shift is important as it captures early cycle behavior thus ensuring higher power nodes are identified correctly for accurate depletion.

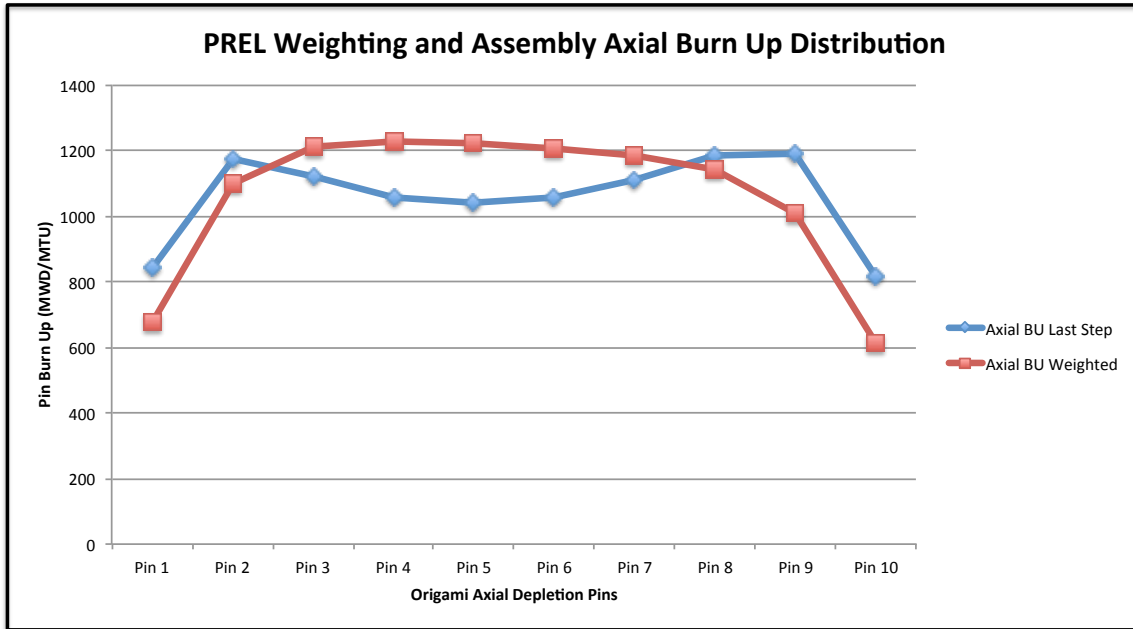


Figure 21: Weighted PRELZ vs Non-Weighted PRELZ Axial Burnup

Figure 21 is a comparison of burnup for PRELZ weighted and non-weighted ORIGAMI depletion models of the target assembly. Using PRELZ weighting does not alter the final assembly burnup but shifts nodal burnup to more accurately reflect core behavior. Central nodes had a higher burnup than axial nodes due to an increase in relative power.

When coupling NESTLE to ORIGAMI, it was important to ensure both programs had the equivalent assembly burnup. The ORIGAMI power history block replicates an assembly burnup close to the equivalent to the NESTLE-provided assembly average burnup. It is difficult to directly match the NESTLE and ORIGAMI burnup.

Appendix D provides an in-depth comparison of burnup weighted vs. non-burnup weighted isotope analysis. Using assembly burnup to weight the impact of relative power alters the distribution of isotopes results. High power nodes, centrally located in the assembly, have a lower mass of ^{235}U than low power nodes. This is expected as the nodes contributing greatest to power production also undergo more fission. Analysis of the impact of burnup weighted PRELZ on isotopes ^{238}U and ^{239}Pu can be found in Appendix D.

3.6 Plutonium Production and Safeguards

Both the mass and isotopic content of plutonium determine the feasibility of weapons use. Table 3 provides a summary of plutonium grades with respect to safeguards that will be used throughout this project. For this paper, all “even numbered” plutonium isotopes (PuEven) are considered detrimental to weapons performance rather than just ^{240}Pu . Even-numbered plutonium isotopes such as ^{240}Pu , ^{242}Pu , and ^{238}Pu have a high spontaneous fission rate and a high decay heat.[28, 31] This makes these isotopes less attractive for use in weapons.[28] The Pu isotope distribution of the assembly is quite significant when determining the feasibility of a plutonium production pathway. A fissile content of 93% or greater (7% or less PuEven) is considered weapons-grade for this project. A review literature in Chapter 2 illustrates there is great debate as to the suitability of plutonium for weapons use with a ^{240}Pu content between 7% and 30%. This project limits the scope of evaluation to the use of a LWR for producing only weapons-grade plutonium but will acknowledge throughout the assessment the production of fuel-grade plutonium because within the scientific community there is debate about material suitability for weapons use.

When describing plutonium content, this paper uses the term “Pu fissile content” to mean the percentage of plutonium that is fissile. This paper collected the top 5 Pu isotopes from the VVER assemblies modeled and assessed their Pu fissile content using the following equations.

$$Pu^{all} = Pu^{238} + Pu^{239} + Pu^{240} + Pu^{241} + Pu^{242} \quad \text{Eq. 7}$$

$$fissile\ content = \frac{(Pu^{239} + Pu^{241})}{Pu^{all}} \quad \text{Eq. 8}$$

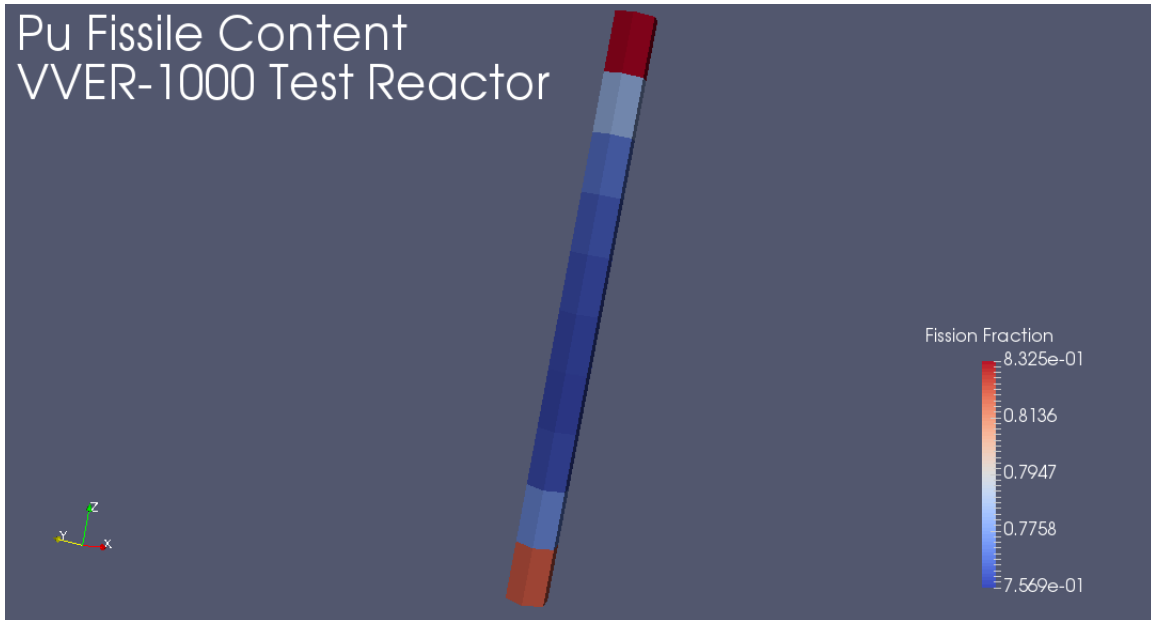


Figure 22: Pu Fissile Content Using Burnup Weighted PRELZ NESTLE to ORIGAMI Coupling

Figure 22 shows the Pu fissile content of the target assembly from the VVER-1000 test reactor. Using Table 3, one sees that the Pu fissile content of this assembly is well below weapons grade level. The highest fissile content is in the axial nodes and is approximately 83%, making it fuel grade. The central nodes of the assembly are all under 80% fissile and reactor grade. The isotopic content is reflective of a high burnup LWR fuel assembly. The distribution of the fissile content reveals that the nodes on either the bottom or the top of the assembly are highest in fissile content and therefore most likely to be targeted for manipulation by an operator.

Using the modeling framework described in this chapter, it is now possible model changes in core behavior and see the impact those changes have on axial isotope distribution. The VVER-1000 Test model and target assembly seen in Figure 22 will be modified as part of the scenario assessment for two potential LWR plutonium production scenarios. Using the NESTLE to ORIGAMI coupling framework detailed in this chapter and its supporting appendixes, it is possible to evaluate the feasibility of the plutonium production scenarios.

Chapter 4: Plutonium Production Scenario: Control Rod Insertion

4.1 Introduction

This chapter is the first of two demonstrations of the nonproliferation application of NESTLE to ORIGAMI coupling. In the scenario modeled for this chapter, an operator attempts to produce weapons grade plutonium in a LWR using control rod positioning. The operator goal is to increase the fissile content of a single assembly by reduce losses within the assembly from ^{239}Pu fission. Recall from Chapter 1 that ^{239}Pu fission losses are primarily from thermal neutron fission. By inserting a control rod into the assembly, the operator will change thermal neutron utilization in assembly nodes in proximity to the control rod. This will reduce the number of thermal neutrons absorbed in the fuel and thus reduce the number of fissions. This could result in a Pu fissile content higher than in an assembly without a control rod.

The target assembly used throughout this report (Assembly #139) does not normally have a control rod cluster associated with it however this project assumes it does. In order to allow for comparisons of results throughout the project, the decision was made to use the same assembly with the understanding that this differed physically from the VVER-1000. The VVER-1000 does have some FA 13AU assemblies with RCCAs. Should the pathway be deemed feasible, it would be possible confirm results using an assembly associated with a control rod working group.

4.2 Modeling

The control rod models were built upon the NESTLE VVER-1000 Test model. The burndata and reactor information remained the same for the control rod test models with the exception of the control rod bank definitions. A single control rod group was added to the model at the Assembly #139 location. NESTLE set the critical boron level necessary to maintain the reactor at critical and the core remained critical from BOC to 13,000 MWD/MTHM. As with previous cases all assembly data analysis was performed

only up to a core burnup of 12,000 MWD/MTHM. Figure 23 and Figure 24 show a full core model of the nodal relative power at BOC. In this model, the target assembly control rod is fully inserted. The reduction in power is clearly evident.

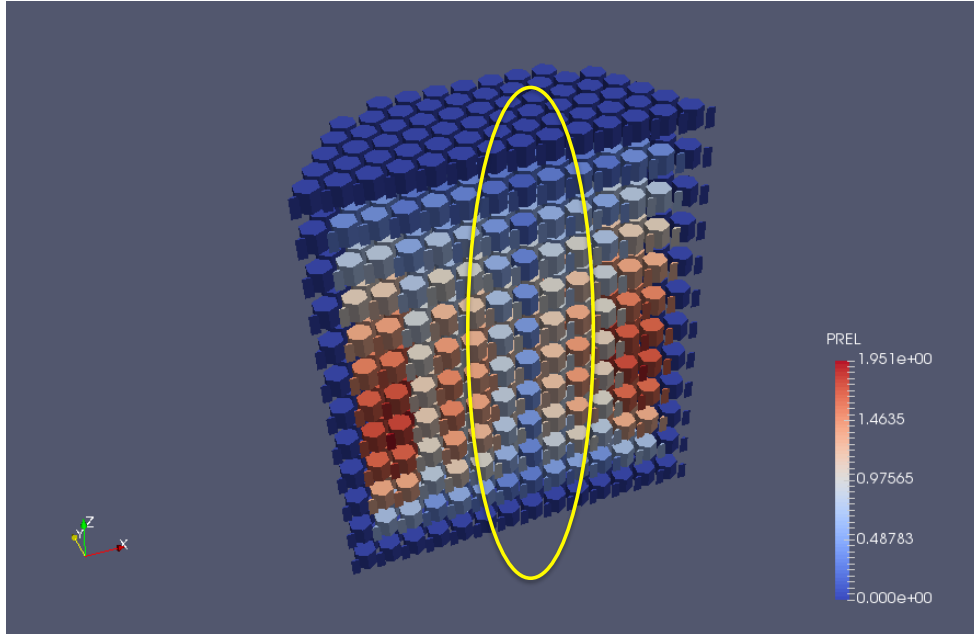


Figure 23: NESTLE VVER-1000 Relative Power with Target Control Rod Fully Inserted

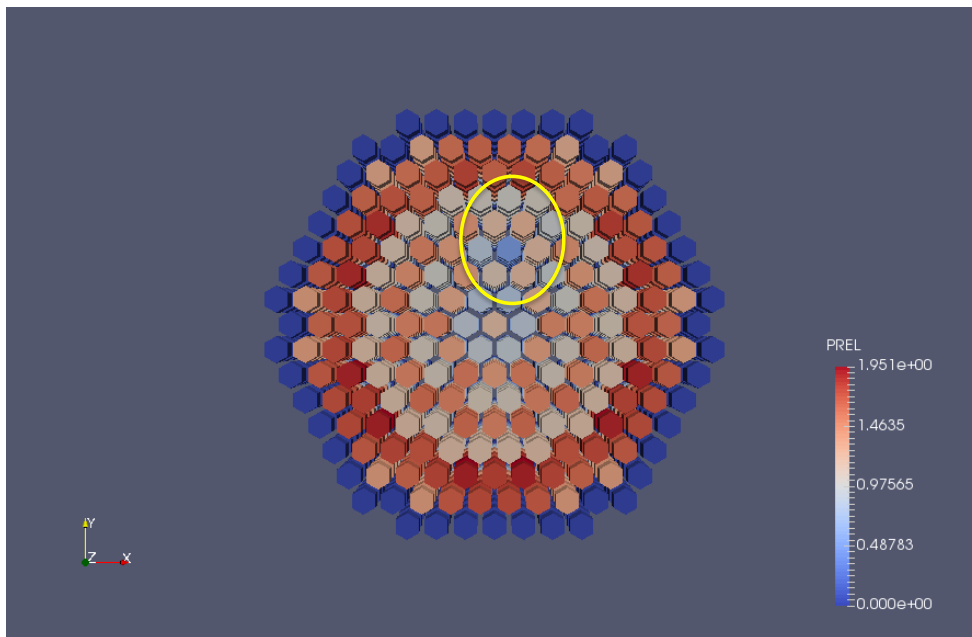


Figure 24: NESTLE VVER-1000 Relative Power with Target Control Rod Fully Inserted, Top View, Mid-Core

Figure 25 and Figure 26 show a full core model of the nodal thermal flux at BOC. In this model, the target assembly control rod is fully inserted. The reduction in thermal flux is clearly evident.

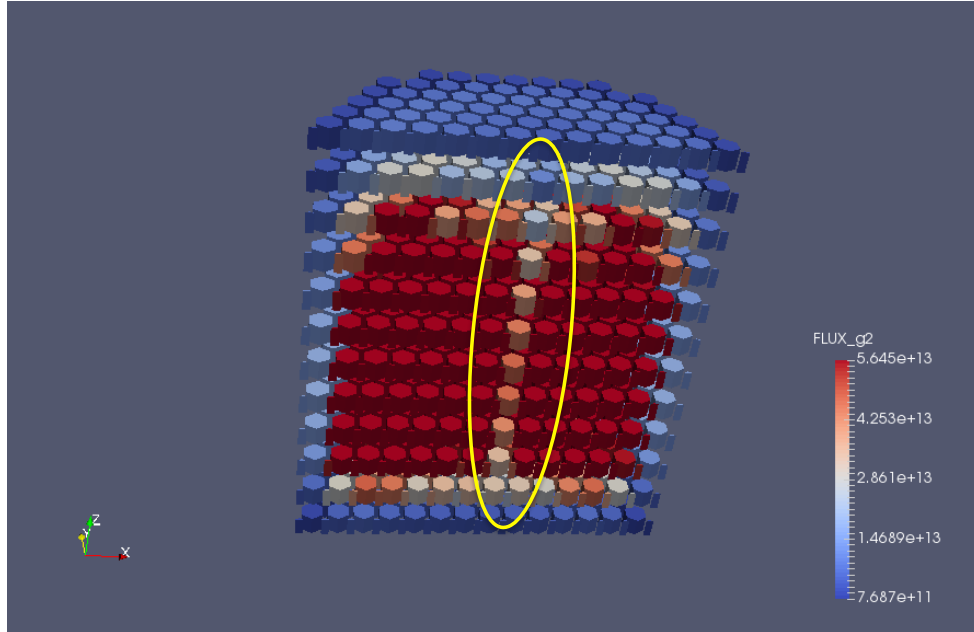


Figure 25: NESTLE VVER-1000 Thermal Flux with Target Control Rod Fully Inserted

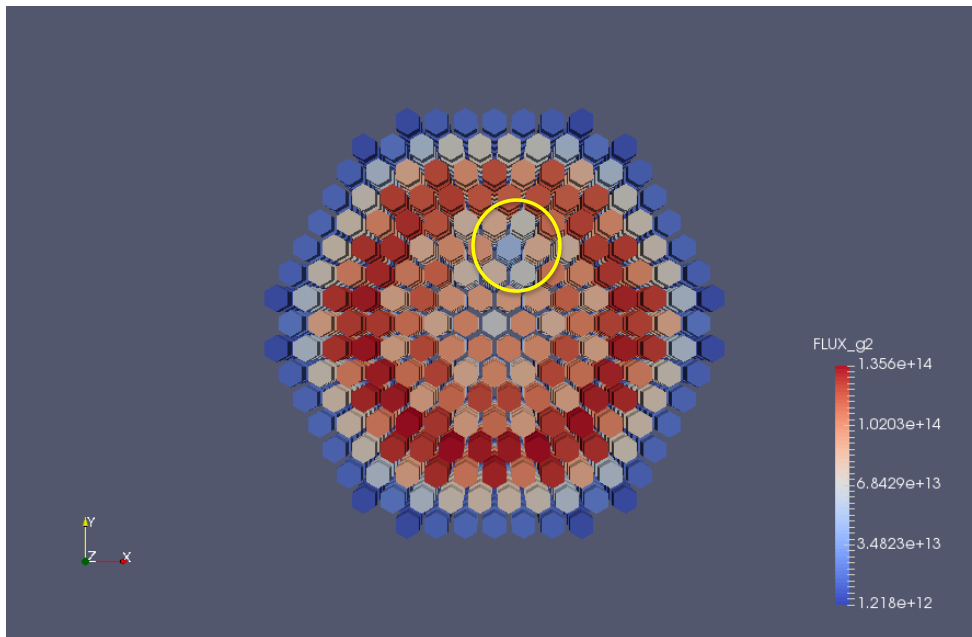


Figure 26: NESTLE VVER-1000 Thermal Flux with Target Control Rod Fully Inserted, Top View, Mid-Core

Ten unique models were used to define the position of the control rod by nodal depth of insertion. The control rod was modeled from a depth of fully inserted to top fuel node only. The VVER-1000 Test model has 12 axial nodes. The top and bottom nodes are reflectors. Therefore the control rod is inserted from a depth of full insertion (11 nodes) to top fuel node only (2 nodes). Figure 27 is an illustration of a control rod insertion depth of 8 nodes, of which only 7 are fuel nodes.

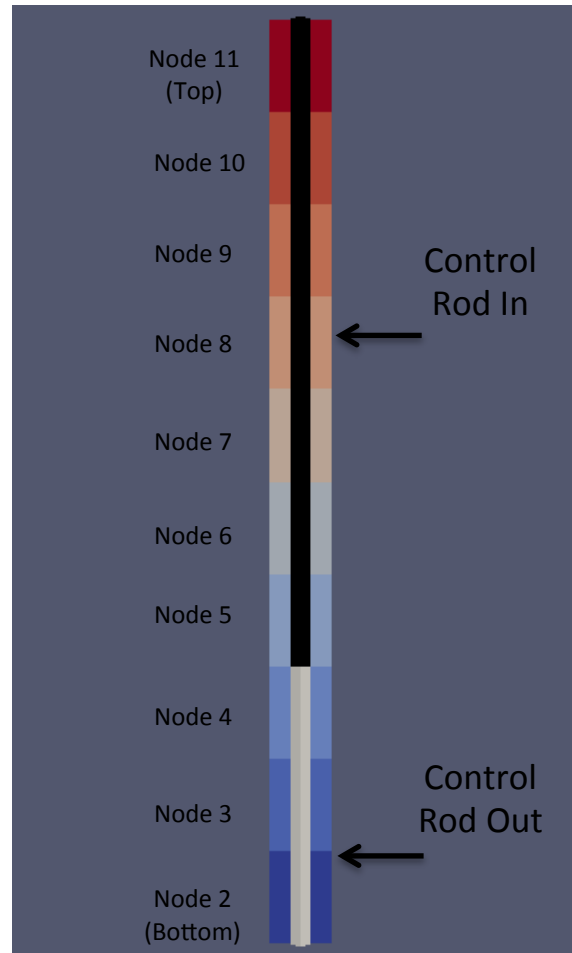


Figure 27: Control Rod Insertion Model

For each NESTLE model, the target assembly nodal group fluxes, relative power, and burnup were extracted at each core burnup step. The PRELZ weighting function was then used to construct a burnup weighted PRELZ for the assembly. The burnup-weighted PRELZ and assembly average burnup were input into ORIGAMI for depletion analysis.

Table 7 shows the NESTLE generated assembly burnup, the burnup input into ORIGAMI, and the difference between the two variables. Assembly burnup increased with removal of the control rod.

Table 7: Control Rod Depth and Burnup

Control Rod Depth: Nestle and Origami Burnup			
Number Nodes of CR Depth	Nestle Assembly BU (MWD/MTHM)	Origami (MWD/MTU)	
		Modeled BU	Origami BU Difference
11 (fully inserted)	6360.47	6374.99	-14.52
10	6836.97	6842.50	-5.53
9	7356.92	7352.50	4.42
8	7879.47	7862.52	16.95
7	8395.95	8415.01	-19.06
6	8903.78	8925.01	-21.23
5	9401.66	9392.51	9.15
4	9878.87	9860.00	18.87
3	10302.74	10285.00	17.74
2 (Top Node Only)	10560.22	10540.01	20.21

Modeling the insertion of a control rod into the assembly in ORIGAMI required the use of two separate libraries. One library contained cross-sections with the CRI and the other contained cross-sections with CRO. Appendix A describes the process to generate these cross-sections.

Modeling axial heterogeneity in an assembly was a larger challenge than expected. While ORIGAMI allows for user specification of multiple cross-section libraries for radial locations, multiple cross-section libraries for different axial zones are not currently supported.[13] ORIGAMI does include an “offset” feature that breaks the assembly axially into two problems and allows the user to call a different cross-section library for each problem. [13] The “offset” feature artificially cuts an assembly into two problems and treats these problems independently. As such, it normalizes the power history for each model separately. This proved to be problematic as the PRELZ and assembly power were defined for a complete assembly. Methods to circumvent the normalization of the power history to preserve the NESTLE PRELZ resulted in erroneous burnup or isotope results.

Due to the challenges creating an axial model in ORIGAMI, this project re-defined the assembly in the XY plane. By redefining the assembly from a nodal z-axis model to a one row, ten column XY plane, it now was possible to model the assembly using the XY pin-map feature of ORIGAMI. The XY pin-map feature allows the user to call multiple ORIGEN libraries in the same file. The user can specify the relative power of the pins as well. The XY pin-map requires a square lattice. It was determined that an assembly, with properties defined axially, could be input in a square array by using the first row of pins as axial nodes and defining all other rows with zeros. ORIGAMI ignores rows with an input of zero and therefore only completed calculations on the first row. Figure 28 is an example of the XY pin-map model used to model axial heterogeneity in the target assembly.

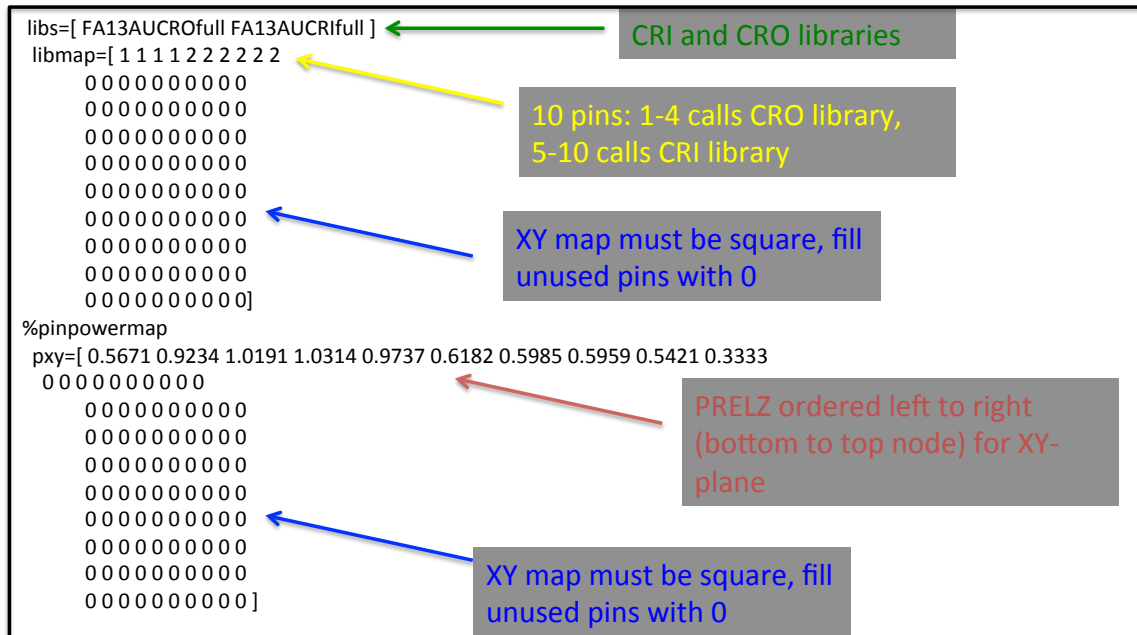


Figure 28: ORIGAMI Assembly XY Model Format

4.3 Results

Ten NESTLE simulations modeled control rod insertion into Assembly #139 at depths varying from fully inserted to top fuel node only. Each NESTLE simulation was coupled to ORIGAMI using burnup weighted PRELZ. ORIGAMI depleted the assembly to approximately the same assembly-average burnup as calculated by NESTLE. Axial node

maps were created for each assembly for eleven isotopes of interest. The relationship between control rod depth and nodal isotope content was then plotted using MATLAB's 3D surface plot feature and Paraview plotting.[53, 54]

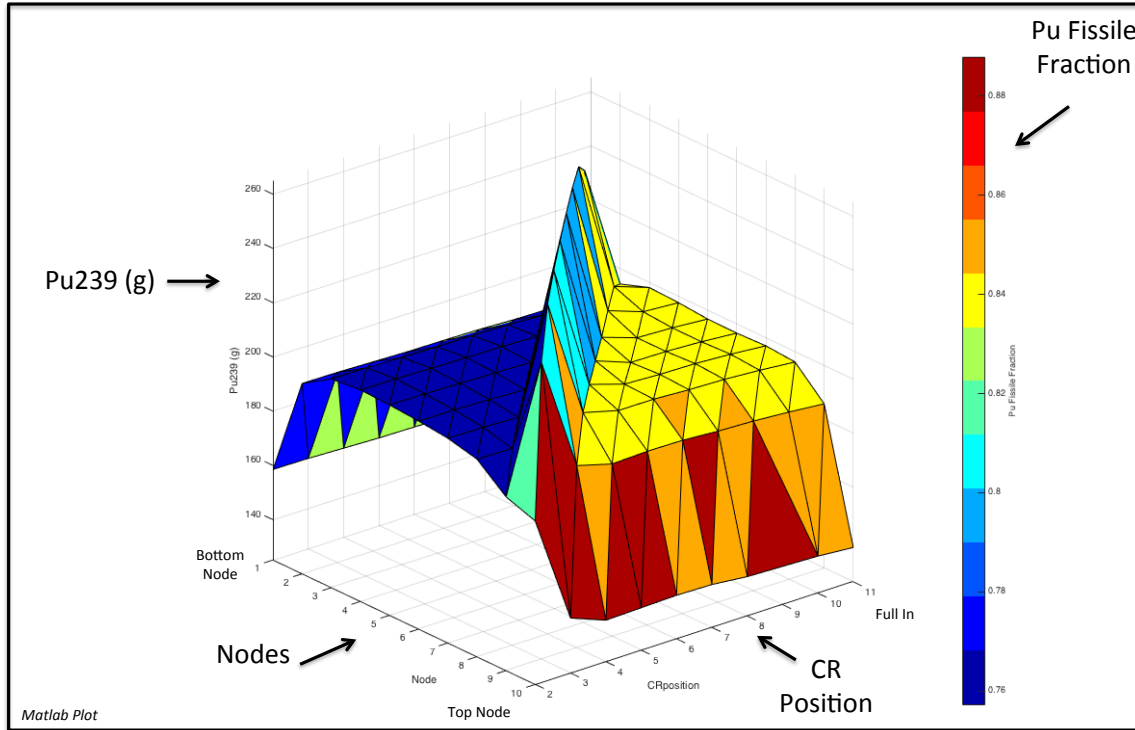


Figure 29: Nodal Impact of Control Rod Insertion on ^{239}Pu mass and Pu Fissile Fraction (MATLAB)

Figure 29 provides a four dimensional plot of the control rod insertion test results. In the XY plane are axial node and control rod position. Only the 10 fuel nodes are modeled. The assembly bottom is node 1 and the top is node 10. Control rod depth is defined by number of nodes in which the rod is inserted. Therefore a fully inserted control rod has a depth of node 11. On the z-axis is the mass of the ^{239}Pu in grams for each node. The color overlay provides the Pu fissile content for each node.

Figure 30 is the same plot as Figure 29 however it is slightly tilted to illustrate key relationship features. A number of observations can be made using this figure about the impact of a control rod on plutonium production. The most distinct feature on this plot is the ridge visible at the CRO-CRI boundary. At the CRO-CRI boundary there is a significant increase in ^{239}Pu production.

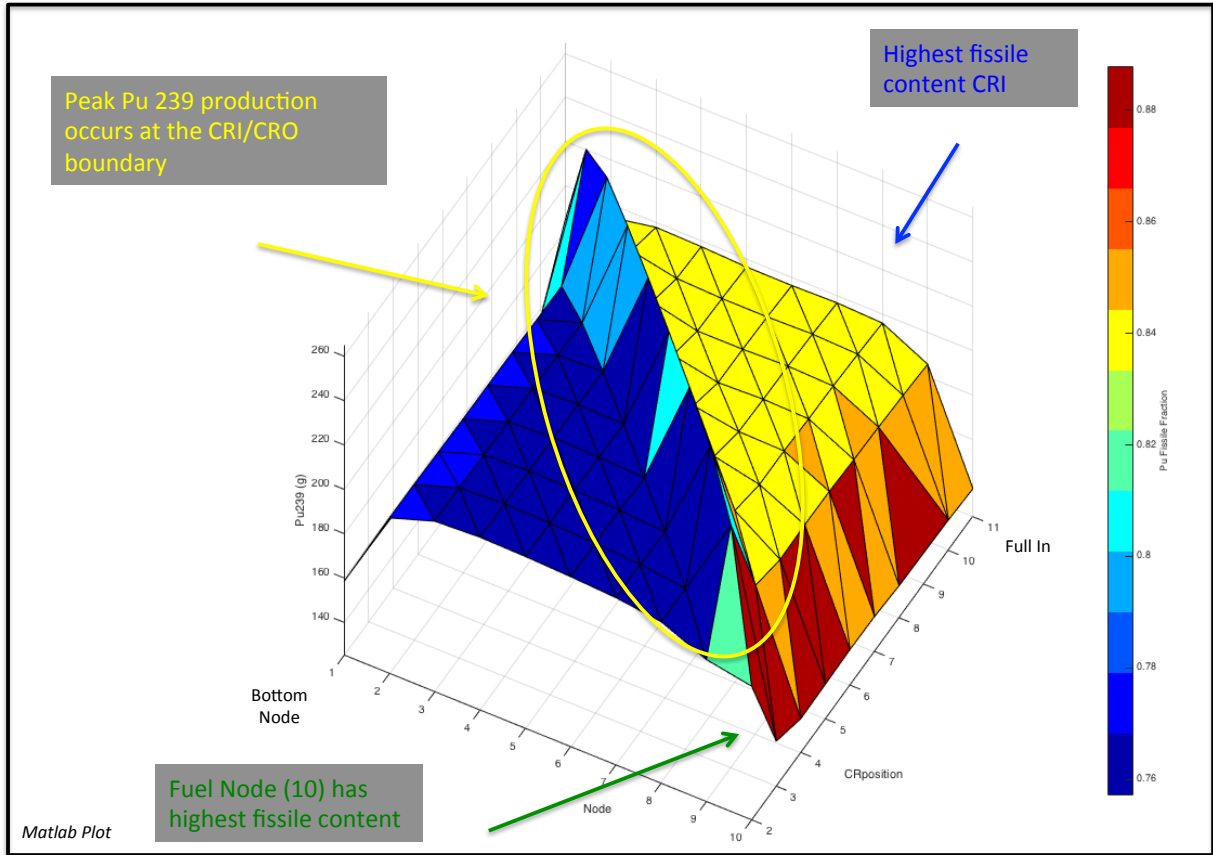


Figure 30: Observations of Nodal Impact of Control Rod Insertion on ^{239}Pu mass and Pu Fissile Fraction (MATLAB)

Figure 30 also demonstrates a clear relationship between control rod presence and Pu fissile content. Nodes with a control rod have a higher Pu fissile content than those without a control rod. Node 10 appears to consistently have the highest Pu fissile content likely because it is modeled with CRI for all simulations. The surface plots clearly show that a ^{239}Pu production peak occurs at the CRO-CRI boundary. The node with the highest ^{239}Pu mass shifts axially as the control rod is withdrawn. Pu fissile content also correlates to the position of the control rod but one can see from Table 8 that at the node of peak ^{239}Pu production, the fissile content is lower than other CRI nodes.

Table 8 lists the axial node distribution of the ^{239}Pu mass and fissile content for assemblies with control rod insertion at two different depths. Table 8 reveals that trade off exists between ^{239}Pu mass and Pu fissile content. A node with a high ^{239}Pu mass may not have the highest Pu fissile content.

Table 8: Pu Mass and Pu Fissile Content Comparison

Pu239 and Control Rod Interface Relationship				
Case	Control Rod: 7 Fuel Nodes		Control Rod: 3 Fuel Nodes	
Nodes	Pu239 (g)	Pu Percent Fissile	Pu239 (g)	Pu Percent Fissile
1 (bottom)	156.63	82.52%	157.98	82.38%
2	193.69	77.25%	194.87	77.12%
3	200.39	76.13%	201.67	75.97%
4	252.49	79.87%	202.71	75.79%
5	202.42	83.86%	202.29	75.86%
6	198.24	84.18%	201.36	76.02%
7	198.96	84.12%	199.94	76.27%
8	198.39	84.17%	246.81	80.39%
9	188.22	84.94%	192.30	84.65%
10 (top)	140.15	88.62%	140.42	88.61%
Key	CRO			
	CRI			

Table 9 shows the total assembly change in ^{239}Pu mass caused by the control rod. The largest gain is 36.7 g. Given that substantial ^{239}Pu gains are found at the CRO-CRI boundary it is likely that those nodes have the largest contribution to total gains. Full insertion of the control rod reduces the neutron spectrum such that ^{239}Pu mass is reduced.

Table 9: Assembly Total ²³⁹Pu Change

Assembly Pu239		
CR Depth	Pu239 (kg)	Pu239 Difference (g)
11 (fully in)	1.8842	-20.9573
10	1.9133	8.1490
9	1.9243	19.1995
8	1.9296	24.4614
7	1.9384	33.3250
6	1.9418	36.7181
5	1.9408	35.6408
4	1.9403	35.2225
3	1.9413	36.1925
2	1.9368	31.6921
1 (out)	1.9051	

4.3.1: CRO-CRI boundary

The boundary of CRO-CRI nodes exhibits unique behavior. This section looks only at the two nodes along the CRO-CRI boundary. Figure 31 highlights the CRO-CRI boundary and is modeled using Paraview.[53] The CRI node has a mass of ^{239}Pu higher than the CRO node on its axial border by an average of 42 grams. The CRI node has a higher Pu fissile content than the CRO node by approximately 3-4%.

Figure 32 is a plots the difference in ^{239}Pu mass and Pu fissile content between the CRO and CRI nodes with respect to depth of control rod insertion. One vertical axis plots the mass increase of ^{239}Pu between CRO to CRI. Plotted on a separate axis is the increase in Pu fissile content between the CRO and CRI nodes. Using the plot in Figure 32 one can see that the increase in ^{239}Pu mass on the CRO-CRI boundary occurs when the control rod is at near full insertion. The lowest change in mass between boundary nodes is in cases of shallow insertion. The increase in Pu fissile content is opposite that of the ^{239}Pu mass. Assemblies with a control rod inserted to near full have the lowest change in Pu fissile content at the CRO-CRI boundary. Shallow insertions, however, result in the largest increase in Pu fissile content. Control rod insertions to central node depths between nodes 8 through 5 appear to have a relatively consistent increase in both ^{239}Pu mass and Pu fissile fraction.

4.3.2: Plutonium Production Pathway

The assembly most likely to be used as a plutonium production pathway will maximize both ^{239}Pu mass and Pu fissile content. Using Figure 32, this project chose to examine the assembly with a control rod depth of node 4 as seen in Table 10. Recall a control rod depth of node 4 means the control rod is inserted into one reflector node (axial top) and three fuel nodes. Table 10 provides a comparison of ^{239}Pu mass, Pu fissile content, burnup, and PRELZ for the control rod model and the non-control rod model. Using a node-to-node comparison, the assembly with a CRI experiences increases in ^{239}Pu mass and Pu fissile content while experiencing decreases in nodal burnup and PRELZ. The CRI assembly also experiences a decrease in total burnup and an increase in total ^{239}Pu mass.

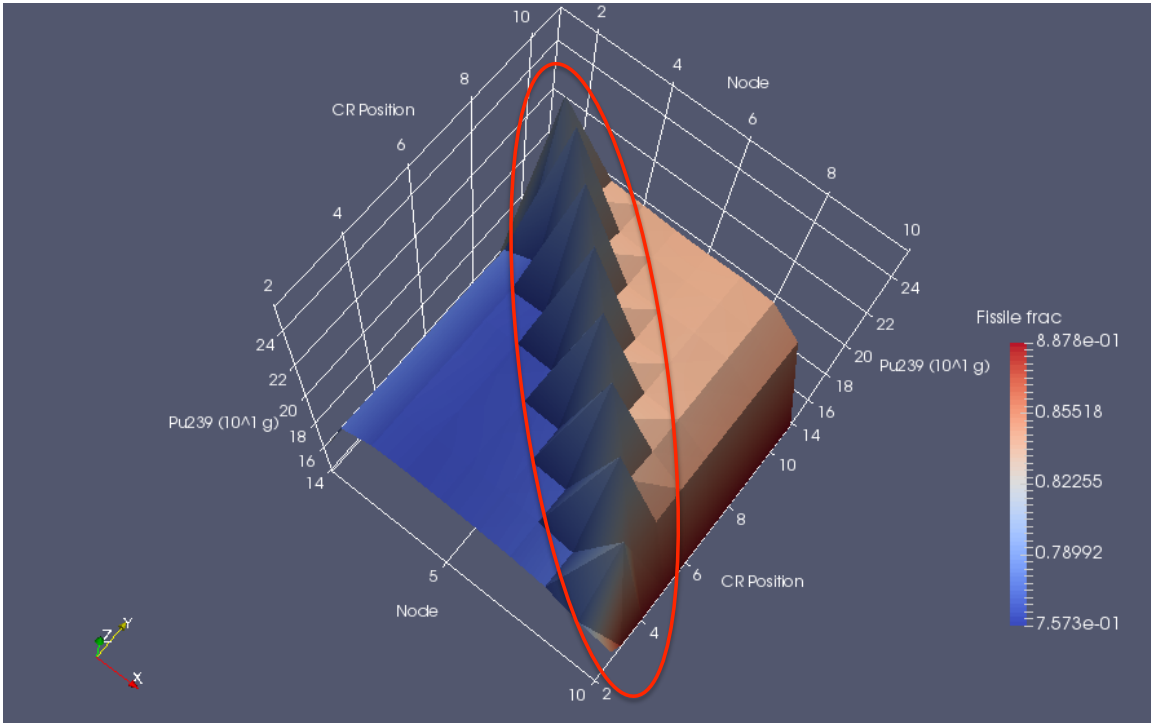


Figure 31: CRO-CRI Boundary

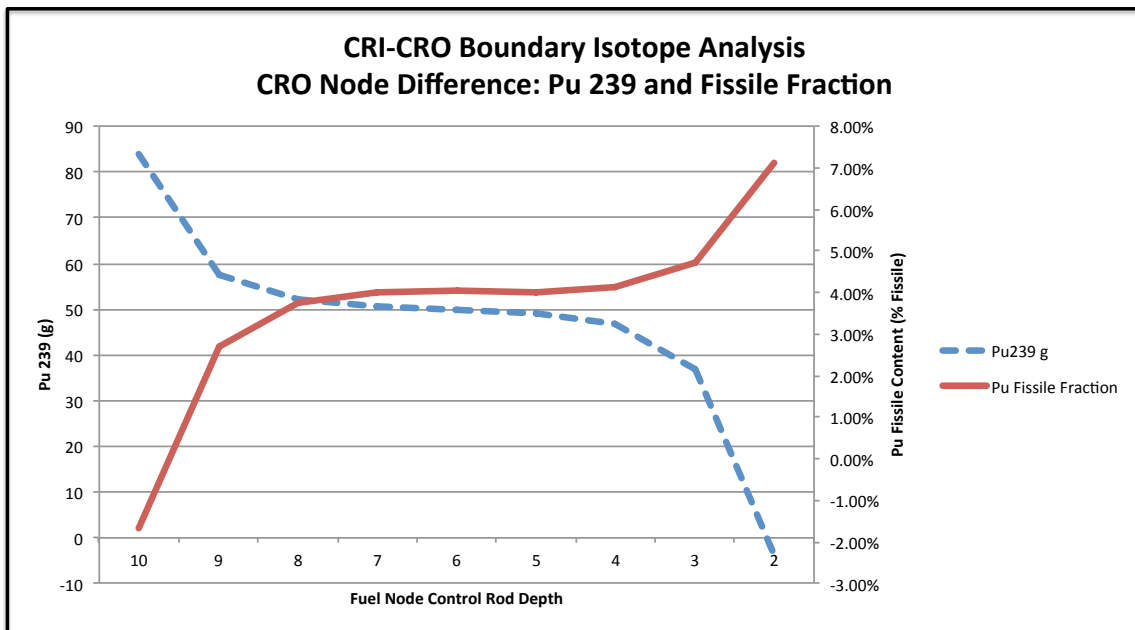


Figure 32: CRI-CRO Boundary Node Isotope Difference

Table 10: Nodal Assembly Analysis Control Rod Depth Node 4

Control Rod: 3 Fuel Nodes					No Control Rod				
Nodes	Pu239 (g)	Pu Percent Fissile	Burnup	PRELZ	Nodes	Pu239 (g)	Pu Percent Fissile	Burnup	PRELZ
1 (bottom)	157.98	82.38%	668.81	0.5668	1 (bottom)	158.87	82.28%	675.89	0.5663
2	194.87	77.12%	1086.88	0.9211	2	195.63	77.01%	1097.77	0.9198
3	201.67	75.97%	1198.62	1.0158	3	202.37	75.86%	1209.98	1.0138
4	202.71	75.79%	1217.15	1.0315	4	203.39	75.69%	1228.35	1.0292
5	202.29	75.86%	1209.59	1.0251	5	202.97	75.76%	1220.73	1.0228
6	201.36	76.02%	1193.19	1.0112	6	202.11	75.91%	1205.34	1.0099
7	199.94	76.27%	1168.65	0.9904	7	200.88	76.12%	1183.91	0.9920
8	246.81	80.39%	1078.5	0.9140	8	198.30	76.57%	1140.31	0.9554
9	192.30	84.65%	652.17	0.5527	9	189.47	78.00%	1007.44	0.8441
10 (top)	140.42	88.61%	386.44	0.3275	10 (top)	151.13	83.25%	612.78	0.5134
Pu239 total (kg)	1.9403	Burnup total	9860.00		Pu239 total (kg)	1.9051	Burnup total	10582.5	
Key	CRO								
	CRI								

Figure 33 shows the ^{239}Pu content of the target assembly with a control rod inserted to a depth of node 4. The control rod is visibly represented as an axially aligned black cylinder at a depth of three nodes. Recall that the isotope modeling only shows fuel nodes so an insertion depth of node four would show only three fuel nodes and the axial reflector node would not be pictured. Figure 33 shows that the ^{239}Pu mass increases by approximately 35 g at the CRO-CRI boundary to a level of 246.8 g.

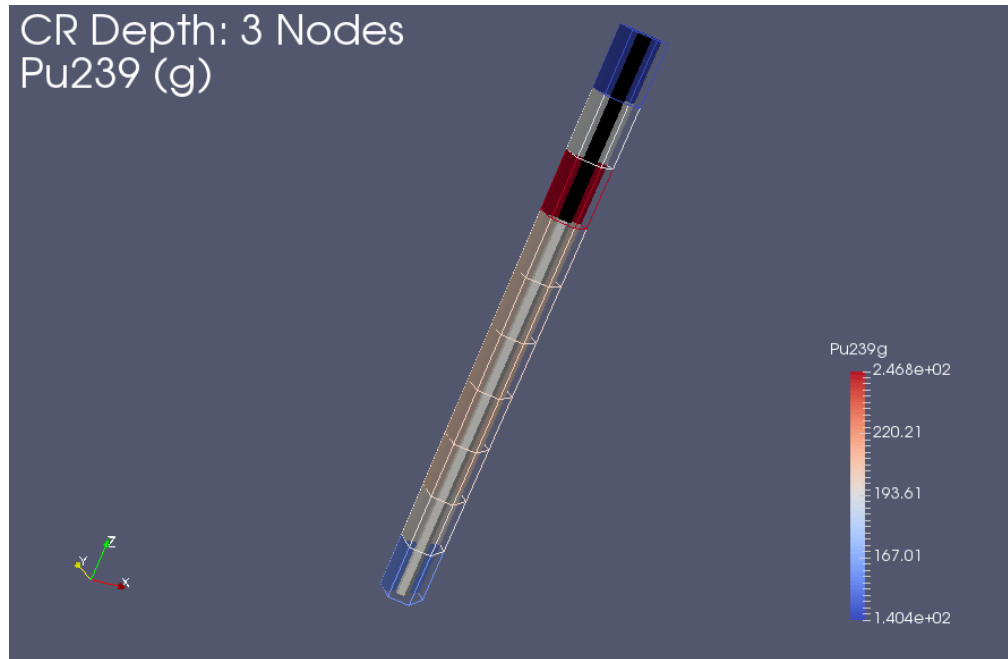


Figure 33: ^{239}Pu (g) Control Rod Depth Node 4

Figure 34 shows the ^{239}Pu content of the target assembly without a control rod and has a maximum nodal ^{239}Pu mass of approximately 203.4 g. ^{239}Pu production in the assembly without a control rod is lower and more uniformly distributed axially in the assembly. Only the nodes on the ends of the assemblies appear to have a significant difference in ^{239}Pu mass.

Figure 35 shows the fissile content of the target assembly with a control rod inserted to a depth of node 4. When comparing to Figure 36, which shows the same assembly with no control rod, one can see that the CRI nodes have a higher Pu fissile content. The top node has the highest fissile fraction at 88.6% making it fuel grade and revealing an increase of 5.36% from the non-control rod assembly.



Figure 34: ^{239}Pu (g) No Control Rod

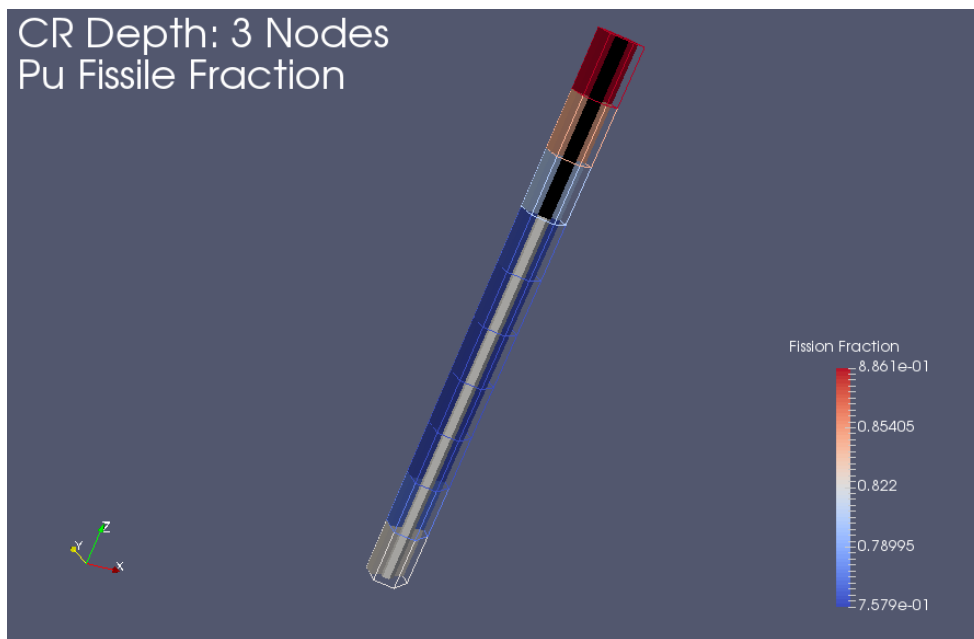


Figure 35: Pu Fissile Content Control Rod Depth Node 4

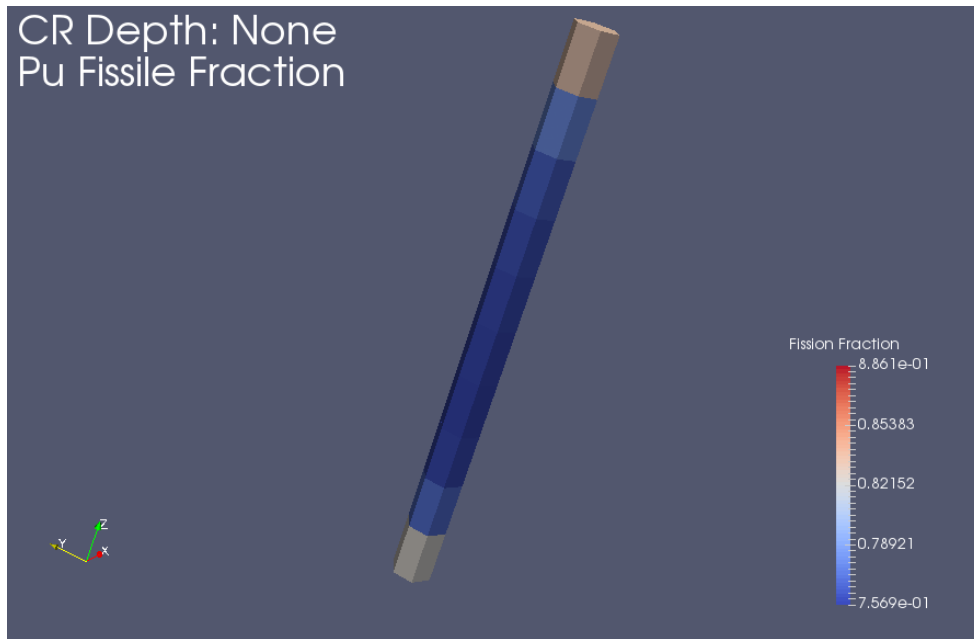


Figure 36: Pu Fissile Content No Control Rod

Figure 37 and Figure 38 illustrate the impact of the control rod on assembly burnup. One can see in Figure 37 that the presence of the control rod at the top of the assembly greatly reduced the burnup in those nodes whereas the assembly in Figure 38 has a more uniform axial burnup distribution. The axial disparity in assembly burnup could possibly be an identifying signature for control rod movement and undeclared activity could be a sign of misuse. This signature will be discussed in future chapters.

4.4 Conclusion

The ability to model axially heterogenous assemblies using NESTLE to ORIGAMI coupling offers new insights into how control rods impact LWR assembly isotopes. While it has been understood that a control rod will reduce the assembly burnup and relative power, this research provided more fidelity as to where within the assembly those reductions take place. Nodes in proximity to the control rod experience a decrease in burnup that flattens the shape of the burnup profile when compared to the non-control rod nodes.

The boundary of nodes with and without a control rod (CRO-CRI boundary) is the region the highest ^{239}Pu production. In each case, the CRI node on the boundary produced an increase in ^{239}Pu mass as compared to its neighboring nodes. Despite this increase, the assembly total ^{239}Pu mass did not increase substantially with the highest gain being only 36 grams. When compared to the total ^{239}Pu produced in the assembly, approximately 1.9 kg, the increase is small and was made almost entirely at the CRO-CRI boundary.

Axial nodes with a control rod have a higher Pu fissile fraction than those without a control rod. Nodal increases in Pu fissile fraction were between 3-5%. The node with the highest Pu fissile fraction produced was fuel grade at 88.7%. Despite the correlation between increase in fissile fraction and control rod presence, the majority of nodes in the assembly models were reactor grade, remaining well below the peak fissile fraction of 88.7%. While some individual nodes did achieve fuel grade fissile fractions, this method of producing plutonium does not effectively utilize the majority of the assembly and is thus inefficient.

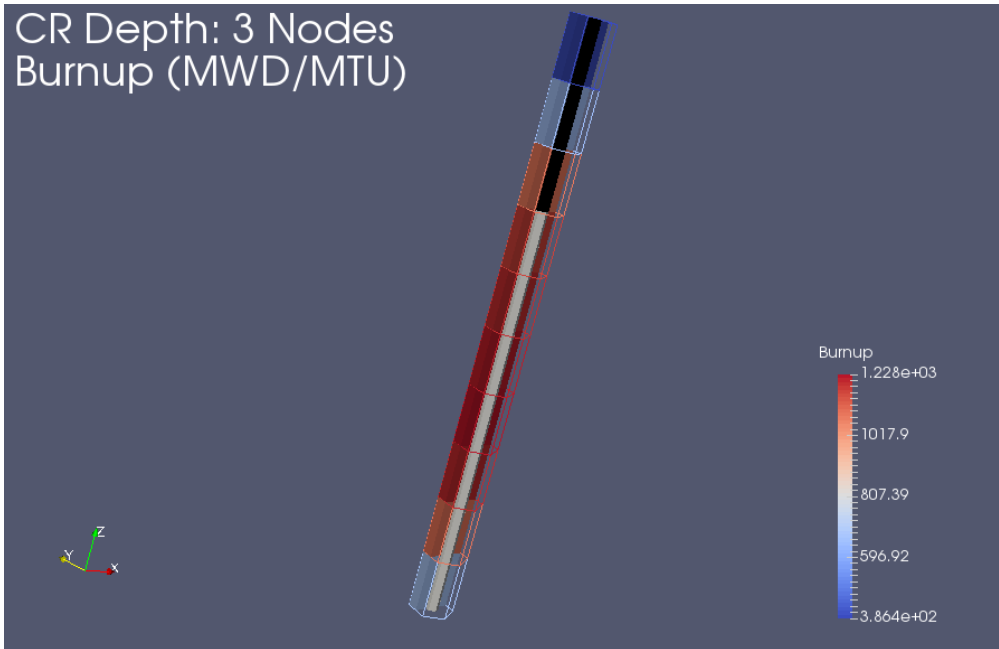


Figure 37: Burnup Control Rod Depth Node 4

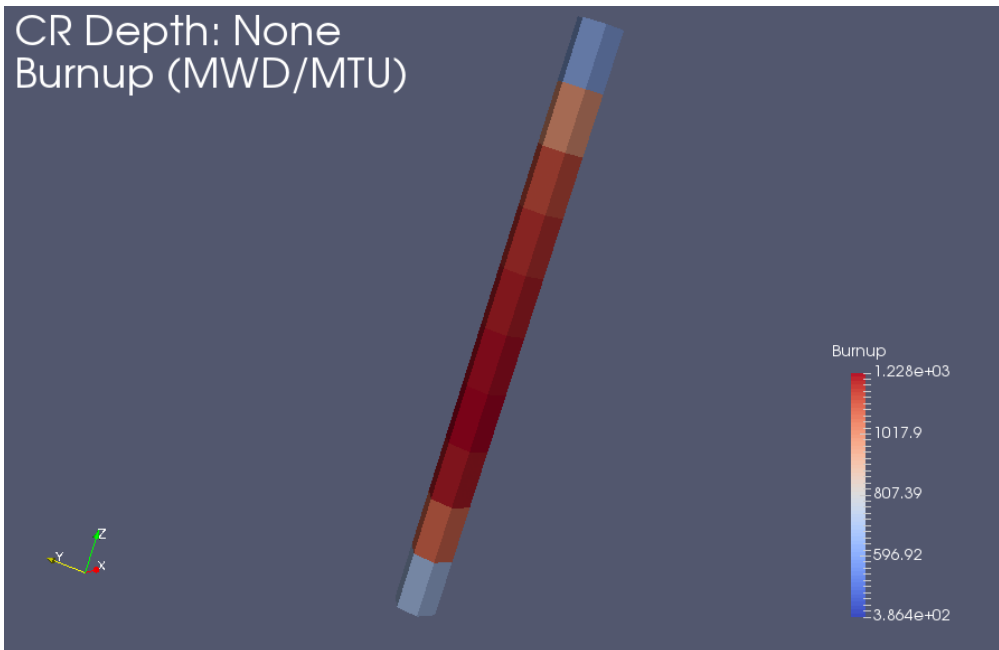


Figure 38: Burnup No Control Rod

The presence of a control rod can increase the amount of ^{239}Pu in an assembly and increase the Pu fissile fraction. The total mass increase in ^{239}Pu is only a few tens of grams and typically occurs centrally within the assembly at the CRO-CRI boundary. Accessing this point without disturbing the rest of the assembly would likely be quite challenging. Additionally, the Pu fissile fraction remains below weapons grade making the material less desirable for weapon use. Pu fissile fraction is highest in the top nodes but these nodes are also lowest in ^{239}Pu mass.

NESTLE to ORIGAMI coupling allowed for the rapid analysis for 10 permutations of the control rod insertion scenario. An axial isotope map was created using a common modeling framework. The axial isotope map was a useful tool when assessing the feasibility of the plutonium production pathway and then narrowing the analysis to a specific assembly of interest. When used in this manner, NESTLE to ORIGAMI coupling aids the nonproliferation professional faced with an abnormal reactor condition by identifying the problem sets of greatest concern. Nonproliferation professionals can then allocate limited resources in a more targeted effort by identifying the assemblies with fissile contents of concern for priority measurement in the spent fuel pond.

Chapter 5: Plutonium Production Scenario: SS316 “Dummy” Material

5.1 Introduction

This chapter is the second of two demonstrations of the nonproliferation application of NESTLE to ORIGAMI coupling. The scenario for this chapter models an operator’s attempts to produce weapons-grade plutonium in a LWR by modifying the assembly with dummy material. The operator fills the control rod guide tubes with SS316 rather than moderator so as to reduce moderation locally inside the assembly. Reducing the moderation inside the assembly cause less neutrons to slow to thermal energies inside the assembly fuel and thus result in less ^{239}Pu fission. The flux local to the assembly will experience a hardening of the flux distribution, as the ratio of fast to thermal flux should increase.

^{239}Pu has a fission cross-section of 1.74 bn at fast energies so increased losses from fast fission are possible.[14] Losses from fast fissions however are likely to be offset by the reduction in thermal neutron losses. The thermal neutron capture and fission cross-sections for ^{239}Pu are 271 bn and 748 bn respectively, effectively offsetting any increases in ^{239}Pu fast fissions.[14]

5.2 2-D Flux Spectrum Analysis

5.2.1: Fast Flux Spectrum Shift

Figure 39 is a 2D plot of the fast flux spectrum for a normal FA 13AU assembly. In this plot, the control rod and instrument guide tubes are filled with moderator (blue). The fast flux is lowest in the guide tubes where the moderator is most present. Fuel near the guide tubes also has the lowest fast flux. Moving radially out from the center of the assembly, the fast flux steadily increases and is at its peak in the assembly corners.

Figure 40 shows an assembly now modified by the operator with SS316 filled control rod guides tubes.

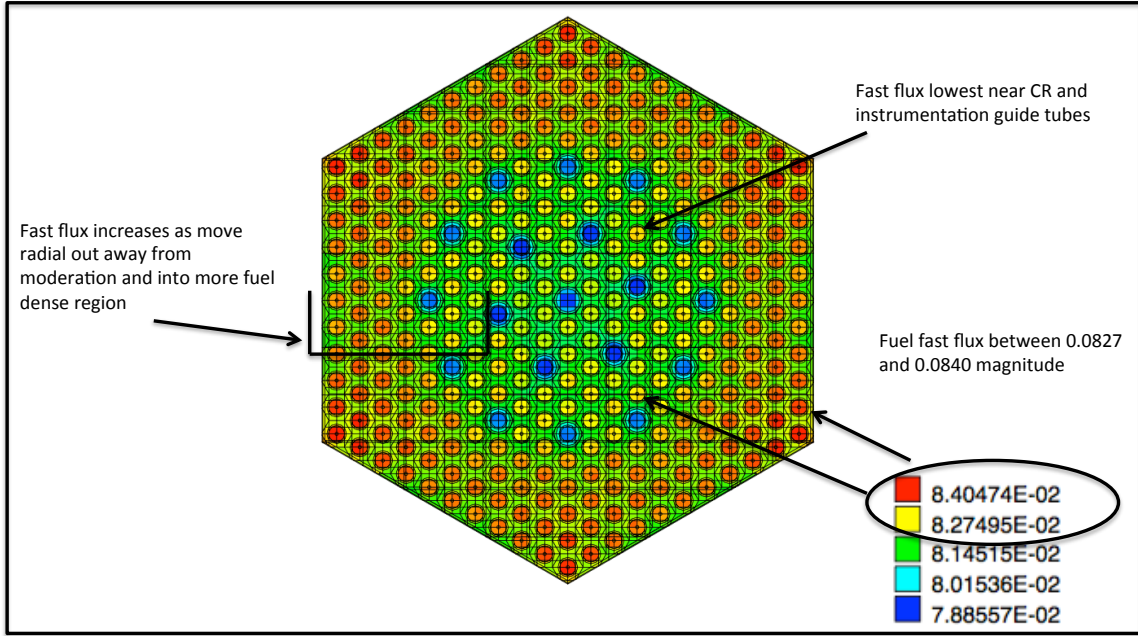


Figure 39: FA13AU Fast Flux Normal Assembly T-NEWT

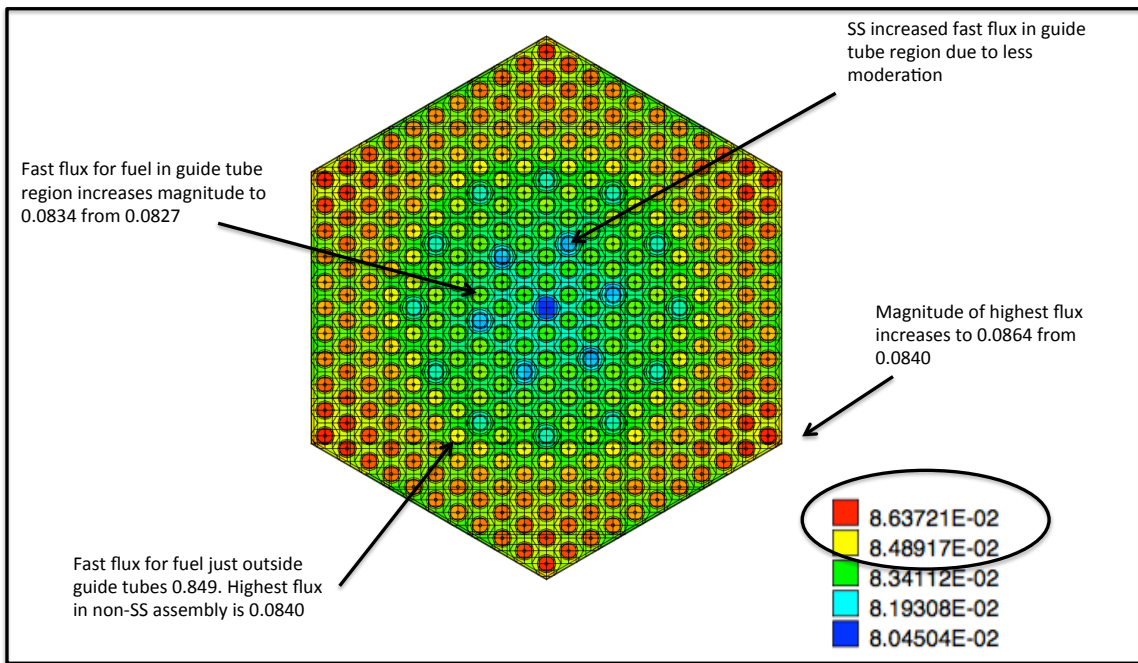


Figure 40: FA13AU Fast Flux SS316 Assembly T-NEWT

Note that each plot is independently generated and as such, the scale on the plot is unique to the plot. Adding SS316 to the guide tubes increased the fast flux by 2.96%. Moving radially away from the guide tube region, the fast flux increases between 2.59% and 2.77%.

The most noticeable shift of the fast flux occurs in fuel located in close proximity to the SS316. Moving radially out from the center of the assembly, the fast flux increase to a magnitude higher than the peak unmodified fast flux in fuel just outside the control rod guide tube region.

5.2.2: Thermal Flux Spectrum Shift

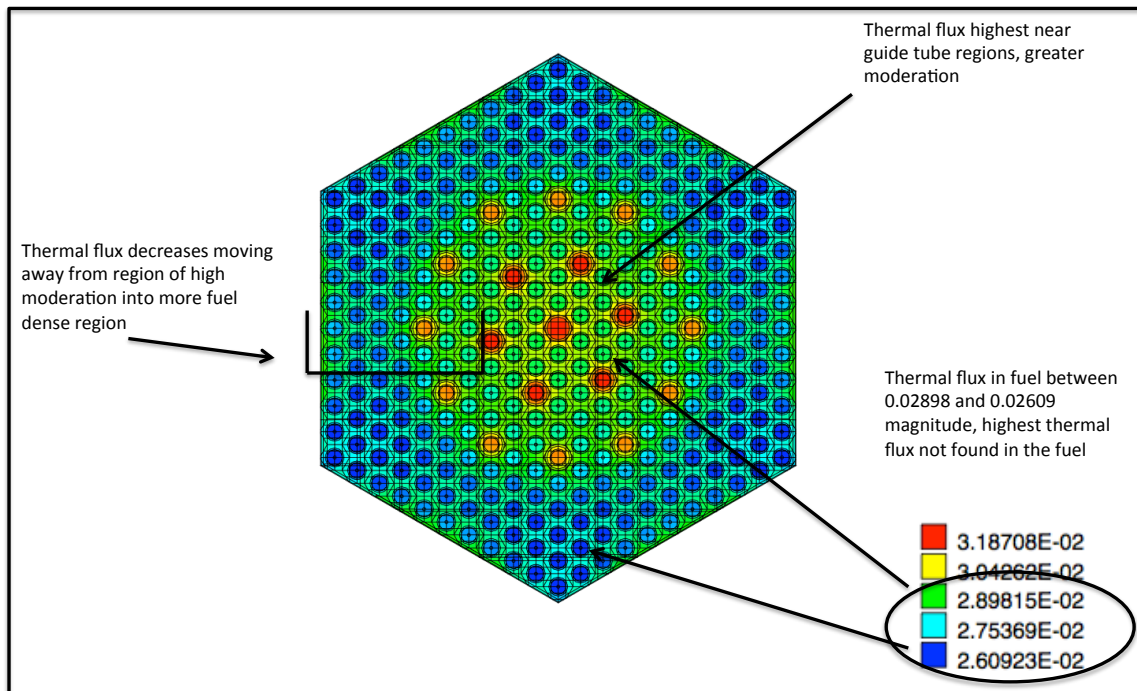


Figure 41: FA13AU Thermal Flux Normal Assembly T-NEWT

Figure 41 shows the thermal flux for the unmodified FA13AU assembly. The moderator filled control rod and instrumentation tubes are clearly visible, in red, as they have the highest thermal flux. Fuel near the tubes also has the highest thermal flux. Thermal flux then decreases moving radially out from the center of the assembly with the lowest thermal flux being in the fuel cornered by the stiffening angles.

Figure 42 shows the thermal flux from a SS316 modified FA13AU. The thermal flux is significantly reduced in the fuel near the SS316 guide tubes. This is especially apparent as the instrumentation tube, which remains filled with moderator, has a high thermal flux. The fuel pellets surrounding the instrumentation tube have a higher flux their neighboring fuel pellets, which are in close proximity to the SS316 modification.

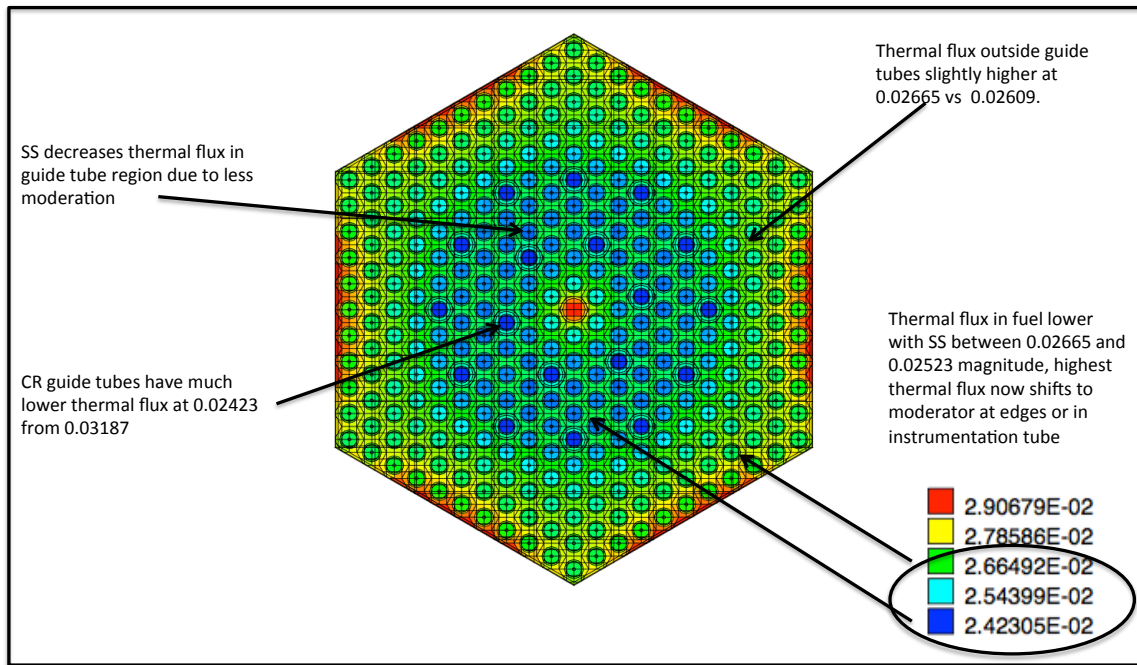


Figure 42: FA13AU Thermal Flux SS316 Assembly T-NEWT

Thermal flux in the control rod guide tubes was reduced by 24.0% with the addition of SS316. Fuel adjacent to these tubes experienced a reduction in flux of 12.8%. Surprisingly there was a 2.1% increase in thermal flux in the fuel just outside the control rod guide tubes.

5.3 SS316 Modification Results

5.3.1: NESTLE VVER-1000 SS Model Results

The NESTLE VVER-1000 SS model includes an assembly modified with SS316 at assembly location #139. The VVER-1000 SS model was run using the same variables as the VVER-1000 Test model.

Figure 43 provides a side-by-side comparison of the flux spectrum hardness for the normal FA13AU assembly and the SS316 modified assembly. The addition of SS316 hardened the flux spectrum in the assembly by reducing the thermal flux and slightly increasing the fast flux. Based on the SCALE T-NEWT models the reduction in thermal flux most likely occurred in fuel pellets located in close proximity to the SS316 filled control rod guide tubes.

Figure 44 is a map of the percent increase in flux spectrum hardness by axial node. The nodes experiencing the highest increase in flux spectrum hardness were those centrally located in the assembly. These nodes experienced approximately an 8-9% increase in flux spectrum hardness or the ratio between the fast and thermal flux. Axial nodes experienced the smallest increase. Figure 45 shows a side-by-side comparison of the burnup weighted axial relative power distribution of the unmodified and SS316 assembly. The SS316 assembly produced less power in the central nodes. Figure 44 shows these same nodes also experienced a hardening of their flux spectrum, due mostly likely to reduced thermal flux. Thus it is likely that that the reduction in power from the central nodes is due to reduced thermal fissions.

Table 11 shows how the impact of SS316 on the assembly burnup as modeled in both NESTLE and ORIGAMI. Lower assembly power reduced the assembly burnup by approximately 900 MWD/MTU. Exploring the radial change in isotope production through NESTLE to ORIGAMI coupling would require both axial and assembly pin-power outputs from NESTLE. Unfortunately at the time of this research, pin-power reconstruction was a developmental feature of NESTLE. Incorporating pin-power coupling to ORIGAMI is an area of further research. This assessment is limited to axial isotope distribution modeling using burnup weighted axial power shaping factor (PRELZ). Figure 46 side-by-side comparison shows that SS316 modified assembly has a slightly higher mass of ^{235}U . This is due to a reduction in ^{235}U fissions from suppressed assembly thermal flux. Figure 47 shows a slightly higher mass of ^{238}U in the SS316 assembly. ^{238}U transmutes via thermal neutron capture. The reduction in thermal flux internally to the assembly likely also reduced the amount of ^{238}U transmutation.

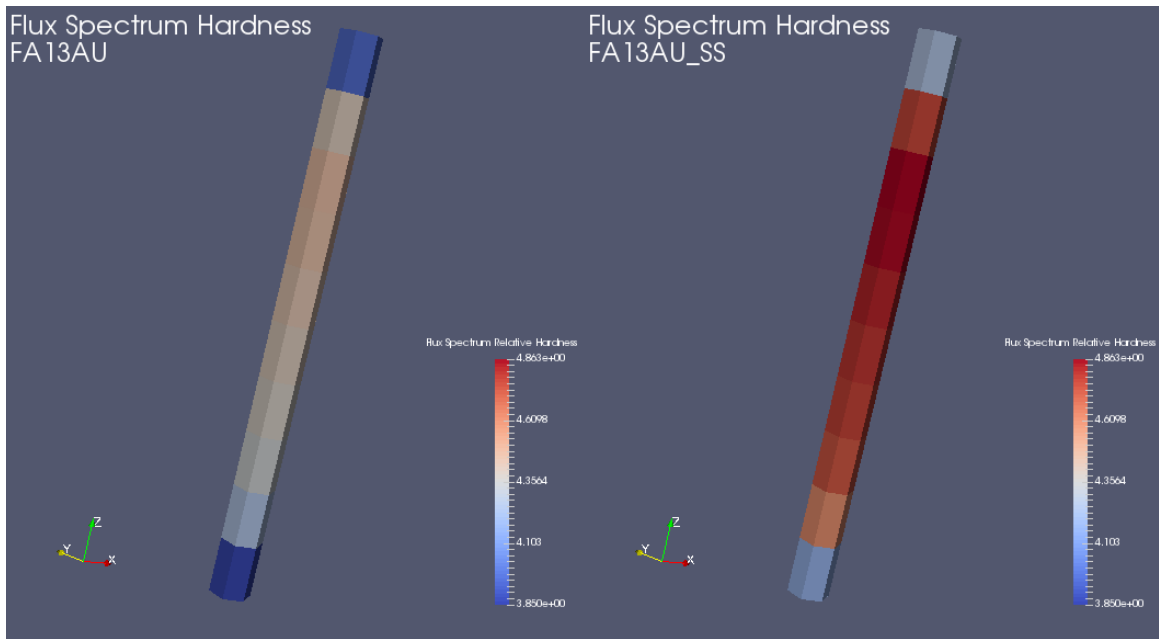


Figure 43: Flux Spectrum Hardness (G1/G2) Comparison between Reference Assembly (left) and an Assembly Modified with SS316 in the Control Rod Guide Channels (right)

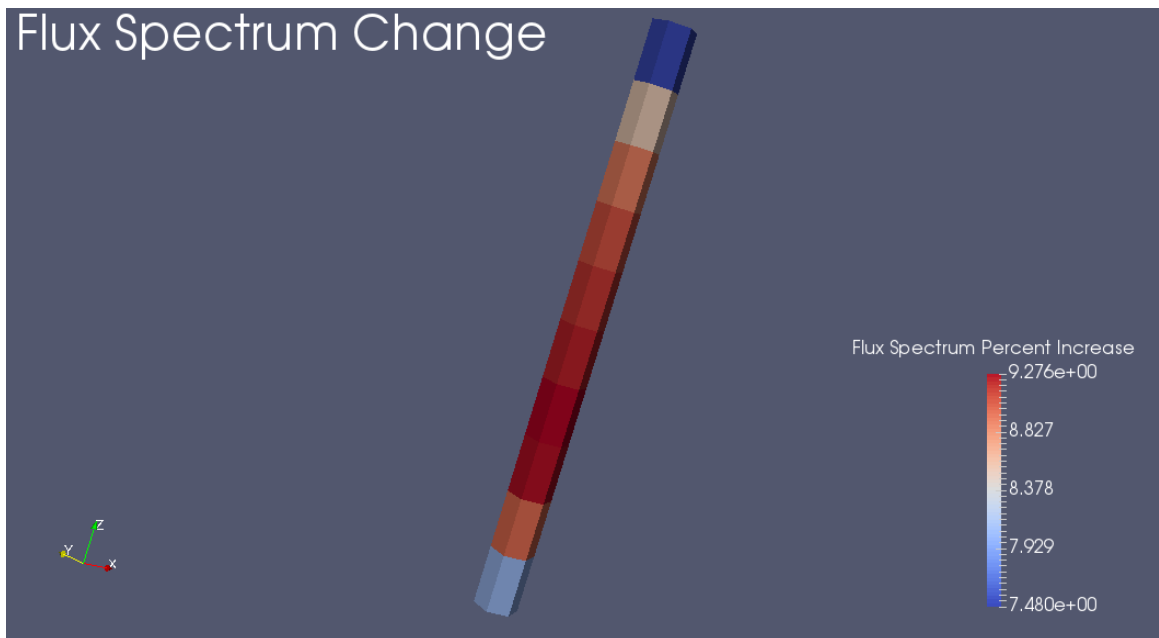


Figure 44: Axial Model of Change in Flux Spectrum Hardness (G1/G2) to the Assembly with the Insertion of SS316 into the Control Rod Guide Tubes

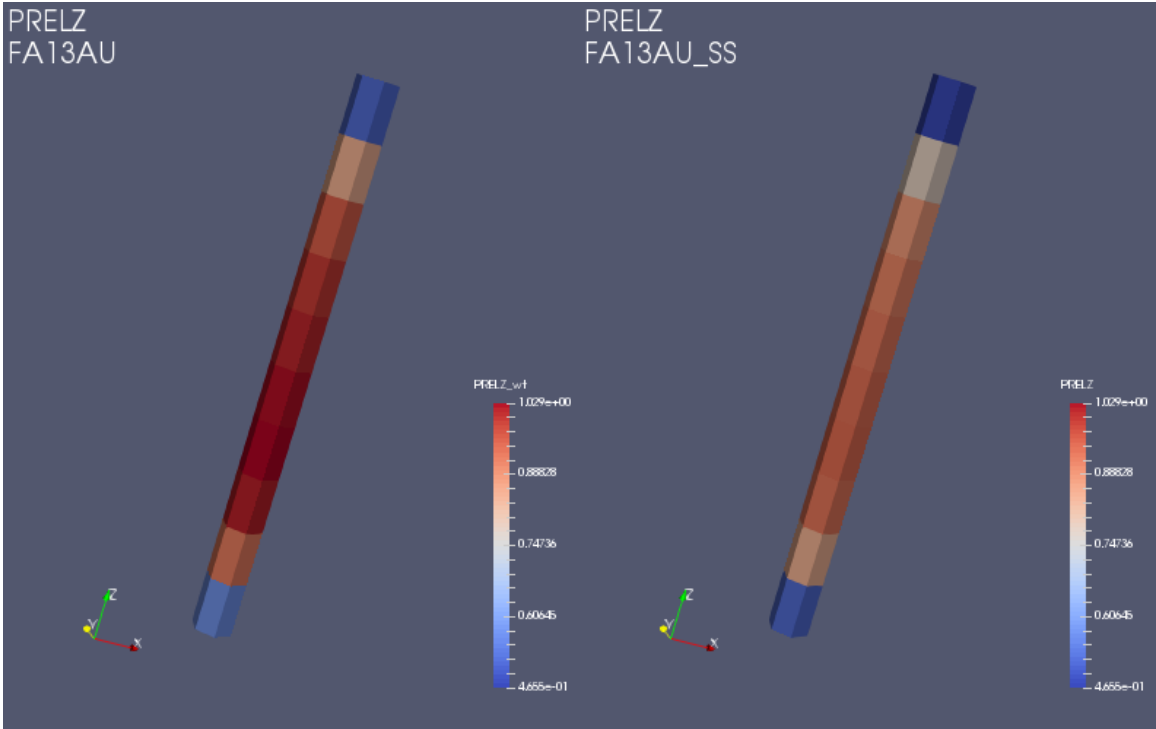


Figure 45: Axial Power Shape Factor Comparison between Reference Assembly (left) and the Assembly with SS316 Insertion into the Control Rod Guide Tubes (right)

Table 11: Flux Spectrum Hardening and Assembly Burnup

Flux Spectrum Hardening and Burnup		
Pin	Burnup FA13AU Normal (MWD/MTU)	Burnup FA13AU SS (MWD/MTU)
Pin 1	675.89	609.62
Pin 2	1097.77	999.86
Pin 3	1209.98	1104.25
Pin 4	1228.35	1120.46
Pin 5	1220.73	1113.61
Pin 6	1205.34	1100.62
Pin 7	1183.91	1082.57
Pin 8	1140.31	1043.49
Pin 9	1007.44	919.35
Pin 10	612.78	553.67
Origami Assembly BU	10582.5	9647.5
Nestle Assembly AVG BU	10560.22	9652.89
Change in Burnup	Nestle	Origami
	907.33	935

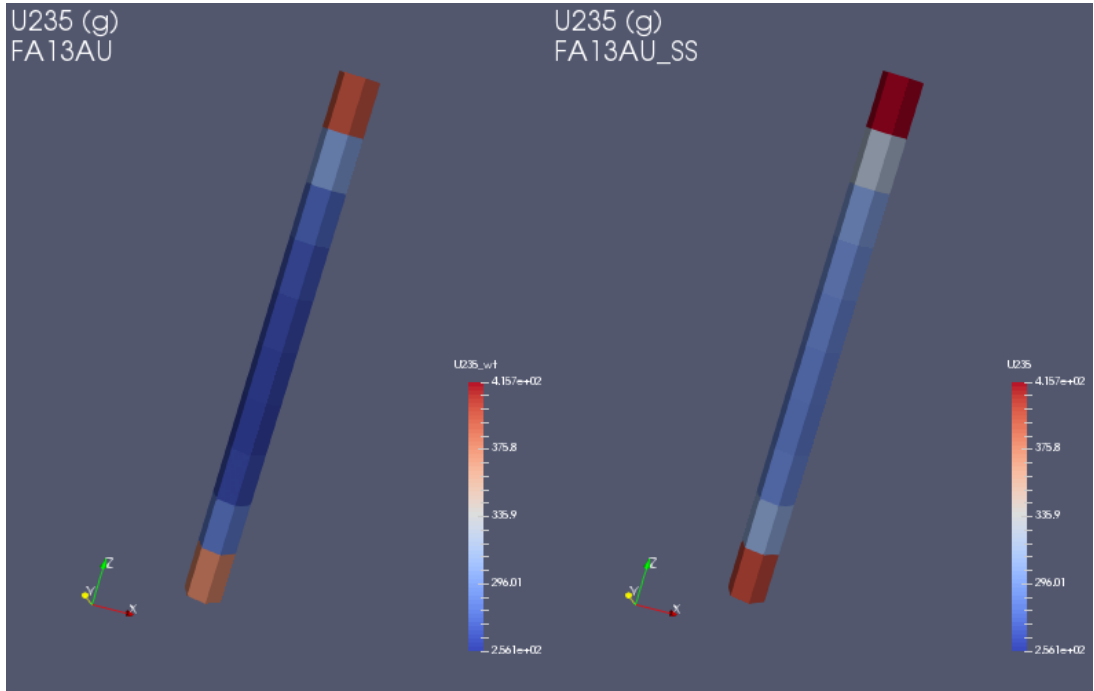


Figure 46: ^{235}U Comparison between Reference Assembly (left) and the Assembly with SS316 Insertion into the Control Rod Guide Tubes (right)

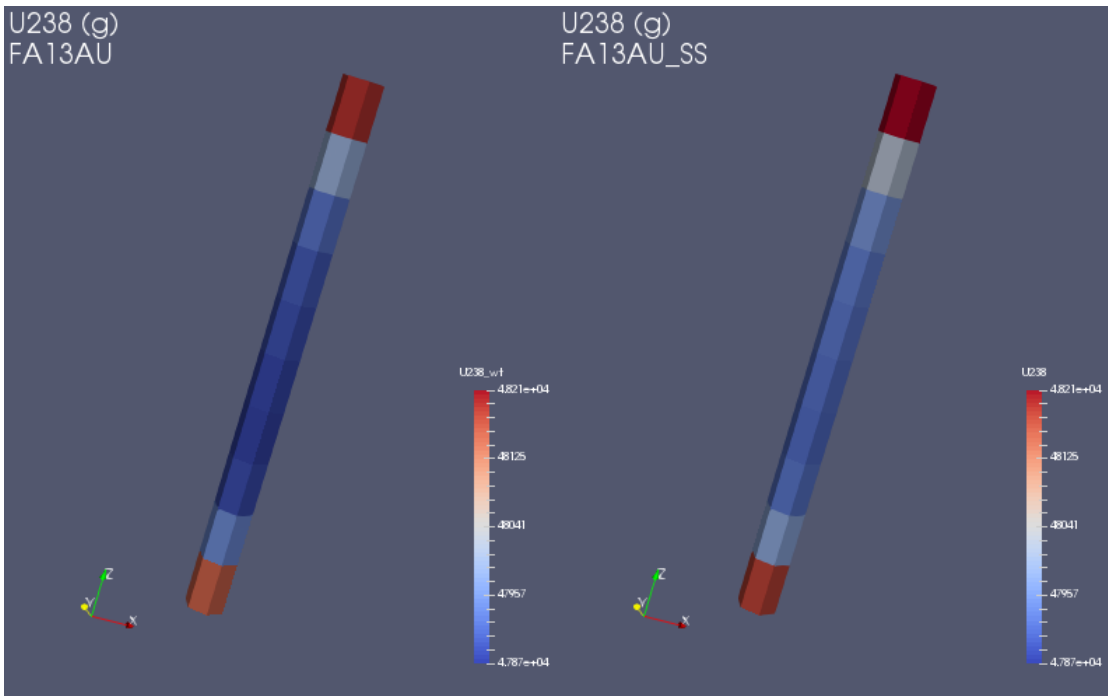


Figure 47: ^{238}U Comparison between Reference Assembly (left) and the Assembly with SS316 Insertion into the Control Rod Guide Tubes (right)

5.3.2: Plutonium Production Pathway

Figure 48 shows that in the relative reduction in thermal flux caused by reduced moderation had a slight impact on the ^{239}Pu distribution. The axially central nodes, where the thermal flux change was most noticeable (Figure 44) had 3-4 more grams of ^{239}Pu than those same nodes in the unmodified assembly. The axial nodes of the SS316 assembly however, had 1-2 grams less ^{239}Pu than the unmodified assembly.

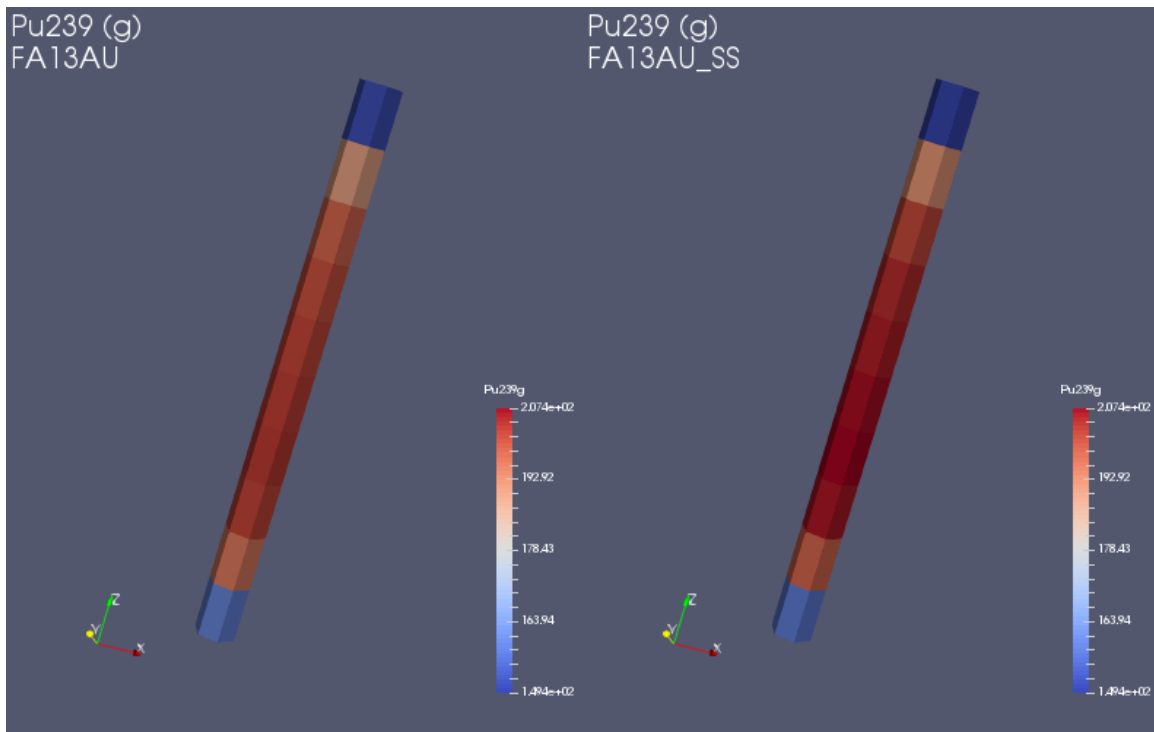


Figure 48: ^{239}Pu Comparison between Reference Assembly (left) and the Assembly with SS316 Insertion into the Control Rod Guide Tubes (right)

Figure 49 and Figure 50 show the impact of the SS316 modification on the Pu fissile fraction. Figure 49, a side-by-side comparison of Pu fissile content, shows that even with the flux spectrum shift, the nodes central to the assembly remain reactor grade, having a fissile content of approximately 77%. The axial nodes are fuel grade at around 83-84% fissile plutonium (Table 3). Figure 50 shows the change in Pu fissile content with the SS316 modification. The central nodes experience an increase in the Pu fissile content of only 1-2%. Axial nodes experienced minimal change in Pu fissile content.

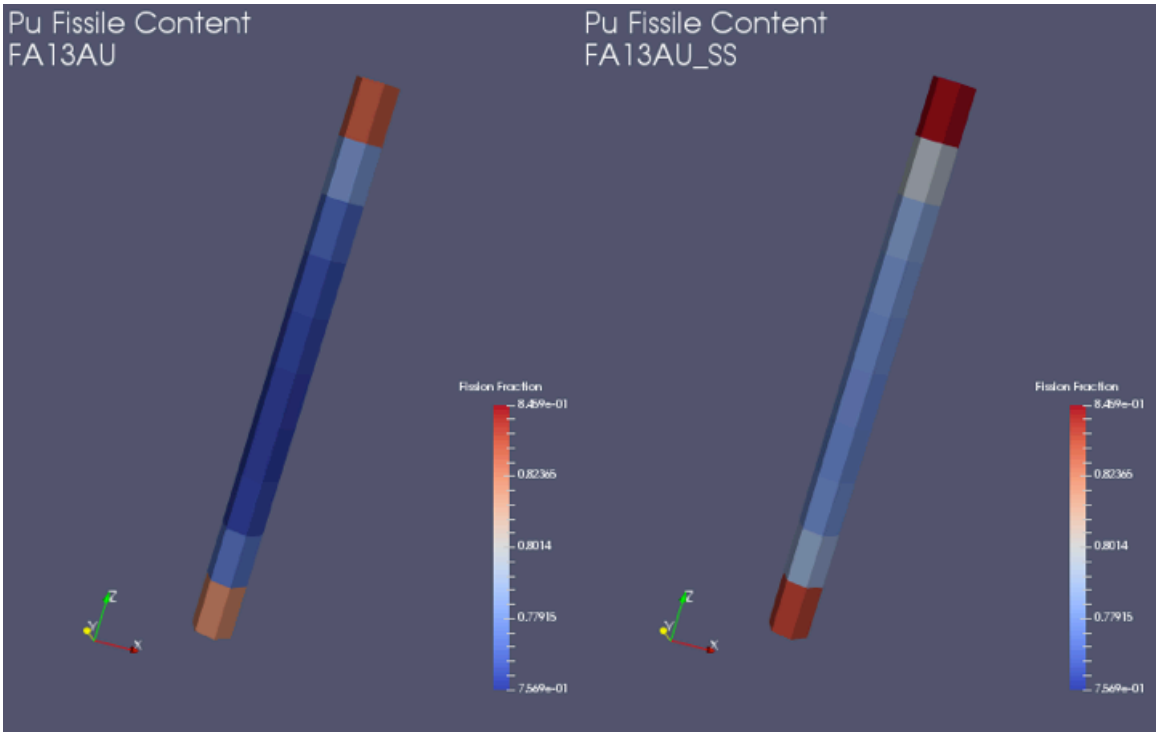


Figure 49: Pu Fissile Fraction Comparison between Reference Assembly (left) and the Assembly with SS316 Insertion into the Control Rod Guide Tubes (right)

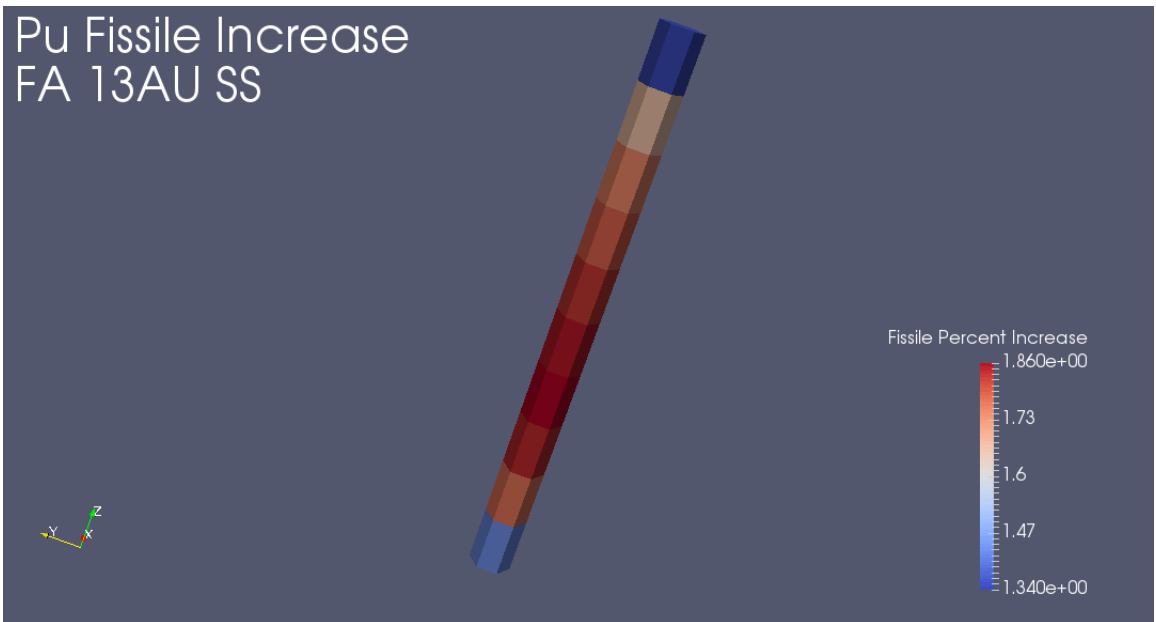


Figure 50: Relative Increase in Fissile Pu Fissile Fraction Resulting from SS316 Modification

5.4 Conclusion

Inserting a dummy material, SS316, in to the fuel assembly control rod guide channels of a VVER-1000 succeeded in locally hardening the flux spectrum of the assembly. The modified assembly had more ^{235}U and ^{238}U mass than the unmodified assembly meaning that a thermal flux reduction was the source of the hardened spectrum. T-NEWT modeling indicated that fuel pellets in close proximity to the SS316 would experience the most significant reduction in thermal flux.

The reduction in thermal flux resulted in a slight increase of both ^{239}Pu mass and Pu fissile content. The most noticeable change in Pu isotope distribution was found in mid-core nodes however the magnitude of the increase in ^{239}Pu and Pu fissile content was minimal. An increase of only 3-4 grams ^{239}Pu and 1-2% Pu fissile content was observed in mid-core nodes. Axial nodes, which this project has observed as having the highest Pu fissile content in most cases, actually experienced a reduction in ^{239}Pu mass. [55]

The plutonium production gains made using SS316 as a dummy material were minimal. The plutonium remained primarily reactor grade with only the end nodes having fuel grade material (Table 3). No weapons grade plutonium was produced using this pathway. This pathway has limited value as a plutonium production pathway due to minimal gains in mass that have an isotope content that experiences only a few percent increase in fissile content keeping the material outside the range of weapons usable.

Further analysis is needed to determine if at the pin-by-pin level, changes in isotope distribution would be more acute. T-NEWT modeling revealed localized thermal flux reduction in close proximity to the dummy material. Further research using the pin-power developmental feature in NESTLE could provide insights as to if individual fuel pellets had greater gains in ^{239}Pu mass or Pu fissile content. It may also be possible to use a dummy material that includes a strong neutron absorber. The combination of reduced moderation and neutron absorption may further reduce thermal flux so as to cause increases in ^{239}Pu mass and fissile content.

Chapter 6: Scenario Feasibility Assessment

6.1 Introduction

This chapter completes the feasibility assessment of the two plutonium production scenarios detailed in earlier chapters using two criteria; detection and production rate. The detectability of the scenario is assessed by making a comparison of SNF isotopic signatures from the target assembly in the VVER-1000 Test model and in the production pathway models. The chapter then examines the time needed to generate enough material to have a significant quantity. Finally, the chapter looks at any other factors that could impact the feasibility of the pathways such as reactor configurations or accessibility.

From Chapter 4, the model with a control rod inserted to a depth of four nodes (three fuel nodes), was selected for analysis. This assembly will be referred to as CR_3 throughout this chapter. From Chapter 5, only a single assembly was modeled with the SS316 and it impacted all axial nodes.

Table 12: Assembly Selection

Plutonium Pathway Feasibility									
Case	VVER1000			Control Rod: 3 Nodes			VVER 1000 SS		
Nodes	Pu239 (g)	Pu Mass Total (g)	Pu Percent Fissile	Pu239 (g)	Pu Mass Total (g)	Pu Percent Fissile	Pu239 (g)	Pu Mass Total (g)	Pu Percent Fissile
1 (bottom)	158.87	208.77	82.28%	157.98	207.14	82.38%	157.44	201.69	83.70%
2	195.63	290.11	77.01%	194.87	288.23	77.12%	198.47	284.57	78.77%
3	202.37	308.51	75.86%	201.67	306.67	75.97%	206.29	303.57	77.70%
4	203.39	311.41	75.69%	202.71	309.62	75.79%	207.42	306.43	77.54%
5	202.97	310.21	75.76%	202.29	308.42	75.86%	206.95	305.22	77.61%
6	202.11	307.77	75.91%	201.36	305.80	76.02%	206.04	302.93	77.74%
7	200.88	304.33	76.12%	199.94	301.84	76.27%	204.74	299.72	77.92%
8	198.30	297.22	76.57%	246.81	346.63	80.39%	201.86	292.65	78.32%
9	189.47	274.43	78.00%	192.30	244.32	84.65%	191.7	269.12	79.66%
10 (top)	151.13	194.52	83.25%	140.42	164.55	88.61%	149.44	187.90	84.59%
Total Pu239 (kg)	1.91			1.94			1.93		
Assembly Burnup (MWD/MTU)	10583			9860			9648		
Key	CRO			CRI			SS Rod In		
	CRI			SS Rod In					
	SS Rod In								

Table 12 provides information about the three assemblies used for comparison in this chapter. The table presents nodal information pertaining to ²³⁹Pu mass, Pu fissile content,

and the presence of any modification such as a control rod or SS316. Table 12 shows total assembly burnup and total assembly ^{239}Pu production. Highlighted in the red are two nodes per assembly. The first node has the highest ^{239}Pu produced and the second node has the highest Pu percent content. The nodes are also color-coded to indicate the presence or absence of modifiers.

6.2 Detection Assessment

6.2.1: Spent Nuclear Fuel Signatures

This assessment examines the ability of safeguards equipment to detect the plutonium production scenarios from previous chapters. SNF safeguards focus on verifying operator declarations. Burnup is the single most important declared variable of an operator when assessing spent nuclear fuel. Thus this sections seeks to answer the following questions about the scenario burnup declarations:

- Can the inspector confirm the accuracy of the declaration?
- Would an inspector be able to recognize an unusual, albeit truthful, declared burnup?

SNF safeguards is challenging in terms of size, scope, and complexity. Hundreds of assemblies are held for cooling in spent fuel cooling ponds for many years. When an inspector arrives to inventory the pond, the sheer number of assemblies presents a challenge. Unlike fresh fuel assemblies, which can easily be assayed with hand-held devices, SNF is highly radioactive and thus must be inspected from a distance and behind shielding, which is typically water. Additionally, what were once easily discernable, direct signatures in fresh fuel assemblies become masked by fission product emissions thus requiring the use of proxy signatures to very irradiation history.[56]

Inspectors typically conduct a visual inventory of the SFP from a bridge above the assemblies. One of the most effective methods is for a team of inspectors to work together, with one inspector visually inspecting the assembly and making a verbal call out while the other inspectors compares the results to the operator declaration.[57] A more detailed inspection can be made in order to confirm discrepancies by lifting the assembly

from the storage rack. Delays in the SFP inspection, to include having to remove an assembly from the storage rack, can be disruptive to the operator. Deviations from the scheduled inspection, including having to conduct a more detailed analysis of individual assemblies, can be stressful for both the operator and the inspector.[56]

The following is a list of common SNF equipment used to confirm operator declarations.

1. *Cerenkov Viewing Device* (ICVD, DCVD): The ICVD is an image-intensifying device that amplifies Cerenkov radiation. Cerenkov radiation is emitted when electrons with energies exceeding the speed of light de-excite. It is directly produced from β emissions and from γ -absorption in water. The intensity of the “Cerenkov glow” can be used to confirm the presence or absence of irradiated material, voids, or structural materials. The ICVD is capable of detecting the diversion of material from spent fuel assemblies such as replacing pins with a dummy material however it does not provide any information about assembly burnup or cooling time.[57] Additionally, the emission is only visible with the presence of water and cloudy or dirty water conditions can limit viewing.[57, 58] The ICVD is the primary tool of safeguards inspectors when conducting SFP inventories and does not require assembly movement for inspection. The ICVD is a gross measurement tool that confirms the presence or absence of nuclear fuel. The sensitive of detector depends greatly on the device, water quality, assembly burnup, and operator. Assemblies with a low burnup or long cooling time can be difficult to view with an ICVD.[57]
2. *FORK detector* (FDET): The FDET is a passive NDA tool that uses a correlation between gross neutron and γ -emissions to determine burnup. ^{242}Cm and ^{244}Cm are the isotopes associated with neutron emissions in SNF.[56, 57] Neutron emissions correlate to burnup exponentially by a factor of about 3.0 to 4.0.[59] Use of the FDET requires that the assembly of interest be lifted from the SNF storage rack.[57] The FDET cannot perform spectroscopy and instead uses the correlation between total neutron and total gamma counts to determine burnup with an accuracy of about 5%.[59, 60]
3. *IRAT* (Irradiate Fuel Attribute Tester): The IRAT is a passive gamma spectroscopy device that uses a spectrum of gamma emissions to determine irradiation history. Common isotopes used in SNF gamma spectroscopy include ^{134}Cs , ^{137}Cs , ^{154}Eu , ^{144}Pr , and ^{60}Co . [57] Gross measurements of ^{137}Cs correlate linearly to burnup with an accuracy of 1%-4%. [59] The ratios of $^{134}\text{Cs}/^{137}\text{Cs}$ and $^{154}\text{Eu}/^{137}\text{Cs}$ correlate linearly to burnup and cooling time. Ratios of isotopes are particularly useful in spent fuel safeguards as they eliminate the need for calculation adjustments based on geometric efficiencies.[59] The IRAT uses a CdZnTe detector and requires that the assembly be lifted from the storage rack for examination.[56, 57] The CdZnTe detector provides lower spectral resolution than an HPGe detector however it does not require cooling so is more useful in a

field based safeguards situations.[61] Using an HPGe detector, measurements of ^{137}Cs and $^{134}\text{Cs}/^{137}\text{Cs}$ had accuracies on average between 4.9% and 4.6% respectively.[59] Using a less sensitive detector such as a CdZnTe will likely result in reduction in accuracy. Combining the accuracy of the liner correlation to burnup with the ability of the detector to resolve spectrum analysis, this research assumes a burnup determination accuracy of 10% for detectors using CdZnTe.

4. *SFAT* (Spent Fuel Attribute Tester): The SFAT is a passive gamma spectroscopy device and measures the same spectrum of signatures as the IRAT to determine irradiation history. The SFAT takes measurements positioned over the top of the assembly and does not require assembly movement. This is operationally advantageous as the inspection is not slowed due to the manipulation of the fuel assembly in the pond.[56, 57] As with the IRAT, this paper assumes an uncertainty of 10% in the SFAT measurements when correlating to burnup.

Detection analysis in this project compares the activity of isotopes in Table 13 for each of the three target assemblies. These isotopes emit signatures detectable by the device listed in Table 13. ORIGAMI depletion analysis for the target assemblies calculated both the gross (total) and nodal (axial distribution) isotope activity in Curies. Some equipment only uses gross counts, such as the ICVD and the SFAT while other detectors may be able to see a nodal distribution by examining the assembly axially.

Table 13: Detection Tools and Isotope Signatures ([56, 57, 59, 60])

Detection and Isotope Signatures				
Isotope	Device	Measurement Type	Notes	Uncertainty
^{137}Cs	CVD, DCVD	Gross	High energy gamma ray emitted at 662 keV from Cs137 that deposits energy in water producing Cerenkov emission, Correlates directly to burnup, Using as a proxy for CVD signature	^{137}Cs correlates to burnup within 1%-4%, CVD is a visual inspection tool that does not make quantitative measurements
Ratio ^{134}Cs to ^{137}Cs	IRAT, SFAT	Gross, Nodal	Used in γ spec, correlates to burnup	10%
^{244}Cm	FDET	Nodal	Used in conjunction with ^{137}Cs	5%
^{154}Eu	IRAT, SFAT	Gross, Nodal	Used in γ spec	10%

6.2.2: Detection Analysis

Verification of operator declared burnup is at the heart of a spent fuel safeguards program. Figure 51 shows the difference in activity for the detection isotopes of each scenario as compared to the VVER-1000 reference assembly. Also listed is the difference in assembly burnup between the scenarios and the reference assembly.

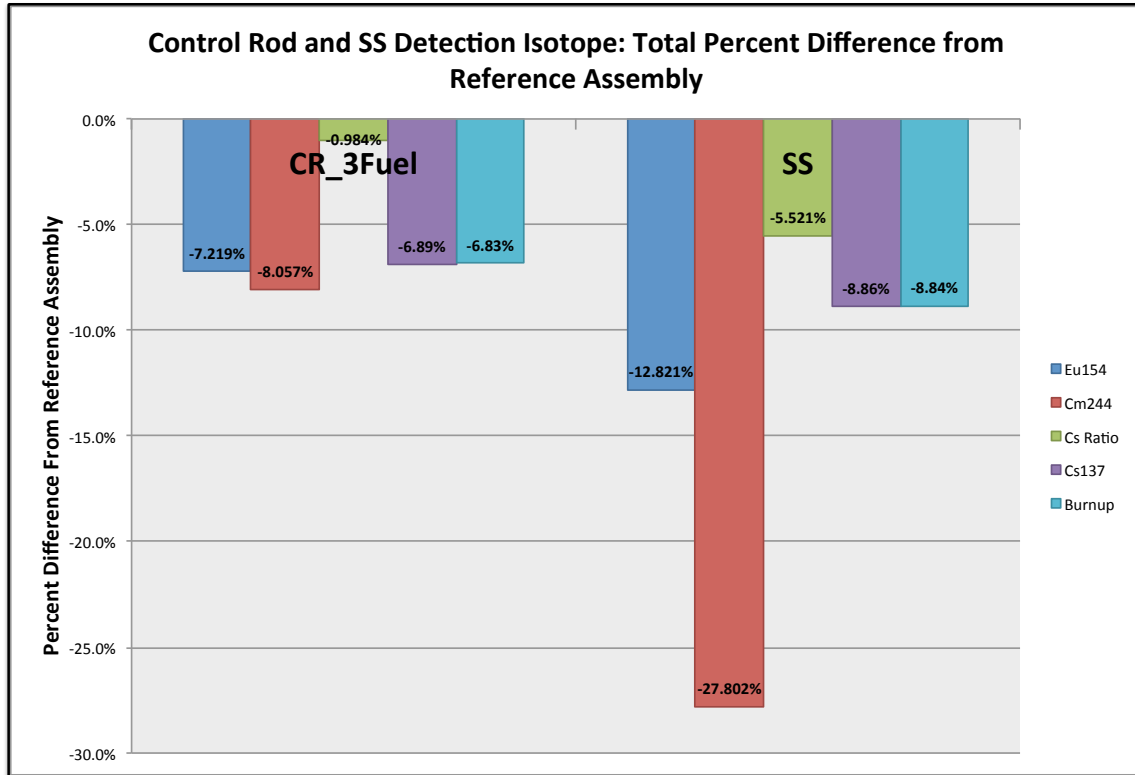


Figure 51: Pathway Gross Isotope Signature Percent Difference from Reference Assembly

All detector analysis of SNF first begins with a burnup declaration. If the isotopic signature of an assembly corresponds to the declared burnup, then it is reasonable to assume the declaration to be truthful.

Thus, if isotopic signatures of the scenarios differ from the reference assembly but in proportion to the change in burnup, it is likely that an interpretation of those signatures will confirm the operator declaration. If the isotope signature is proportionally different than the change in burnup, the operation declaration will not match the signature. The

following safeguards analysis compares the change in key detection isotopes with respect to the change in burnup using Figure 51

¹³⁷Cs (ICVD, DCVD)

Recall from Table 13 that ¹³⁷Cs correlates linearly to assembly burnup within 4% and is being used as a proxy variable for the Cerenkov signature. Figure 51 shows that the change in ¹³⁷Cs activity for both the control and SS316 case are nearly equal to the change in burnup and greater than 4% indicating that ¹³⁷Cs is an isotope of interest when confirming operator declared burnup. The scenario assemblies would appear as irradiated material with a burnup that agrees with a truthful operator declaration. Should the operator burnup declaration be false, a large discrepancy would also be noticeable.

Unlike the other SNF safeguards tools mentioned in Table 13, the ICVD does not have the ability to make quantitative measurements. It is a viewing device that allows inspectors to discern fuel from non-fuel material in the assembly. Using ¹³⁷Cs as a proxy for the ICVD signature only means that when viewed through the eyes of an inspector, the CR_3 and SS316 will appear to be irradiated and have a visual signature consistent with the declared truthful burnup. The assembly will not appear to be either a low burnup or high burnup assembly when using the ICVD unless it truly is.

Ratio ¹³⁴Cs to ¹³⁷Cs (IRAT, SFAT)

Figure 51 shows that CR_3 fuel had a decrease of only 0.984% for ¹³⁴Cs/¹³⁷Cs ratio when compared to the reference assembly despite having a burnup reduction of 6.83% or 723 MWD/MTU. The isotope signature differs from a truthful burnup declaration by 5.846%. Spectrum analysis from a highly accurate HPGe detector could possibly ascertain that the isotope signature did not agree with a truthful burnup declaration but less precise measurement tools would find this discrepancy to be within their margin of error.

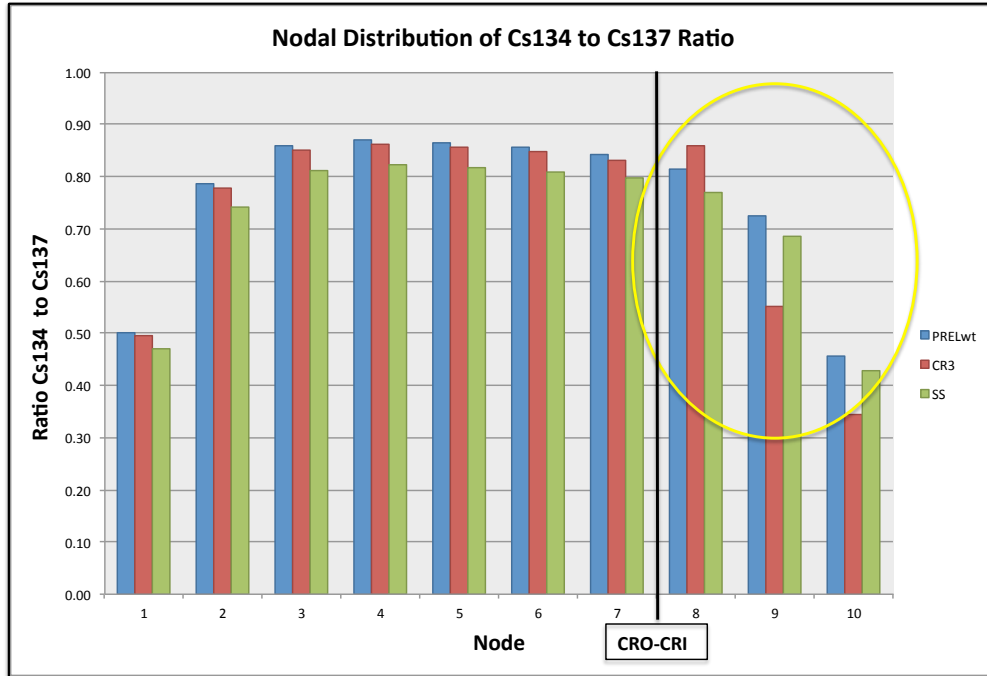


Figure 52: Axial Distribution of $^{134}\text{Cs}/^{137}\text{Cs}$ for Test Assemblies

Figure 52 shows the axial distribution for the ratio of ^{134}Cs activity to ^{137}Cs activity for the reference and scenario assemblies. Highlighted in yellow are the nodes modified by a control rod in the CR_3 fuel case. Note that at the CRO-CRI boundary (node 8), the ratio is actually higher than the reference assembly. No other node has a $^{134}\text{Cs}/^{137}\text{Cs}$ ratio higher than the reference assembly.

An IRAT could be used axially to observe the peak in signature at the CRO-CRI boundary followed by suppressed activity. With a detector limitation of 10%, one possible method to identify this activity would be to compare the CRO-CRI boundary node and the next subsequent node (higher). A ratio difference of 0.308 (35.9%) exists between node 8 and node 9 as compared to the reference assembly, which only has a difference of 0.087 (10.7%) between those same nodes. This tool would only be useful if the operator fails to declare the control rod behavior. Declaring the behavior may invite additional scrutiny, as it is abnormal to leave a single control rod in the core for the duration of the fuel cycle without it being caused by a malfunction.

²⁴⁴Cm and ¹³⁷Cs (FDET)

The FDET uses both a ¹³⁷Cs gamma signature and the neutron signature of ²⁴⁴Cm to confirm irradiation history.[56] Figure 51 shows that while the ¹³⁷Cs activity changed proportional with burnup for both the CR_3 and the SS316, the ²⁴⁴Cm activity did not linearly proportional change. In the case of the SS316, the ²⁴⁴Cm activity was 27.80% lower than the reference assembly while the burnup was reduced by only 8.84%. In the case of CR_3 the ²⁴⁴Cm activity was only 1.23% lower than the reference assembly. As stated above, the activity of ²⁴⁴Cm is quadratically correlated to burnup (Eq. 9), therefore a direct correlation is not as straightforward as with Cs isotopes.[59]

$$neutron\ emission = \alpha(burnup)^\beta \tag{Eq. 9}$$

The constant α in Eq. 9 is dependent on enrichment and assumed to be the same for all scenarios and β was assumed to be 4.0.[59] The constant α was found by comparing the reference assembly neutron emission and burnup. The neutron emission of ²⁴⁴Cm was derived from its activity based on a spontaneous fission probability of 0.000137 [14] and assuming 2.691 neutrons produced per fission[62]. The predicted neutron emission and activity for each proliferation scenario was then calculated using Eq. 9 and the assembly declared burnup. Table 14 shows a comparison of the predicted ²⁴⁴Cm activity (Eq. 9) to the modeled ²⁴⁴Cm activity.

Table 14: ²⁴⁴Cm Activity Predicted and Modeled for Proliferation Scenarios

Case	Burnup	Cm244 (Ci) Predicted	Cm244 (Ci) Actual	Difference	% Difference
CR3	9860	40.325	49.197	8.872	22.00%
SS	9647.5	36.960	38.632	1.672	4.52%

Table 14 shows that in both proliferation scenarios, truthfully declared assemblies will have a ²⁴⁴Cm signature that is higher than the relationship predicted by Eq. 9. In the case of the CR_3 scenario, this deviation is likely to be detectable as it exceeds the uncertainty of the FDET.

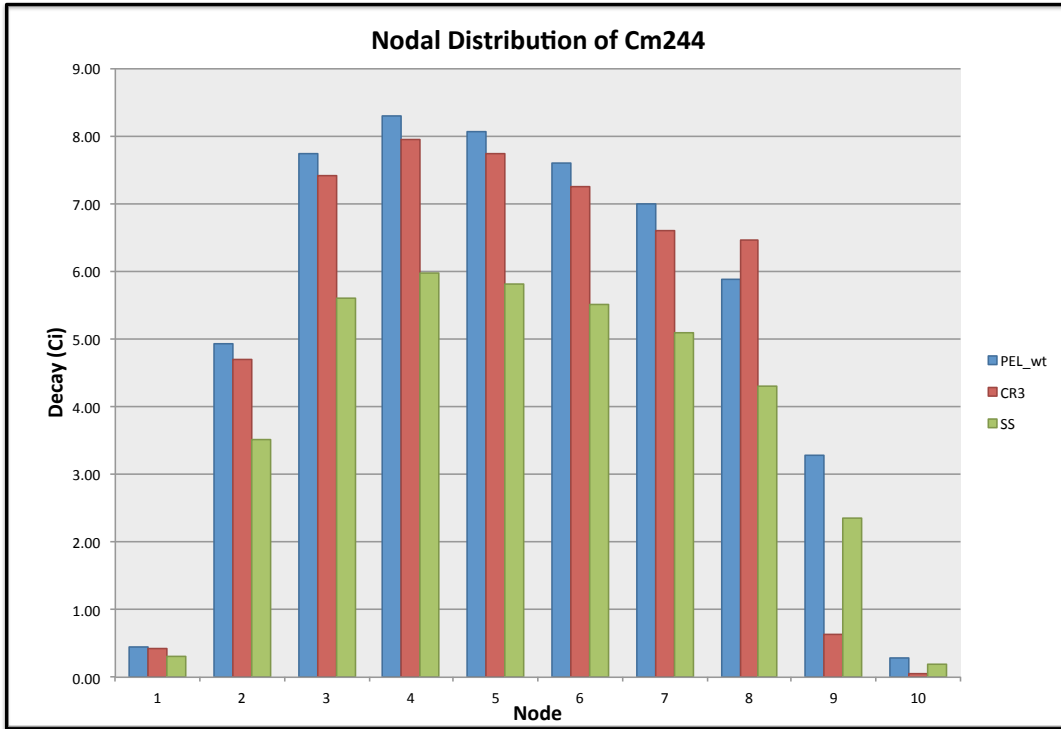


Figure 53: Axial Distribution ²⁴⁴Cm for Test Assemblies

Figure 53 also shows that nodes 8 through 10 for CR_3 exhibit the same identifying signature as observed with ¹³⁴Cs/¹³⁷Cs ratio. At the CRO-CRI boundary, the ²⁴⁴Cm activity is higher than the reference assembly. Moving to node 9, the ²⁴⁴Cm activity is reduced by 5.84 Ci, which is a 90.28% reduction from the activity of node 8. This variation in axial signature would be detectable by an FDET.

¹⁵⁴Eu (IRAT, SFAT)

Figure 51 shows that the ¹⁵⁴Eu activity was reduced proportional with burnup for the CR_3 assembly. The SS316 ¹⁵⁴Eu activity was reduced by 12.82% while the burnup reduction was 8.84%. With a difference of 3.98% between a truthful declaration and the modified assembly signature, it is unlikely that either an IRAT or SFAT would detect this signature discrepancy. Figure 54 shows the nodal distribution of ¹⁵⁴Eu activity for the scenarios. Once again, the CR_3 exhibits a higher activity than the reference assembly at the CRO-CRI boundary and is then suppressed for the remaining CRI nodes. The difference between node 8 and node 9 is 43.58 Ci representing a 62.25% decrease between the nodes.

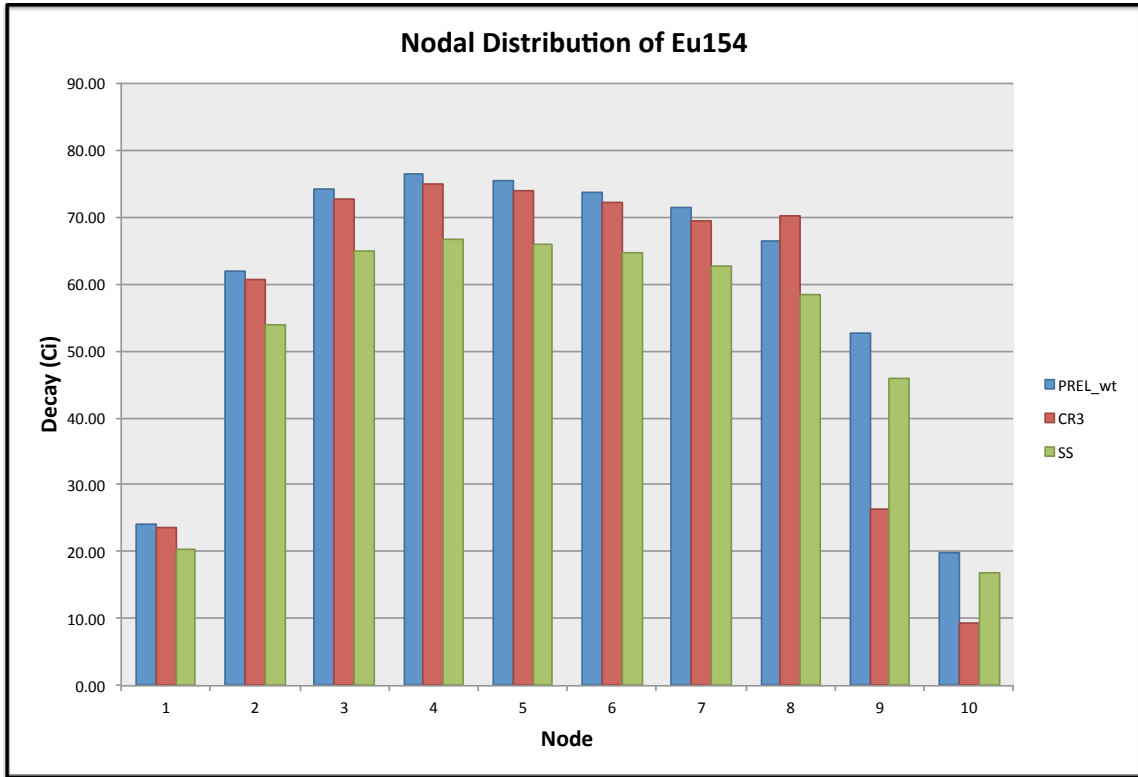


Figure 54: Axial Distribution ^{154}Eu for Test Assemblies

6.2.3: Detection Summary

A comparison of the test assemblies' detection isotope signatures reveals the following.

1. Truthful burnup declarations verified by the ^{137}Cs signature. The ICVD can provide a broad approximation for an inspector as to the general burnup, such as low or high, but as it is not quantitative, it cannot be used to discern minor changes in burnup such as the ones presented in these scenarios.
2. Using a ratio of isotopes or a two-isotope signature increases the chance of detecting a scenario with an accurate burnup declaration but unusual isotope production. Without a more sensitive detector, it would be difficult to discern unusual Cs isotope activity. An FDET has the sensitivity to detect changes in the ^{244}Cm signature with respect to ^{137}Cs however the extent of that deviation is greatly dependent on activity of ^{244}Cm with respect to burnup. The CR_3 scenario emitted a detectable deviation in the ^{244}Cm signature that was not consistent with the accepted relationship to burnup.
3. The control rod insertion case may exhibit a unique axial isotope signature with an increased level of activity at the CRO-CRI boundary followed by suppressed activity. An operator that fails to declare the control rod activity could be discovered. An operator that chooses to declare the activity would need to provide further justification of the unusual operating practice asymmetrically inserting a single control rod rather than the more standard practice of a symmetric working group.

6.3 Production Assessment

This section examines the rate of production for the scenarios. The assessment is framed around the time needed for an operator to produce a significant quantity of plutonium. Table 3 provides a list of plutonium grades and definitions used throughout this paper. Recall from Chapter 4 and Chapter 5 that in all modeled cases, neutron spectrum manipulation did not result in Pu fissile content achieving weapons desirable levels. The majority of the nodes were reactor grade, while the top and bottom assembly nodes were fuel grade. The nodes central to assembly produce the largest amount of material while the nodes on either end of the assembly produce the highest fissile material. Using either scenario as a pathway, regardless of rate of production, results in material that is less than desirable for direct weapons use.

Two nodes from each scenario are identified in red in Table 12. These nodes have the highest mass ^{239}Pu and the highest Pu fissile content. Production rate analysis using these nodes will result in either the shortest time required to make a single SQ or the time required to make an SQ of the highest plutonium quality for the scenario. Production rates were determined based on the extraction of 25%, 50%, and 100% of the pellets in each node.

A single assembly and multi-assembly scenario was also examined. The multi-assembly scenario uses six modified assemblies should the operator seek to increase the rate of production. Using six assemblies would maintain core symmetry. The practicality of extracting pins from the center of the assembly is not addressed in this section but will be addressed later.

6.3.1: Scenario-Control Rod Insertion

Table 15: Production Statistics Control Rod Insertion Model

Pu Nodal Production		
Case	Control Rod: 3 Nodes	
Nodes	8	10
Pu (g)	346.63	164.55
Pu239 (g)	246.81	140.42
Pu (g) per pin	1.11	0.53
Pu Percent Fissile	80.39%	88.61%
Nodal Pins For SQ	7201	15168

Table 15 provides the production statistics for the control rod insertion model. Node 8 had the highest production mass of ^{239}Pu . By uniformly distributing the mass of the ^{239}Pu over the 312 fuel pins in the assembly, Table 15 shows that it takes 7200 pins to make an SQ of plutonium. Node 10 had the highest Pu fissile content at 88.61% but had a low ^{239}Pu mass per pin. It takes over 15,000 pins from node 10 to make an SQ.

Table 16: Rate of Production Control Rod Insertion Model

CR_3 Node				
Node 8	Single Assembly		6 Assemblies	
Pins removed per cycle	Total Cycles	Years	Total Cycles	Years
25%	92	59	15	10
50%	46	29	8	5
100%	23	15	4	2
Node 10	Single Assembly		6 Assemblies	
Pins removed per cycle	Total Cycles	Years	Total Cycles	Years
25%	194	124	32	21
50%	97	62	16	10
100%	49	31	8	5

Table 16 illustrates the rate of production for the control rod insertion model. Single assembly production requires at one to two decades to produce an SQ of plutonium assuming 100% pin extraction. The multi-assembly model could produce an SQ of plutonium in a few as 2 years assuming total diversion of pins in the node. No weapons grade plutonium was produced in this model. These rates of production assume that the proliferator is only using plutonium from the nodes of interest. In reality, it is likely that the proliferator would use material from other nodes either intentionally or due to difficulties in extracting a single node’s worth of material. Any additional material harvested by the proliferator would have a fissile content of lower desirability. Therefore, ignoring this assumption results in an increase in the production rates but a decrease the quality of the material.

6.3.2: Scenario-Stainless Steel Modification

Table 17 provides the production statistics for the SS316 dummy material model. Node 4 had the highest production mass of ²³⁹Pu. Table 17 shows that it takes a little over 8,100 pins to make an SQ of plutonium. Node 10 had the highest Pu fissile content at 84.59% but had a low ²³⁹Pu mass per pin. It takes over 13,200 pins from node 10 to make an SQ. No weapons grade plutonium was produced in this model. SS316 scenario had lower mass ²³⁹Pu and lower Pu fissile content than the control rod insertion model.

Table 17: Production Statistics SS316 Model

Pu Nodal Production		
Case	VVER 1000 SS	
Nodes	4	10
Pu (g)	306.43	187.90
Pu239 (g)	207.42	149.44
Pu (g) per pin	0.98	0.60
Pu Percent Fissile	77.54%	84.59%
Nodal Pins For SQ	8146	13283

Table 18: Rate of Production SS316 Model

VVER 1000 SS				
Node 4	Single Assembly		6 Assemblies	
Pins removed per cycle	Total Cycles	Years	Total Cycles	Years
25%	104	65	17	11
50%	52	32	9	5
100%	26	16	4	3
Node 10	Single Assembly		6 Assemblies	
Pins removed per cycle	Total Cycles	Years	Total Cycles	Years
25%	170	106	28	18
50%	85	53	14	9
100%	43	26	7	4

Table 18 lists the rate of production for the SS316 model. Single assembly production requires one to two decades to produce an SQ of plutonium assuming 100% pin extraction. The multi-assembly model could produce an SQ of plutonium in a few as 3 years assuming total diversion of the node. All plutonium produced is below weapons grade. As stated in Chapter 5, adding SS316 to the VVER-1000 assembly had minimal impact on Pu production or fissile content.

6.4 Feasibility Assessment

There are a number of additional feasibility challenges for both scenarios. This research assumed the LWR assemblies were irradiated for only one cycle. Such behavior would be unusual and attract attention from inspectors. LWR fuel assemblies go through multiple fuel cycles before movement to the SFP.

An assembly that is truthfully declared to be a single cycle assembly would require some additional explanation. Pulling an assembly out early is costly and inefficient. An assembly that is only irradiated for a single fuel cycle would be unusual. The projection rates also assumed the core configuration did not change between cycles. Such an assumption is not realistic. In power reactor operation, core configurations change with each cycle and fuel is routinely shuffled.

Material added to the control rod guide tubes would need to be removed before placing in the spent fuel pond. Such material, as in the SS316 case, would be visible from the pond bridge with the ICVD or maybe even the naked eye. Finally, any efforts to extract pellets from “middle” nodes would almost certainly require damaging or destroying the pin. Accessing the assembly in order to gain retrieve to the pin would require justification but could be disguised as part of an effort to remove damaged pins. Once removed, the absence or replacement of a single pin would be difficult to detect with only an ICVD.

Manipulation of LWR assembly isotope content with either control rod insertion or stainless steel dummy material is detectable but may require the use of more than one signature for confirmation. Inaccurate burnup declarations are likely to be observed using an ICVD. Using more than one isotope for signature analysis allows for the detection of isotope discrepancies despite accurate burnup declarations. Both the CR_3 and the SS316 model had some signatures consistent with their declared burnup while others were not. Using multiple isotopes to confirm the declaration of a suspect assembly provides a more complete understanding of the irradiation history. The CR_3 model exhibited a distinct signature at the CRO-CRI boundary, which might be useful for identifying control rod manipulation.

The number of assemblies in the spent fuel pond does present a safeguards challenge due mostly to the number of man-hours required to conduct the inspection. Pre-inspection modeling could help safeguards officials prepare for the expected isotope signatures and identify assemblies of concern.

Misusing LWRs to produce plutonium via spectrum manipulation is slow and inefficient. No weapons-grade plutonium was produced in the reactor in the scenarios evaluated herein. The manipulation efforts modeled in this project, which aimed on improving production rates, had minimal impact. Both models had low production rates requiring a minimum of 1-2 decades to produce an SQ. Multi-assembly production increased the production rate to 2-3 years however this also seems unfeasibly as it would increase the chance of detection.

A safeguarded LWR reactor is not a good candidate for producing plutonium. The quality of the plutonium is not ideal for weapons use and the rate of production is slow. Any effort to increase the production rate or improve the plutonium quality would be detected using routine SNF safeguards. Pre-inspection modeling and the use of multiple isotopes to confirm the declaration increase the odds of detecting malicious behavior. Extraction of the material from the assembly would almost certainly be detected. The reactor technology of a LWR ensures that it is inherently peaceful. Any efforts to subvert the peaceful nature of technology are detectable using routine monitoring.

Chapter 7: Conclusion and Future Work

Nuclear energy is an attractive option to meet the energy capacity shortages of the developing world. As new states develop infrastructure to support nuclear energy programs, the challenge of prioritizing safeguards resources will increase. This paper puts forth a versatile nuclear modeling tool that allows researchers to directly observe the impact of core environmental changes on LWR assembly isotope production. When used in a nonproliferation capacity, this tool gives safeguards professionals a method by which to confirm the burnup declarations of spent nuclear fuel following an unexpected operator event such as control rod insertion. This tool will allow safeguards professionals to identify assemblies of concern prior to an inspection as well as quickly assess any unforeseen scenarios encountered during an inspection.

This project began by developing a VVER-1000 core model using information found in a series of benchmark publication and generating cross-section information with SCALE 6.2.1 lattice physics software. A NESTLE VVER-1000 model was used to replicate two scenarios of proliferation attempts. Burnup weighted relative power calculated by NESTLE was coupled to ORIGAMI for depletion analysis. The proliferation scenarios were assessed for feasibility based on detectability and production capacity. Control rod manipulation and SS316 flux spectrum hardening failed to produce weapons grade plutonium in the LWR assembly. Neither pathway had a useful production capacity. Both pathways emitted isotope signatures that would be detectable using standard safeguards equipment. Using NESTLE to ORIGAMI coupling, two potential LWR proliferation scenarios were demonstrated to be unfeasible.

NESTLE to ORIGAMI coupling offers a quick analysis tool for proliferation assessments. Constructing a reactor specific NESTLE model is a time intensive endeavor, however once constructed, the NESTLE simulation executes quickly. Using a core map and simple script, it is possible to extract a wide range of information from NESTLE for post processing. Relative power is extracted from NESTLE and weighted with burnup. Burnup weighted relative power serves as a conduit for the impact of core environment changes to be captured during depletion analysis. ORIGAMI allows the user to specify

relative power distributions in three dimensions. This project used the axial power distribution provided from NESTLE to shape ORIGAMI depletion. Through NESTLE to ORIGAMI coupling, the isotopic impact of control rod insertions and SS316 modifications were directly observable.

There are many opportunities for future work to expand this project. It was noted that the NESTLE VVER-1000 model did not agree with the benchmark results. Efforts to improve the model accuracy will improve results. The next step in confirming the accuracy of NESTLE to ORIGAMI coupling is to compare results to the isotope concentrations found in the third benchmark publication.[18] The 2011 benchmark publication provides isotope concentrations derived from multiple modeling sources for a number of nuclides. Comparing the NESTLE to ORIGAMI nuclide concentrations to those modeled using different software programs would aid in confirm the accuracy of the results. Comparing results of NESTLE to ORIGAMI coupling to NDA analysis of a spent fuel assembly would be the final step in verifying the accuracy of this modeling technique.

This work examined axial variations in isotope production. As the capabilities of NESTLE improve, to include radial pin-power modeling, it will be possible to examine isotope production in three dimensions. NESTLE pin-power modeling coupled to ORIGAMI provides the safeguards professional the ability to assess proliferation scenarios at the scale of the individual pin. Reexamining the SS316 scenario with a pin-by-pin level assessment could demonstrate the strength of this modeling tool by illustrating the isotope changes in the pins within close proximity to the SS316.

Meeting the energy demand of the future will likely require changes in nuclear reactor technology. Small module reactor technology offers the potential to address energy shortages without overwhelming an immature electrical infrastructure. NESTLE to ORIGAMI is a flexible modeling tool that can replicate a variety of core conditions and materials. Some small modular reactors are intended to operate autonomously or in austere locations. Such conditions raise concerns about the proliferation of material within the SMR core. Using NESTLE to ORIGAMI coupling, a nonproliferation

professional can address these concerns by assessing the feasibility of potential proliferation scenarios for the technology. By directly addressing proliferation concerns associated with new reactor technology, NESTLE to ORIGAMI coupling helps to ensure the peaceful application of nuclear energy and improve the lives of peoples around the world.

List of References

1. Teller, E. and J. Shoolery, *Memoirs, A Twentieth-Century Journey in Science and Politics*. 2001, Cambridge MA: Perseus Publishing.
2. U.S. Energy Information Administration, *International Energy Outlook 2016*, 2016, Office of Energy Analysis in U.S. Department of Energy: Washington DC.
3. International Atomic Energy Agency, *Energy, Electricity, and Nuclear Power Estimates for the Period up to 2050*, in *Reference Data Series No 12016*: Vienna.
4. International Atomic Energy Agency, *Climate Change and Nuclear Power 2016*, 2016: Vienna.
5. Frayer, K. and Getty Images, *A Coal Fired Plant on outskirts of Beijing.*, in *Polluted Skies Heighten Challenge for Chinese Government*, E. Wong, Editor 2015, NY Times: Accessed Online at <https://www.nytimes.com/2015/12/11/world/asia/china-smog-challenge.html> on July 2, 2017.
6. World Nuclear Association, *World Nuclear Performance Report 2017*, 2017: Published online at <http://www.world-nuclear.org/our-association/publications/online-reports/world-nuclear-performance-report.aspx>.
7. International Atomic Energy Agency, *Power Reactor Information System*, 2016, IAEA: <https://www.iaea.org/pris/>.
8. International Atomic Energy Agency, *IAEA Annual Report 2015*, in *IAEA Annual Reports 2015*: Vienna.
9. World Nuclear Association. *Nuclear Power in Germany*. 2017 May 30 [cited 2017 July 2]; Available from: <http://www.world-nuclear.org/information-library/country-profiles/countries-g-n/germany.aspx>.
10. International Atomic Energy Agency, *Evaluation of the Status of National Nuclear Infrastructure Development*, in *IAEA Nuclear Energy Series 2016*: Vienna.
11. Calma, D. *How IAEA Safeguards Contribute to International Peace and Security* IAEA Photo Essay [Online Photo Essay] June 11, 2015 [cited 2015 October 14]; Available from: <https://www.iaea.org/newscenter/multimedia/photoessays/how-iaea-safeguards-contribute-international-peace-and-security>.
12. Rearden, B.T. and M.A. Jessee, Eds., *SCALE Code System*, ORNL/TM-2005/39, Version 6.2.1, Oak Ridge National Laboratory: Oak Ridge, Tennessee (2016). Available from Radiation Safety Information Computational Center as CCC-834.
13. Williams, M.L., et al., *5.4 Origami: A Code for Computing Assembly Isotopics with ORIGEN*, in *SCALE Code System*, B.T. Rearden and M.A. Jessee, Editors.

- 2016, Oak Ridge National Laboratory: Oak Ridge, TN. Available from Radiation Safety Information Computational Center as CCC-834.
14. International Atomic Energy Agency. *Live Chart of the Nuclides*. [interactive database] December 2016 [cited 2017 April 5]; Available from: <https://www-nds.iaea.org/relnsd/vcharthtml/VChartHTML.html>.
 15. Brookhaven National Laboratory. *Evaluated Nuclear Data File ENDF/B-VII.1*. [cited 2015; Available from: <http://www.nndc.bnl.gov/exfor/endl00.jsp>.
 16. Lotsch, T., V. Khalimonchuk, and A. Kuchin, *Proposal of a Benchmark for Core Burnup Calculations for a VVER-1000 Reactor Core*, in *19th AER Symposium on VVER Reactor Physics and Reactor Safety 2009*, INIS: Bulgaria.
 17. Lotsch, T., V. Khalimonchuk, and A. Kuchin. *Corrections and additions to the proposal of a benchmark for core burnup calculations for a WWER-1000 reactor. in 21st Symposium of Atomic Energy Research*. 2010. Hungary.
 18. Lotsch, T., V. Khalimonchuk, and A. Kuchin. *Solutions for the Task 1 and Task 2 of the Benchmark for Core Burnup Calculations for a VVER-1000 Reactor. in 21st Symposium of Atomic Energy Research on WWER Physics and Reactor Safety*. 2011. Hungary.
 19. Brookhaven National Laboratory, *Evaluated Nuclear Data File (ENDF) Retrieval and Plotting for ENDF/B-VII.1 library*, 2011, Brookhaven National Laboratory, Upton, NY Accessed online at <http://www.nndc.bnl.gov/sigma/> on August 13, 2017.
 20. International Atomic Energy Agency, *Power Reactor Information System*, 2017, IAEA: Accessed Online at <https://www.iaea.org/pris/>.
 21. World Nuclear Association. *Nuclear Power In Russia*. 2017 June 2017 [cited 2017 July 2]; Available from: <http://www.world-nuclear.org/information-library/country-profiles/countries-o-s/russia-nuclear-power.aspx>.
 22. Camas, E., *The Build-Own-Operate (BOO) approach: Advantages and challenges*, in *Technical Meeting on Topical Issues in the Development of Nuclear Power Infrastructure 2014*, IAEA: Vienna, Austria.
 23. International Atomic Energy Agency, *Alternative Contracting and Ownership Approaches for New Nuclear Power Plants*, in *IAEA TECDOC SERIES 2014*: Accessed online at <https://www.iaea.org/inis/> on April 25, 2016.
 24. Boyer, B. and M. Schanfein, *International Safeguards Inspection: An Inside Look at the Process*, in *Nuclear Safeguards, Security, and Non-Proliferation*, J.E. Doyle, Editor. 2008, Butterworth-Heinemann: Burlington, MA.

25. Doyle, J.E., *Nuclear Safeguards, Security, and Nonproliferation; Achieving Security with Technology and Policy*. 2008, Burlington MA: Butterworth-Heinemann.
26. International Atomic Energy Agency, *IAEA Safeguards Glossary*, in *International Nuclear Verification Series 2001*: Accessed online at <http://www-pub.iaea.org/books/IAEABooks/6663/IAEA-Safeguards-Glossary> on April 26, 2016.
27. Pellaud, B., *Proliferation Aspects of Plutonium Recycling*. *Journal of Nuclear Materials Management*, 2002. **31**(1): p. 30-38.
28. Mark, J.C., F. Von Hippel, and E. Lyman, *Explosive Properties of Reactor-Grade Plutonium*. *Science & Global Security*, 2009. **17**(2-3): p. 170-185.
29. Kessler, G., et al., *Potential nuclear explosive yield of reactor-grade plutonium using the disassembly theory of early reactor safety analysis*. *Nuclear Engineering and Design*, 2008. **238**(12): p. 3475-3499.
30. Kessler, G., et al., *A new scientific solution for preventing the misuse of reactor-grade plutonium as nuclear explosive*. *Nuclear Engineering and Design*, 2008. **238**(12): p. 3429-3444.
31. Permana, S., et al., *Study on material attractiveness aspect of spent nuclear fuel of LWR and FBR cycles based on isotopic plutonium production*. *Energy Conversion and Management*, 2013. **72**: p. 19-26.
32. Kimura, Y., M. Saito, and H. Sagara, *Evaluation of Proliferation Resistance of Plutonium Based on Decay Heat*. *Journal of Nuclear Science and Technology*, 2011. **48**(5): p. 715-723.
33. Permana, S., et al. *Irradiation and cooling process effects on material barrier analysis based on plutonium composition of LWR*. in *2013 International Conference on Future Energy and Materials Research, FEMR 2013, June 1, 2013 - June 2, 2013*. 2013. Singapore: Trans Tech Publications Ltd.
34. Permana, S., et al., *Analysis on isotopic plutonium barrier based on spent nuclear fuel of LWR*. *Annals of Nuclear Energy*, 2015. **75**: p. 116-122.
35. Costa, A.L., et al., *A neutronic evaluation of the (Pu-U) and (Am-Pu-U) insertion in a typical fuel of Angra-I*. *Annals of Nuclear Energy*, 2009. **36**(1): p. 1-6.
36. Kimura, Y., M. Saito, and H. Sagara, *Improvement of evaluation methodology of plutonium for intrinsic feature of proliferation resistance based on its isotopic barrier*. *Annals of Nuclear Energy*, 2012. **40**(1): p. 130-140.

37. Bathke, C.G., et al., *The Attractiveness of Materials in Advanced Nuclear Fuel Cycles for Various Proliferation and Theft Scenarios [LA-UR-09-02466]*, 2009, Los Alamos National Laboratory: United States and accessed in the IAEA INIS Database on 7 August 2017.
38. Ade, B.J., *SCALE/TRITON Primer: A Primer for Light Water Reactor Lattice Physics Calculations*, I. Frankl, Editor 2012, U.S. Nuclear Regulatory Commission Office of Nuclear Regulatory Research: Oak Ridge National Laboratory.
39. Jessee, M.A., et al., *3.2 Polaris-2D Light Water Reactor Lattice Physics Model*, in *Scale Code System*, B.T. Rearden and M.A. Jessee, Editors. 2016, Oak Ridge National Laboratory: Oak Ridge, TN. Available from Radiation Safety Information Computational Center as CCC-834.
40. University of Tennessee and North Carolina State University, *DRAFT: NESTLE Version 6.2+ Few-Group Neutron Diffusion Equation Solver Utilizing The Nodal Expansion Method for Eigenvalue, Adjoint, Fixed-Source Steady-State and Transient Problems*, 2015.
41. Oak Ridge National Laboratory, *NESTLE: Code System to Solve the Few-Group Neutron Diffusion Equation Utilizing the Nodal Expansion Method for Eigenvalue, Adjoint, and Fixed-Source Steady-State and Transient Problems, Version 5.1.2*, 2003, Available from Radiation Safety Information Computational Center at Oak Ridge National Laboratory as CCC-641.
42. Galloway, J.D., *Boiling Water Reactor Core Simulation with Generalized Isotope Inventory Tracking for Actide Management, PhD diss*, 2010, University of Tennessee.
43. Ottinger, K.E., *Multi-cycle Boiling Water Reactor Fuel Cycle Optimization, PhD diss*, 2014, University of Tennessee.
44. Collins, P.E., N. Luciano, and G.I. Maldonado, *Modernization and Expansion of isotopic depletion capabilities within the nestle 3D nodal simulator*. Transactions of the American Nuclear Society, 2014. **111**: p. 1230-1233.
45. Luciano, N., P and I. Maldonado, *Two-dimensional hexagonal geometry discontinuity factors at the core periphery*. Annals of Nuclear Energy, 2017. **107**: p. 49-52.
46. Gentry, C.A., *Development of a Reactor Physics Analysis Procedure for the Plank-Based and Liquid Salt Cooled Advanced High Temperature Reactor*, 2016, PhD diss, University of Tennessee: Knoxville TN.
47. Jessee, M.A., et al., *3.1 Triton: A Multipurpose Transport, Depletion, and Sensitivity and Uncertainty Analysis Module*, in *Scale Code System*, B.T. Rearden

- and M.A. Jessee, Editors. 2016, Oak Ridge National Laboratory: Oak Ridge, TN. Available from Radiation Safety Information Computational Center as CCC-834.
48. Luciano, N., *Sensitivity of VVER-1000 Spent Fuel Pin Nuclide Inventory to Operational Parameters*, in *Nuclear Engineering*, 2017, University of Tennessee: Knoxville, TN.
 49. Oak Ridge National Laboratory, *SCALE: A Comprehensive Modeling and Simulation Suite for Nuclear Safety Analysis and Design*, ORNL/TM-2005/39, 2011, Available at Radiation Safety Information Computational Center, CCC-785: Oak Ridge National Laboratory.
 50. Enin, A., D. Pluzhnikov, and Y. Bezborodov, *Improvement of VVER-1000 FA design and manufacturing techniques*, in *10th International Conference on VVER Fuel Performance Modeling and Experimental Support* 2013: Bulgaria.
 51. Oak Ridge National Laboratory, *Scale 6.2 Lattice Physics and Depletion Class (Feb 15-19, 2016)*, 2016: Oak Ridge, TN.
 52. International Atomic Energy Agency. *Advanced Reactor Information System*. [online database] 2017 Last Update July 21, 2011 [cited 2017 June 19]; Available from: <https://aris.iaea.org/default.html>.
 53. Utkarsh, A., *The Paraview Guide: A Parallel Visualization Application*, 2015, Kitware: ISBN 978-1930934306.
 54. MathWorks, *Matlab Surface and Mesh Plots R2015a*, 2017, MathWorks Inc: University of Tennessee Academic License.
 55. LeBlanc, D., *Molten salt reactors: A new beginning for an old idea*. *Nuclear Engineering and Design*, 2010. **240**(6): p. 1644-1656.
 56. Abhold, M.E., *Irradiated Fuel Measurements*, in *Nuclear Safeguards, Security, and Nonproliferation*, J.E. Doyle, Editor. 2008, Butterworth-Heinemann: Burlington, MA. p. 70-75.
 57. International Atomic Energy Agency, *Safeguards Techniques and Equipment*, in *International Nuclear Verification Series (Revised)* 2003, IAEA: Vienna, Austria.
 58. Chen, J.D., et al., *Cerenkov Characteristics of PWR assemblies using a prototype DCVD with Back-Illuminated CCD*, 2003, Canadian Nuclear Safety Commission and Swedish Nuclear Power Inspectorate, accessed from IAEA INIS Database June 27, 2017.
 59. Phillips, J.R., *Chapter 18: Irradiated Fuel Measurements*, in *Passive Nondestructive Assay of Nuclear Materials*, NUREG/CR-5550, D. Reilly, et al., Editors. 1991, U.S. Nuclear Regulatory Commission: Washington DC.

60. ANTECH. *B2102 Series, Fork Detectors (IAEA) 2017* [cited 2017 August 8]; Available from: <http://www.antech-inc.com/products/b2102/>.
61. Chaudhury, S., et al., *Comparison between HPGe and CdZnTe detector for correlation between calculated radioactivity and measured does using an activated concrete sample*. Journal of Radioanalytical and Nuclear Chemistry, 2012. **294**(3): p. 461-464.
62. International Atomic Energy Agency. *IAEA Handbook of Nuclear Data for Safeguards*. 2015 October [cited 2017 18 August]; Available from: <https://www-nds.iaea.org/sgnucdat/>.
63. Wolfram Alpha. *WolframAlpha*. 2016 [cited 2016 February 1]; Available from: <https://www.wolframalpha.com/input/?i=steam+15.7+Mpa+578+K>.
64. Ward, A.M., et al., *Methods and Model Development for Coupled RELAP5/PARCS Analysis of the Atucha-II Nuclear Power Plant*. Science and Technology of Nuclear Installations,, 2010. **2011**.
65. Mittag, S., P.T. Petkov, and U. Grundmann, *Discontinuity factors for non-multiplying material in two-dimensional hexagonal reactor geometry*. Annals of Nuclear Energy, 2003. **30**: p. 1347-1364.
66. Jessee, M.A. and M.D. DeHart, *9.2 NEWT: A New Transport Algorithm for Two-Dimensional Discrete-Ordiantes Analysis in Non-Orthogonal Geometries*, in *SCALE Code System*, B.T. Rearden and M.A. Jessee, Editors. 2016, Oak Ridge National Laboratory: Oak Ridge, TN. Available from Radiation Safety Information Computational Center as CCC-834.
67. World Nuclear Association. *Nuclear Power in Russia*. [Web Page] 2017 May 2017 [cited 2017 June 19]; Available from: <http://www.world-nuclear.org/information-library/country-profiles/countries-o-s/russia-nuclear-power.aspx>.
68. Rinovany, V.D., E.E. Varlashova, and D.N. Suslov, *Dysprosium titanate as an absorber materal for control rods*. Journal of Nuclear Materials, 2000. **281**: p. 84-89.
69. MathWorks, *Matlab Polyfit Tool R2015a*, 2017, MathWorks Inc: University of Tennessee Academic License.
70. Wieselquist, W.A., et al., *ORIGAMI Automator Primer: Automated ORIGEN Source Terms and Spent Fuel Storage Pool Analysis*, 2016, Oak Ridge National Laboratory: Oak Ridge TN, ORNL/TM-2015/49.

Appendices

Appendix A SCALE 6.2.1 Assembly Modeling and Cross-Section Library Generation

A.1: Introduction

The purpose of this Appendix is to present the parameters, assumptions, and branches used in the SCALE 6.2.1 T-Depl assembly models. All data is based on the information provided three VVER-1000 benchmark publications. [16-18] Additionally, ORIGAMI depletion software requires unique, burnup dependent cross-section libraries. This section also describes the model variations to the FA 13AU T-Depl model used to generate unique burnup dependent cross-section libraries for ORIGAMI analysis. Finally, the section describes the modeling method used to create cross-sections for the VVER reflector regions. Reflector cross-sections are used in the NESTLE VVER-1000 model and hexagonal assemblies have particularly challenging ADFs to calculate. This section describes the use of ADFs by nodal core simulators, difficulties calculating hexagonal reflector ADFs, and the approximations made for this project with regards to hexagonal reflector ADFs.

A.2: SCALE 6.2.1 Settings

The following section describes some of the model settings used when executing the TRITON Depletion sequence T-Depl. Features listed below are described fully in the Oak Ridge National Lab publication, *SCALE Code System*. [12]

- *Library = v7-252*: The most comprehensive cross-section library used by Scale is ENDF/B-VII.1 containing 148 fast groups and 104 thermal groups. This library is also the most recent cross section library available.[12] Using v7-252 ensures the most complete and current multigroup cross-section data
- *Parm = weight*: This feature allows for the collapse of the initial 252-group library into a 56-group library. The initial calculation is performed and then collapsed for subsequent calculations. The use of the collapsed group library allows for a reduction in overall CPU time.
- *cmfd=yes*: Course-Mesh Finite Difference Acceleration (cmfd) speeds up the convergence of inner and outer iterations used during the solving of discrete ordinate by NEWT. CMFD homogenizes cells as specified by a user-defined grid. By using the keyword *yes*, Scale 6.2.1 uses the “unstructured” CMFD method that is compatible with hexagonal geometry.

- *xcmfd=1*: This feature allows the user to define the number of fine meshes in the x-direction used by CMFD acceleration. In this case, *1* is selected which tells CMFD to use individual meshes defined for each unit.
- *ycmfd=1*: This feature allows the user to define the number of fine meshes in the y-direction used by CMFD acceleration. In this case, *1* is selected which tells CMFD to use individual meshes defined for each unit.
- This is the recommended *cmfd* parameter configuration according to the Scale 6.2.1 manual.
- *epsilon = 1e-5*: Sets converge criteria for both special and eigenvalue convergence. This value was recommend by the software throughout model development.
- *cell_tol=1e-8*: Increased tolerance suggested by the software during model development due to ray tracing error.
- *Collapse Block = 40r1 16r2*: The collapse block collapses the 252-group (56-group with *parm=weight*) cross sections into a number of energy groups as defined by the user. In this case, there are two final energy groups. The fast group contains 40 energy groups and the thermal group contains 16. This was the 2-group collapse block recommend during Scale 6.2 Lattice Physics Training.[51]
- *Homogenization Block*: The homogenization block facilities collapsing material cross sections for generating few-group cross sections for nodal simulators like NESTLE. Included in this block are all materials located in the fuel assembly. Invoking this block will generate the *xfile016* necessary for NESTLE cross-section generation.
- *ADF Block*: The ADF block must be invoked in conjunction with the homogenization block in order to calculate the ADFs at unit boundaries and ensure continuity current across the boundary for the nodal simulator. For a hexagonal fuel assembly, the ADF must be defined as 12 points representing the 6 line segments that define the assembly boundary. Special treatment of the ADF block is required for generating reflector cross-sections.
- *Boundary conditions = white*: Only the global unit has defined boundary conditions. For non-rectangular units, such as the hexagonal fuel assembly of a VVER1000, the only available conditions are white and vacuum. Because the assemblies modeled will be situated as an array of assemblies inside the core of the reactor, it is not appropriate to model the boundaries as a vacuum. A vacuum condition however, would be appropriate when modeling a reflector region.
- *Alias Block*: All input files utilize an Alias Block. This block allows the user to reduce code input by grouping multiple material identifiers under a single alias, rather than listing each material identifier individually. The alias then corresponds to a unique composition.
- *Shell commands*: All input files include four shell commands. These commands tell the run time environment to save four files generated in the temporary directory. The files saved are *xfile016*, *txtfile016*, *ft33f001.cmbined*, and *ft71001*. The *xfile016* and *txtfile016* are used later to generated a cross-section file for the development of the NESTLE cross-section library. The *ft33f001.cmbined* file is used later for the creation of Origami material libraries. Additional material specific *ft33f001* files were also saved for unique cases.

A.3: Model Assumptions

When building each of the fuel assembly models, the design specifications for the reactor core came from the Lotsch, T, etc, all 2009 Benchmark Proposal and 2010 Corrections and Additions to the Benchmark Proposal. [16, 17] Some information necessary to model a detailed core in SCALE Triton was assumed when not clearly specified in these documents. The following is a list of those assumptions.

- *Moderator Properties:* The 2010 document includes a list of average state parameters.[17] These are assumed to be the nominal state for the reactor. The average moderator temperature is 578K and moderator pressure is 15.7 MPa. The nominal boron concentration of the moderator is 525 ppm (3 g/kg). Steam tables from the website www.WolframAlpha.com were used to calculate the moderator density for the nominal state.[63]
- *Fuel pin gap:* The VVER1000 fuel pin is annular. There is no material defined for the gas in the pin center annulus or in the gap between the fuel and cladding. It is assumed that the gas filling that space is helium and has a temperature of 900K. This temperature is slightly less than that of the 1005K average fuel temperature.
- *Control Rod Guide Tube Material:* The 2009 reference has two tables with conflicting information that describe the material composition of the control rod guide tubes (Tables 3 and 4). Table 3 of that same reference also mentions burnable absorber guide tubes. It is assumed that the mentioned of burnable absorber guide tubes is an error as the BA are part of the mixture comprising fuel pins within of the assembly and there is no mention of BA guide tubes in any subsequent documents. The CR guide tube material is listed as two different materials in the 2009 reference. Table 3 of the 2009 reference lists the material as a type of steel and Table 4 lists it as alloy E635. The 2010 reference lists the CR guide tubes as the same composition as alloy E635 but references a different alloy number. It is therefore assumed that the CR guide tubes are made of Alloy E635 by composition as defined in the 2009 reference, Table 4.
- *Cladding Temperatures:* The cladding temperatures for fuel pins, burnable absorber pins, and control rods are never specifically mentioned in the benchmark data. Therefore it is assumed that the fuel and BA cladding materials have a temperature of 600K. This assumption makes the fuel cladding slightly hotter than the moderator but less hot than the fuel/BA pin material. The control rod cladding is assumed to be the same temperature as the moderator.
- *CR guide tube/Central Guide tube Material Composition:* The composition breakdown of these materials summed, by percentage, to greater than 100%. Therefore, the Zr composition was reduced by 1.07%.
- *BA material:* The burnable absorber composition listed in Table 3 of the 2009 benchmark document seems in error as it does not list gadolinium in the materials for the absorber despite the fact Gd_2O_3 pins are listed later in Table 6. The 2010

document simple states the burnable absorber material is Gd_2O_3 . Therefore, Gd_2O_3 is assumed to be the absorber in the BA pin and it is assumed to have the standard SCALE composition. The burnable absorber pins are 5.0% Gd_2O_3 and 95% UO_2 . The enrichment level of the UO_2 varies depending the fuel assembly modeled.

- *CR material*: The absorbing material in the VVER 1000 control rod is not homogenous. The rod consists of an upper and lower part. The upper part of the rod is 3200 mm and is comprised of B_4C . The lower part of the rod is 300 mm and is comprised of $Dy_2O_3 \cdot TiO_3$. The overall rod length is 3500 mm. This model assumes the rod to be comprised entirely of B_4C .

A.4: Burndata

The VVER1000 lattices modeled have a similar power and cycle life of the reactor studied by Lotsh, T, etc. The reactor had an average power density of 42.5 W/gU and an cycle length of approximately 311 EFPD (effective full power days).[17] During the first operational cycle of the reactor, it takes approximately 50 EFPD for the reactor to reach peak operating power. In subsequent cycles, the reactor is brought to full power more quickly. Since the goals of this model is not to mirror the behavior of the modeled reactor exactly but rather to simply have a plausible reactor model from which to build permutations, the power ramp increase is not modeled. The reactor is modeled at full power for the entire length of cycle.

When determining the depletion scheme, it is important have an adequate number of depletion intervals to accurately address the changing composition of the reactor over time. *The Scale/Triton Primer: A Primer for Light Water Reactor Lattice Physics Calculations* recommends a short depletion step sized based on the presence of fission product poisons (Xe/Sm, ~ first 100 hrs) and impact of burnable absorbers.[38] The depletion scheme present below accounts for the build up of Xenon (and other fission poisons) early in the reactor cycle with small depletion steps. The step size increases for the second depletion interval and covers the remainder of the fuel cycle. The final depletion step provides a wide range of burnup calculations for NESTLE and ORIGAMI libraries. This depletion scheme is standardized across all assemblies in order to facilitate agreement for nodal simulator cross-section library.

- $p = 42.5 \text{ burn} = 4 \text{ nlib} = 5$ (step size 0.034 GWd/MTHM)

- p = 42.5 burn = 307 nlib = 5 (step size 2.610 GWd/MTHM)
- p = 42.5 burn = 100 nlib = 1 (step size 4.250 GWd/MTHM)

A.5: Branches

The nominal branch state is defined as follows:

- Temperature Fuel: 1005 K
- Temperature Moderator: 578 K
- Density Moderator: 0.7176 g/cm³
- Control Rod Status: Out (cr = 0)
- Soluble Boron Concentration: 525 ppm

Branch conditions listed focus primarily on permutations of absorbers in the assembly.

NESTLE determined the boron concentration levels necessary to maintain criticality throughout the scenario modeling. Therefore it was important to have branches covering a wide spectrum of boron concentrations with and without control rod presence.

Table 19 contains the list of branch conditions used for each fuel assembly model.

Table 19: Branch Conditions

Branch Conditions						
Branch	tf (K)	tm (K)	dm (g/cm³)	cr (0=out)	cb (ppm)	Condition Changed
0	1005	578	0.7167	0	525	Nominal
1	1005	578	0.7167	1	525	Rod In
2	1005	578	0.7167	0	1000	Boron Increase
3	1005	578	0.7167	1	1000	Boron Increase, Rod In
4	1005	578	0.7167	0	1500	Boron Increase
5	1005	578	0.7167	1	1500	Boron Increase, Rod In
6	1005	578	0.7167	0	2000	Boron Increase
7	1005	578	0.7167	1	2000	Boron Increase, Rod In
8	1005	578	0.7167	0	0	No Boron
9	1005	578	0.7167	1	0	No Boron, Rod In
10	1005	300	0.7167	0	0	EOC
11	1005	300	0.7167	1	0	EOC, Rod In
12	1500	578	0.7167	0	525	High Fuel Temp
13	2000	578	0.7167	0	525	High Fuel Temp
14	3000	578	0.7167	0	525	High Fuel Temp
15	1005	578	0.6000	0	525	Moderator Density
16	1005	578	0.8500	0	525	Moderator Density
17	1005	578	1.0000	0	525	Moderator Density

A.6: Material Depletion

Materials that contribute to neutron flux through fission require depletion because their compositions will change throughout the fuel cycle. Additionally, the burnable absorber fuel pins require depletion as both the fuel and the absorber materials change in isotopic concentration. Therefore, all fuels are included in the depletion block. The burnable absorber fuel pins are depleted using constant flux and the normal fuel pins are depleted using constant power as recommended by the *Scale/Triton Primer*. [38]

The depletion of materials is highly dependent on the neutron flux. Figure 55 shows fuel assembly 39AWU as modeled using SCALE's Triton T-Newt sequence and illustrates the variation in the 2D neutron flux distribution across the assembly. Factors such as fuel composition, the presence of burnable absorbers, control rods, and moderator filled guide tubes all impact the spatial distribution of neutron flux across the assembly. Each fuel pin experiences a unique flux distribution depending on its location within the assembly. As such, each fuel pin will have a unique depletion and final composition of isotopes.

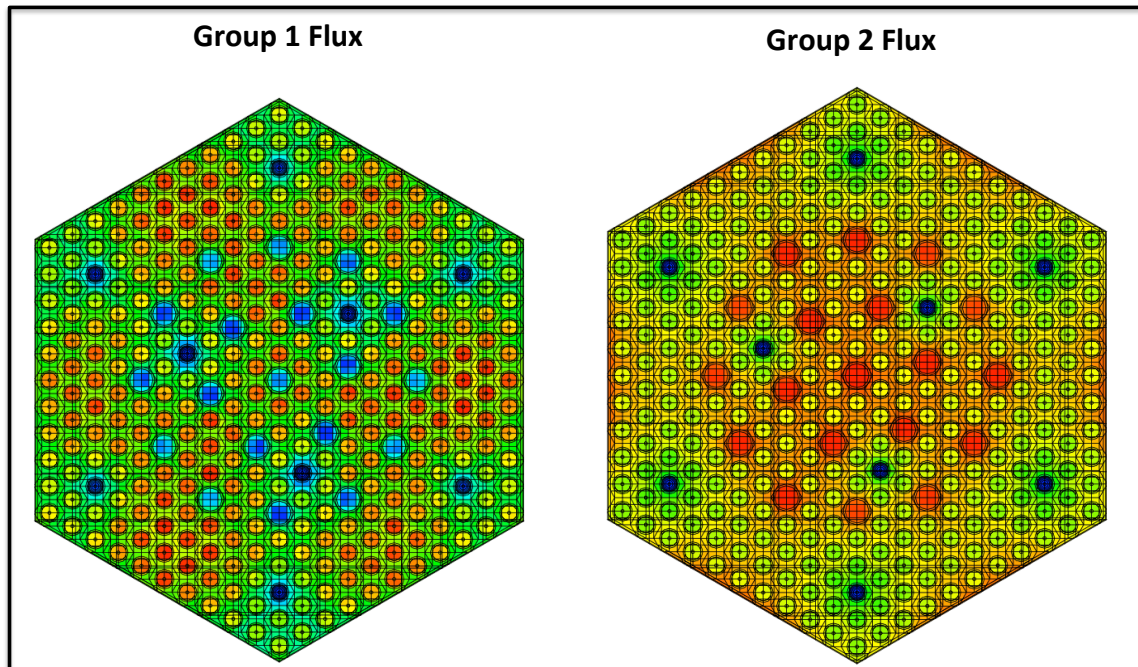


Figure 55: 2 Group Flux Spectrum FA 39AWU modeled with T-Newt

Prior to beginning depletion analysis of materials within an assembly, it is important to understand how ORIGEN, the depletion program used as part of TRITON, constructs a depletion model. ORIGEN is a point depletion code and depletes materials at individual points. These points, identified by the user, correlate to the material identification numbers. All materials defined by the same material identification number will be depleted with either a constant flux or constant power depending on the user defined setting. [38, 49, 51] Thus, in order to get accurate isotope concentrations at depletion, one must define materials in such a way so as to accurately account for the spatial distribution of the neutron flux.

SCALE/TRITON Primer: A Primer for Light Water Reactor Lattice Physics Calculations, proposes using symmetry as a method for incorporating the impact of the spatial flux changes across the assembly when conducting depletion calculations.[38] Fuel assemblies for this project are either 1/3 or 1/6 symmetric depending on the presence of BA pins. Using the symmetry technique involves defining each pin within the region of symmetry with a unique material identifier and then reflecting it to a spatially symmetric location(s) across the assembly. Approximately 104 unique fuel pins would be required to construct a 1/3 symmetric model of assemblies in this project.

Alternatively, it is possible to save computing time by lumping materials with similar flux profiles rather than individually providing each pin with a unique material identity. This project examined assembly thermal flux distributions and grouped pins based on thermal flux exposure. Fuel pins with similar compositions located in a region of similar thermal flux were given the same material identification number and were depleted as a lumped material.

Material lumping saved computing time but does reduce accuracy at the pin level isotope inventory. The following sections described the process of defining material depletion regions used for this project.

A.6.1: 13AU (or 22AU) Material Depletion Regions

Figure 56 shows FA 13AU modeled in T-Newt. The 312 fuel pins in FA 13AU are 1.3% enriched ^{235}U . The pin map is identical for 22AU assembly however the enrichment is slightly higher at 2.2% ^{235}U . The fuel pins are in red. The moderator is in blue. The control rod guide channels are filled with moderator and are colored light green. The central guide tube is filled with moderator and is purple. The stiffening plate is in place on each corner (red).

Figure 57 show the thermal flux profile for the FA 13AU with regions of similar flux identified.

- Region 1: The region contains fuel pins closest to the central guide tube. The central guide tube is used for in-core instrumentation and monitoring. Thus, the volume of the channel is primarily filled with moderator even when taking into consideration of presence of any core instrumentation equipment. This region is unlikely to undergo any changes in its material composition throughout the cycle of the core (Material Regions: green pins).
- Region 2: This region contains fuel pins in close proximity to the inner loop of control rod guide tubes. As seen in Figure 57, the guide tubes, when filled with either moderator (rods out) or with absorber (rods in), alter neutron flux in the fuel pins from the rest of assembly (Material Regions: dark blue pins).
- Region 3: This region contains the fuel pins located in proximity to the outer loop of control rod guide tubes. As with Region 2, the depletion of materials in these fuel pins will differ from other parts of the assembly due to the impact of the guide tube materials on neutron flux (Material Regions: yellow pins).
- Region 4: This region consists of pins located along the edge of the assembly that is not bounded by the corner stiffening plates. Figure 57 illustrates that fuel pins unbounded by the corner stiffening plates have a slightly higher flux than those pins that are bounded by the stiffening plate (Material Regions: light blue pins).
- Region 5: All fuel pins not included in regions 1-4 are part of region 5 (Material Regions: red pins).

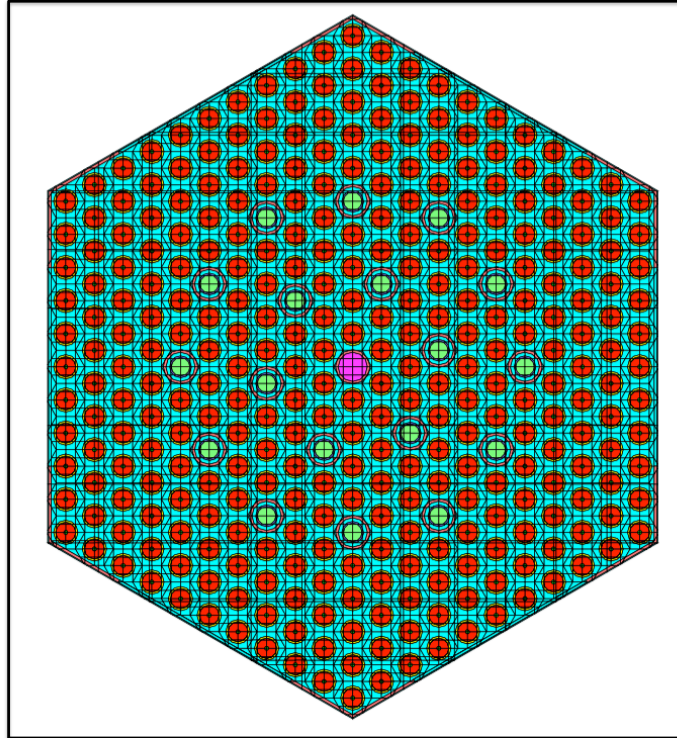


Figure 56: FA 13AU T-Newt Model

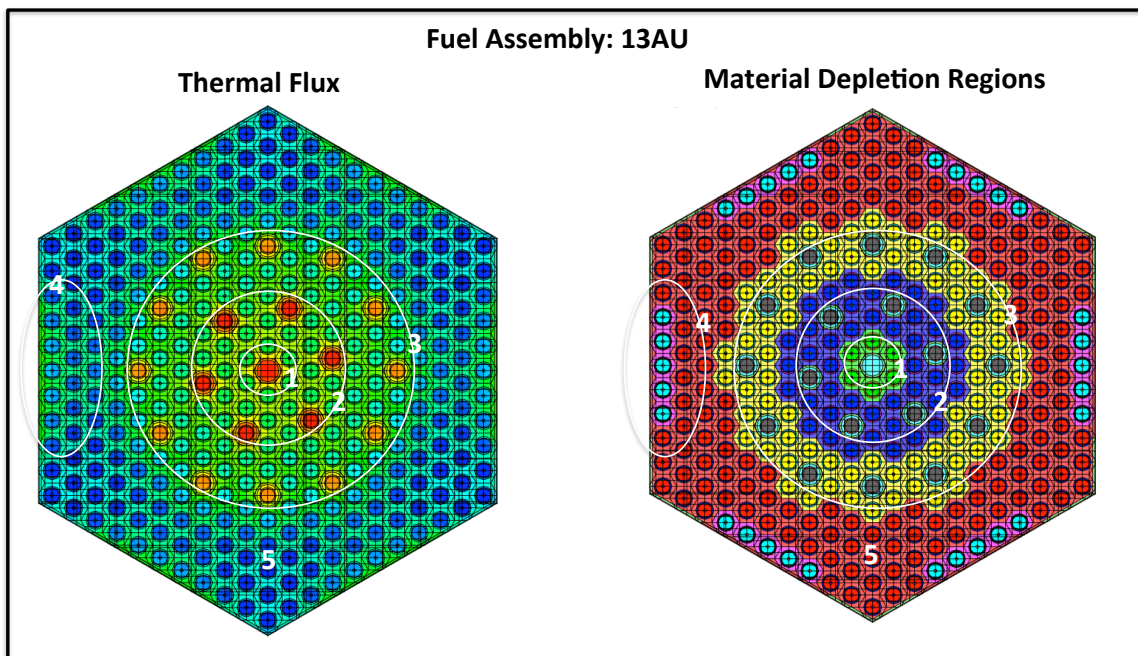


Figure 57: FA 13AU Thermal Flux Profile With Material Regions Defined

A.6.2: 30AV5 Material Depletion Regions

Figure 58 illustrates TVSA FA 30AV5 which consists of 303 fuel pins (red) enriched at 3.00% ^{235}U and 9 burnable absorber (BA) pins (dark).

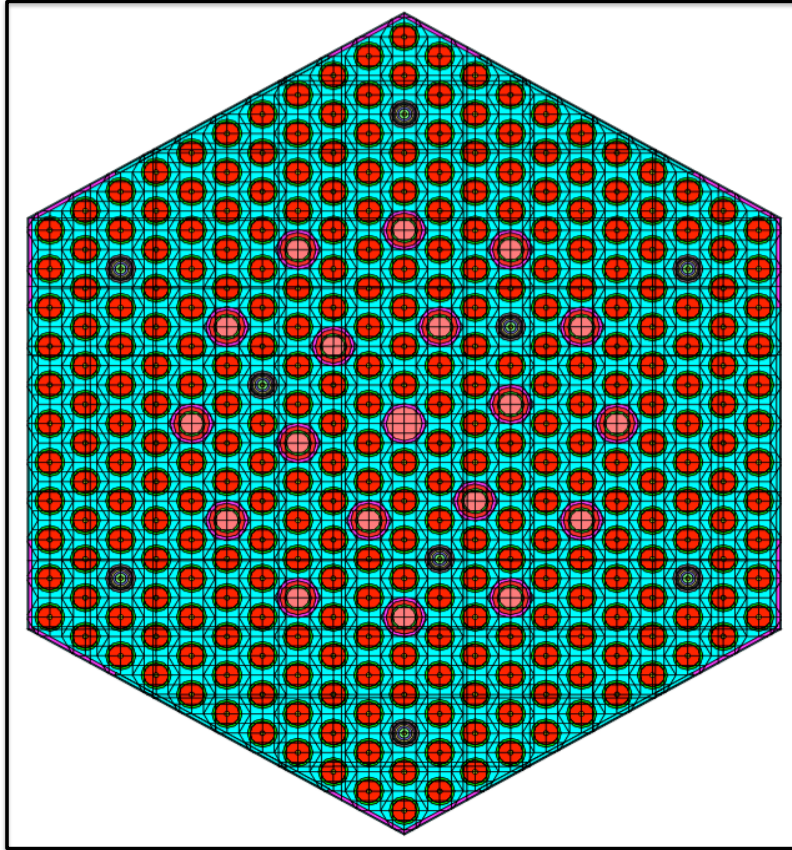


Figure 58: FA 30AV5 Modeled in T-Newt

FA 30AV5 differs from the previous assemblies due to the presence of nine burnable absorber fuel pins. The BA pins are 5% Gd_2O_3 and 95% UO_2 . The UO_2 has a ^{235}U enrichment of 2.4%. [16, 17] These pins require special attention due to the mixing of a strong neutron absorber and the enriched fuel. Modeling BA pins in TRITON requires the use of a multiregion cell with five concentric rings of the fuel/absorber mix.[38] The thermal flux at each of BA pins is depressed by the presence of the absorber. The flux depression will result in differences in depletion of fuel materials not only in the pins themselves but also in surrounding fuel pins.

As the burnable absorber material depletes through the core fuel cycle, the flux profile of the pin changes significantly. The complex nature of the pin necessitates special modeling treatment. Each BA pin is treated as a unique geometric unit. All materials inside the pins, to include each of the five concentric fuel circles, are also unique. Uniquely identifying the materials allows for greater accuracy when depleting the pins over the life of the fuel cycle.

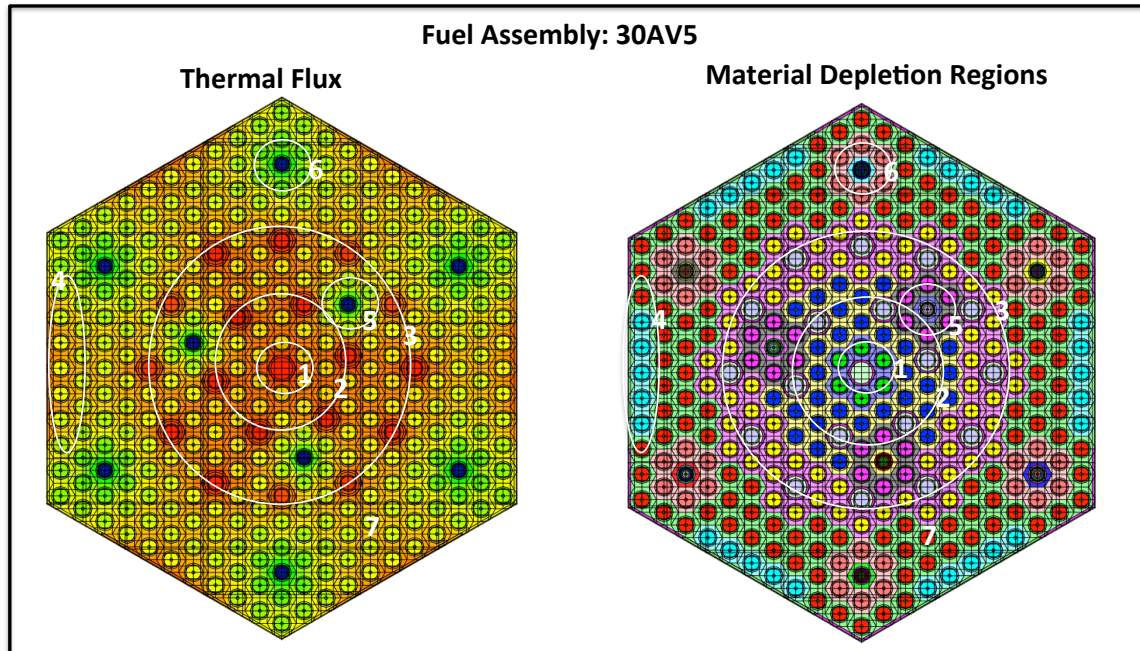


Figure 59: FA 30AV5 Thermal Flux Profile With Material Regions Defined

Figure 59 shows the thermal flux of FA 30AV5. The BA absorber fuel pins are highly visible because they have a much lower thermal neutron flux as compared to the rest of the assembly. Figure 59 also shows the material depletion regions selected.

- Region 1: This region contains fuel pins closest to the central guide tube (green pins).
- Region 2: This region contains fuel pins in close proximity to the inner loop of control rod guide tubes (dark blue pins).
- Region 3: This region contains the fuel pins located in proximity to the outer loop of control rod guide tubes (yellow pins).
- Region 4: This region consists of pins located along the edge of the assembly that are not bounded by the corner stiffening plates (light blue pins).
- Region 5: This region consists for fuel pins surrounding inner loop BA pins. The inner loop BA pins are symmetrically located inside the core and thus have the

same thermal neutron flux distribution. The five fuel pins surrounding each inner BA pin will be most influenced by the decreased thermal neutron flux caused by the presence of the neutron absorber and thus, these pins must be depleted as a separate region (magenta pins).

- Region 6: This region consists for fuel pins surrounding outer loop BA pins. As with Region 5, these fuel pins will be most directly influenced by the presence of the neutron absorber in the BA pin and must be depleted as a separate region (pink pins).
- Region 7: All fuel pins not included in regions 1-6 are part of Region 7 (red pins).

A.6.3: 39AWU Material Depletion Regions

Figure 60 illustrates TVSA FA 39AWU which consists of 243 fuel pins (red) enriched at 4.00% ^{235}U , 60 fuel pins (purple) enriched at 3.60% ^{235}U , and 9 burnable absorber pins (dark).

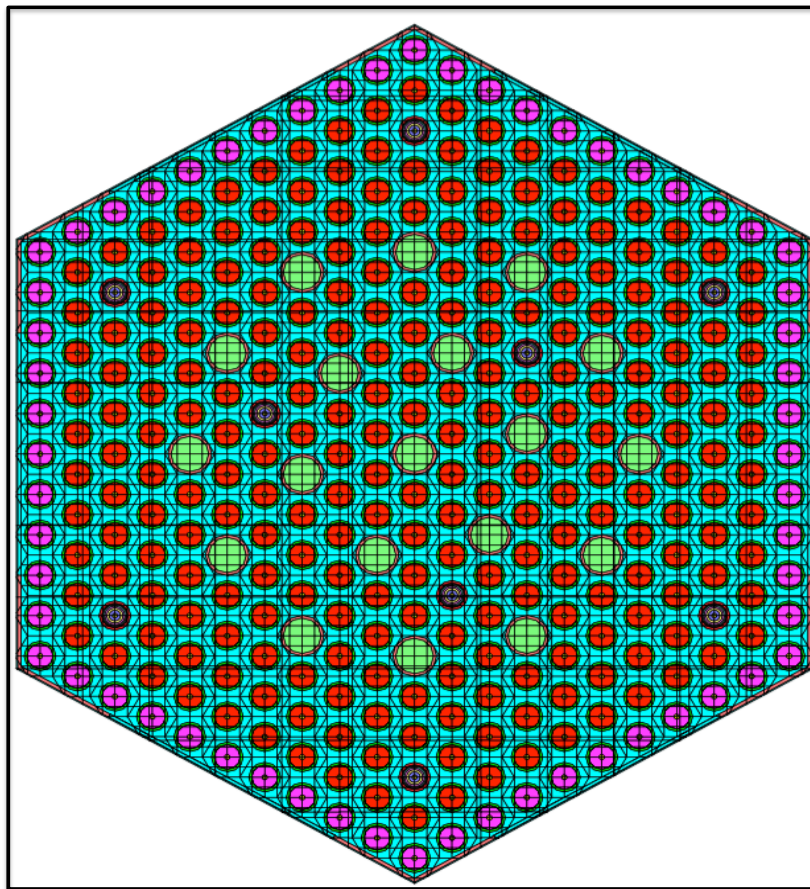


Figure 60: FA 39AWU Model t-newt

The 9 BA pins in FA 39AWU are physically located in the same positions as those found in FA 30AV5. All BA pins consist of 5% Gd₂O₃ and 95% UO₂. The UO₂ has a ²³⁵U enrichment of 3.3%. All fuel pins on the outer edge of the assembly are enriched at 4.00% ²³⁵U. All internal fuel pins are enriched to 3.60% ²³⁵U. [16, 17]

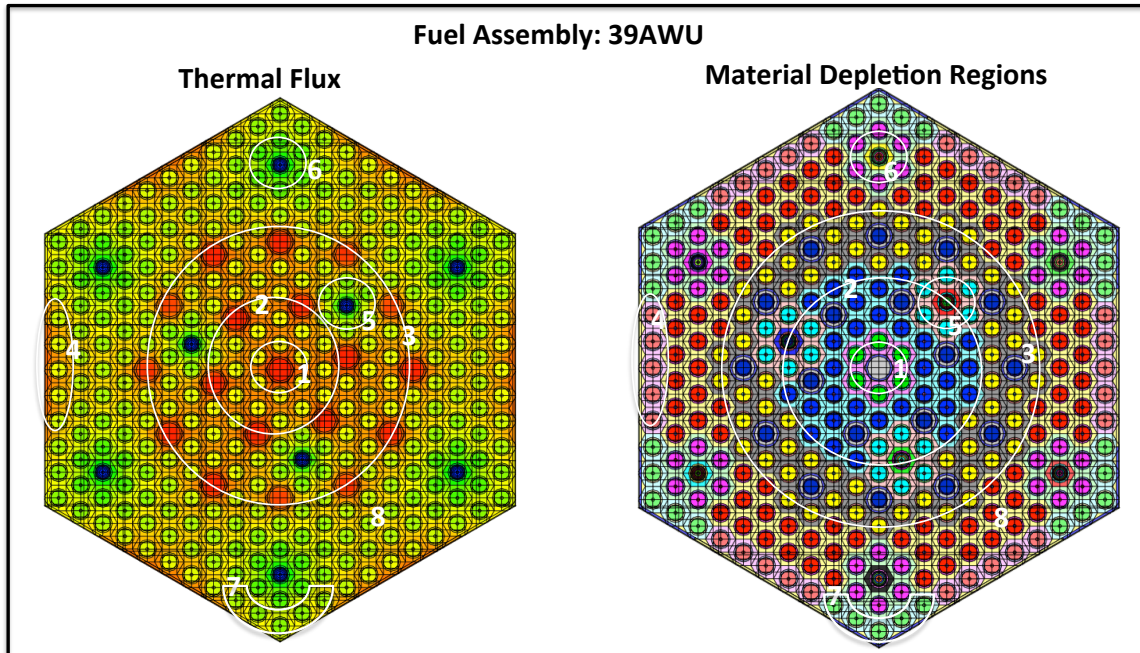


Figure 61: FA 39AWU Thermal Flux Profile With Material Regions Defined

The material depletion regions for FA 39AWU are similar to those in 30AV5 however due to the difference in enrichment of fuel pins on the outer edge of the assembly an additional fuel region is necessary. Figure 61 shows the thermal flux for assembly 39AWU as well as the material depletion regions. The material depletion regions are defined as follows:

- Region 1: This region contains fuel pins closest to the central guide tube (green pins).
- Region 2: This region contains fuel pins in close proximity to the inner loop of control rod guide tubes (dark blue pins).
- Region 3: This region contains the fuel pins located in proximity to the outer loop of control rod guide tubes (yellow pins).
- Region 4: This region consists of pins located along the edge of the assembly that are not bounded by the corner stiffening plates (pink pins).
- Region 5: This region consists for fuel pins surrounding inner loop BA pins (light blue pins).

- Region 6: This region consists for fuel pins surrounding outer loop BA pins (magenta pins).
- Region 7: Fuel pins located on the outer edge of the assembly but bounded by the stiffening angle (light green pins).
- Region 8: All fuel pins not included in regions 1-6 are part of Region 8 (red pins).

A.6.4: 390GO Material Depletion Regions

Figure 62 is a T-Newt model of TVSA FA 390GO which consists of 240 fuel pins (red) enriched at 4.00% ^{235}U , 66 fuel pins (purple) enriched at 3.60% ^{235}U , and 6 centrally located burnable absorber pins (dark/black).

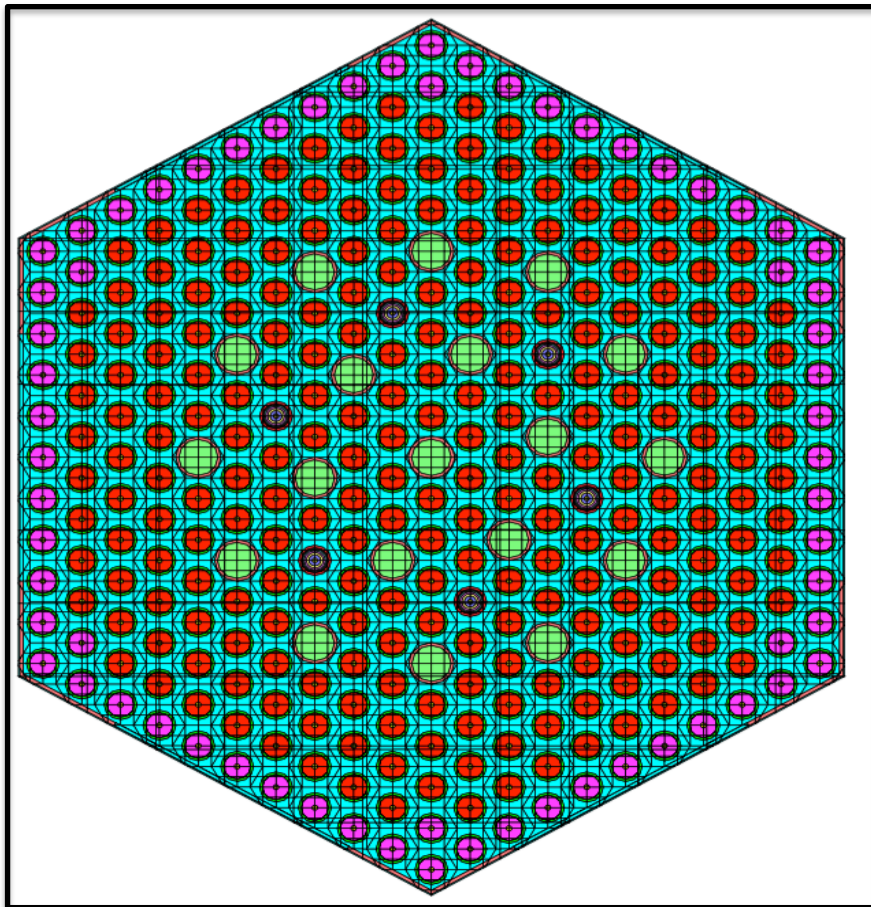


Figure 62: FA 390GO T-Newt Module

Fuel assembly 390GO has 6 burnable absorber pins and all pins are located equidistance from the center of the assembly. The BA pins consist of 5% Gd_2O_3 and 95% UO_2 . The UO_2 is 3.3% ^{235}U enriched. The outer edge of the assembly consists of fuel pins with an enrichment of 4.00% ^{235}U and the internal fuel pins are enriched at 3.60% ^{235}U . There is one additional 4.00% enriched fuel pin at each corner of the assembly. [16, 17]

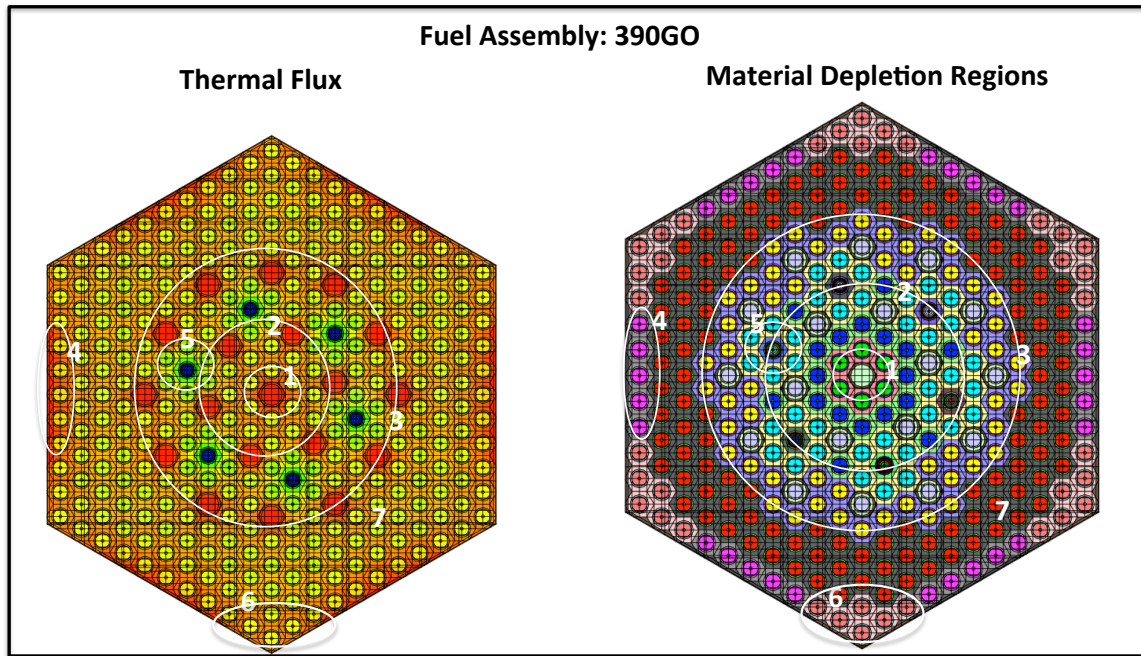


Figure 63: FA 390GO Thermal Flux Profile With Material Regions Defined

Figure 63 shows the thermal flux for assembly 390GO as well as the material depletion regions. The material depletion regions are defined as follows:

- Region 1: This region contains fuel pins closest to the central guide tube (green pins).
- Region 2: This region contains fuel pins in close proximity to the inner loop of control rod guide tubes (dark blue pins).
- Region 3: This region contains the fuel pins located in proximity to the outer loop of control rod guide tubes (yellow pins).
- Region 4: This region consists of pins located along the edge of the assembly that are not bounded by the corner stiffening plates (magenta pins).
- Region 5: This region consists for fuel pins surrounding inner loop BA pins. Only inner loop BA pins are present in this assembly (light blue pins).
- Region 6: Fuel pins located on the outer edge of the assembly but bounded by the stiffening angle. Note the additional fuel pin in each corner of the assembly (light pink pins).

- Region 7: All fuel pins not included in regions 1-6 are part of Region 7 (red pins).

A.7: VVER Assembly Origami Material Libraries

ORIGEN requires a library file (ft33f001 files) containing pre-generated burnup depended cross-sections for materials the user requests to deplete. When using ORIGEN as part of a T-Depl sequence, the code either calls from a selection of pre-supplied libraries or NEWT creates its own ORIGEN libraries depending on how the user defined the problem. SCALE 6.2 contains a robust collection of pre-calculated ORIGEN reactor libraries spanning a wide variety of reactor fuel types, fuel material, enrichment, and moderator properties.[12, 51]

ORIGAMI is a SCALE depletion code that tailors the capabilities of ORIGEN for LWR assembly modeling and provides the user a 3D depletion analysis capability. ORIGAMI can conduct pin-level depletion analysis in the XY plane as well as axial depletion analysis. This greatly expands the ability of a researcher to explore discrete isotopic regions within a LWR fuel assembly. ORIGAMI uses ORIGEN for depletion and therefore also requires pre-generated burnup dependent cross section files for the materials being depleted.[12, 13, 51]

This project used ORIGAMI to model depletion for the FA 13AU assembly only. Unique ORIGEN cross-section libraries were created for FA 13AU for all possible assembly configurations used in this project. Both combined and mixture specific ORIGEN libraries were created for each configuration. The FA 13AU assembly had five material groups defined. Generating both assembly homogenized and material specific cross-section libraries gave the researcher maximum flexibility when studying the VVER assembly.

The T-Depl model used to generate ORIGEN libraries is identical to the model used for generating NESTLE cross-section libraries with the exception of the branch block. When creating ft33f001 files, TRITON does not utilize the branch feature therefore individual T-Depl models were needed for each assembly configuration. The following is a list of

ORIGEN cross-section libraries created for the analysis in this project. These libraries include models with control rods in, control rods out, and SS316 filling the control rod guide tubes. The input files used to generate these cross-section libraries can be found in Appendix E.

- FA 13AU Normal Control Rod Out (CRO)
 - FA13AU6.2.1_CROcombined.f33
 - FA13AU6.2.1_CROmix0001.f33
 - FA13AU6.2.1_CROmix0011.f33
 - FA13AU6.2.1_CROmix0012.f33
 - FA13AU6.2.1_CROmix0013.f33
 - FA13AU6.2.1_CROmix0014.f33
- FA 13AU Normal Control Rod In (CRI)
 - FA13AU6.2.1_CRIcombined.f33
 - FA13AU6.2.1_CRImix0001.f33
 - FA13AU6.2.1_CRImix0011.f33
 - FA13AU6.2.1_CRImix0012.f33
 - FA13AU6.2.1_CRImix0013.f33
 - FA13AU6.2.1_CRImix0014.f33
- FA 13AU Stainless Steel in Control Rod Guide Tubes
 - FA13AU6.2.1_SScmbined.f33
 - FA13AU6.2.1_SSmix0001.f33
 - FA13AU6.2.1_SSmix0011.f33
 - FA13AU6.2.1_SSmix0012.f33
 - FA13AU6.2.1_SSmix0013.f33
 - FA13AU6.2.1_SSmix0014.f33

A.8: VVER Reflector Cross-Sections

NESTLE provides the user the option to define materials as fuel or non-fuel. This gives the user the ability to add material such as structures and reflectors the nodal core simulation. The benchmark study provides information for three reflector regions: a radial reflector, a bottom axial reflector, and a top axial reflector. Incorporating reflectors in the NESTLE VVER 1000 model required the development and incorporation of reflector cross-sections into the cross-section library.

SCALE's discrete ordinate transport code NEWT generates the xfile016 cross-section information for the fuel assemblies as previously discussed. With non-fuel material such as reflectors, depletion analysis is not required so the SCALE sequence used is only T-

NEWT. T-NEWT generates both cross-sections and assembly discontinuity factors (ADF). When collapsing energy groups and homogenizing assembly cross-sections for a nodal simulator, NEWT calculates a unique homogenized flux as part of the transport solution. The homogenous flux can also be thought of as the average flux across the assembly. Because the homogenous flux is an approximation rather than an exact solution, a discontinuity occurs at the boundary of the assembly and cause problems for nodal simulators that calculate flux across a series of assemblies in a core. [12] [51]

In order to compensate for discontinuity at assembly boundaries, nodal simulators use ADFs to preserve reaction rates and currents at assembly boundaries. The true flux of the assembly is the heterogeneous flux and is calculated by NEWT as part of the complete transport solution. At the boundary of an assembly, the true flux is the average surface flux on the boundary. The ADF is the ratio of the heterogeneous flux to the homogenous flux or the ratio of the average boundary surface flux to the assembly average flux. [12] [51] NEWT can calculate reflector ADFs however it only calculates the ADF in one dimension. The VVER 1000 assembly is hexagonal meaning that the fuel assemblies in the core will interact with reflector on more than one face and thus requires 2D treatment. NEWT is unable to calculate a reflector ADF for a boundary with this geometry.

The challenge of calculating VVER reflector ADFs for use in nodal simulators is known. (Ward et al., 2010) modeled the hexagonal fuel-reflector boundary in a manner similar to that of a square lattice with the calculation being done using only one face.[64] While this method allows for the collapsing of few-group homogenized cross-sections in the reflector region the ADFs generated are physically inaccurate. (Mittag et al., 2003) presented a 2D method for calculating ADFs for VVER cores.[65] (Luciano and Maldonado, 2017) improved the Mittag 2D method of calculating ADFs and demonstrated significant improvements the core periphery pin power calculations for VVER nodal simulations.[45] This paper calculates the VVER 1000 reflector cross-sections using an approach similar 1D method presented as a sample problem in the SCALE 6.2.1 manual description of NEWT.[66] The SCALE sample problem models a single radial section of a MOX core bounded by a large water reflector is modeled in 1D to calculate the reflector few-group homogenized cross-section and ADFs. This paper

takes a similar approach when generating radial and axial reflectors for the VVER-1000 core modeled. A single radial (or axial for top and bottom reflectors) slice from core center to the outer reflector boundary is modeled in one dimension. Careful attention is paid to the dimensions of the reflector material so as to ensure material proportions are correct for cross-section processing. The fuel assemblies for all reflector models simply intended to provide a neutron source for the model. The fuel consists of hexagonal 3.00% ^{235}U enriched UO_2 pins with triangular pitch equal to that of the VVER-1000 fuel pins. The pins are arrayed in a cuboid with a length equal to half the pitch of the VVER fuel assembly. The fuel region then uses as many fuel cuboids as needed to have the equivalent dimension of the distance from core center to outer edge of the reflector boundary. Figure 64 illustrates the radial reflector 1D model.

Table 20 lists the reflector material compositions. The benchmark studies provided a composition for steel that is slightly different than SS304s. SS304s contains 0.5% to 1.5% difference in Cr, Fe, Mn, and Ni as well as trace amounts of C, Si, and P. For the top axial reflector, the benchmark composition of moderator, steel and zircaloy (Mod/St.Zr C and Mod/St/Zr D) did not sum to 100% therefore the missing material was assumed to be moderator. The top and bottom axial reflectors include 2 cm of E100, the spacer grid alloy, to account for upper and lower assembly structural material. Table 21 lists the dimensions and materials used when modeling the three reflectors used for this project. The input file for T-NEWT separately homogenized the fuel material and reflector material. The reflector cross sections were manually added to the NESTLE cross-section library. Input files for the reflector models can be found Appendix E. Due to the known inaccuracy of the hexagonal ADF calculation, the NEWT generated ADFs were not used. Instead the ADF for the reflectors was defined such that the heterogeneous flux and homogeneous flux were equal ($\text{ADF} = 1.0$). While inaccurate, the impact of the approximation would be most felt at the core periphery.[45] [65] Analysis for this project focused on the depletion of assemblies internal to the core and not near the periphery. Further improvements to the model could be gained from accurately defining the fuel-reflector boundary discontinuity factors but would likely only impact assemblies on the outer boundary of the core.

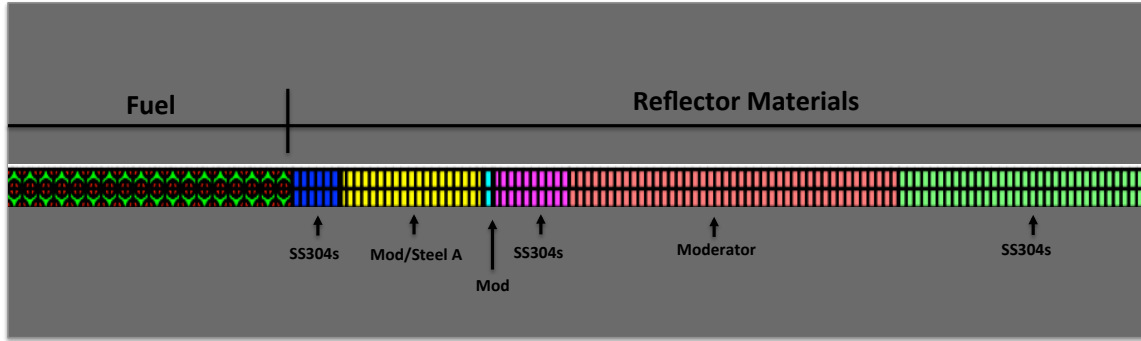


Figure 64: Radial Reflector 1D Newt Model

Table 20: VVER Reflector Material Composition

VVER Reflector Compositions					
Material Name	Composition		Material Name	Composition	
	Material	% Comp		Material	% Comp
Mod/Steel A	Moderator	45.6	Mod/St/Zr A	Moderator	58
	SS304s	54.4		SS304s	7
Mod/Steel B	Moderator	67		Zirc4	35
	SS304s	33	Mod/St/Zr B	Moderator	57
Mod/Steel C	Moderator	98.9		SS304s	33
	SS304s	1.1		Zirc4	10
E110	Zirconium	98.97	Mod/St/Zr C	Moderator	56
	Niobium	1		SS304s	2
	Hafnium	0.03		Zircaloy	11.8
Steel Temp: 563.15 K (coolant inlet temp)			Mod/St/Zr D	Moderator	56
Steel used is SS304s from Scale Standard composition				SS304s	1.9
				Zirc4	30.6

Table 21: VVER Reflector Model Dimensions

VVER Reflector Models							
Radial							
Region	Fuel	Reflector					
Material	UO ₂ 3.00% Enriched U235	SS304s	Mod/Steel A	Moderator	SS304s	Moderator	SS304s
Dimension (cm)	149.175	4	11.3	1	6	26.45	19.8
Bottom Axial							
Region	Fuel	Reflector					
Material	UO ₂ 3.00% Enriched U235	E110 Spacer	Mod/St/Zr A	Mod/St/Zr B	Mod/Steel B		
Dimension (cm)	172.125	2	2.3	1.7	25		
Top Axial							
Region	Fuel	Reflector					
Material	UO ₂ 3.00% Enriched U235	E110 Spacer	Mod/St/Zr C	Mod/St/Zr D	Mod/Steel C		
Dimension (cm)	172.125	2	22.2	4.5	5.5		

Appendix B NESTLE VVER-1000 Model Benchmark Comparison

This appendix presents a detailed description of the NESTLE VVER-1000 model created and compares its results to those of the benchmark publications. The VVER-1000 benchmark publications used throughout this analysis are a series of three documents from Lotsch T., Khalimonchuk V., and Kuchin A presented from 2009-2011 in the *Symposium of Atomic energy Research on WWER Physics and Reactor Safety*. [16-18]

B.1: VVER-1000 Benchmark Reactor

The VVER series of pressurized light-water reactors (PWR) are incredibly common throughout the world. Russia's national nuclear energy company ROSATOM has a robust reactor export program.[67] The VVER reactor series differs significantly from Western PWRs. Most noticeable is the core configuration, which uses triangular pitch lattice as opposed to a square pitch lattice. The hexagonal core requires a different geometric treatment than Western square lattice configurations. VVERs also have a different number and orientation for their steam generators. VVER-1000 reactors have four steam generators, orientated horizontally, while Western PWRs orient their two steam generators vertically.[52] Other core characteristics are similar to Western PWRs such as power output, reactor pressure, and coolant/moderator properties.

Table 22 provides a list of general reactor characteristics for the VVER-1000. Figure 65 illustrates the first cycle core loading. Each fuel assembly has 312 annular fuel pins with differing levels of enrichment. The core of a VVER consists of 163 hexagonal fuel assemblies. The fuel assembly has 18 control rod guide tubes and one central guide tube. The reactor uses borated water as both a coolant and a moderator.

There are 61 RCCAs that insert 18 $Dy_2O_3 \cdot TiO_3$ and B_4C control rods. Reactivity is also controlled early in the cycle through the presence of burnable absorber pins that contain a mixture of 5.00% Gd_2O_3 and 95% UO_2 (differing levels of uranium enrichment).

Figure 66 shows the location of the control rod working groups for the first core load. Both Figure 65 and Figure 66 were taken directly from the 2009 benchmark publication [16]

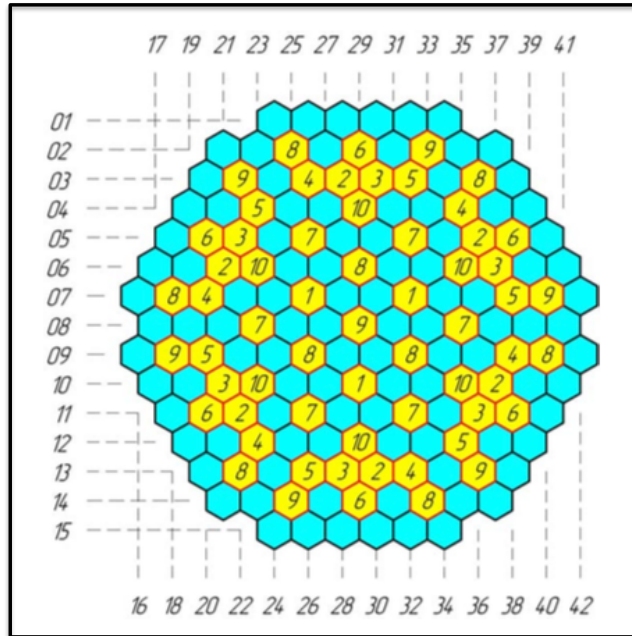


Figure 66: Control Rod Working Groups First Core Load (Adapted from Figure 5 in [16])

Figure 67 shows the locations of the VVER-1000 core control rod clusters as modeled in NESTLE from the data provided in Figure 66.

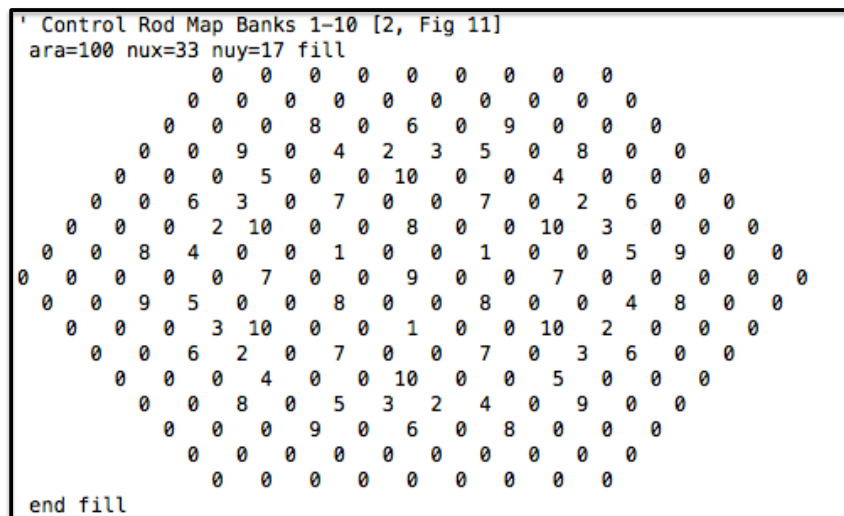


Figure 67: NESTLE Input File Control Rod Array

The reactor in the first benchmark cycle operated for 311 EFPD. Unlike typical reactor cycles that try to operate at a constant power level, this reactor had a variety of power fluctuations during its first cycle. Full power was not reached until approximately 50 EFPD. The researchers in the benchmark study attribute both the first cycle power build-up and fluctuations to initial cycle core testing but do not specify the nature of the testing.[16] Figure 68 shows a graph of the reactor percent power for the first cycle. The initial power build up is noticeable as well as power fluctuations in the later part of the cycle

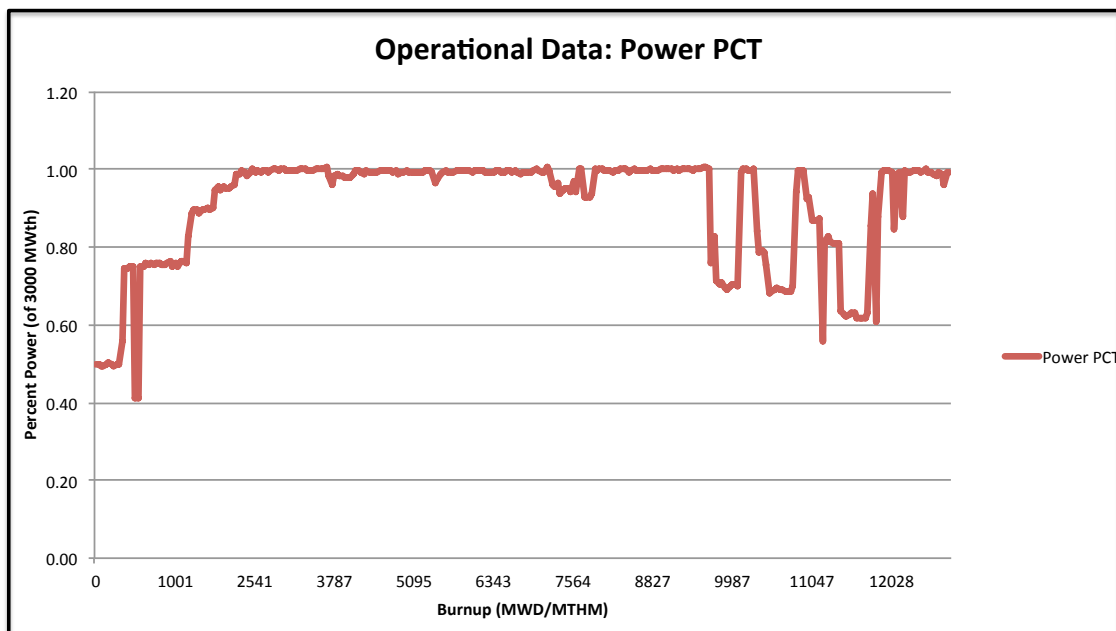


Figure 68: First Cycle Power History

B.2: NESTLE VVER-1000 Benchmark Model

NESTLE requires geometric, thermodynamic, and nuclear operating information to build a nodal core simulation. The following section provides an overview of the inputs used to create a NESTLE VVER-1000 model. The NESTLE input files for this project are found in Appendix E.

A single node in the NESTLE VVER-1000 model is hexagonal in shape with a bundle pitch of 9.2441 inches and an axial dimension of 13.898 inches. The total core model consists of 211 radial nodes arranged in a hexagonal array. A radial slice of the core

consists of nodes representing five fuel assemblies surrounding by one ring of radial reflector nodes. Figure 69 shows the NESTLE input defining a single radial slice of the core. The lattice ID numbers in Figure 69 correspond to the assembly specific, burnup dependent cross-sections found in the cross-section library.

```
' Core loading map for fuel [1, Figure 16]
ara=1 nux=33 nuy=17 fill
  0  1  1  1  1  1  1  1  1  0
    1  1  8  7  7  7  7  8  1  1
      1  8  6  5  6  5  6  5  6  8  1
        1  7  5  5  4  4  4  4  5  5  7  1
          1  7  6  4  4  6  5  6  4  4  6  7  1
            1  7  5  4  6  5  4  4  5  6  4  5  7  1
              1  7  6  4  5  4  6  5  6  4  5  4  6  7  1
                1  8  5  4  6  4  5  4  4  5  4  6  4  5  8  1
                  0  1  6  5  4  5  6  4  6  4  6  5  4  5  6  1  0
                    1  8  5  4  6  4  5  4  4  5  4  6  4  5  8  1
                      1  7  6  4  5  4  6  5  6  4  5  4  6  7  1
                        1  7  5  4  6  5  4  4  5  6  4  5  7  1
                          1  7  6  4  4  6  5  6  4  4  6  7  1
                            1  7  5  5  4  4  4  4  5  5  7  1
                              1  8  6  5  6  5  6  5  6  8  1
                                1  1  8  7  7  7  7  8  1  1
                                  0  1  1  1  1  1  1  1  0
end fill
```

Figure 69: NESTLE Core Input

There are 12 axial layers in the core. Axial nodes 2-11 consist of fuel and radial reflector material and are arrayed as specified in Figure 69. Axial nodes 1 and 12 are the bottom and top reflector respectively. NESTLE requires additional inputs through the use of keywords defining characteristics of the fuel, number of fuel pins, and the fuel to moderator ratio. This information is available on the input file found in Appendix E.

Control rod positions are defined for each burnup step. The benchmark documentation implies that control rod working groups 1-9 are used for shutdown only and thus they are modeled as fully out of the core. The position of control rod working group 10 is provided in the cycle 1 operating data and changes slightly with each burnup step.

The NESTLE VVER-1000 model defines the control rods as B₄C only. This is a deviation from the benchmark that defines the lower portion of the rod as Dy₂O₃•TiO₃ and the upper portion as B₄C.

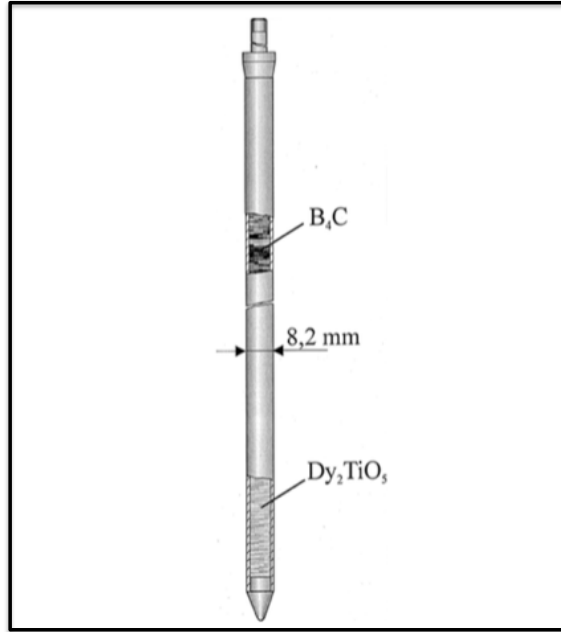


Figure 70: B_4C and Dy_2TiO_3 Rod Example taken from Figure 10 in [68]

Figure 70 illustrates a VVER fuel rod with a $Dy_2O_3 \cdot TiO_3$ and B_4C composition.[68] The decision to model the control rod as B_4C only was done for ease of modeling. Tracking the axial position of the $Dy_2O_3 \cdot TiO_3$ and B_4C sections of the rod with respect to the core, while achievable, would be input intensive when studying the control rod scenario. This approximation could be a source of model error and will be discussed in future sections.

Other core characteristics not modeled in the NESTLE VVER-1000 model are the self-powered neutron detectors (SPND) and assembly spacer grids. The benchmark study provides a core map detailing both the radial and axial position of the SPND.[17] Modeling the SPND would require significant input file modification and reduce user flexibility. Each assembly has 13 spacer grids in the active fuel portion of the assembly. [17] Fuel-region spacer grids were not modeled in NESTLE however the spacer grids at the top and bottom of the assemblies were included in the modeling of the axial reflector cross-sections.

The power density of the core was calculated to be 111.68 kw/liter. The calculation involved multiplying the fuel power density by the fraction of the fuel that is uranium and

the density of the fuel. NEWT volume fractions were used to find the fraction of the fuel that is uranium. The fuel density provide by the 2009 benchmark gave a range of UO_2 densities from $10.4 \text{ g}\cdot\text{cm}^3$ to $10.7 \text{ g}\cdot\text{cm}^3$. [16] The modeling for this project assumed an average density of $10.55 \text{ g}\cdot\text{cm}^3$. The core power density seems higher than expected. The Advanced Reactor Information System (ARIS), an IAEA database, lists the VVER-1000 as having a power density of 108 kw/l . [52] Likely the density of UO_2 provided in the benchmark is at room temperature and does not account for the reactor operating temperature. In order to ensure agreement between cross-section files and the three modeling codes, density of the fuel was maintained at $10.55 \text{ g}\cdot\text{cm}^3$ and could be a potential source error. The impact of the higher than expected power density will be discussed in future sections.

The core coolant flow rate, provided in the benchmark study, is $88,000 \text{ m}^3/\text{hr}$. [17] The core coolant is borated water. The benchmark provided the thermodynamic information is found in Table 23.

Table 23: VVER-1000 Benchmark Coolant Properties

VVER-1000 Benchmark	
Core Thermodynamic Properties	
Power (MWth)	3000
Average Moderator Temperature (K)	578
Coolant Outlet Pressure (MPa)	15.7
Coolant Flow Rate (m^3/hr)	88000
Coolant Temp at Core Inlet (K)	563.15
Coolant Temp at Core Outlet (K)	592.75

When calculating the necessary NESTLE thermodynamic inputs, the coolant is assumed to be water. Wolfram Alpha steam tables were used to calculate additional coolant information. [63] MATLAB polyfit tool was used to generate a number of NESTLE required thermodynamic fit coefficients. [69] These inputs and fit coefficients can be found in Appendix E in the NESTLE input files.

The core begins in a clean configuration, with no xenon or samarium present, and then goes to equilibrium after the first burnup step. While this is physically inaccurate, it is not possible in NESTLE to model the fission product buildup and equalization that occurs early in a fuel cycle. Since isotope analysis of core assemblies occurs at late in the cycle, this limitation should not be a factor.

B.3: NESTLE VVER-1000 Benchmark Results

The benchmark publication provided 323 points of operating data for the first cycle. This data included EFPD, percent power, control rod position, percent coolant flow rate, boron concentration, and coolant inlet temperature. Two models were created using this data. One modeled contained all 323-data points while the other used every 5th measurement resulting in a faster running 63-point model.

To verify the accuracy of the NESTLE VVER-1000 model and determine model bias, two tests were run. The first test involved running VVER-1000 model using the cycle 1 operating specifications provided in the benchmark. Both the 323-point and 63-point data models were run for this test.

It was assumed that the reactor operator would set control parameters such that the reactor would at critical for the entirety of the fuel cycle. Therefore the first test compared the NESTLE VVER-1000 k-eff to a criticality of 1.0. Figure 71 shows the results of the 323-point model. Figure 71 shows a number of operating fluctuations consistent with the cycle-1 power history in Figure 68.

Figure 72 shows the results of the abbreviated 63-point model. It too shows evidence of the operating fluctuations throughout cycle-1 however to a lesser extent than the full 323-point model.

Both the 323-point and 63-point models reveal a reactor that is less than critical. Figure 73 shows that the k-eff for the NESTLE VVER-1000 model remains about 1000 pcm below critical.

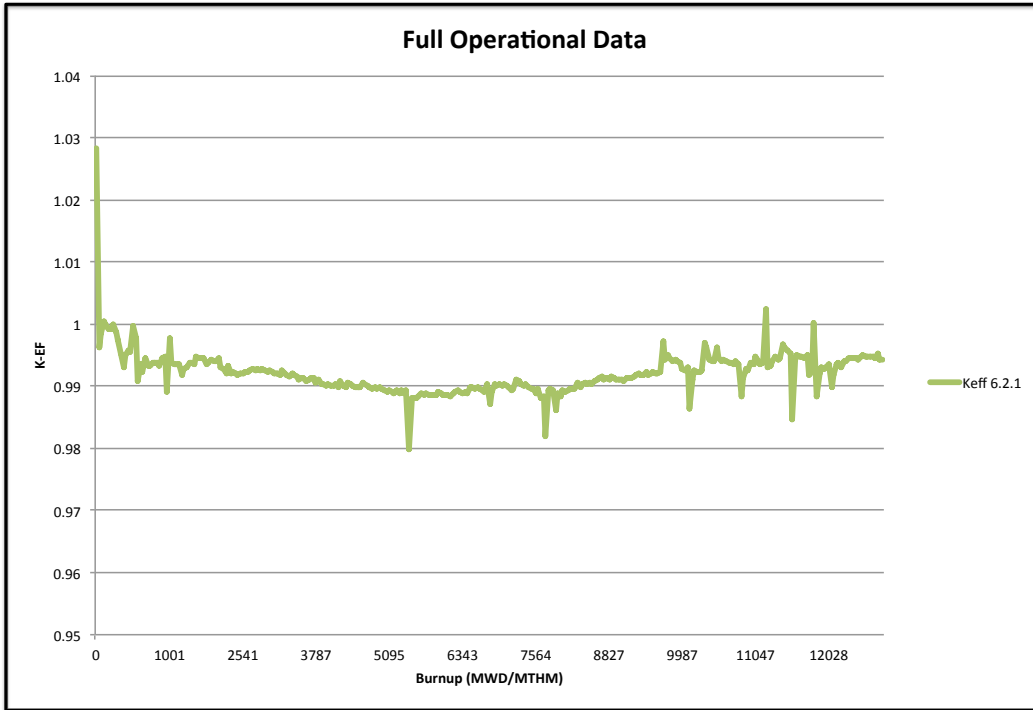


Figure 71: NESTLE k-eff VVER-1000 Model 323 Data Points

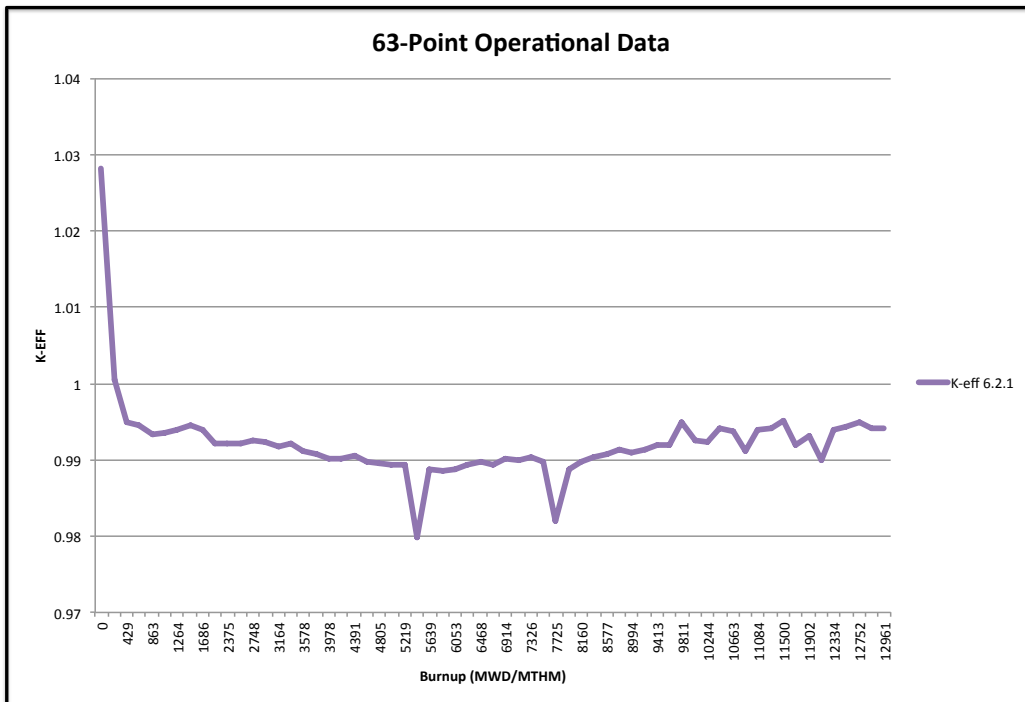


Figure 72: NESTLE k-eff VVER-1000 Model 63 Data Points

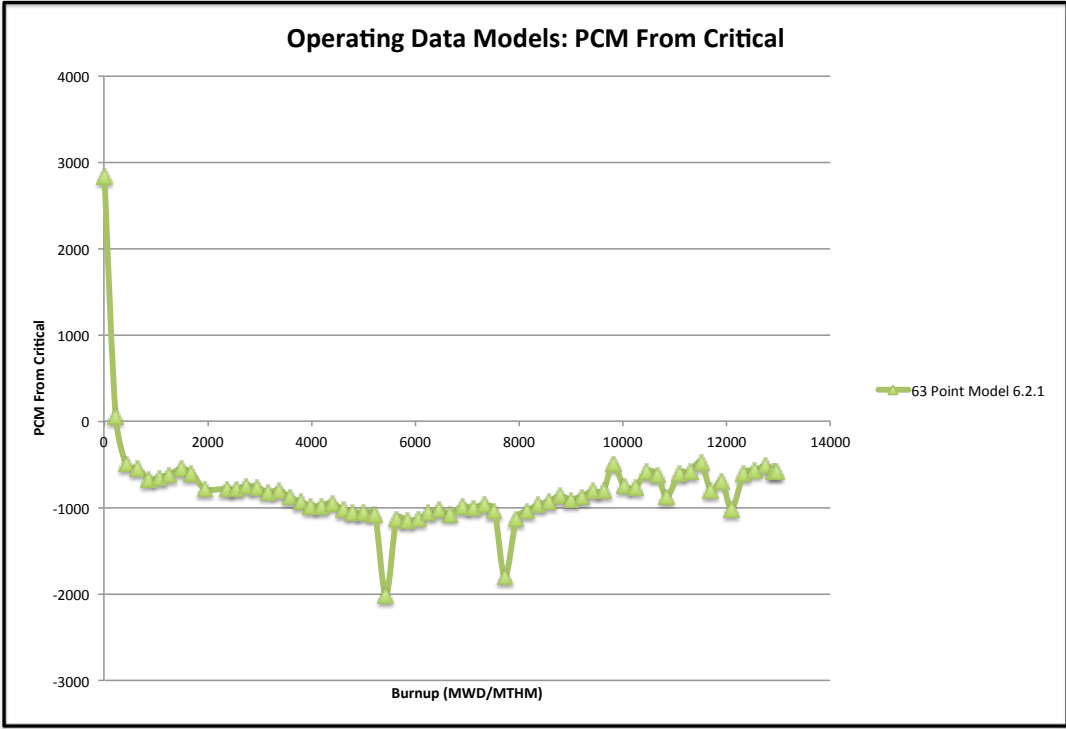


Figure 73: PCM from Critical (k-eff 1.0) 63-Point Model

The second test used to verify the accuracy and bias of the NESTLE VVER-1000 model used the critical boron level and compared it to the boron concentrations provided in the benchmark document. NESTLE has the capability to do criticality searches wherein it fixes criticality and allows another variable to fluctuate. In the case of boron letdown modeling, NESTLE assumes a criticality of 1.0 and calculates the necessary boron concentration. For this test, all benchmark parameters remained the same with exception of boron, which was calculated by NESTLE. The second test used only the 63-point model.

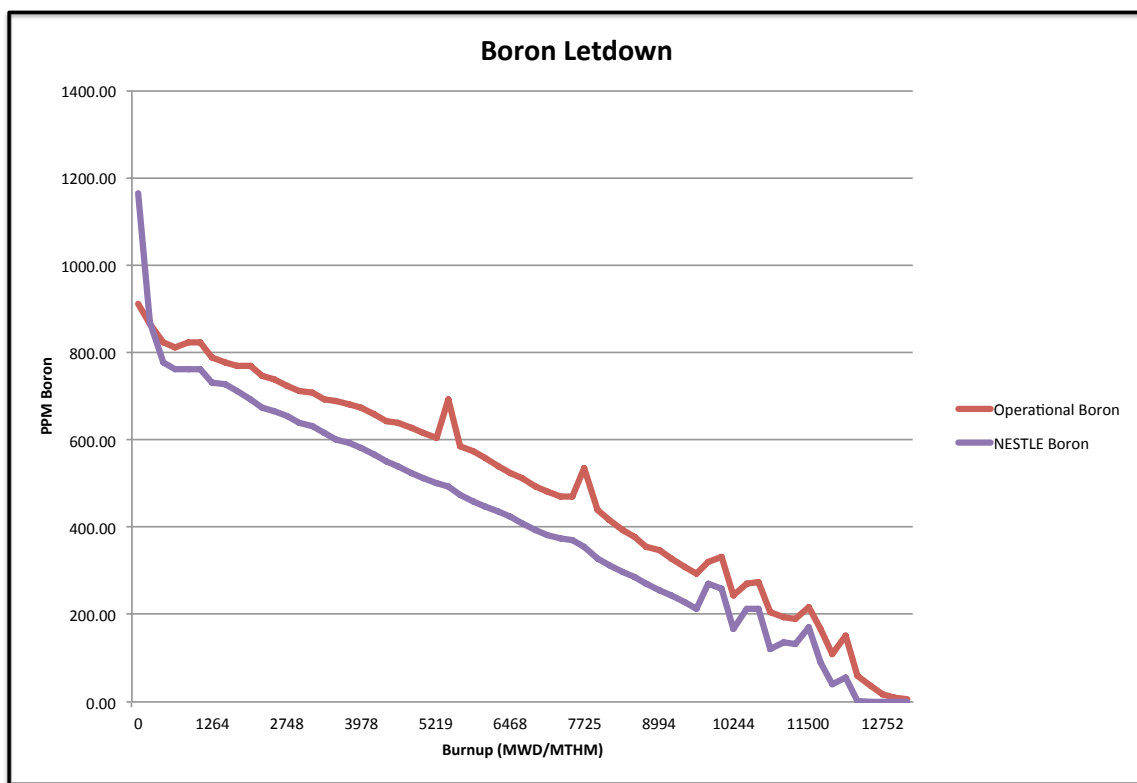


Figure 74: Boron Letdown Modeling

Figure 74 illustrates that the critical boron level for the NESTLE model is significantly lower than the operational boron levels provided. The NESTLE model has 0.00 ppm boron at 296 EFPD rather than the 311 EFPD in the benchmark.

This result is in agreement with the first test. Using the inputs from the benchmark study result in a subcritical reactor with the likely source of error being excessive boron in the system used to compensate for excessive reactivity not present in the NESTLE model. It

is worth noting that the benchmark researchers had a similar boron discrepancy with their first cycle model that was not seen in later cycles.[17]

B.4: Error Analysis and Bias Assessment

Figure 71 through Figure 74 show that the NESTLE VVER-1000 model has a lower reactivity than the benchmark model. A number of modeling assumptions and simplifications, some previously mentioned, could account for the loss of reactivity. It is likely that these error sources contribute collectively to the model's negative bias. One likely source of error is the core power density. Modeling the core with a higher power density than the benchmark reactor will result in a lower reactivity. Ensuring uniformity of input across the modeling software was vital to the project so the decision was made to maintain the fuel density at 10.55 g/cm^3 . To re-address this error would require the development of new cross-section libraries, which is quite time consuming. Future work would involve addressing the question of reactor power density.

The reactor model could be neutronically leaky. The ADF boundary defined as 1.0 may contribute to a miscalculation of flux at the fuel-reflector boundary. It is possibly that the core loses fewer neutrons than modeled. (Luciano and Maldonado, 2017) present a method to more accurately modeling the fuel-reflector boundary of a VVER using an ADF solution method involving multiple dimensions.[45] Accurate fuel-reflector discontinuity factors are unlikely to make a significant difference across the entirety of the core but 2D ADFs will likely improve the model at the periphery.

Another source of modeling error could come from the composition of the control rods. Boron-10 has a thermal neutron capture cross-section of 3837 bn. Dysprosium is about 33% of the material in the rod lower section. Dysprosium-164, which is the largest dysprosium isotope by weight percent in the control rod, has a thermal neutron capture cross-section of 2650 bn. The other Dy isotopes thermal neutron capture cross-sections are well below Dy-164, with the next highest cross section being 600 bn.[14, 17] It is possible that by modeling the control rod as B_4C only, the control rod neutron absorption was too high.

It is also possible that the operators did in fact keep the level of boron intentionally or unintentionally high during the first cycle. Were this the case, assuming a k-eff of 1.0 would be incorrect. It is clear from the power history that the first cycle was not nearly as constant as the subsequent cycles. The benchmark researchers had a similar reactivity issues with their first cycle modeling.

B.5: Conclusion

This project assumes the benchmark data to be true and therefore concludes that the NESTLE VVER-1000 model has a negative bias. The bias is not so large as to make the operational results unrealistic. The purpose of this research is to demonstrate the versatile modeling capability of NESTLE to ORIGAMI coupling for LWR assembly isotope analysis. Modeling two possible LWR proliferation scenarios and presenting an assessment of scenario feasibility demonstrate the nonproliferation applications of NESTLE to ORIGAMI coupling. Improving model accuracy will result in a more complete assessment of the possible proliferation scenarios but is not necessary to demonstrate the versatility of the tool.

Appendix C Testing Framework

C.1: VVER-1000 Test Reactor

Demonstrating the nonproliferation capabilities of NESTLE to ORIGAMI coupling first required the development of a reactor testing framework. The VVER-1000 benchmark data was operating data and therefore not consistent. A VVER-1000 Test model was built using the VVER-1000 benchmark model but the burndata and operator inputs were standardized to allow for scenario modeling. The visualizations in this section were created using Paraview. [53]

The VVER-1000 Test model had a core burnup of Core burnup of 13,0000 MWD/MTHM. This is a close representation of the VVER-1000 Benchmark cycle one model which had an EOC burnup of 12,961 MWD/MTHM. The NESTLE burndata step size 1000 MWD/MTHM. Standardizing the burnup step allowed for post processing programs to quickly search the NESTLE output file and extract information.

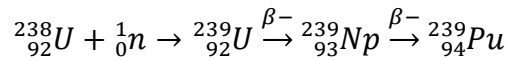
The core was started in a clean configuration and progressed to equilibrium with the next burnup. The core power was 99% for all steps but was modeled with a 50% power coast down for the last step. The reduction in power at the last burnup step was designed to mirror an end of core “coast down” similar to the power history described as “coast down” in the ORIGAMI Automator Primer.[70] The coolant inlet temperature was set at 549°F.

As with the benchmark model, the default control rod position was working groups 1-9 fully out. Working group 10 inserted into the top fuel node only. An additional working group was used to model the control rod induced production scenario. NESTLE determined the critical boron level at each burnup step through the use of the “ppm search” keyword in the burndata block and core remained critical for all models. The NESTLE VVER-1000 Test input file can be found in Appendix E.

C.2: Assembly Identification

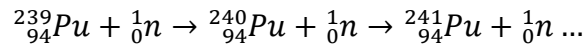
C.2.1: Theory

Plutonium production in a LWR is closely related to neutron flux. ^{239}Pu is produced during ^{238}U neutron capture and β - decay.



^{238}U has a capture cross-section for thermal neutrons of 2.68 bn[14] and less than 1 bn for neutrons with an energy above 1 MeV[15]. ^{239}U decays to ^{239}Np with half-life of 23.45 min. ^{239}Np subsequently decays to ^{239}Pu with a 2.36 d half-life.[14, 15]

Plutonium losses are greatly impacted by neutron flux. ^{239}Pu transmutes to additional plutonium isotopes primarily through neutron capture. ^{239}Pu has a thermal neutron capture cross section of 271 bn.[14] At 1 MeV, the capture cross section is 0.04 bn.[15]



Fission is the greatest source of ^{239}Pu isotope loss in a reactor. ^{239}Pu undergoes fission at thermal and fast energies. ^{239}Pu has a thermal fission cross-section of 748 bn [14] and a fast fission cross-section of 1.74 bn at 1 MeV. [15]

The scenarios modeled using NESTLE to ORIGAMI coupling attempt to use a LWR to produce plutonium for weapons use. The FA 13AU assembly was chosen as a target assembly for modeling production scenarios in order to maximize the mass of ^{239}Pu in a single assembly.

The ratio of fast neutron flux to thermal neutron flux (G1/G2) was used to identify a single FA 13AU assembly for modeling. Thermal fission is the largest contributor to ^{239}Pu inventory losses. The scenarios modeled sought to reduce ^{239}Pu inventory losses from thermal fission. A reduction in thermal flux will result in a higher G1/G2 ratio. Therefore, the assembly with a high G1/G2 ratio prior to assembly modification was well positioned for isotope production.

The fast to thermal flux ratio will be referred to as the G1/G2 flux henceforth. It is also referred to at times as flux spectrum hardness.

C.2.2: Assembly #139 Identification

Linux and python scripting facilitated the identification of the FA 13AU target assembly. A program was written to extract data from the NESTLE output file. The program extracted the fast and thermal flux for all assemblies in the core and calculated the flux spectrum hardness for each node of each assembly. The information for the FA 13AU assemblies was separately identified. For each axial plane, the FA 13AU node with the highest flux spectrum hardness was identified. The assembly with the highest number of identified nodes was selected to be the target assembly.

Figure 75 shows the spectrum hardness for the VVER-1000 benchmark reactor at EOC. Figure 76 shows only the FA13AU core load. Figure 77 shows the FA13AU core load in relation to the other assemblies. Figure 78 and Figure 79 show the VVER-1000 operational model flux spectrum hardness. The FA13AU fuel assemblies have been visually modified for ease of identification. FA 13AU assemblies have lower flux spectrum hardness than the surrounding assemblies.

Linux and python scripts were used to extract and calculate the maximum flux spectrum hardness for each axial node. All flux spectrum data was extracted at EOC. The core was then examined to determine which FA 13AU assembly had the most axial nodes with high flux spectrum hardness.

Figure 80 provides a front view the assembly from the VVER-1000 Operational Data. The target assembly is identified with a yellow circle. Figure 81 shows a top-down view of the assembly. The assembly identified in Figure 80 and Figure 81 is assembly #139. The numerical tracking method used to identify the assembly is project specific and has no meaning beyond the scope of this paper.

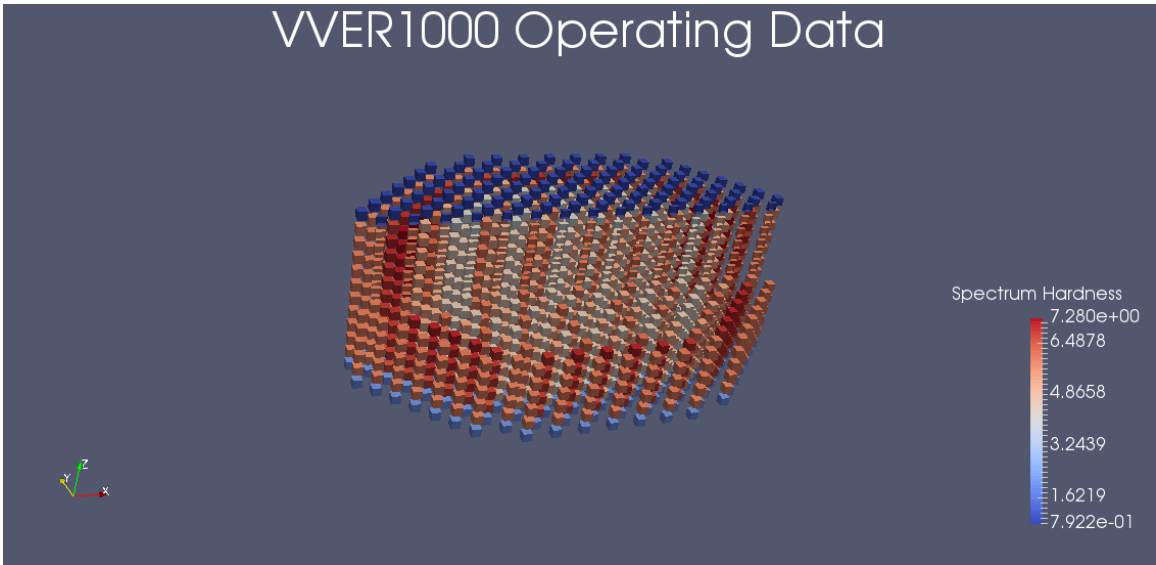


Figure 75: VVER-1000 Operational Data Flux Spectrum Hardness

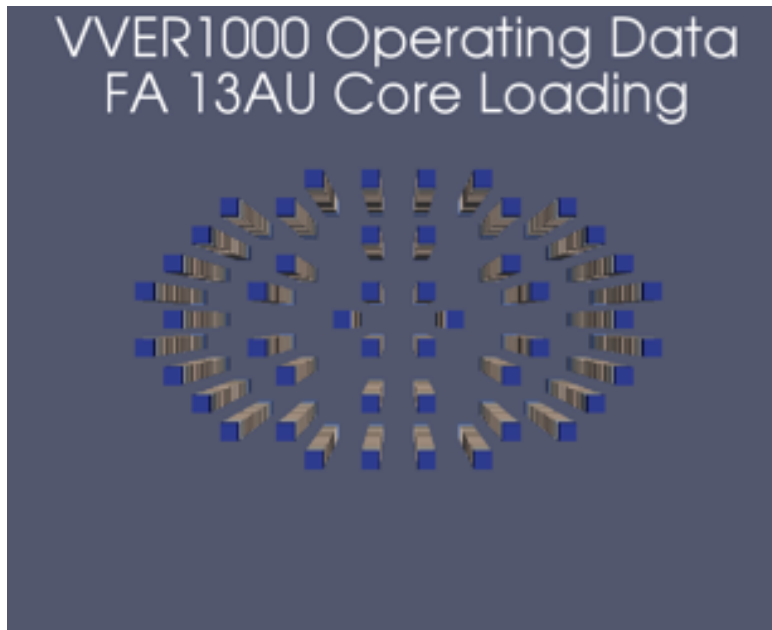


Figure 76: FA13AU Core Load

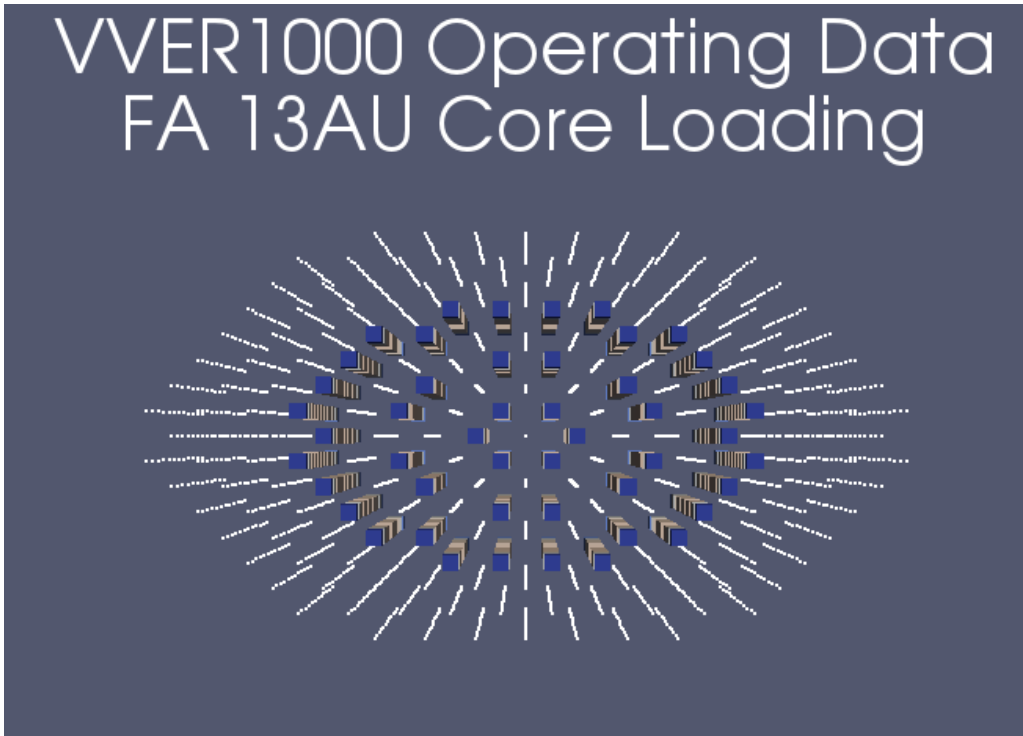


Figure 77: FA13AU VVER-1000 Locations

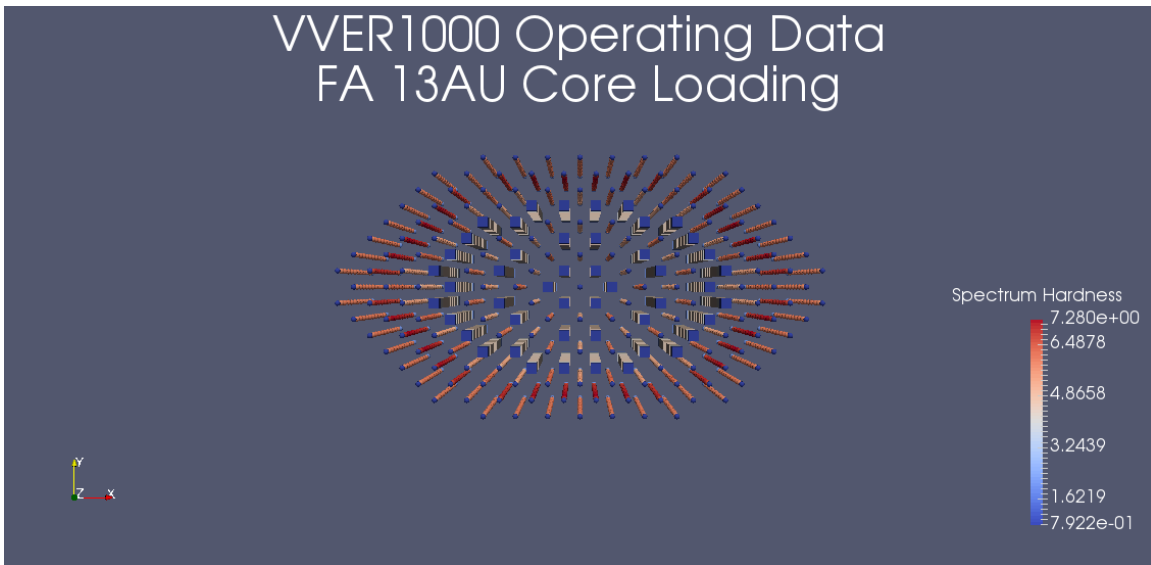


Figure 78: VVER-1000 Operating Data Flux Spectrum Hardness

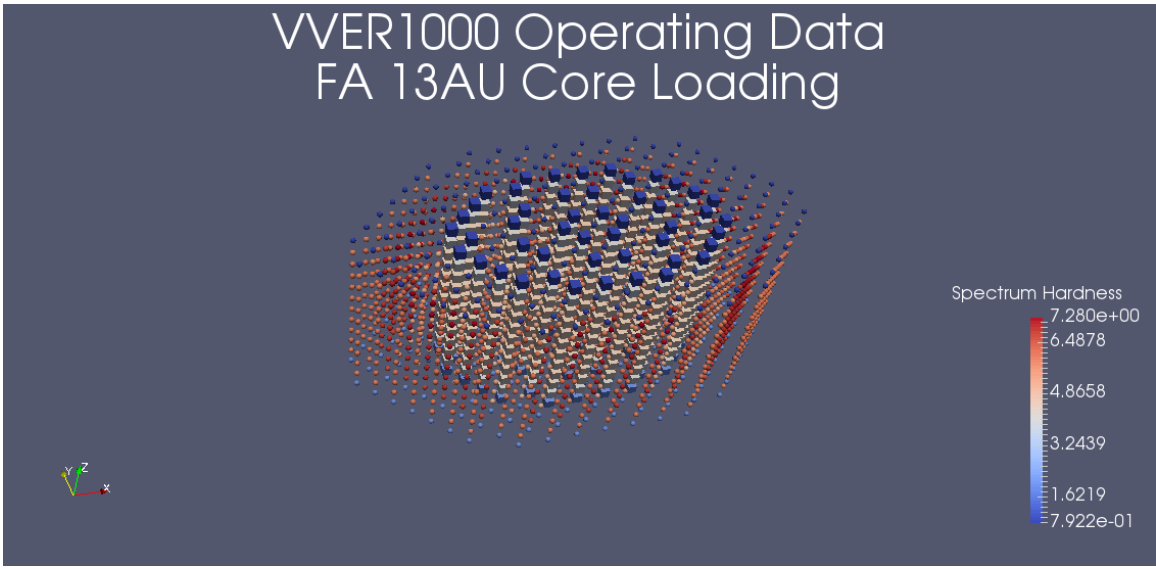


Figure 79: VVER-1000 Operating Data Flux Spectrum Hardness (2)

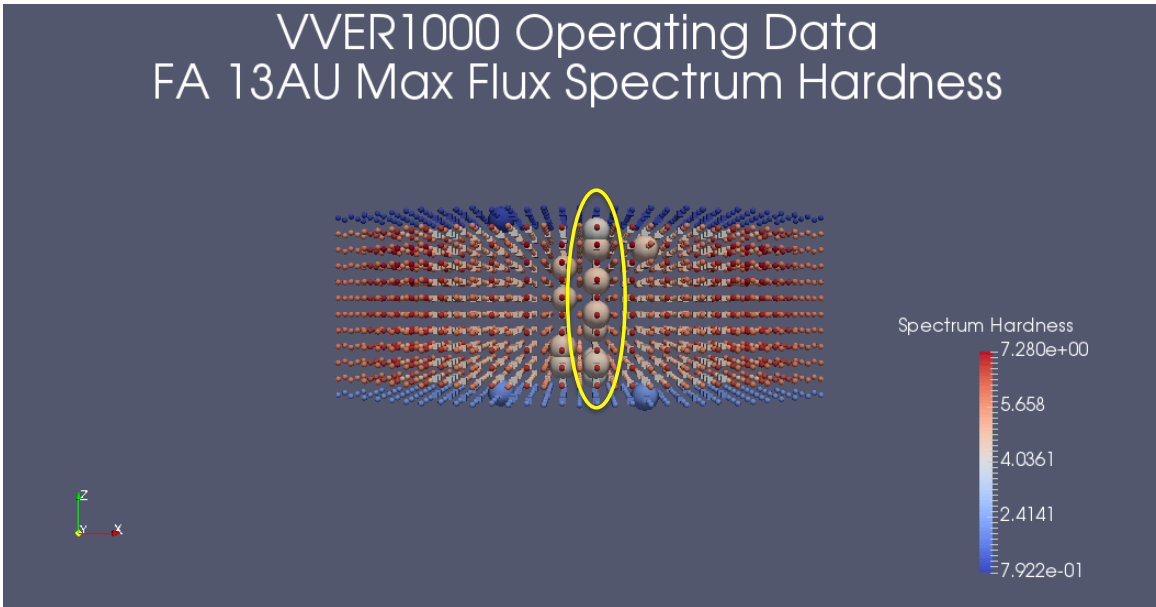


Figure 80: Assembly ID using Flux Spectrum Hardness

VVER1000 Operating Data FA 13AU Max Flux Spectrum Hardness

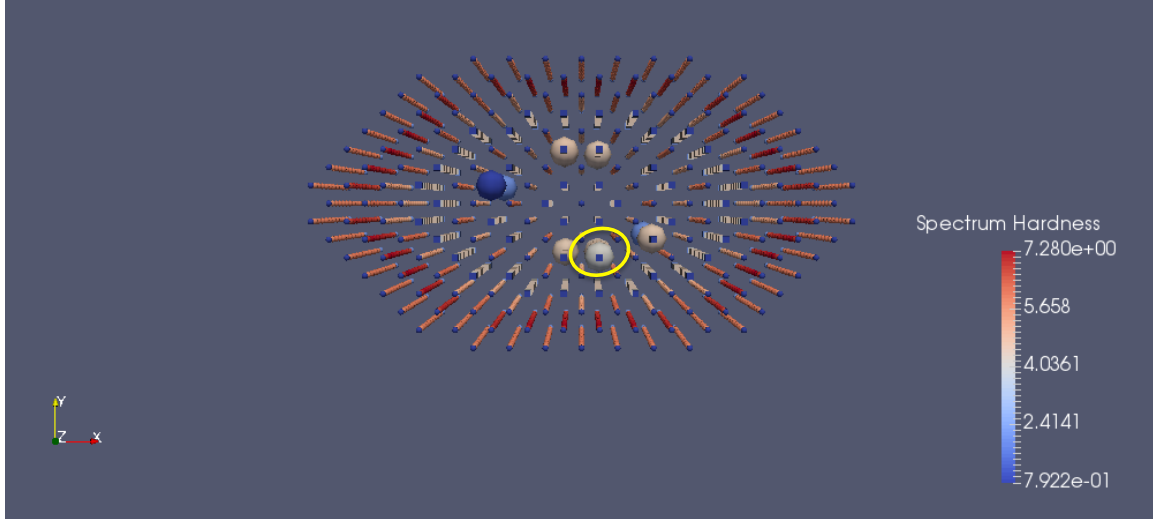


Figure 81: Assembly ID using Flux Spectrum Hardness (top view)

Figure 82 shows the axial flux spectrum of assembly #139 from the VVER-1000 operational model. Note that only 10 nodes are visible in Figure 82.



Figure 82: FA13AU #139 Flux Spectrum Hardness

While each assembly in the core consists of 12 axial nodes, nodes 1 and 12 are reflector material. ^{239}Pu buildup will occur only in the fuel nodes so the reflector node information is not extracted from NESTLE output files. Figure 82 shows that the highest flux spectrum hardness occurs in the center of the assembly.

The same assembly identification process was used for to find the target assembly in the VVER-1000 Test model. Figure 83 shows the VVER-1000 Test model and identifies the assembly with the highest flux spectrum hardness. Assembly #139 had the most nodes with a high flux spectrum hardness Assembly #139 was selected to be the target assembly for ^{239}Pu production in this project.

FA13AU Maximum Flux Spectrum Hardness VVER1000 Test Reactor

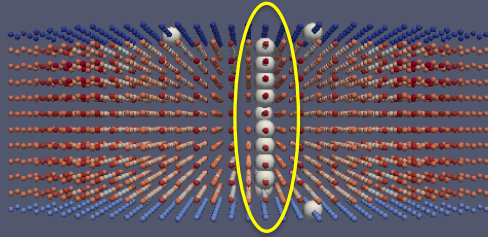


Figure 83: VVER-1000 Test Model Flux Spectrum Hardness

Appendix D Burnup Weighted Relative Power

D.1: Axial Power Distribution and Isotope Production

ORIGAMI, a new tool for depletion modeling, was released in SCALE 6.2. ORIGAMI is designed specifically to model depletion in LWR fuel assemblies. ORIGAMI expands the inputs available to the user to capture the impact local power distributions on the assembly. SCALE 6.2.1 TRITON requires the user to define power based on an average assembly power history. TRITON does not allow the user to define a heterogeneous power distribution. ORIGAMI provides the user the capability define both an axial power distribution for an assembly as well as radial, pin-by-pin power distributions. This effectively gives the user the ability to define the power distributions in three dimensions for single assembly model.[13]

Figure 84 shows the flux spectrum hardness of the target assembly from the VVER-1000 benchmark model. Axial variations in the assembly flux are apparent. Allowing the user to specify an assembly specific power distribution results in a more accurate depletion analysis. The power distribution of an assembly is greatly shaped by the reactor environment. Changes in local flux distributions will directly impact assembly power. The proximity to other assemblies, the presence of absorbing material, or proximity to core structures influences local flux distributions. Flux directly correlates to assembly power and depletion modeling. Evidence of the heterogeneity of assembly flux and power is most noticeable when looking at the axial profiles of an assembly.

Figure 85 is a model of the NESTLE generated nodal power distribution for the target assembly at EOC for the VVER-1000 benchmark model. Power produced by the assembly differs depending on axial location. Figure 86 illustrates a depletion model of the target assembly using a flat power distribution rather than the power distribution in Figure 85. Variations in isotope content are masked.

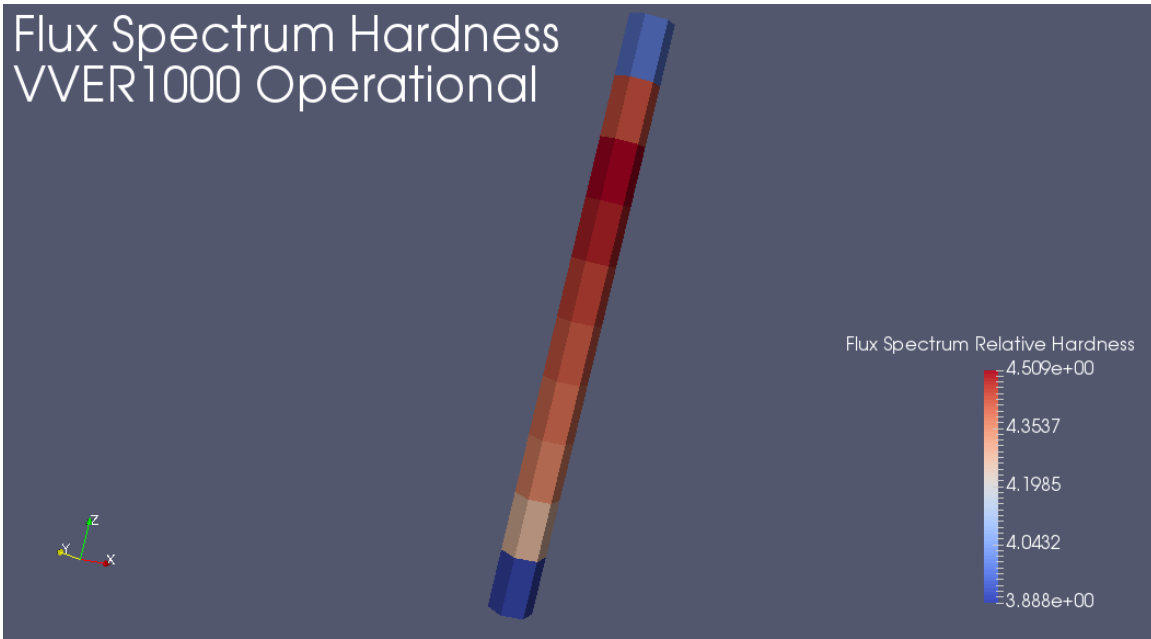


Figure 84: Assembly #139 VVER-1000 Benchmark Model Flux Spectrum Hardness

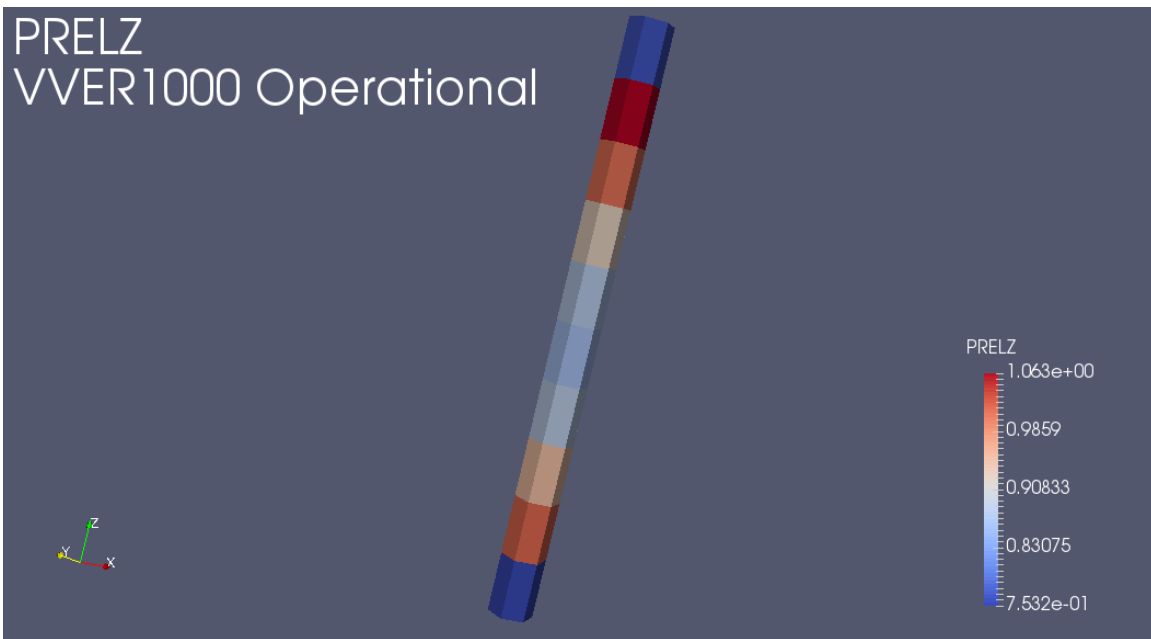


Figure 85: Assembly #139 VVER-1000 Benchmark PRELZ

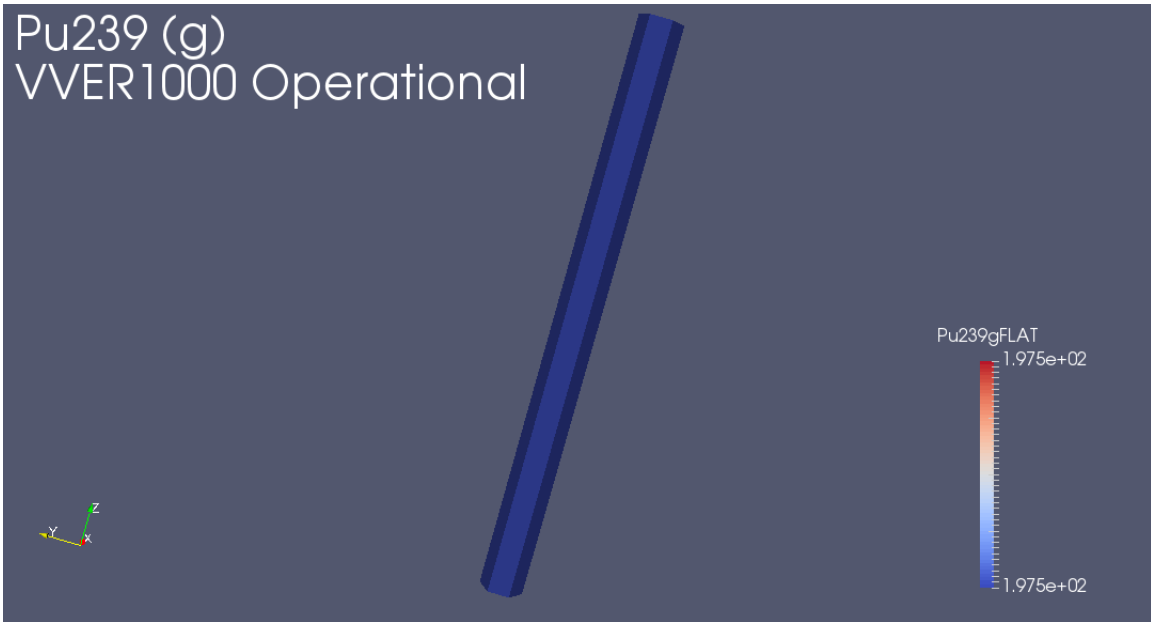


Figure 86: ^{239}Pu (g) Flat PRELZ VVER-1000 Benchmark

Figure 87 is a depletion model of the target assembly using the NESTLE generated EOC PRELZ from Figure 85 in ORIGAMI. Figure 87 illustrates variations in ^{239}Pu content with the highest mass ^{239}Pu produced in locations similar to high PRELZ.

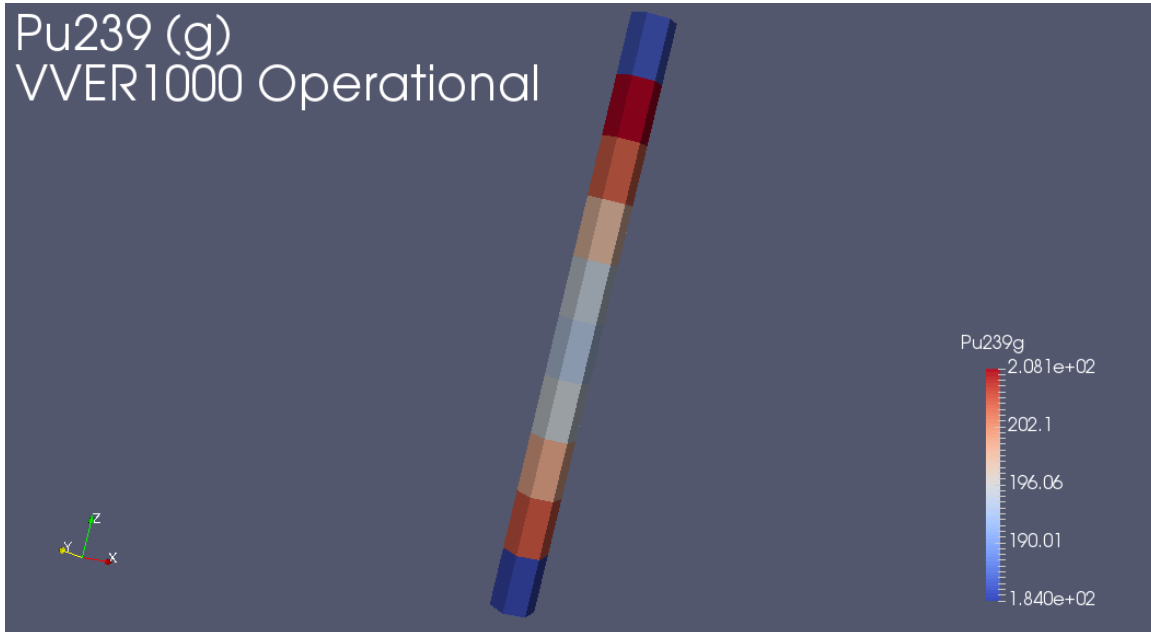


Figure 87: ^{239}Pu using PRELZ EOC VVER-1000 Benchmark

The release of ORIGAMI with SCALE 6.2.1 gave the user a powerful new tool with which to accurately model the impact of power distribution on isotope production. NESTLE outputs relative power distributions in three dimensions when modeling core simulations. It is now possible to correlate behavior modeled in NESTLE to isotope production using relative power to link the simulations.

D.2: Relative Power Weighting

Assembly axial power distribution changes throughout the fuel cycle. Figure 88 illustrates the changes in nodal power distribution of the target assembly with respect to burnup for the VVER-1000 Test model. At BOC nodes have a wide variation in axial power distribution. As the reactor operates, the variation in axial power distribution reduces until reaching EOC. The top and bottom nodes of the assembly steadily increased in relative power with burnup. The central fuel nodes reached peak power early in the cycle and then converged at the end of cycle.

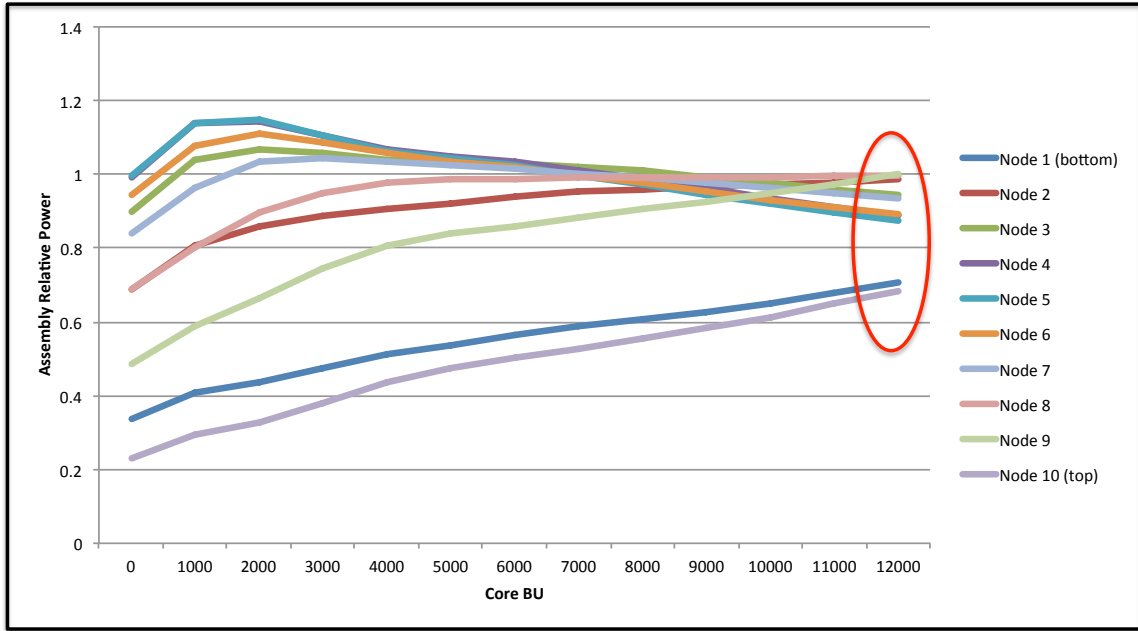


Figure 88: VVER-1000 Test Nodal PRELZ

The axial power distribution used by ORIGAMI has a significant impact on depletion analysis. ORIGAMI currently only allows the user to input a single axial or radial power distribution per model. Therefore it became evident that a method was needed to capture the changes in power distribution with respect to assembly burnup.

In order to accurately model the axial relative power of the assembly, a method was devised that aggregated the relative power of the node from each burnup step into a weighted solution. The weighted PRELZ was more representative of the power distribution experienced by that node over the complete cycle.

Eq. 1 through Eq. 6 provides the weighting formula and inputs for relative power weighting with burnup.

$$i = \text{nestle calculation iteration } [0,1,2 \dots 12] \quad \text{Eq. 9}$$

$$\text{step} = i + 1 [1,2,3 \dots 12] \quad \text{Eq. 10}$$

$$n = \text{nestle axial node } [0,1,2, \dots 12] \quad \text{Eq. 11}$$

$$\Delta BU_{n,\text{step}} = BU_{n,i+1} - BU_{n,i} \quad \text{Eq. 12}$$

$$\overline{PREL}_{n,\text{step}} = \frac{(PREL_{n,i} - PREL_{n,i+1})}{2} \quad \text{Eq. 13}$$

$$PREL_n = \frac{\sum_1^{12} [(\Delta BU_{n,\text{step}})(\overline{PREL}_{n,\text{step}})]}{\sum_1^{12} \Delta BU_{n,\text{step}}} \quad \text{Eq. 14}$$

To facilitate calculation of the burnup weighted relative power, a Linux script was created that extracted the nodal burnup and PREL for each core burnup step as well as the final assembly burnup. The Linux script then called a python program that calculated the weighted PRELZ using Eq. 6 and output the PRELZ for use in ORIGAMI. All Linux and python scripts can be found in Appendix F.

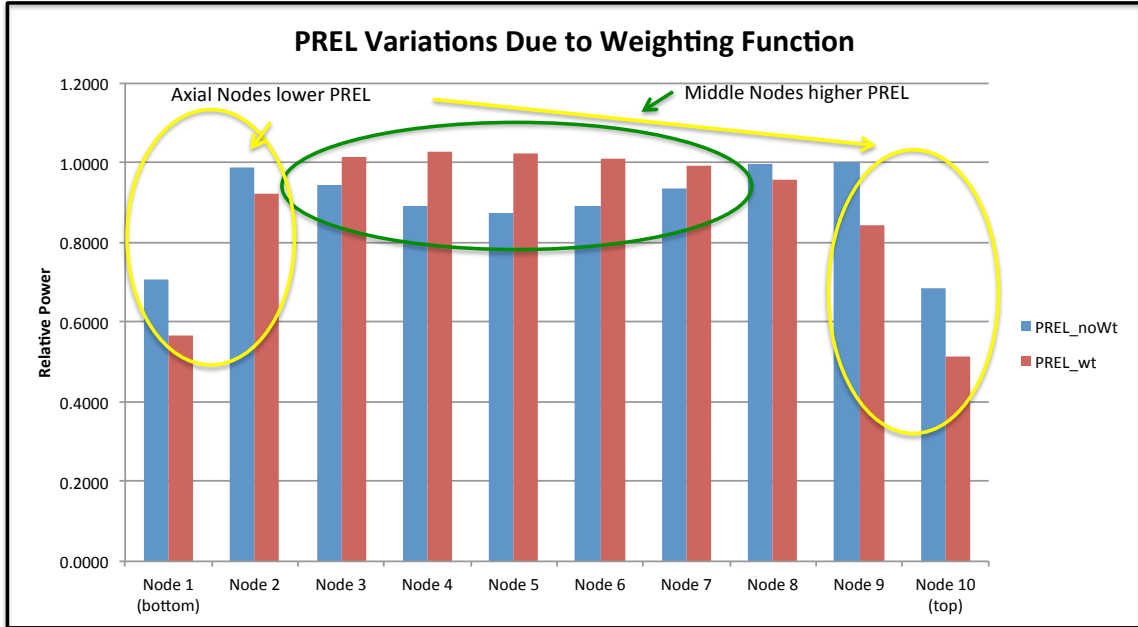


Figure 89: Axial Relative Power Distribution PRELZ Weighting

Analysis of the VVER-1000 test assembly using the weighted PREL reveals a shift in axial power distribution. Figure 89 shows that the burnup weighted PRELZ increases the relative power of the center fuel nodes and reduces the relative power of the axial end fuel nodes. With weighed PRELZ, ORIGAMI has a more realistic representation of the assembly power distribution from which to model depletion.

Figure 90 overlays the data from Figure 89 on to a model of the target fuel assembly. Figure 90 illustrates a weighted PRELZ solution results in the assembly power provided to the reactor coming primarily from core central nodes. This shift is important as it captures early cycle behavior thus ensuring higher power nodes are identified correctly for accurate depletion.

D.3: Weighted PRELZ and Origami Modeling

When constructing the weighted PRELZ function, it was important to ensure that the weighting function did not alter the final assembly burnup. NESTLE outputs the average assembly burnup for each depletion step. The Linux script in Appendix F extracted the nodal burnup data as part of its weighting calculations as well as the final assembly burnup from the NESTLE output file.

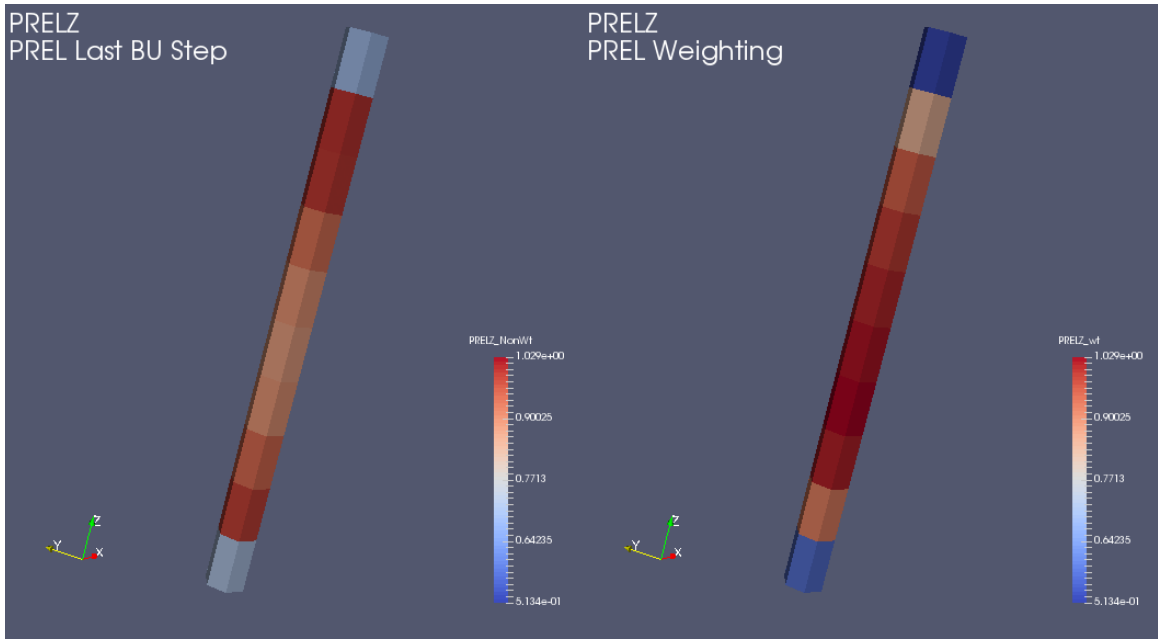


Figure 90: PRELZ for Target Assembly EOC (left) vs. Weighted (right)

The ORIGAMI power history block is then defined so as to have an assembly burnup as close to the equivalent to the NESTLE provided assembly average burnup as possible. The ORIGAMI model uses the assembly average power multiplied by the number of days irradiated as part of its burnup calculation. Ensuring agreement with the ORIGEN libraries required adjusting the number of irradiation days rather than the assembly power to achieve the assembly average burnup provided by NESTLE calculations.

```
hist[
  cycle{ power=42.5 burn=4 nlib=5 }
  cycle{ power=42.5 burn=245 nlib=5 }]
```

Figure 91: ORIGAMI Power History Block VVER-1000 Test Assembly #139

Figure 91 shows the power history block from assembly #139 in the VVER-1000 Test model. NESTLE determined that at a core burnup of 12,000 MWD/MTHM assembly #139 had a burnup of 10560.22 MWD/MTHM. Keeping the average assembly power at 42.5 MW, the total cycle length was defined a 249 days to get an assembly burnup of 10582.5 MWD/MTU.

Table 24 illustrates the impact of weighted PRELZ on the assembly burnup. The total assembly burnup remains unchanged. The nodal burnup however has shifted with the use of weighted PRELZ. Weighted PRELZ moves the distribution of power and burnup to nodes central to the assembly. The term node and pin are used interchangeable in this project.

Figure 92 provides the same data in Table 24 however more clearly shows the burnup shift of the central fuel nodes. It was assumed that the assembly UO₂ had an initial distribution that was axially uniform. Thus, increased power in the central nodes should be the result of increased reaction rates in the center of the assembly. This will lead to a higher burnup. As a result, one would expect to see less ²³⁵U in the central nodes due to a higher number of fissions.

Table 24: Weighted PRELZ and Burnup

Flux Spectrum Hardening and Burnup		
Pin	Burnup FA13AU Normal (MWD/MTU)	Burnup FA13AU SS (MWD/MTU)
Pin 1	675.89	609.62
Pin 2	1097.77	999.86
Pin 3	1209.98	1104.25
Pin 4	1228.35	1120.46
Pin 5	1220.73	1113.61
Pin 6	1205.34	1100.62
Pin 7	1183.91	1082.57
Pin 8	1140.31	1043.49
Pin 9	1007.44	919.35
Pin 10	612.78	553.67
Origami Assembly BU	10582.5	9647.5
Nestle Assembly AVG BU	10560.22	9652.89
Change in Burnup	Nestle	Origami
	907.33	935

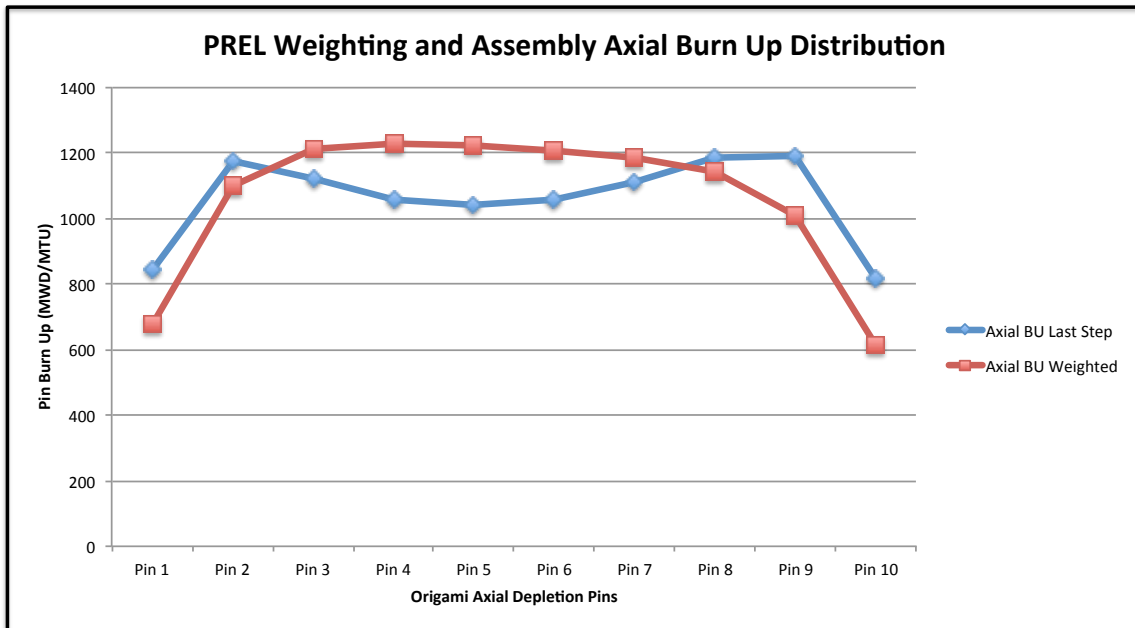


Figure 92: Weighted vs. EOC PRELZ Comparison

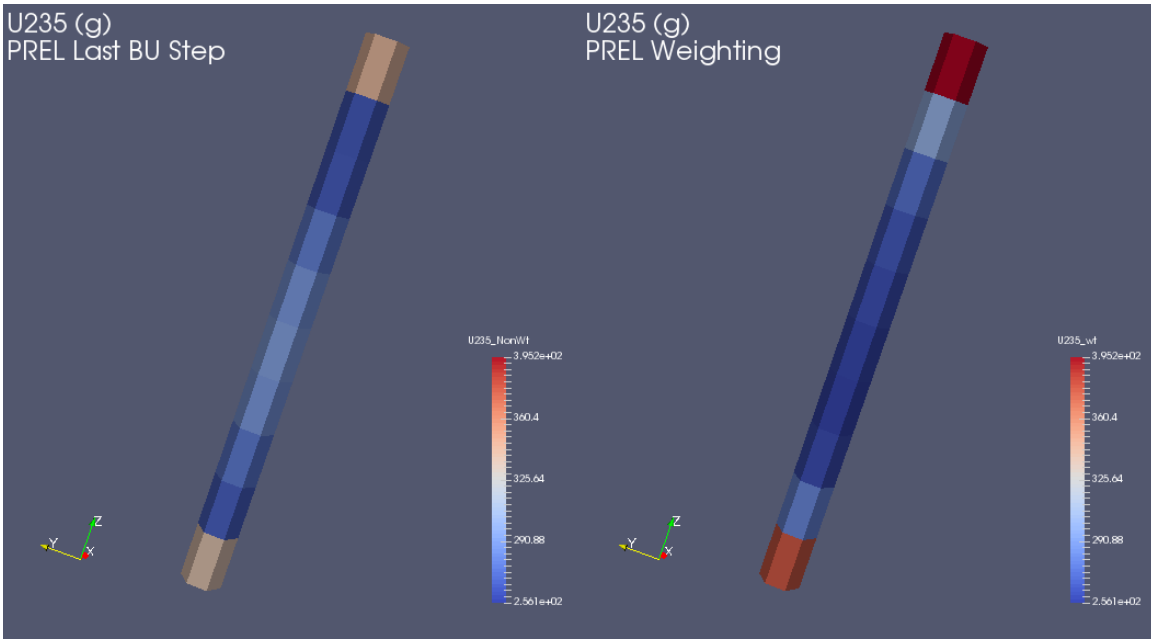


Figure 93: ²³⁵U Mass EOC (left) vs PRELZ Weighted (right) Comparison

Figure 93 and Figure 94 show the impact of PRELZ weighting on ²³⁵U mass. PRELZ weighting resulted in lower ²³⁵U mass in the central nodes. This is the expected result since the central fuel nodes have a higher burnup than the axial end fuel nodes.

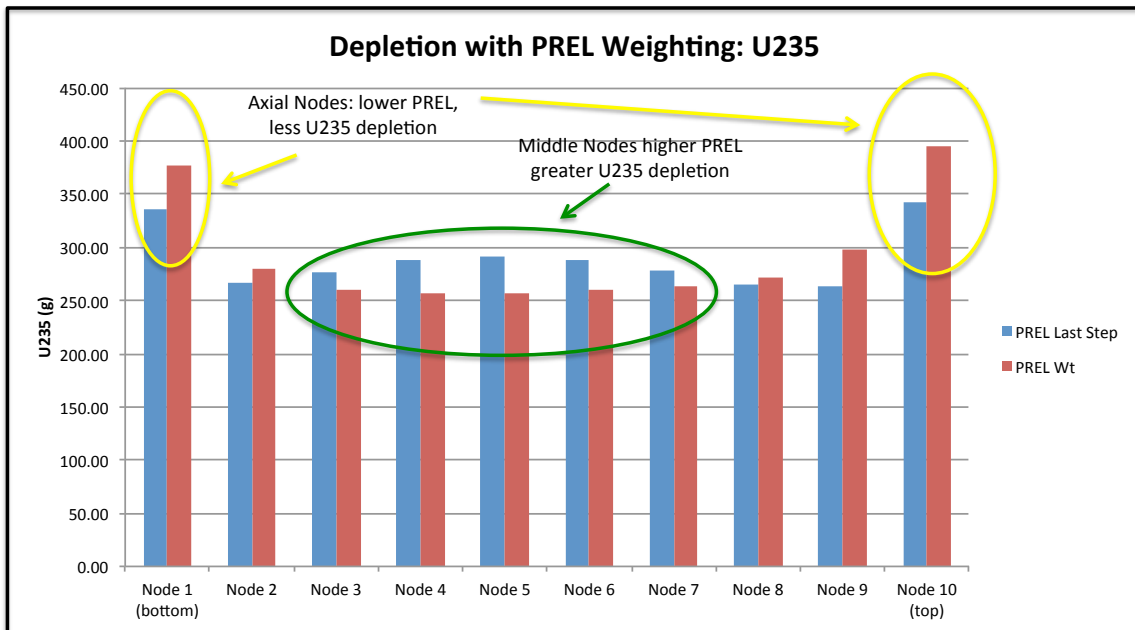


Figure 94: ²³⁵U Mass Distribution Weighted vs. EOC PRELZ Comparison

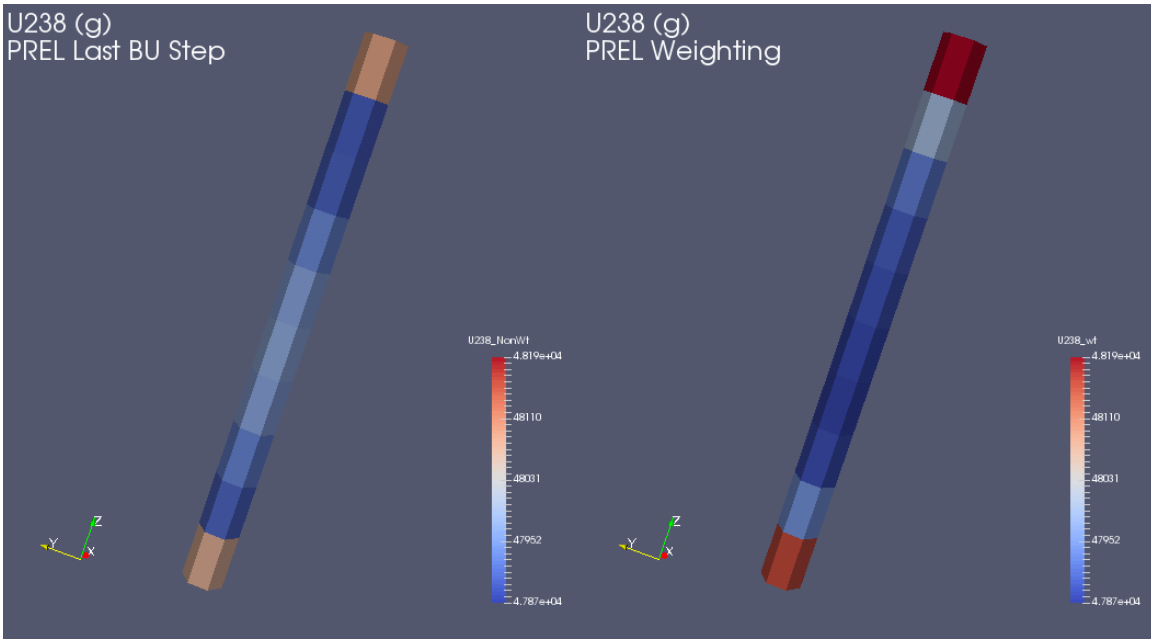


Figure 95: ^{238}U Mass EOC (left) vs PRELZ Weighted (right) Comparison

Figure 95 and Figure 96 show the impact of PRELZ weighting on the mass of ^{238}U in the target assembly. Weighting PRELZ increased ^{238}U transmutation and reduced the mass of ^{238}U in the central nodes.

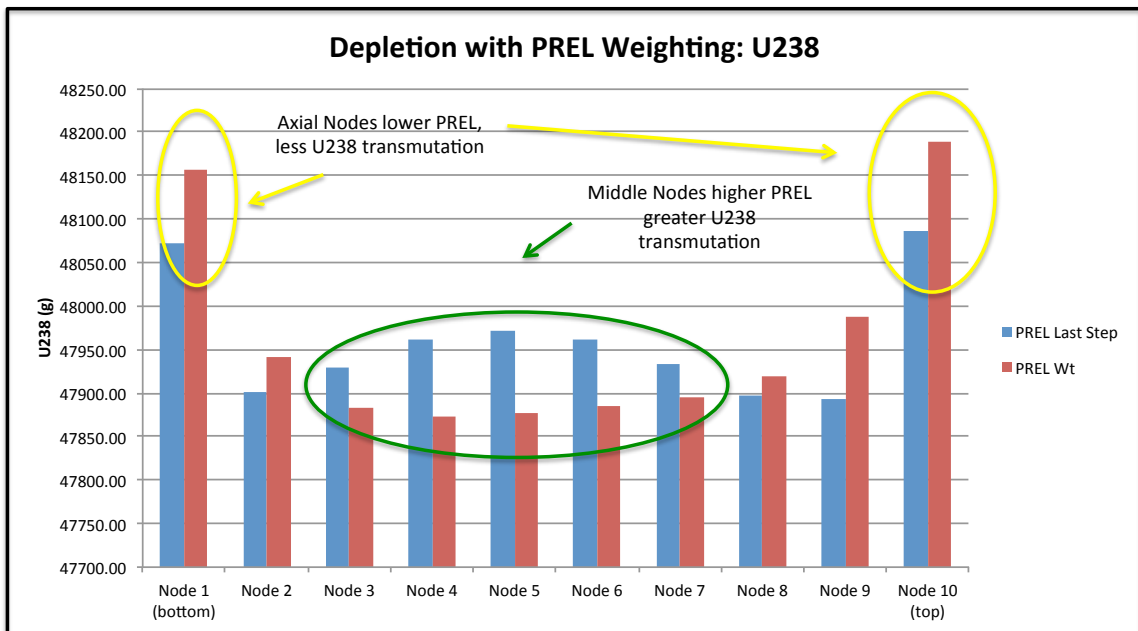


Figure 96: ^{238}U Mass Distribution Weighted vs. EOC PRELZ Comparison

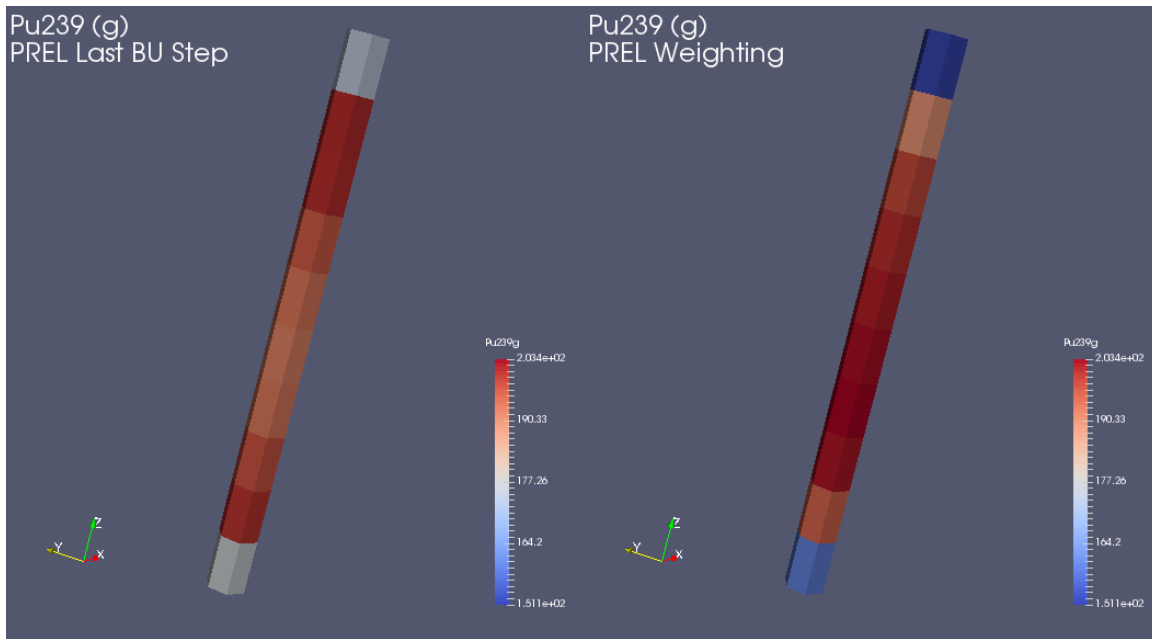


Figure 97: ^{239}Pu Mass EOC (left) PRELZ Weighted (right) Comparison

Figure 97 and Figure 98 show the change in mass of ^{239}Pu (g) due to PRELZ weighting. There is an increase in the mass of ^{239}Pu for the center fuel nodes and a reduction in the mass of ^{239}Pu at the axial nodes for the weighted assembly. The mass increase in the central nodes is not the same magnitude as the ^{238}U mass loss seen in Figure 95 and Figure 96. ^{239}Pu in the reactor core will contribute to assembly power from fission. ^{239}Pu will also continue to transmute into higher Pu isotopes. Fission and transmutation losses account for the disparity in magnitude.

D.4: Plutonium Production and Safeguards

Both the mass and isotopic content of plutonium determine the feasibility of weapons use. Table 3 is a summary of information about plutonium with regards to safeguards. For this paper, all “even numbered” plutonium isotopes (PuEven) are considered detrimental to weapons performance rather than just Pu240. Even number plutonium isotopes such as ^{242}Pu and ^{238}Pu have a high spontaneous fission rate and a high decay heat.[28, 31] This makes these isotopes less attractive for use in weapons.[28]

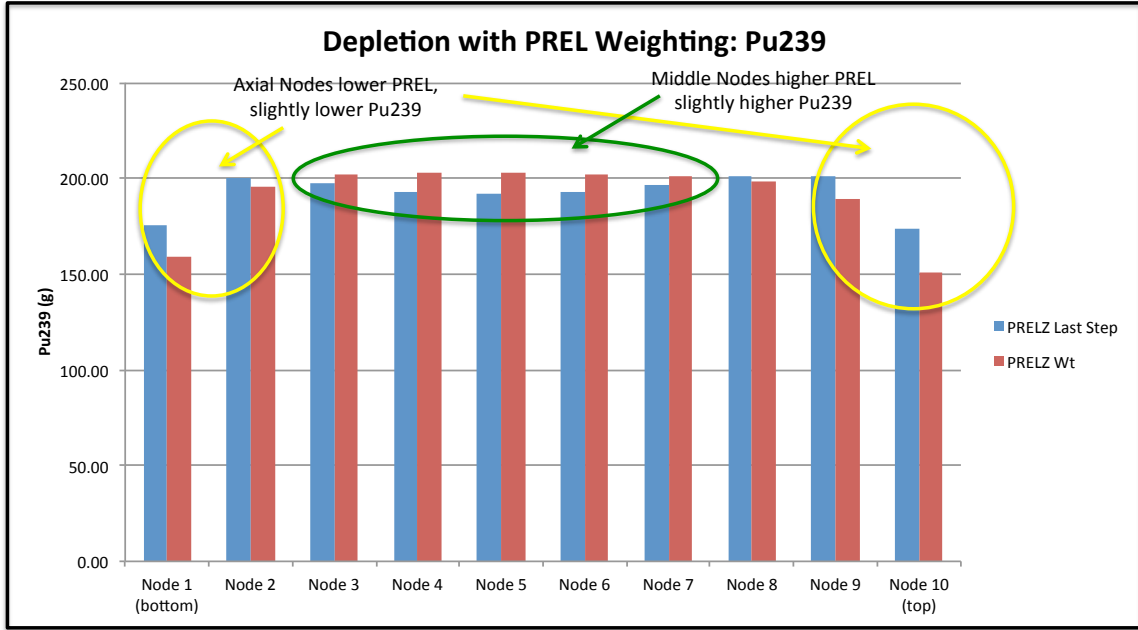


Figure 98: ²³⁹Pu Mass Distribution Weighted vs EOC PRELZ Comparison

The Pu isotope distribution of the assembly is quite significant when determining the feasibility of a plutonium production pathway. A fissile content of 93% or greater (7% or less PuEven) is considered weapons grade for this project. When describing plutonium content, this paper uses the term “Pu fissile content” to mean the percentage of plutonium that is fissile. This paper collected the top 5 Pu isotopes from the VVER assemblies modeled and assessed their Pu fissile content using the following equations.

$$Pu^{all} = Pu^{238} + Pu^{239} + Pu^{240} + Pu^{241} + Pu^{242} \quad \text{Eq. 15}$$

$$fissile\ content = \frac{(Pu^{239} + Pu^{241})}{Pu^{all}} \quad \text{Eq. 16}$$

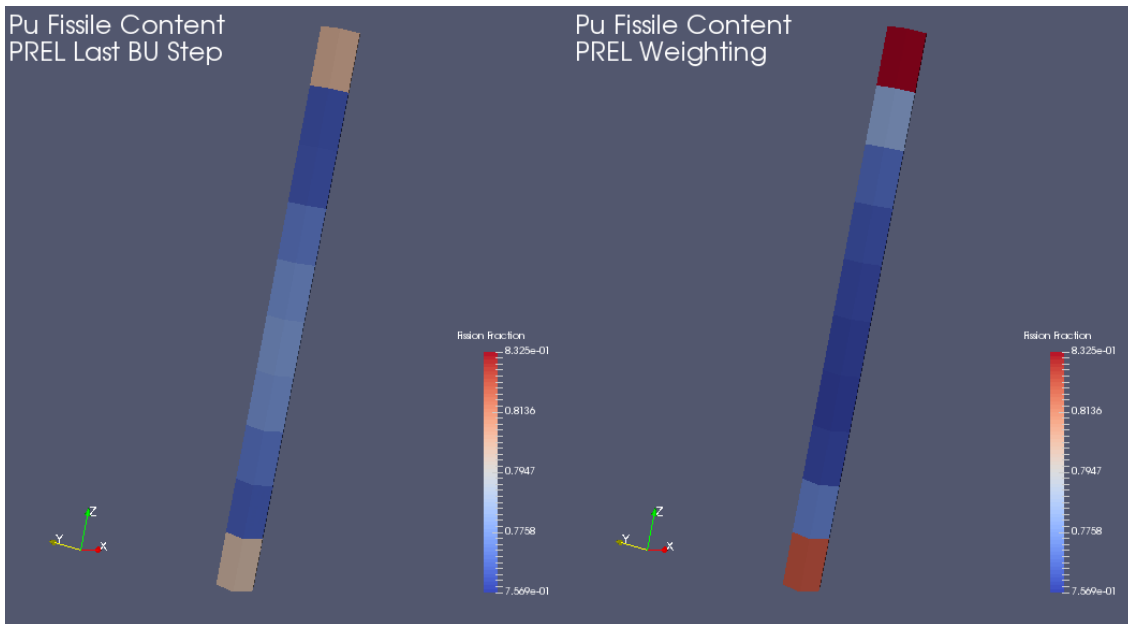


Figure 99: Pu Fissile Content Weighted vs. EOC PRELZ Comparison

Figure 99 shows that in areas of high power and high burnup, the fissile fraction is lower. This is due to fission and transmutation of fissile isotopes. The top and bottom nodes, which have a lower PRELZ, have a higher Pu fissile content due to less fission and transmutation losses. Figure 100 shows that the losses from fission and transmutation, which impact the suitability of the material for weapons application, are most evident in the central fuel nodes.

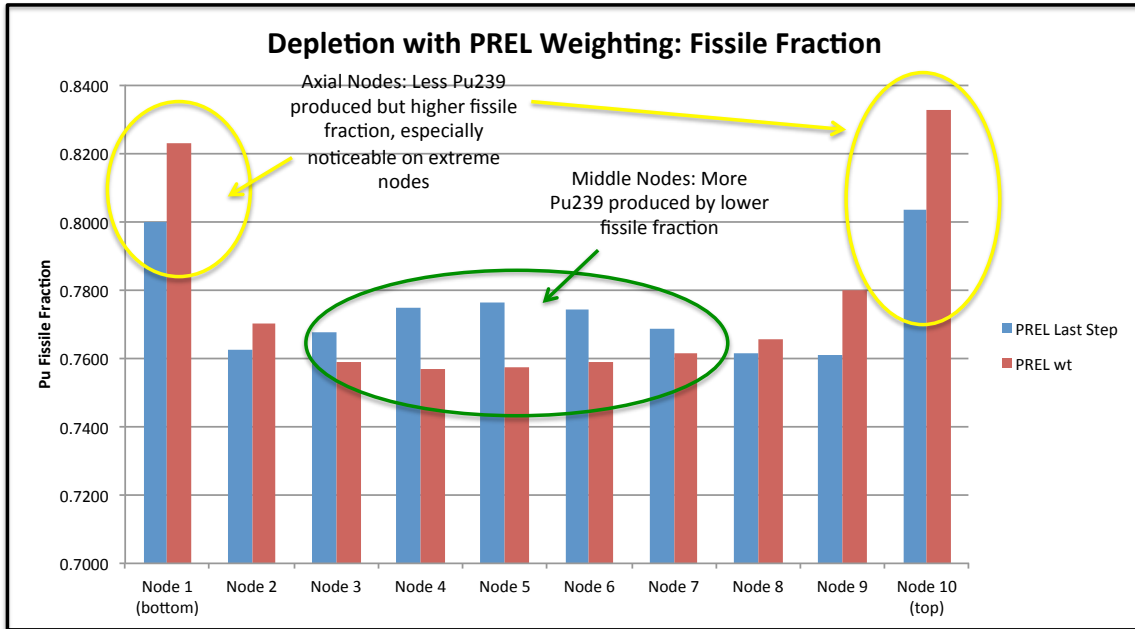


Figure 100: Pu Fissile Content Weighted vs EOC PRELZ Comparison

From a safeguards standpoint, it is important to note that even the nodes with the highest Pu fissile content are well below weapons grade. The target assembly in the VVER-1000 Test model had an axial Pu fissile content of 83% which makes it reactor grade. The central nodes were all under 80% fissile.

D.5: Conclusion

SCALE 6.2.1 ORIGAMI code allows the user to link full core simulation results to a depletion code through the use of relative power distribution. Due to limitation in ORIGAMI input, the user must ensure the axial power distribution provided is reflective of the assembly power over the entirety of the core cycle. In order to capture the behavior of the power distribution early in the cycle, a weighting method for the axial power distribution burnup was developed using burnup. Coupling NESTLE to ORIGAMI using burnup weighted PRELZ provides the user a flexible interface with which to explore the impact of core inputs on individual assembly isotope production.

Appendix E Select Input Files

E.1: Introduction

The following appendix contains select examples of input files used throughout this project. Each model included represents a key geometric, material, or modeling technique addressed in previous chapters. The following input files are included:

- SCALE 6.2.1 TRITON and NEWT Models: 13AU, 30AV5, Radial Reflector (T-NEWT), Bottom Axial Reflector (T-NEWT)
- NESTLE Models: VVER-1000 Benchmark (63-point model), VVER-1000 Test Reactor, NESTLE VVER-1000 Control Rod Insertion Node Depth 4, VVER-1000 SS316
- ORIGAMI: 13AU Assembly #139 VVER-1000 Test Model, 13AU Assembly #139 Control Rod Insertion Node Depth 4

The models not included in this appendix are as follows:

- SCALE 6.2.1 TRITON and NEWT Models: 22AU, 39AWU, 390GO, 13AU SS316, Top Axial Reflector (T-NEWT), 13AU Origami library modeling CRO, 13AU Origami library modeling CRI, 13AU Origami library modeling SS316
- NESTLE Models: VVER-1000 Benchmark 323-point model, VVER-1000 Control Rod Insertion Depth 2,3,5-11 Nodes
- ORIGAMI: 13AU Assembly #139 Benchmark Model, 13AU Assembly #139 CR 2,3,5-11 Node, 13AU Assembly #139 SS

Input files not included can be obtained by contacting the author.

E.2: SCALE Triton Input Files

E.2.1: 13AU Cross-Section File

'VVER1000 FA13AU Depletion

'1.3% ²³⁵U Enriched, depletion

'Created by Margaret Kurttis

*****Assumptions and References*****

'1. Lotsch, T., V. Khalimonchuk, and A. Kuchin, Proposal of a Benchmark for Core Burnup Calculations for a VVER-1000 Reactor Core, 2009

'2. Lotsch, T., V. Khalimonchuk, and A. Kuchin. Corrections and additions to the proposal of a benchmark for core burnup calculations for a WVER-1000 reactor, 2010.

'Table 4 [1]-materials for fuel, guide tube, spacer.

'Table 3 [1]-materials for control rods

'Table 5 [1]-materials for stiffing plate

'Table 1 [1]-reactor temperature data

'Tab 1 [2]-Moderator Boron Concentration, fuel temperature

'Moderator density based off properties of water at 15.7 MPa and 578 K, Table 1 [1], used www.wolframalpha.com

'Burndata comes from [2] for power (42.5 MW/MTU) and the core was shut down after 311.74 EFPD [1,2]

'Figure 1 [1] shows operating data for cycle 1. It took ~50 days for the core to reach full power

'**Assume Gap is helium and gap temp is 900K

'**Assume clad temp 600k**'

'**Assume moderator temperature is average temp of 578 K (Table 1)

'**Alloy E635 is slightly less Zr % than in Table 4 [1]. Did not sum to 100%.

'Final Assembly

=t-depl parm=(centrm, weight)

13AU VVER1000 Fuel Lattice

v7-252

'-----

'----ALIAS BLOCK-----

read alias

\$fuel 1 11 12 13 14 end

\$mod 4 401- 404 end

\$CRmod 41 42 43 end

\$clad 3 31 - 34 end

\$gapi 2 21 23 25 27 end

\$gapo 20 22 24 26 28 end

end alias

'-----

'----COMPOSITION BLOCK-----

read composition

'-----Fuel-----

uo2 \$fuel den=10.55 1 1005

92234 0.0054
92235 1.3
92238 98.6946 end

'-----Gap:Fuel Pin-----'

helium \$gapi 1 900 end

helium \$gapo 1 900 end

'-----Cladding Alloy E110:Fuel-----'

wtptE110 \$clad 6.4516 3

40000 98.97
41000 1.0
72000 0.03

1 600 end

'-----Moderator-----'

h2o \$mod den=0.7167 1 578 end

boron \$mod den=0.7167 525e-6 578 end

h2o \$CRmod den=0.7167 1 578 end

boron \$CRmod den=0.7167 525e-6 578 end

'-----Guide Tube Alloy E635-----'

wtptE635 5 6.55 4

40000 97.40
41000 1.0
50000 1.3
26000 0.3

1 578 end

'-----Control rod-----'

b4c 70 den=1.8 1 1005

5010 19.8
5011 80.2 end

'-----Control Rod Clad Steel-----'

wtptCRclad 80 7.8 4

26000 69.5
24000 18.0
28000 11.0
25000 1.5
1 578 end

'-----Spacer Grid-----

end composition

'-----

'----CELL DATA BLOCK -----

read cell

latticecell atriangpitch imodr=0.075 \$gapi fuelr=0.3785 \$fuel gapr=0.3865 \$gapo clad=0.455 \$clad hpitch=0.6375 \$mod end

end cell

'-----

'----BURNDATA BLOCK -----

read burndata

power=42.5 burn=4 nlib=5 end

power=42.5 burn=307 nlib=5 end

power=42.5 burn=100nlib=1 end

end burndata

'-----

'----BRANCH BLOCK -----

read branch

define fuel \$fuel end

define mod \$mod \$SCRmod end

define crout 42 43 end

define crin 70 80 end

tf=1005 tm=578 dm=0.7167 cr=0 sb=525 end

cr=1 end

sb=1000 end

cr=1 sb=1000 end

sb=1500 end

```

cr=1 sb=1500 end

sb=2000 end

cr=1 sb=2000 end

sb=0 end

cr=1 sb=0 end

tm=300 end

tm=300 cr=1 end

tf=1500 end

tf=2000 end

tf=3000 end

dm=0.6 end

dm=0.85 end

dm=1.0 end

end branch

'-----
'----DEPLETION BLOCK -----
read depletion

$fuel end

end depletion

'-----

read model

'----PARAMETER BLOCK -----

read parameters

cmfd=yes

xcmfd=1

ycmfd=1

epsilon=1e-5

echo=yes

converge=cell

drawit=yes

prtmxtab=no

```

```

timed=yes

cell_tol=1.0e-8

prtflux=yes

end parameters

'-----
'----MATERIALS BLOCK -----

read materials

mix=$fuel pn=1 com='1.3% enrich UO2 fuel' end

mix=$gapi pn=1 com='helium gap, inner pin' end

mix=$gapo pn=1 com='helium gap btw fuel and clad' end

mix=$clad pn=1 com='fuel pin cladding, zircalloy E110' end

mix=$mod pn=2 com='moderator H2O and boron' end

mix=$CRmod pn=2 com='guide tube moderator when rods out' end

mix=5 pn=1 com='guide tube alloy E635' end

mix=70 pn=1 com='control rod material' end

mix=80 pn=1 com='control rod clad' end

end materials

'-----
'----GEOMETRY BLOCK -----

read geometry

unit 1

com='fuel pin Region 5'

cylinder 10      0.075

cylinder 20      0.3785

cylinder 30      0.3865

cylinder 40      0.455

rhexprism      50      0.6375

media 2 1      10

media 1 1      1      20 -10

media 20 1      30 -20

media 3 1      40 -30

```

```

media 4 1      50 -40

boundary 50 4 4

unit 101

com='fuel pin Region 1'

cylinder 10      0.075

cylinder 20      0.3785

cylinder 30      0.3865

cylinder 40      0.455

rhexprism      50      0.6375

media 21 1      10

media 11      1      20 -10

media 22 1      30 -20

media 31 1      40 -30

media 401      1      50 -40

boundary 50 4 4

unit 102

com='fuel pin Region 2'

cylinder 10      0.075

cylinder 20      0.3785

cylinder 30      0.3865

cylinder 40      0.455

rhexprism      50      0.6375

media 23 1      10

media 12      1      20 -10

media 24 1      30 -20

media 32 1      40 -30

media 402      1      50 -40

boundary 50 4 4

unit 103

com='fuel pin Region 3'

cylinder 10      0.075

```

```

cylinder 20      0.3785
cylinder 30      0.3865
cylinder 40      0.455
rhexprism      50      0.6375
media 25 1      10
media 13 1      1      20 -10
media 26 1      30 -20
media 33 1      40 -30
media 403      1      50 -40
boundary 50 4 4

```

unit 104

com='fuel pin Region 4'

```

cylinder 10      0.075
cylinder 20      0.3785
cylinder 30      0.3865
cylinder 40      0.455
rhexprism      50      0.6375
media 27 1      10
media 14 1      1      20 -10
media 28 1      30 -20
media 34 1      40 -30
media 404      1      50 -40
boundary 50 4 4

```

unit 2

com='central guide tube'

```

cylinder 10      0.55
cylinder 20      0.65
rhexprism      30      0.6375
media 41 1      1      10
media 5 1      1      20 -10
media 4 1      30 -20

```

boundary 30 4 4

unit 3

com='guide tube, with room for rod'

cylinder 10 0.35

cylinder 20 0.41

cylinder 30 0.55

cylinder 40 0.65

rhexprism 50 0.6375

media 42 1 10

media 43 1 20 -10

media 41 1 30 -20

media 5 1 40 -30

media 4 1 50 -40

boundary 50 4 4

unit 4

com='stiffening angle'

hexprism 10 11.6

hexprism 20 11.7

media 5 1 20 -10

boundary 20

unit 40

com='stiffing angle gap'

cuboid 10 .05 -.05 3.825 -3.825

media 4 1 10

boundary 10

global unit 100

com='fuel assembly'

hexprism 10 11.74

array 1 10 place 11 11 0 0

hole 4 origin x=0 y=0

hole 40 origin x=-11.65 y=0

hole 40 origin x=11.65 y=0

hole 40 origin x=-5.68 y=10.1625 rotate a1=-60

hole 40 origin x=5.68 y=10.1625 rotate a1=60

hole 40 origin x=5.68 y=-10.1625 rotate a1=-60

hole 40 origin x=-5.68 y=-10.1625 rotate a1=60

media 4 1 10

boundary 10 12 12

end geometry

'-----

'----ARRAY BLOCK -----

read array

ara=1 typ=rhexagonal nux=21 nuy=21

fill

0	0	0	0	0	0	0	0	0	0	1	1	1
	0	0	0	0	0	0	0	0	0	0		
0	0	0	0	0	0	0	104	1	1	1	1	
	1	104	0	0	0	0	0	0	0	0		
0	0	0	0	0	104	104	1	1	1	1	1	
	1	1	104	104	0	0	0	0	0	0		
0	0	0	104	104	1	1	1	1	1	1	1	
	1	1	1	1	104	104	0	0	0	0		
0	1	1	1	1	1	1	103	1	103	103	103	
	1	103	1	1	1	1	1	1	0			
1	1	1	1	1	1	103	3	103	103	3	103	
	103	3	103	1	1	1	1	1	1	1		
1	1	1	1	1	103	103	103	103	102	103	102	
	103	103	103	103	1	1	1	1	1	1		
1	1	1	1	103	3	103	102	102	3	102	102	
	102	102	103	3	103	1	1	1	1	1		
104	1	1	1	103	103	103	102	102	102	102	102	
	3	102	103	103	103	1	1	1	104			
104	1	1	103	103	103	102	3	102	101	101	101	
	102	102	102	103	103	103	1	1	104			
104	1	1	103	3	103	102	102	102	101	2	101	
	102	3	102	103	3	103	1	1	104			
104	1	1	1	103	103	102	102	102	102	101	102	
	102	102	102	103	103	1	1	1	104			

104	1 102	1 102	1 103	103 3	3 103	103 1	102 1	3 1	102 104	102	3
1	1 102	1 103	1 103	103 103	103 103	103 1	103 1	102 1	102 1	102	102
1	1 103	1 3	1 103	1 1	1 1	103 1	3 1	103 1	103 1	103	103
1	1 103	1 103	1 103	1 1	1 1	103 1	103 1	103 1	103 1	3	103
0	0 1	1 1	104 1	1 1	1 1	1 104	1 1	1 0	1 0	103	1
0	0 1	0 1	0 1	104 104	104 104	1 0	1 0	1 0	1 0	1	1
0	0 1	0 104	0 104	0 0	0 0	104 0	104 0	1 0	1 0	1	1
0	0 1	0 0	0 0	0 0	0 0	0 0	0 0	1 0	1 0	1	1
0	0 0	0 0	0 0	0 0	0 0	0 0	0 0	0 0	0 0	1	0

end array

'-----

'----COLLAPSE BLOCK -----

read collapse

40r1 16r2

end collapse

'-----

'----HOMOG BLOCK -----

read hmog

500 AssemAU 1 11 12 13 14 4 401 402 403 404 3 31 32 33 34 2 21 23 25 27 20 22 24 26 28 5 41 42 43 end

end hmog

'-----

'----ADF BLOCK -----

read adf

3 500

0.00000 13.55618 11.74000 6.77809

11.74000 6.77809 11.74000 -6.77809

11.74000 -6.77809 0.00000 -13.55618

```

0.00000 -13.55618 -11.74000 -6.77809
-11.74000 -6.77809 -11.74000 6.77809
-11.74000 6.77809 0.00000 13.55618

end adf

'-----
'----BOUNDARY CONDITIONS BLOCK-----

read bnds

all=white

end bnds

'-----

end model

end

=shell

cp $TMPDIR/xfile016 $RTNDR/$BASENAME.x16

cp $TMPDIR/txtfile16 $RTNDR/$BASENAME.t16

cp $TMPDIR/ft33f001.cmbined $RTNDR/$BASENAME.f33

cp $TMPDIR/ft71001 $RTNDR/$BASENAME.f71

end

```

E.2.2: 30AV5 Cross-Section File

```

'VVER1000 FA30AV5 DEPL

'3.00 235U Enriched, 5% Gd2O3 2.4% 235U BA pin

'Created by Margaret Kurtts

'*****Assumptions and References*****

'1. Lotsch, T., V. Khalimonchuk, and A. Kuchin, Proposal of a Benchmark for Core Burnup Calculations for a VVER-1000 Reactor Core, 2009

'2. Lotsch, T., V. Khalimonchuk, and A. Kuchin. Corrections and additions to the proposal of a benchmark for core burnup calculations for a WVER-1000 reactor, 2010.

'Table 4 [1]-materials for fuel, guide tube, spacer.

'Table 3 [1]-materials for control rods, burnable absorbers

'Table 5 [1]-materials for stiffing plate

'Table 1 [1]-reactor temperature data

```

'Tab 1 [2]-Moderator Boron Concentration and fuel temperature

'Table 3 [1]-BA materials, specifications

'Moderator density based off properties of water at 15.7 MPa and 578 K, Table 1 [1], used www.wolframalpha.com

***Assume Gap is helium and gap temp is slightly less than fuel

Assume fuel clad and BA clad temp 600k

***Assume moderator temperature is average temp of 578 K (Table 1)

***Assume fuel/BA cladding temp is slightly higher than moderator at 600K

***Alloy E635 is slightly less Zr % than in Table 4 [1]. Did not sum to 100%.

***BA material composition in [1] seems in error. [2] does not provide details beyond Gd2O3. Assume SCALE Standard composition for Gd2O3

***CR/BA tubes are different than guide tubes and cladding Table 3 [1]. This seems in error. Not mentioned in [2].

***Table 3 [1] CR/BA tubes not used. Cladding and guide tubes used (table 3 and 4, [1])

'Final

=t-depl parm=(centrm,weight)

30AV5 VVER1000 Fuel Lattice

v7-252

'-----

'----ALIAS BLOCK-----

read alias

\$fuel 1 11 12 13 14 15 16 end

\$fuelBA 130 - 174 end

\$mod 4 401- 406 end

\$CRmod 41 42 43 end

\$clad 3 31 - 36 end

\$gapi 2 21 23 25 27 29 291 end

\$gapo 20 22 24 26 28 280 282 end

\$BAGapi 600 - 608 end

\$BAGapo 700 - 708 end

\$BAclad 800 - 808 end

\$BAMod 900 - 908 end

```

end alias

'-----COMPOSITION BLOCK -----

read composition

'-----Fuel-----

uo2 $fuel den=10.55 1 1005

                                92234 0.0054

                                92235 3.00

                                92238 96.9946 end

uo2 $fuelBA den=10.376 0.95 1005

                                92234 0.0054

                                92235 2.400

                                92238 97.5946 end

gd2o3 $fuelBA den=10.376 0.05 1005 end

'-----Gap:Fuel Pin-----

helium $gapi 1 900 end

helium $gapo 1 900 end

'-----Cladding Alloy E110:Fuel and Spacer Grid-----

wtptE110 $clad 6.4516 3

                                40000 98.97

                                41000 1.0

                                72000 0.03

                                1 600 end

'-----Moderator-----

h2o $mod den=0.7167 1 578 end

boron $mod den=0.7167 525e-6 578 end

h2o $CRmod den=0.7167 1 578 end

boron $CRmod den=0.7167 525e-6 578 end

'-----Guide Tube Alloy and Stiffening Plate E635-----

wtptE635 5 6.55 4

                                40000 97.40

                                41000 1.0

```

```

50000 1.3
26000 0.3
1 578 end

'-----BA Cladding-----
wptBAclad $BAclad 6.4516 3
40000 98.97
41000 1.00
72000 0.03
1 600 end

'-----BA Gap-----
helium $BAgapi 1 900 end
helium $BAgapo 1 900 end

'-----BA moderator-----
h2o $BAmo den=0.7167 1 578 end
boron $BAmo den=0.7167 525e-6 578 end

'-----Control rod-----
b4c 70 den=1.8 1 1005
5010 19.8
5011 80.2 end

'-----Control Rod Clad Steel-----
wptCRclad 80 7.8 4
26000 69.5
24000 18.0
28000 11.0
25000 1.5
1 578 end

'-----Spacer Grid-----
end composition
'-----
'-----CELL DATA BLOCK -----
read cell

```

latticell atiangpitch imodr=0.075 \$gapi fuelr=0.3785 \$fuel gapr=0.3865 \$gapo cladr=0.455 \$clad hpitch=0.6375 \$mod end

multiregion cylindrical left_bdy=reflected right_bdy=white end

600 0.075

130 0.1695

131 0.2397

132 0.2936

133 0.3390

134 0.3790

700 0.3860

800 0.4550

900 0.6694

end zone

multiregion cylindrical left_bdy=reflected right_bdy=white end

601 0.075

135 0.1695

136 0.2397

137 0.2936

138 0.3390

139 0.3790

701 0.3860

801 0.4550

901 0.6694

end zone

multiregion cylindrical left_bdy=reflected right_bdy=white end

602 0.075

140 0.1695

141 0.2397

142 0.2936

143 0.3390

144 0.3790

702 0.3860

802 0.4550

902 0.6694

end zone

multiregion cylindrical left_bdy=reflected right_bdy=white end

603 0.075

145 0.1695

146 0.2397

147 0.2936

148 0.3390

149 0.3790

703 0.3860

803 0.4550

903 0.6694

end zone

multiregion cylindrical left_bdy=reflected right_bdy=white end

604 0.075

150 0.1695

151 0.2397

152 0.2936

153 0.3390

154 0.3790

704 0.3860

804 0.4550

904 0.6694

end zone

multiregion cylindrical left_bdy=reflected right_bdy=white end

605 0.075

155 0.1695

156 0.2397

157 0.2936

158 0.3390

159 0.3790

705 0.3860

805 0.4550

905 0.6694

end zone

multiregion cylindrical left_bdy=reflected right_bdy=white end

606 0.075

160 0.1695

161 0.2397

162 0.2936

163 0.3390

164 0.3790

706 0.3860

806 0.4550

906 0.6694

end zone

multiregion cylindrical left_bdy=reflected right_bdy=white end

607 0.075

165 0.1695

166 0.2397

167 0.2936

168 0.3390

169 0.3790

707 0.3860

807 0.4550

907 0.6694

end zone

multiregion cylindrical left_bdy=reflected right_bdy=white end

608 0.075

170 0.1695

171 0.2397

172 0.2936
173 0.3390
174 0.3790
708 0.3860
808 0.4550
908 0.6694

end zone

end cell

'-----

'----BURNDATA BLOCK -----

read burndata

power=42.5 burn=4 nlib=5 end

power=42.5 burn=307 nlib=5 end

power=42.5 burn=100nlib=1 end

end burndata

'-----

'----BRANCH BLOCK -----

read branch

define fuel \$fuel \$fuelBA end

define mod \$mod \$SCRmod end

define crout 42 43 end

define crin 70 80 end

tf=1005 tm=578 dm=0.7167 cr=0 sb=525 end

cr=1 end

sb=1000 end

cr=1 sb=1000 end

sb=1500 end

cr=1 sb=1500 end

sb=2000 end

cr=1 sb=2000 end

sb=0 end

```

cr=1 sb=0 end

tm=300 end

tm=300 cr=1 end

tf=1500 end

tf=2000 end

tf=3000 end

dm=0.6 end

dm=0.85 end

dm=1.0 end

end branch

'-----
'-----DEPLETION BLOCK -----
read depletion

$fuel flux $fuelBA end

end depletion

'-----

read model

'-----PARAMETER BLOCK -----

read parameters

cmfd=yes

xcmfd=1

ycmfd=1

epsilon=1e-5

echo=yes

converge=cell

drawit=yes

prtmxtab=no

timed=yes

cell_tol=1.0e-8

prtflux=yes

end parameters

```

'-----MATERIALS BLOCK -----

read materials

mix=\$fuel pn=1 com='1.3% enrich UO2 fuel' end
mix=\$gapi pn=1 com='helium gap, inner pin' end
mix=\$gapo pn=1 com='helium gap btw fuel and clad' end
mix=\$clad pn=1 com='fuel pin cladding, zircalloy E110' end
mix=\$mod pn=2 com='moderator H2O and boron' end
mix=\$CRmod pn=2 com='guide tube moderator when rods out' end
mix=\$fuelBA pn=1 com='BA fuel 2.4% enriched ²³⁵U, 5% enrich Gd' end
mix=\$BAgapi pn=1 com='helium center BA pins' end
mix=\$BAgapo pn=1 com='helium gap BA pins' end
mix=\$BAclad pn=1 com='cladding BA bins' end
mix=\$BAmod pn=2 com='moderator around BA pins' end
mix=5 pn=1 com='guide tube alloy E635' end
mix=70 pn=1 com='control rod material' end
mix=80 pn=1 com='control rod clad' end

end materials

'-----GEOMETRY BLOCK -----

read geometry

unit 1

com='fuel pin Region 5--all others'

cylinder	10	0.075	
cylinder	20	0.3785	
cylinder	30	0.3865	
cylinder	40	0.455	
rhexpism	50	0.6375	
media 2	1	10	
media	1	1	20 -10

```

media 20 1      30 -20

media 3  1      40 -30

media 4  1      50 -40

boundary 50 4 4

unit 101

com='fuel pin near central guide tube, Region 1'

cylinder 10     0.075

cylinder 20     0.3785

cylinder 30     0.3865

cylinder 40     0.455

rhexprism 50    0.6375

media 22 1      10

media  11      1      20 -10

media 23 1      30 -20

media 31 1      40 -30

media 401      1      50 -40

boundary 50 4 4

unit 102

com='fuel pin Region 2---inner guide channels'

cylinder 10     0.075

cylinder 20     0.3785

cylinder 30     0.3865

cylinder 40     0.455

rhexprism 50    0.6375

media 23 1      10

media  12      1      20 -10

media 24 1      30 -20

media 32 1      40 -30

media 402      1      50 -40

boundary 50 4 4

unit 103

```

com='fuel pin Region 3--outer guide channels'

cylinder 10 0.075
cylinder 20 0.3785
cylinder 30 0.3865
cylinder 40 0.455
rhexprism 50 0.6375
media 25 1 10
media 13 1 20 -10
media 26 1 30 -20
media 33 1 40 -30
media 403 1 50 -40
boundary 50 4 4

unit 104

com='fuel pin Region 4---edges b/w corners stiffening'

cylinder 10 0.075
cylinder 20 0.3785
cylinder 30 0.3865
cylinder 40 0.455
rhexprism 50 0.6375
media 27 1 10
media 14 1 20 -10
media 28 1 30 -20
media 34 1 40 -30
media 404 1 50 -40
boundary 50 4 4

unit 105

com='fuel pin Region 6---around inner BA pins'

cylinder 10 0.075
cylinder 20 0.3785
cylinder 30 0.3865
cylinder 40 0.455

rhexprism	50	0.6375
media 29 1	10	
media 15	1	20 -10
media 280	1	30 -20
media 35 1	40 -30	
media 405	1	50 -40
boundary 50 4 4		

unit 106

com='fuel pin Region 7--around outer BA pins'

cylinder 10	0.075
cylinder 20	0.3785
cylinder 30	0.3865
cylinder 40	0.455
rhexprism	50 0.6375
media 291	1 10
media 16	1 20 -10
media 282	1 30 -20
media 36 1	40 -30
media 406	1 50 -40
boundary 50 4 4	

unit 10

com='BA fuel pin 1, 5% Gd2O3 2.4% ²³⁵U'

cylinder 10	0.075
cylinder 20	0.1695
cylinder 30	0.2397
cylinder 40	0.2936
cylinder 50	0.3390
cylinder 60	0.3790
cylinder 70	0.3860
cylinder 80	0.4550

rhexprism	90	0.6375
media 600	1	10
media 130	1	20 -10
media 131	1	30 -20
media 132	1	40 -30
media 133	1	50 -40
media 134	1	60 -50
media 700	1	70 -60
media 800	1	80 -70
media 900	1	90 -80

boundary 90 4 4

unit 11

com="BA fuel pin 2, 5% Gd2O3 2.4% ²³⁵U,

cylinder 10	0.075
cylinder 20	0.1695
cylinder 30	0.2397
cylinder 40	0.2936
cylinder 50	0.3390
cylinder 60	0.3790
cylinder 70	0.3860
cylinder 80	0.4550
rhexprism	90 0.6375
media 601	1 10
media 135	1 20 -10
media 136	1 30 -20
media 137	1 40 -30
media 138	1 50 -40
media 139	1 60 -50
media 701	1 70 -60
media 801	1 80 -70

media 901 1 90 -80

boundary 90 4 4

unit 12

com="BA fuel pin 3, 5% Gd2O3 2.4% ²³⁵U,

cylinder 10 0.075

cylinder 20 0.1695

cylinder 30 0.2397

cylinder 40 0.2936

cylinder 50 0.3390

cylinder 60 0.3790

cylinder 70 0.3860

cylinder 80 0.4550

rhexprism 90 0.6375

media 602 1 10

media 140 1 20 -10

media 141 1 30 -20

media 142 1 40 -30

media 143 1 50 -40

media 144 1 60 -50

media 702 1 70 -60

media 802 1 80 -70

media 902 1 90 -80

boundary 90 4 4

unit 13

com="BA fuel pin 4, 5% Gd2O3 2.4% ²³⁵U,

cylinder 10 0.075

cylinder 20 0.1695

cylinder 30 0.2397

cylinder 40 0.2936

cylinder 50 0.3390

cylinder 60	0.3790
cylinder 70	0.3860
cylinder 80	0.4550
rhexprism	90 0.6375
media 603	1 10
media 145	1 20 -10
media 146	1 30 -20
media 147	1 40 -30
media 148	1 50 -40
media 149	1 60 -50
media 703	1 70 -60
media 803	1 80 -70
media 903	1 90 -80

boundary 90 4 4

unit 14

com="BA fuel pin 5, 5% Gd2O3 2.4% ²³⁵U,

cylinder 10	0.075
cylinder 20	0.1695
cylinder 30	0.2397
cylinder 40	0.2936
cylinder 50	0.3390
cylinder 60	0.3790
cylinder 70	0.3860
cylinder 80	0.4550
rhexprism	90 0.6375
media 604	1 10
media 150	1 20 -10
media 151	1 30 -20
media 152	1 40 -30
media 153	1 50 -40

media 154 1 60 -50
media 704 1 70 -60
media 804 1 80 -70
media 904 1 90 -80

boundary 90 4 4

unit 15

com='BA fuel pin 6, 5% Gd2O3 2.4% ²³⁵U,

cylinder 10 0.075
cylinder 20 0.1695
cylinder 30 0.2397
cylinder 40 0.2936
cylinder 50 0.3390
cylinder 60 0.3790
cylinder 70 0.3860
cylinder 80 0.4550

rhexprism 90 0.6375

media 605 1 10
media 155 1 20 -10
media 156 1 30 -20
media 157 1 40 -30
media 158 1 50 -40
media 159 1 60 -50
media 705 1 70 -60
media 805 1 80 -70
media 905 1 90 -80

boundary 90 4 4

unit 16

com='BA fuel pin 7, 5% Gd2O3 2.4% ²³⁵U,

cylinder 10 0.075
cylinder 20 0.1695

cylinder	30		0.2397
cylinder	40		0.2936
cylinder	50		0.3390
cylinder	60		0.3790
cylinder	70		0.3860
cylinder	80		0.4550
rhexprism	90		0.6375
media	606	1	10
media	160	1	20 -10
media	161	1	30 -20
media	162	1	40 -30
media	163	1	50 -40
media	164	1	60 -50
media	706	1	70 -60
media	806	1	80 -70
media	906	1	90 -80

boundary 90 4 4

unit 17

com='BA fuel pin 8, 5% Gd2O3 2.4% ²³⁵U'

cylinder	10		0.075
cylinder	20		0.1695
cylinder	30		0.2397
cylinder	40		0.2936
cylinder	50		0.3390
cylinder	60		0.3790
cylinder	70		0.3860
cylinder	80		0.4550
rhexprism	90		0.6375
media	607	1	10
media	165	1	20 -10

media	166	1	30 -20
media	167	1	40 -30
media	168	1	50 -40
media	169	1	60 -50
media	707	1	70 -60
media	807	1	80 -70
media	907	1	90 -80

boundary 90 4 4

unit 18

com="BA fuel pin 9, 5% Gd2O3 2.4% ²³⁵U,

cylinder	10	0.075	
cylinder	20	0.1695	
cylinder	30	0.2397	
cylinder	40	0.2936	
cylinder	50	0.3390	
cylinder	60	0.3790	
cylinder	70	0.3860	
cylinder	80	0.4550	

rhexprism	90	0.6375	
-----------	----	--------	--

media	608	1	10
media	170	1	20 -10
media	171	1	30 -20
media	172	1	40 -30
media	173	1	50 -40
media	174	1	60 -50
media	708	1	70 -60
media	808	1	80 -70
media	908	1	90 -80

boundary 90 4 4

unit 2

com='central guide tube'

cylinder 10 0.55

cylinder 20 0.65

rhexprism 30 0.6375

media 41 1 10

media 5 1 20 -10

media 4 1 30 -20

boundary 30 4 4

unit 3

com='guide tube, with room for rod'

cylinder 10 0.35

cylinder 20 0.41

cylinder 30 0.55

cylinder 40 0.65

rhexprism 50 0.6375

media 42 1 10

media 43 1 20 -10

media 41 1 30 -20

media 5 1 40 -30

media 4 1 50 -40

boundary 50 4 4

unit 4

com='stiffening angle'

hexprism 10 11.6

hexprism 20 11.7

media 5 1 20 -10

boundary 20

unit 40

com='stiffing angle gap'

cuboid 10 .05 -.05 3.825 -3.825

media 4 1 10

```

boundary 10

global unit 100

com='fuel assembly'

hexprism 10      11.74

array 1  10      place 11 11 0 0

hole 4 origin x=0 y=0

hole 40 origin x=-11.65 y=0

hole 40 origin x=11.65 y=0

hole 40 origin x=-5.68 y=10.1625 rotate a1=-60

hole 40 origin x=5.68 y=10.1625 rotate a1=60

hole 40 origin x=5.68 y=-10.1625 rotate a1=-60

hole 40 origin x=-5.68 y=-10.1625 rotate a1=60

media 4  1      10

boundary 10 12 12

end geometry

```

```
'-----
```

```
'-----ARRAY BLOCK -----
```

```
read array
```

```
ara=1 typ=rhexagonal nux=21 nuy=21
```

```
fill
```

```

0      0      0      0      0      0      0      0      0      1      1      1
      0      0      0      0      0      0      0      0      0
0      0      0      0      0      0      0      104     1      106     106     106
      1      104     0      0      0      0      0      0      0      0
0      0      0      0      0      104     104     1      1      106     16      106
      1      1      104     104     0      0      0      0      0
0      0      0      104     104     1      1      1      1      1      106     1
      1      1      1      1      104     104     0      0      0
0      1      1      1      1      1      1      103     1      103     103     103
      1      103     1      1      1      1      1      1      1      0
1      106     106     106     1      1      103     3      103     103     3      105
      103     3      103     1      1      106     106     106     1
1      106     15      106     1      103     103     103     103     102     105     11
      105     103     103     103     1      106     17      106     1

```

1	1 105	106 102	1 103	103 3	3 103	103 1	102 106	102 1	3 1	105	105
104	1 3	1 102	1 103	103 103	103 103	103 1	102 1	102 1	102 104	102	102
104	1 102	1 102	103 102	103 103	103 103	102 103	3 1	102 1	101 104	101	101
104	1 102	1 3	103 102	3 103	105 3	105 103	105 1	102 1	101 104	2	101
104	1 102	1 105	1 102	103 103	105 103	12 1	105 1	102 1	102 104	101	102
104	1 105	1 10	1 105	103 3	3 103	105 1	102 1	3 1	102 104	102	3
1	106 105	106 105	106 105	103 103	103 103	103 106	103 106	102 106	102 1	102	102
1	106 103	14 3	106 103	1 1	1 1	103 106	3 18	103 106	103 1	103	103
1	1 103	106 103	1 103	1 1	1 1	103 1	103 106	103 1	103 1	3	103
0	0 1	1 1	104 1	1 1	1 1	1 104	1 1	1 0	1 0	103	1
0	0 1	0 1	0 1	104 104	104 104	1 0	1 0	1 0	106 0	106	106
0	0 1	0 104	0 104	0 0	0 0	104 0	104 0	1 0	106 0	13	106
0	0 1	0 0	0 0	0 0	0 0	0 0	0 0	1 0	1 0	106	1
0	0 0	0 0	0 0	0 0	0 0	0 0	0 0	0 0	0 0	1 end fill	0

end array

'-----

'----COLLAPSE BLOCK -----

read collapse

40r1 16r2

end collapse

'-----

'----HOMOG BLOCK -----

read hmog

500 30AV5

1 11 12 13 14 15 16

```

130      131      132      133      134      135      136      137      138      139      140      141
        142      143      144      145

146      147      148      149      150      151      152      153      154      155      156      157
        158      159      160      161

162      163      164      165      166      167      168      169      170      171      172      173
        174

4        401      402      403      404      405      406

41       42       43

3        31       32       33       34       35       36

2        21       23       25       27       29       291

20       22       24       26       28       280      282

600      601      602      603      604      605      606      607      608

700      701      702      703      704      705      706      707      708

800      801      802      803      804      805      806      807      808

900      901      902      903      904      905      906      907      908

```

5

70

80 end

end hmog

'-----

'----ADF BLOCK-----

read adf

3 500

0.00000 13.55618 11.74000 6.77809

11.74000 6.77809 11.74000 -6.77809

11.74000 -6.77809 0.00000 -13.55618

0.00000 -13.55618 -11.74000 -6.77809

-11.74000 -6.77809 -11.74000 6.77809

-11.74000 6.77809 0.00000 13.55618

end adf

'-----

'----BOUNDARY CONDITIONS BLOCK-----

```

read bnds

  all=white

end bnds

'-----

end model

end

=shell

cp $TMPDIR/xfile016 $RTNDR/$BASENAME.x16

cp $TMPDIR/txfile16 $RTNDR/$BASENAME.t16

cp $TMPDIR/ft33f001.cmbined $RTNDR/$BASENAME.f33

cp $TMPDIR/ft71001 $RTNDR/$BASENAME.f71

end

```

E.2.3: Radial Reflector NEWT Model

```

=t-newt parm=(centrm)

1DReflector

'1D reflector slice. Uses matching materials as final model

'v7-238

v7-252

read composition

uo2    303 den= 10.55  0.667033 1005.0

      92234 0.0054

      92235 3.000000

      92238 96.9946          end

helium  303      0.182418 1005.0  end

wtpt-mix 303  6.451600 3

      40000 98.97

      41000 1.000000

      72000 0.03

              0.150549 1005.0 end

h2o     304 den=0.716700 0.999475 578.0 end

```

```

boron    304 den=0.716700 0.000525 578.0 end
ss304s   100 den=7.94000  1.0           563.15 end

ss304s   200 den=7.94000  0.544000 563.15 end
h2o      200 den=0.746500 0.455761 563.15 end
boron    200 den=0.746500 0.000239 563.15 end

h2o      300 den=0.746500 0.999475 563.15 end
boron    300 den=0.746500 0.000525 563.15 end
ss304s   400 den=7.940000 1.00    563.15 end
h2o      500 den=0.746500 0.999475 563.15 end
boron    500 den=0.746500 0.000525 563.15 end
ss304s   600 den=7.940000 1.00    563.15 end
end composition

```

```

read cell
' 30av5 Fuel Pin
  latticecell
    triangpitch
    fuelr= 0.455000 303
    hpitch= 0.637500 304      end
end cell

```

```

read model
  read parameters
    prthmmix=yes
'  cmfd=yes
  timed=yes
  converge=mix
  drawit=yes

```

```

echo=yes

' prtflux=yes

' If reflective boundary conditions are desired for hexagonal-domain
' configurations, product quadrature sets must be used and nazim must
' be a multiple of 3.
' nazim=3
' npolar=2
'Eigenvalue mode followed by a buckling correction
' solntype=b1

'Turns on the use of the B1 approximation to determine the critical spectrum
' useb1=yes

epseigen=1e-05
epsinner=1e-05
epsouter=1e-05

outers=1000

end parameters

read materials

*** Lattice 30av5

mix=303 pn=1 com='30av5 Fuel pin 1' end
mix=304 pn=2 com='Water' end
mix=100 pn=1 com='steel' end
mix=200 pn=2 com='ss304-h20' end
mix=300 pn=2 com='h2o ' end
mix=400 pn=1 com='ss304' end
mix=500 pn=2 com='h2o ' end
mix=600 pn=1 com='ss304' end

end materials

read geometry

***** Global 1D slice *****

```

global unit 1

com="1D_Ref1"

cuboid 10 217.725 0.00 1.104182 -1.104182

cuboid 11 149.175 0.00 1.104182 -1.104182

cuboid 100 153.175 149.175 1.104182 -1.104182

cuboid 200 164.475 153.175 1.104182 -1.104182

cuboid 300 165.475 164.475 1.104182 -1.104182

cuboid 400 171.475 165.475 1.104182 -1.104182

cuboid 500 197.925 171.475 1.104182 -1.104182

cuboid 600 217.725 197.925 1.104182 -1.104182

hole 100 origin x=0.0

hole 100 origin x=11.475

hole 100 origin x=22.95

hole 100 origin x=34.425

hole 100 origin x=45.9

hole 100 origin x=57.375

hole 100 origin x=68.85

hole 100 origin x=80.325

hole 100 origin x=91.8

hole 100 origin x=103.275

hole 100 origin x=114.75

hole 100 origin x=126.225

hole 100 origin x=137.7

media 304 1 11

media 100 1 100

media 200 1 200

media 300 1 300

media 400 1 400

media 500 1 500

media 600 1 600

boundary 10 353 2

***** LATTICE 1 *****

unit 100

com="1D_Refl"

cuboid 10 11.475 0.00 1.104182 -1.104182

' Top Row

hole 14 origin x=0.00 y=1.104182

hole 12 origin x=1.275 y=1.104182

hole 12 origin x=2.550 y=1.104182

hole 12 origin x=3.825 y=1.104182

hole 12 origin x=5.100 y=1.104182

hole 12 origin x=6.375 y=1.104182

hole 12 origin x=7.650 y=1.104182

hole 12 origin x=8.925 y=1.104182

hole 12 origin x=10.200 y=1.104182

hole 16 origin x=11.475 y=1.104182

' Middle Row

hole 10 origin x=0.6375

hole 10 origin x=1.9125

hole 10 origin x=3.1875

hole 10 origin x=4.4625

hole 10 origin x=5.7375

hole 10 origin x=7.0125

hole 10 origin x=8.2875

hole 10 origin x=9.5625

hole 10 origin x=10.8375

' Bottom Row

hole 13 origin x=0.00 y=-1.104182

hole 11 origin x=1.275 y=-1.104182

hole 11 origin x=2.550 y=-1.104182

hole 11 origin x=3.825 y=-1.104182
hole 11 origin x=5.100 y=-1.104182
hole 11 origin x=6.375 y=-1.104182
hole 11 origin x=7.650 y=-1.104182
hole 11 origin x=8.925 y=-1.104182
hole 11 origin x=10.200 y=-1.104182
hole 15 origin x=11.475 y=-1.104182
media 304 1 10
boundary 10 9 2

*** Lattice 1, Pin 1 *****

unit 10
com="Fuel pin"
cylinder 13 0.4550
media 303 1 13
boundary 13 2 2

*** Lattice 1, Pin 1 *****

unit 11
com="Fuel pin"
cylinder 13 0.4550 chord +y=0.0
media 303 1 13
boundary 13 2 1

*** Lattice 1, Pin 1 *****

unit 12
com="Fuel pin"
cylinder 13 0.4550 chord -y=0.0
media 303 1 13
boundary 13 2 1

*** Lattice 1, Pin 1 *****

unit 13
com="Fuel pin"

```

cylinder 13 0.4550 chord +y=0.0 chord +x=0.0

media 303 1 13

boundary 13 1 1

*** Lattice 1, Pin 1 ****
unit 14

com="Fuel pin"

cylinder 13 0.4550 chord -y=0.0 chord +x=0.0

media 303 1 13

boundary 13 1 1

*** Lattice 1, Pin 1 ****
unit 15

com="Fuel pin"

cylinder 13 0.4550 chord +y=0.0 chord -x=0.0

media 303 1 13

boundary 13 1 1

*** Lattice 1, Pin 1 ****
unit 16

com="Fuel pin"

cylinder 13 0.4550 chord -y=0.0 chord -x=0.0

media 303 1 13

boundary 13 1 1

end geometry

read bnds

-x=reflect

+x=vacuum

-y=reflect

+y=reflect

end bnds

read collapse

213r1 39r2

```

```

' 199r1 39r2
' 30r1 19r2
end collapse

read hmog
5000 Assembly 303 304 end
5001 Reflector 100 200 300 400 500 600 end
end hmog

read adf
' Assembly Discontinuity Factors
2 5000 5001 w=149.175
end adf

end model

end

=shell
cp $TMPDIR/xfile016 $RTNDR/$BASENAME.x16
cp $TMPDIR/txfile16 $RTNDR/$BASENAME.t16
cp $TMPDIR/ft33f001.cmbined $RTNDR/$BASENAME.f33
cp $TMPDIR/ft71001 $RTNDR/$BASENAME.f71
end

```

E.2.4: Bottom Axial Reflector

```

=t-newt parm=(centrm)
1DReflector Bottom Reflector
'1D reflector slice for Axial Bottom Reflector. Uses matching materials as final model
'v7-238
v7-252

read composition

```

uo2 303 den= 10.55 0.667033 1005.0

92234 0.0054

92235 3.000000

92238 96.9946 end

helium 303 0.182418 1005.0 end

wtpt-mix 303 6.451600 3

40000 98.97

41000 1.000000

72000 0.03

0.150549 1005.0 end

h2o 304 den=0.716700 0.999475 578.0 end

boron 304 den=0.716700 0.000525 578.0 end

'E110 is Spacer grid between end of active fuel and reflector

wtptE110 100 6.4516 3

40000 98.97

41000 1.0

72000 0.03

1 563.15 end

ss304s 200 den=7.94000 0.07 563.15 end

h2o 200 den=0.746500 0.5796955 563.15 end

boron 200 den=0.746500 0.0003045 563.15 end

zirc4 200 den=6.56 0.35 563.15 end

ss304s 300 den=7.94000 0.33 563.15 end

h2o 300 den=0.746500 0.56970075 563.15 end

boron 300 den=0.746500 0.00029925 563.15 end

zirc4 300 den=6.56 0.1 563.15 end

ss304s 400 den=7.94000 0.33 563.15 end

h2o 400 den=0.746500 0.66964825 563.15 end

```

boron    400 den=0.746500 0.00035175 563.15 end
end composition

read cell

' 30av5 Fuel Pin

latticecell

triangpitch

fuelr= 0.455000 303

hpitch= 0.637500 304          end

end cell

read model

read parameters

prthmmix=yes

' cmfd=yes

timed=yes

converge=mix

drawit=yes

echo=yes

' prtflux=yes

' If reflective boundary conditions are desired for hexagonal-domain
' configurations, product quadrature sets must be used and nazim must
' be a multiple of 3.

' nazim=3

' npolar=2

' Eigenvalue mode followed by a buckling correction

' solntype=b1

' Turns on the use of the B1 approximation to determine the critical spectrum

' useb1=yes

epseigen=1e-05

epsinner=1e-05

epsouter=1e-05

```

```

    outers=2000

end parameters

read materials

*** Lattice 30av5

    mix=303 pn=1 com='30av5 Fuel pin 1' end

    mix=304 pn=2 com='Water' end

    mix=100 pn=1 com='E110 Spacer Grid' end

    mix=200 pn=1 com='steel-h2o-zirc' end

    mix=300 pn=1 com='steel-h2-zirc' end

    mix=400 pn=1 com='steel-h2' end

end materials

read geometry

***** Global ID slice *****

*****

global unit 1

    com="ID_Refl"

    cuboid 10 203.125 0.00 1.104182 -1.104182

    cuboid 11 172.125 0.00 1.104182 -1.104182

    cuboid 100 174.125 172.125 1.104182 -1.104182

    cuboid 200 176.425 174.125 1.104182 -1.104182

    cuboid 300 178.125 176.425 1.104182 -1.104182

    cuboid 400 203.125 178.125 1.104182 -1.104182

        hole 100 origin x=0.0

    hole 100 origin x=11.475

    hole 100 origin x=22.95

    hole 100 origin x=34.425

    hole 100 origin x=45.9

    hole 100 origin x=57.375

    hole 100 origin x=68.85

    hole 100 origin x=80.325

```

hole 100 origin x=91.8
hole 100 origin x=103.275
hole 100 origin x=114.75
hole 100 origin x=126.225
hole 100 origin x=137.7
hole 100 origin x=149.175
hole 100 origin x=160.65
media 304 1 11
media 100 1 100
media 200 1 200
media 300 1 300
media 400 1 400
boundary 10 328 2

***** LATTICE 1 *****

unit 100

com="1D_Refl"

cuboid 10 11.475 0.00 1.104182 -1.104182

' Top Row

hole 14 origin x=0.00 y=1.104182

hole 12 origin x=1.275 y=1.104182

hole 12 origin x=2.550 y=1.104182

hole 12 origin x=3.825 y=1.104182

hole 12 origin x=5.100 y=1.104182

hole 12 origin x=6.375 y=1.104182

hole 12 origin x=7.650 y=1.104182

hole 12 origin x=8.925 y=1.104182

hole 12 origin x=10.200 y=1.104182

hole 16 origin x=11.475 y=1.104182

' Middle Row

hole 10 origin x=0.6375

hole 10 origin x=1.9125
hole 10 origin x=3.1875
hole 10 origin x=4.4625
hole 10 origin x=5.7375
hole 10 origin x=7.0125
hole 10 origin x=8.2875
hole 10 origin x=9.5625
hole 10 origin x=10.8375

' Bottom Row

hole 13 origin x=0.00 y=-1.104182
hole 11 origin x=1.275 y=-1.104182
hole 11 origin x=2.550 y=-1.104182
hole 11 origin x=3.825 y=-1.104182
hole 11 origin x=5.100 y=-1.104182
hole 11 origin x=6.375 y=-1.104182
hole 11 origin x=7.650 y=-1.104182
hole 11 origin x=8.925 y=-1.104182
hole 11 origin x=10.200 y=-1.104182
hole 15 origin x=11.475 y=-1.104182

media 304 1 10

boundary 10 9 2

*** Lattice 1, Pin 1 *****

unit 10

com="Fuel pin"

cylinder 13 0.4550

media 303 1 13

boundary 13 2 2

*** Lattice 1, Pin 1 *****

unit 11

com="Fuel pin"

```

cylinder 13 0.4550 chord +y=0.0

media 303 1 13

boundary 13 2 1

*** Lattice 1, Pin 1 ****
unit 12

com="Fuel pin"

cylinder 13 0.4550 chord -y=0.0

media 303 1 13

boundary 13 2 1

*** Lattice 1, Pin 1 ****
unit 13

com="Fuel pin"

cylinder 13 0.4550 chord +y=0.0 chord +x=0.0

media 303 1 13

boundary 13 1 1

*** Lattice 1, Pin 1 ****
unit 14

com="Fuel pin"

cylinder 13 0.4550 chord -y=0.0 chord +x=0.0

media 303 1 13

boundary 13 1 1

*** Lattice 1, Pin 1 ****
unit 15

com="Fuel pin"

cylinder 13 0.4550 chord +y=0.0 chord -x=0.0

media 303 1 13

boundary 13 1 1

*** Lattice 1, Pin 1 ****
unit 16

com="Fuel pin"

cylinder 13 0.4550 chord -y=0.0 chord -x=0.0

```

```

media 303 1 13

boundary 13 1 1

end geometry

read bnds

-x=reflect

+x=vacuum

-y=reflect

+y=reflect

end bnds

read collapse

213r1 39r2

' 199r1 39r2

' 30r1 19r2

end collapse

read hmog

5000 Assembly 303 304 end

5001 Reflector 100 200 300 400 end

end hmog

read adf

' Assembly Discontinuity Factors

2 5000 5001 w=172.125

end adf

end model

end

=shell

cp $TMPDIR/xfile016 $RTNDR/$BASENAME.x16

cp $TMPDIR/txtfile16 $RTNDR/$BASENAME.t16

```

cp \$TMPDIR/ft33f001.cmbined \$RTNDR/\$BASENAME.f33

cp \$TMPDIR/ft71001 \$RTNDR/\$BASENAME.f71

end

E.3: Nestle Input Files

E.3.1: VVER 1000 Benchmark 63 Point Data

VVER1000_fullcore_all_reflectors

read parameter

*****Assumptions and References*****

'Created by Margaret Kurttis

'REF1. Lotsch, T., V. Khalimonchuk, and A. Kuchin, Proposal of a Benchmark for Core Burnup Calculations for a VVER-1000 Reactor Core, 2009

'REF2. Lotsch, T., V. Khalimonchuk, and A. Kuchin. Corrections and additions to the proposal of a benchmark for core burnup calculations for a WVER-1000 reactor, 2010.

'REF3. Wolfram Alpha Computational Knowledge Engine. [Online Database and Computational Tool] [cited 2016 May 24]; Available from: <http://www.wolframalpha.com/>.

'REF4. Nuclear Power: Convert/Calculator-Boric Acid. [Web page] [cited 2016 May 25]; Available from: <http://www.nuclear-power.net/glossary/boron-10/convertcalculator-boric-acid/>.

'Table 4 [1]-materials for fuel, guide tube, spacer.

'Table 3 [1]-materials for control rods, burnable absorbers

'Table 5 [1]-materials for stiffing plate

'Table 1 [1]-reactor temperature data

'Tab 1 [2]-Moderator Boron Concentration and fuel temperature

'Burndata comes from [2] for power (42.5 MW/MTU) and the core was shut down after 311.74 EFPD [1,2]

'Figure 1 [1] shows operating data for cycle 1. It took ~50 days for the core to reach full power

'Full core using 5 fuels, radial reflector

*****Assumptions and References*****

xsecfile=FUEL621.XSEC

outputfile=VVER1000OP_6.2.1rodfix63.out

output_format=new

*****Power Density Calculation*****

'power density calculated is based on average fuel power density provided in benchmark, not thermal power/core V

'Methodology used to ensure agreement with Triton models used to generate cross sections

```

'average fuel power density 42.5 W/gU ([1],table 1)

'U/UO2 fraction = 0.881475

'fuel fraction=0.282572 (calculated using mixture vf ratios from Newt, and %fuel mixture that is fuel

'fuel density (UO2)=10.55

'power den=42.5*10.55*0.282572*0.881475=111.68

'power den=111.68

*****

powerden=111.68

prcnt=100.0

t2n=yes

diffusionmethod=nem

thfeedback=yes

thsolver=hem

accel=cheby

problemtyp=evp

sym=full

printscreen=yes

geometry=hexa

end parameter

read edit

power dim=2 dist=avg scale=yes plot=yes end plot

power visit=123 geom=full coreline=solid

flux visit=456 geom=full coreline=solid

end edit

read plot

visit=123 gap=0.2 0.2 .5 scale=yes center=xyz color_scale=rel

        colors=0.0 "blue" 0.25 "cyan" 0.5 "green" 0.75 "yellow" 1.0 "red" endcolors end visit

visit=456 gap=0.2 0.2 0.5 scale=yes center=xyz color_scale=rel

        colors=0.0 "blue" 0.25 "cyan" 0.5 "green" 0.75 "yellow" 1.0 "red" endcolors end visit

```

```

end plot

read heattransfer

*****Heat Transfer Information and Calculations*****

' All steam table data, properties of water generated from Wolfram Alpha at www.wolframalpha.com

' Coolant Pressure at Core Outlet = 15.7 MPa [2, Table 3]

' Coolant Temperature at core Outlet = 592.75 K [2, Table 3] = 607.28 F

' Coolant Density at core outlet: Temp 592.75 K, Pres 15.7 MPa, dens=683.8 kg/m^3 [3]

' Coolant Temp at Core inlet = 563.15 K [2, Table 3] = 554 F

' Coolant Density at Core inlet: Temp 563.15 K, Pres 15.7 MPa, dens=746.5 kg/m^3 [3]

' Average coolant temp = 578 K [2, Table 3] = 580.73 F

' Coolant Density Average: Temp 578 K Pres 15.7 MPa,dens=716.7 kg/m^3 [3]

' Coolant flow rate = 88000 m^3/hr [2, Table 3]

' Saturation Temperature of water at 15.7 MPa is 619 K = 654.53 F [3]

' Density of water at saturation at 15.7 MPa 590.7 kg/m^3, 36.876 lbm/ft^3 [3]

' Density of steam at saturation at 15.7 MPa 104.1 kg/m^3, 6.499 lbm/ft^3 [3]

' Internal energy of water at saturation at 15.7 MPa is 1.611x10^6 J/kg = 692.6 BTU/lbm [3]

' Internal energy of steam at saturation at 15.7 MPa is 2.439x10^6 J/kg = 1048.6 BTU/lbm [3]

' Inlet Coolant Mass Flow Velocity

' Density of coolant at inlet (above)= 746.5 kg/m^3

' Mass flow rate = coolant density*coolant flow rate = 746.5 kg/m^3 * 88000 m^3/hr = 6.5692E07 kg/hr

' Mass flow rate conversion: 6.5692E07 kg/hr = 1.44826E08 lbm/hr

' Area of bundles = 163*477 =77751 cm^2 = 83.6905 ft^2

' Wet area of bundles = wtfro*area bundles = .5554*83.6905=46.4817 ft^2

' Coolant Mass Flow Velocity = Mass flow/Wet Area of bundles

' (1.44826E08 lbm/hr)/ 46.4817 ft^2 = 3.11576E06 lbm/hr-ft^2

*****

' Inlet Coolant Mass FlowVelocity (lb/hr-ft^2)

g=3.11576E06

' bypass region = 0 (no bypass)

bypass=0.0

' Sat temp at 15.7 MPa (F)

```

tsat=654.53

' Density coolant vapor at Sat at 15.7 MPa (lbm/ft^3)

rhovsat=6.499

' Internal energy of coolant vapor at sat at 15.7 MPa (BTU/lbm)

uvsat=1048.6

' Temp of coolant at inlet (F)

tinlet=554

*****Coolant Fit Generation at 15.7 MPa [3]*****

'Temperature (K) (lbm/ft^3)	Temperature (F)	Internal Energy (J/kg)	Internal Energy (BTU/Lbm)	Density (kg/m^3)	Density
'550		530.33 770	1.196E+06	48.070	514.28
'560		548.33 752.4	1.247E+06	46.971	536.21
'570		566.33 733.3	1.299E+06	45.778	558.57
'580		584.33 712.3	1.354E+06	44.467	582.22
'590		602.33 688.8	1.411E+06	43.000	606.73
'600		620.33 661.8	1.472E+06	41.315	632.96

'Fits generated using MATLAB Polyfit tool

t_vs_ufit -97.1512972 1.594225239 -0.000727706 end t_vs_ufit

u_vs_tfit 362.6758597 -0.593634149 0.001658951 end u_vs_tfit

rho_vs_ufit 53.18310251 0.028116898 -7.4028469E-05 end rho_vs_ufit

end heattransfer

read fuelmech

*****Fuel Mech Calculations*****

'''fuel pin

' Number of fuel pins per assembly 312

' Number of fuel assembly types (colors) in xsec file = 1

' Area of fuel assembly (from above)=477.014 cm² 0.5135 ft²

' Pin Diameter = 0.91 cm [2, table 1]

' Pin Radius =0.455 cm or 0.1791 in

' Pin Inner Clad Diam = 0.773 cm [2, table 1]

' Pin Outer fuel Diam = 0.757 cm [2, table 1] 0.2980 in

' Pin fuel rad = 0.3785 cm 0.1490 in

' Pin area = pi*(.91/2)² = 0.6504 cm²

' total area of fuel pins in assembly = 312*0.6504 = 202.9211 cm²

'''Control Rod

' CR guide tube outer diam = 1.26 cm [2, table 1]

' CR guide tube inner diam = 1.09 cm [2, table 1]

' CR clad outer diam = 0.82 cm [2, table 1]

' Area of guide tube = pi*(1.26/2)² = 1.247 cm²

' Area of CR wet (RO) = pi*(1.09/2)² = 0.933 cm²

' Area of guide tube material = (pi*(1.26/2)²)-(pi*(1.09/2)²)= 0.31377 cm²

' Area of CR material = pi*(0.82/2)² = 0.5281 cm²

' Number of CR guide tubes in TVSA = 18 [2, table 1]

' Assembly CR guide tube area = 18*1.246 = 22.444 cm²

' Assembly CR guide tube material area = 18*0.31377 = 5.6478 cm²

' Assembly CR material (R/I) = 18*0.5281 = 9.5058 cm²

'''Central Guide Tube

' CG tube inner diam = 1.1 cm [2, table 1]

' CG tube outer diam = 1.3 cm [2, table 1]

' CG tube material area = (pi*(1.3/2)²)-(pi*(1.1/2)²)=0.3770 cm²

'''Stiffening angle plate

' thickness of stiffening plate = 0.1 cm [1, figure 10]

' Assembly side gap NOT covered by stiffening plate = side - 7.65 cm = 13.55-7.65=5.9 cm [1, figure 10]

' Area of single stiffening plate corner = 5.9*0.1 =0.59 cm²

' Number of Stiffening plates per assembly = 6 [1, Table 5]

' Assembly area with stiffening material = 6*0.59 = 3.54 cm²

' Fuel fraction (single assembly) =202.9211/477.014 = 0.4254

'''Wet Fraction Rods Out

' Material (not water) area / assembly area = (fuel pin+CR guide tubes+CG guide tube+stiffangle)/area

' wtmaterialNOTwetRO=(202.9211+5.6478+0.377+3.54)/477.014=0.44545

' wtfro=1-wtmaterialNOTwetRO=0.55455

'''Wet Fraction Rods In

' Material (not water)area/assembly =(fuelpins+CRguidetubes+CRmaterial+CGguidetube+stiffangle)/area

' wtmaterialNOTwetRI=(202.9211+5.6478+9.506+0.377+3.54)/477.014=0.46534

' wtfri=1-wtmaterialNOTwetRI=0.53462

'''wtfro and wtfri calculation for reflector region

' Wet fraction for the reflector region is the same RI and RO

'-----Reflector Region Wet Fraction Calcs (VF from Newt)-----

Mixture ID	Name	VF total	VF Colors	VF material/color	V mixture Wet	Fraction Wet
	WTFRO/WTFRI					
'303	Fuel(2) 0.00E+00	0.53802	3.17E-01	6.85E-01 4.62E-01		0
'304	Mod(2) 1		3.69E-01 5.38E-01		5.38E-01	
'100	Steel(1) 0.00E+00	0.47557	1.84E-02	3.15E-01 5.84E-02		0
'200	Stel/Mod(1) 7.51E-02	5.19E-02			1.65E-01	0.455761
'300	mod(1) 1		4.59E-03 1.46E-02		1.46E-02	
'400	steel(1) 0.00E+00	2.76E-02			8.75E-02	0
'500	mod(1) 1		1.21E-01 3.86E-01		3.86E-01	
'600	Steel(1) 0.00E+00	9.09E-02			2.89E-01	0

' Wet Fraction of Radial Reflector Region: 0.47557

' Wet Fraction of Bottom Reflector Region: 0.61461 (calcs similar to above, not listed here)

' Wet Fraction of Top Reflector Region: 0.80741 (calcs similar to above, not listed here)

' fuel density = 10.55 g/cc [1, table 4 average of values, consistant with scale files]

' fuel density = 658.6 lbm/ft^3

```

fiss_frac=1.0

fuelden=658.6

numfrods 3r0.0 5r312 end numfrods

bunarea 3r0.0 5r0.5135 end bunarea

frodrad 3r0.0 5r0.1490 end frodrad

'Fuel fraction calculations use single assembly fuel material VF from NEWT calcs

fuelfrac 3r0.0 2r0.282562 0.282585 0.282584 0.282577 end fuelfrac

wtfro 0.47557 0.61461 0.80741 5r0.55455 end wtfro

wtfri 0.47557 0.61461 0.80741 5r0.53462 end wtfri

'The following fits were pulled out of the regression test file NESTLE.XSC.MACRO.PWR

wc=1.00

wp=0.85

heff_vs_t 0.78363116E-01 -0.19203380E-04 0.73696720E-08 end heff_vs_t

tavg_vs_lpd 0.56955571E+3 0.16964059E+03 -0.2916911E+1 end tavg_vs_lpd

tsurf_vs_lpd 0.56955571E+3 0.924990E+2 0.432861000 -0.377884E-1 end tsurf_vs_lpd

cp_vs_tfit 0.8110000193E-01 end cp_vs_tfit

'lattice ID below

lattice_ids 1 2 3 4 5 6 7 8 end lattice_ids

end fuelmech

read burndata

pres=2277.092

*****Burnup Calculations*****

'BOC burn data

'Coolant inlet temp = 563.15 K=554.0 F

*****

burnup=0.00 sm=no xe=no pctpwr=49.690 crod_id=1 pctflow=100.694 ppm=909.43
tinlet=540.68 end

burnup=228.80 sm=eq xe=eq pctpwr=49.547 crod_id=2 pctflow=100.615 ppm=865.71
tinlet=540.14 end

burnup=428.84 sm=eq xe=eq pctpwr=74.623 crod_id=3 pctflow=100.518 ppm=821.99
tinlet=544.82 end

```

burnup=646.39 end	sm=eq	xe=eq	pctpwr=75.360	cro_d_id=4	pctflow=100.550	ppm=809.74	tinlet=545
burnup=862.69 tinlet=545.54 end	sm=eq	xe=eq	pctpwr=75.690	cro_d_id=5	pctflow=100.495	ppm=821.99	
burnup=1056.89 tinlet=546.08 end	sm=eq	xe=eq	pctpwr=76.433	cro_d_id=6	pctflow=100.492	ppm=821.99	
burnup=1264.44 tinlet=548.42 end	sm=eq	xe=eq	pctpwr=89.650	cro_d_id=7	pctflow=100.279	ppm=788.76	
burnup=1488.65 tinlet=548.78 end	sm=eq	xe=eq	pctpwr=90.083	cro_d_id=8	pctflow=100.374	ppm=778.26	
burnup=1685.78 tinlet=548.96 end	sm=eq	xe=eq	pctpwr=95.057	cro_d_id=9	pctflow=100.328	ppm=767.77	
burnup=1951.25 tinlet=549.5 end	sm=eq	xe=eq	pctpwr=98.933	cro_d_id=10	pctflow=100.265	ppm=767.77	
burnup=2375.09 tinlet=549.68 end	sm=eq	xe=eq	pctpwr=99.093	cro_d_id=11	pctflow=100.113	ppm=746.78	
burnup=2540.55 tinlet=549.5 end	sm=eq	xe=eq	pctpwr=99.237	cro_d_id=12	pctflow=100.261	ppm=739.79	
burnup=2747.67 tinlet=549.68 end	sm=eq	xe=eq	pctpwr=99.403	cro_d_id=13	pctflow=100.235	ppm=724.05	
burnup=2955.63 tinlet=549.32 end	sm=eq	xe=eq	pctpwr=99.990	cro_d_id=14	pctflow=100.294	ppm=713.55	
burnup=3163.60 tinlet=549.32 end	sm=eq	xe=eq	pctpwr=99.520	cro_d_id=15	pctflow=100.465	ppm=708.31	
burnup=3371.97 tinlet=549.32 end	sm=eq	xe=eq	pctpwr=99.717	cro_d_id=16	pctflow=100.335	ppm=692.57	
burnup=3577.85 tinlet=549.32 end	sm=eq	xe=eq	pctpwr=100.027	cro_d_id=17	pctflow=100.398	ppm=687.32	
burnup=3787.06 tinlet=549.5 end	sm=eq	xe=eq	pctpwr=98.513	cro_d_id=18	pctflow=100.193	ppm=682.07	
burnup=3978.35 tinlet=549.32 end	sm=eq	xe=eq	pctpwr=98.157	cro_d_id=19	pctflow=100.363	ppm=675.08	
burnup=4183.82 tinlet=549.5 end	sm=eq	xe=eq	pctpwr=99.580	cro_d_id=20	pctflow=100.457	ppm=659.34	
burnup=4390.53 tinlet=549.5 end	sm=eq	xe=eq	pctpwr=99.400	cro_d_id=21	pctflow=100.413	ppm=643.60	
burnup=4598.07 tinlet=549.32 end	sm=eq	xe=eq	pctpwr=99.663	cro_d_id=22	pctflow=100.407	ppm=638.35	
burnup=4805.20 tinlet=549.32 end	sm=eq	xe=eq	pctpwr=99.530	cro_d_id=23	pctflow=100.354	ppm=627.86	
burnup=5012.33 tinlet=549.14 end	sm=eq	xe=eq	pctpwr=99.397	cro_d_id=24	pctflow=100.455	ppm=617.36	

burnup=5219.45 tinlet=549.5 end	sm=eq	xe=eq	pctpwr=99.347	cro_d_id=25	pctflow=100.334	ppm=605.12
burnup=5432.42 tinlet=549.86 end	sm=eq	xe=eq	pctpwr=96.623	cro_d_id=26	pctflow=100.341	ppm=690.82
burnup=5638.71 tinlet=549.68 end	sm=eq	xe=eq	pctpwr=99.433	cro_d_id=27	pctflow=100.402	ppm=584.14
burnup=5845.42 tinlet=549.68 end	sm=eq	xe=eq	pctpwr=99.690	cro_d_id=28	pctflow=100.414	ppm=573.64
burnup=6053.38 tinlet=549.5 end	sm=eq	xe=eq	pctpwr=99.593	cro_d_id=29	pctflow=100.322	ppm=559.65
burnup=6260.51 tinlet=549.5 end	sm=eq	xe=eq	pctpwr=99.317	cro_d_id=30	pctflow=100.317	ppm=540.41
burnup=6468.47 tinlet=549.32 end	sm=eq	xe=eq	pctpwr=99.263	cro_d_id=31	pctflow=100.515	ppm=524.67
burnup=6673.52 tinlet=549.86 end	sm=eq	xe=eq	pctpwr=99.783	cro_d_id=32	pctflow=100.479	ppm=514.18
burnup=6914.40 tinlet=549.5 end	sm=eq	xe=eq	pctpwr=99.443	cro_d_id=33	pctflow=100.476	ppm=491.44
burnup=7122.36 tinlet=549.32 end	sm=eq	xe=eq	pctpwr=99.447	cro_d_id=34	pctflow=100.530	ppm=480.95
burnup=7325.74 tinlet=549.14 end	sm=eq	xe=eq	pctpwr=96.673	cro_d_id=35	pctflow=100.574	ppm=470.46
burnup=7524.12 tinlet=548.6 end	sm=eq	xe=eq	pctpwr=94.177	cro_d_id=36	pctflow=100.487	ppm=470.46
burnup=7724.58 tinlet=549.68 end	sm=eq	xe=eq	pctpwr=92.660	cro_d_id=37	pctflow=100.551	ppm=535.17
burnup=7951.29 tinlet=549.68 end	sm=eq	xe=eq	pctpwr=99.883	cro_d_id=38	pctflow=100.568	ppm=438.98
burnup=8159.67 tinlet=549.5 end	sm=eq	xe=eq	pctpwr=99.853	cro_d_id=39	pctflow=100.318	ppm=416.24
burnup=8368.46 tinlet=549.68 end	sm=eq	xe=eq	pctpwr=99.987	cro_d_id=40	pctflow=100.515	ppm=395.25
burnup=8576.84 tinlet=549.68 end	sm=eq	xe=eq	pctpwr=99.793	cro_d_id=41	pctflow=100.396	ppm=377.76
burnup=8785.64 tinlet=549.68 end	sm=eq	xe=eq	pctpwr=100.037	cro_d_id=42	pctflow=100.498	ppm=356.78
burnup=8994.43 tinlet=549.5 end	sm=eq	xe=eq	pctpwr=100.177	cro_d_id=43	pctflow=100.398	ppm=346.28
burnup=9203.64 tinlet=549.5 end	sm=eq	xe=eq	pctpwr=100.153	cro_d_id=44	pctflow=100.403	ppm=328.79
burnup=9412.85 tinlet=549.5 end	sm=eq	xe=eq	pctpwr=100.213	cro_d_id=45	pctflow=100.606	ppm=307.81

burnup=9622.07 tinlet=549.5 end	sm=eq	xe=eq	pctpwr=100.417	cro_d_id=46	pctflow=100.514	ppm=292.07
burnup=9811.27 tinlet=544.1 end	sm=eq	xe=eq	pctpwr=71.193	cro_d_id=47	pctflow=100.766	ppm=320.05
burnup=10020.07 tinlet=544.1 end	sm=eq	xe=eq	pctpwr=70.643	cro_d_id=48	pctflow=100.799	ppm=330.54
burnup=10243.87 tinlet=549.32 end	sm=eq	xe=eq	pctpwr=99.850	cro_d_id=49	pctflow=100.514	ppm=243.10
burnup=10459.75 tinlet=545.18 end	sm=eq	xe=eq	pctpwr=75.413	cro_d_id=50	pctflow=100.810	ppm=269.33
burnup=10663.12 tinlet=544.28 end	sm=eq	xe=eq	pctpwr=68.650	cro_d_id=51	pctflow=100.874	ppm=274.58
burnup=10846.91 tinlet=550.04 end	sm=eq	xe=eq	pctpwr=99.853	cro_d_id=52	pctflow=100.676	ppm=206.37
burnup=11083.63 tinlet=547.52 end	sm=eq	xe=eq	pctpwr=86.847	cro_d_id=53	pctflow=100.668	ppm=194.13
burnup=11292.01 tinlet=546.98 end	sm=eq	xe=eq	pctpwr=81.577	cro_d_id=54	pctflow=100.653	ppm=188.88
burnup=11499.55 tinlet=544.1 end	sm=eq	xe=eq	pctpwr=62.557	cro_d_id=55	pctflow=100.826	ppm=215.12
burnup=11705.01 tinlet=548.42 end	sm=eq	xe=eq	pctpwr=85.380	cro_d_id=56	pctflow=100.500	ppm=167.90
burnup=11902.14 tinlet=548.78 end	sm=eq	xe=eq	pctpwr=99.730	cro_d_id=57	pctflow=100.691	ppm=108.43
burnup=12097.18 tinlet=548.96 end	sm=eq	xe=eq	pctpwr=84.727	cro_d_id=58	pctflow=100.617	ppm=150.41
burnup=12334.32 tinlet=549.5 end	sm=eq	xe=eq	pctpwr=99.403	cro_d_id=59	pctflow=100.410	ppm=61.21
burnup=12543.53 tinlet=549.86 end	sm=eq	xe=eq	pctpwr=99.880	cro_d_id=60	pctflow=100.257	ppm=38.48
burnup=12752.32 tinlet=549.5 end	sm=eq	xe=eq	pctpwr=98.470	cro_d_id=61	pctflow=100.215	ppm=19.24
burnup=12919.44 tinlet=549.32 end	sm=eq	xe=eq	pctpwr=99.220	cro_d_id=62	pctflow=100.071	ppm=9.62
burnup=12961.12 tinlet=549.32 end	sm=eq	xe=eq	pctpwr=99.100	cro_d_id=63	pctflow=100.143	ppm=6.12

end burndata

read geom

"reflection

down=noentry

```

up=noentry

outer=noentry

inner=cyclic

numrings=8

"xy mesh

' bundle pitch = 23.48 cm = 9.2441 in

' half pitch = 4.62205

' side length 13.55 cm = 5.3346 in

' 6-14 x assemblies

' 15 y assemblies

bpitch=9.2441

deltax 6r4.2205 end deltax

deltay 15r5.334 end deltay

' # nodes

"z direction calculations

' Core active fuel height 353 cm = 138.98 in

' 12 axial nodes. 1 bottom Refl, 10 fuel, 1 top refl

' deltaz= 138.98/10 = 13.898

deltaz 12r13.898 end deltaz

figure 2 10r1 3 end figure

bottomfuelnode=2

topfuelnode=11

*****Control Rod Bank Information*****

' Working control rod group = 10 [2, para 3.1.1, pg 6]

' All Control Rods in groups 1-9 assumed to be fully OUT. Not specified.

' Model Z dimension 12*13.898 = 166.776, CR fullout = 166.776

' CRG 1-9 are at 166.776 (fully out)

*****

crload= topdown

crbank 1 100 9r166.776 132.50 end crbank

crbank 2 100 9r166.776 131.98 end crbank

```

crbank	3	100	9r166.776 125.23	end crbank
crbank	4	100	9r166.776 120.63	end crbank
crbank	5	100	9r166.776 127.79	end crbank
crbank	6	100	9r166.776 128.64	end crbank
crbank	7	100	9r166.776 130.34	end crbank
crbank	8	100	9r166.776 123.85	end crbank
crbank	9	100	9r166.776 126.11	end crbank
crbank	10	100	9r166.776 131.03	end crbank
crbank	11	100	9r166.776 131.28	end crbank
crbank	12	100	9r166.776 131.88	end crbank
crbank	13	100	9r166.776 132.57	end crbank
crbank	14	100	9r166.776 133.46	end crbank
crbank	15	100	9r166.776 133.38	end crbank
crbank	16	100	9r166.776 134.02	end crbank
crbank	17	100	9r166.776 132.23	end crbank
crbank	18	100	9r166.776 132.38	end crbank
crbank	19	100	9r166.776 130.89	end crbank
crbank	20	100	9r166.776 132.07	end crbank
crbank	21	100	9r166.776 132.38	end crbank
crbank	22	100	9r166.776 131.00	end crbank
crbank	23	100	9r166.776 129.89	end crbank
crbank	24	100	9r166.776 130.79	end crbank
crbank	25	100	9r166.776 131.48	end crbank
crbank	26	100	9r166.776 126.24	end crbank
crbank	27	100	9r166.776 131.04	end crbank
crbank	28	100	9r166.776 131.42	end crbank
crbank	29	100	9r166.776 132.20	end crbank
crbank	30	100	9r166.776 130.79	end crbank
crbank	31	100	9r166.776 132.43	end crbank
crbank	32	100	9r166.776 132.16	end crbank
crbank	33	100	9r166.776 132.23	end crbank

```
crbank 34 100 9r166.776 132.21 end crbank
crbank 35 100 9r166.776 134.20 end crbank
crbank 36 100 9r166.776 132.48 end crbank
crbank 37 100 9r166.776 129.14 end crbank
crbank 38 100 9r166.776 137.44 end crbank
crbank 39 100 9r166.776 136.38 end crbank
crbank 40 100 9r166.776 136.80 end crbank
crbank 41 100 9r166.776 137.78 end crbank
crbank 42 100 9r166.776 136.84 end crbank
crbank 43 100 9r166.776 137.34 end crbank
crbank 44 100 9r166.776 139.20 end crbank
crbank 45 100 9r166.776 137.87 end crbank
crbank 46 100 9r166.776 139.74 end crbank
crbank 47 100 9r166.776 115.24 end crbank
crbank 48 100 9r166.776 114.24 end crbank
crbank 49 100 9r166.776 137.38 end crbank
crbank 50 100 9r166.776 116.60 end crbank
crbank 51 100 9r166.776 111.18 end crbank
crbank 52 100 9r166.776 135.57 end crbank
crbank 53 100 9r166.776 123.48 end crbank
crbank 54 100 9r166.776 119.91 end crbank
crbank 55 100 9r166.776 112.16 end crbank
crbank 56 100 9r166.776 126.03 end crbank
crbank 57 100 9r166.776 140.09 end crbank
crbank 58 100 9r166.776 115.44 end crbank
crbank 59 100 9r166.776 137.88 end crbank
crbank 60 100 9r166.776 140.02 end crbank
crbank 61 100 9r166.776 140.63 end crbank
crbank 62 100 9r166.776 142.87 end crbank
crbank 63 100 9r166.776 143.79 end crbank
end geom
```

read arrays

*****TVSA Fuel Bundle Information*****

' Color Cross Section # ²³⁵U Pins Gd Absorber Pins

' TVSA	²³⁵ U Enrichment	# UPins	%Gd	% ²³⁵ U	# Pins
'4	13AU	1.30	312		
'5	22AU	2.2	312		
'6	30AV5	3.00	303	5.00	2.40 9
'7	39AWU	4.00	243	5.00	3.30 9
'		3.60	60		
'8	390GO	4.00	240	5.00	3.30 6
'		3.60	66		

'1 Radial Reflector

'2 Bottom Reflector

'3 Top Reflector

' Core loading map for fuel [1, Figure 16]

ara=1 nux=33 nuy=17 fill

```
0 1 1 1 1 1 1 1 0
1 1 8 7 7 7 7 8 1 1
1 8 6 5 6 5 6 5 6 8 1
1 7 5 5 4 4 4 4 5 5 7 1
1 7 6 4 4 6 5 6 4 4 6 7 1
1 7 5 4 6 5 4 4 5 6 4 5 7 1
1 7 6 4 5 4 6 5 6 4 5 4 6 7 1
1 8 5 4 6 4 5 4 4 5 4 6 4 5 8 1
0 1 6 5 4 5 6 4 6 4 6 5 4 5 6 1 0
1 8 5 4 6 4 5 4 4 5 4 6 4 5 8 1
1 7 6 4 5 4 6 5 6 4 5 4 6 7 1
```

```
1 7 5 4 6 5 4 4 5 6 4 5 7 1
1 7 6 4 4 6 5 6 4 4 6 7 1
1 7 5 5 4 4 4 4 5 5 7 1
1 8 6 5 6 5 6 5 6 8 1
1 1 8 7 7 7 7 8 1 1
0 1 1 1 1 1 1 1 0
```

end fill

'Bottom Reflector Array

ara=2 nux=33 nuy=17 fill

```
0 2 2 2 2 2 2 2 0
2 2 2 2 2 2 2 2 2
2 2 2 2 2 2 2 2 2
2 2 2 2 2 2 2 2 2
2 2 2 2 2 2 2 2 2
2 2 2 2 2 2 2 2 2
2 2 2 2 2 2 2 2 2
2 2 2 2 2 2 2 2 2
0 2 2 2 2 2 2 2 2 2 2 2 2 2 2 2 0
2 2 2 2 2 2 2 2 2 2 2 2 2 2 2
2 2 2 2 2 2 2 2 2 2 2 2 2
2 2 2 2 2 2 2 2 2 2 2
2 2 2 2 2 2 2 2 2 2 2
2 2 2 2 2 2 2 2 2 2
2 2 2 2 2 2 2 2 2
2 2 2 2 2 2 2 2 2
0 2 2 2 2 2 2 0
```

end fill

'Top Reflector Array

ara=3 nux=33 nuy=17 fill

```
0 3 3 3 3 3 3 3 0
3 3 3 3 3 3 3 3 3
```

```

3 3 3 3 3 3 3 3 3 3 3
3 3 3 3 3 3 3 3 3 3 3
3 3 3 3 3 3 3 3 3 3 3
3 3 3 3 3 3 3 3 3 3 3
3 3 3 3 3 3 3 3 3 3 3
3 3 3 3 3 3 3 3 3 3 3
0 3 3 3 3 3 3 3 3 3 3 3 0
3 3 3 3 3 3 3 3 3 3 3 3
3 3 3 3 3 3 3 3 3 3 3 3
3 3 3 3 3 3 3 3 3 3 3
3 3 3 3 3 3 3 3 3 3 3
3 3 3 3 3 3 3 3 3 3 3
3 3 3 3 3 3 3 3 3 3 3
3 3 3 3 3 3 3 3 3 3 3
3 3 3 3 3 3 3 3 3 3 3
0 3 3 3 3 3 3 3 0

```

end fill

' Control Rod Map Banks 1-10 [2, Fig 11]

ara=100 nux=33 nuy=17 fill

```

0 0 0 0 0 0 0 0 0 0
0 0 0 0 0 0 0 0 0 0
0 0 0 8 0 6 0 9 0 0 0
0 0 9 0 4 2 3 5 0 8 0 0
0 0 0 5 0 0 10 0 0 4 0 0 0
0 0 6 3 0 7 0 0 7 0 2 6 0 0
0 0 0 2 10 0 0 8 0 0 10 3 0 0 0
0 0 8 4 0 0 1 0 0 1 0 0 5 9 0 0
0 0 0 0 0 7 0 0 9 0 0 7 0 0 0 0 0
0 0 9 5 0 0 8 0 0 8 0 0 4 8 0 0
0 0 0 3 10 0 0 1 0 0 10 2 0 0 0
0 0 6 2 0 7 0 0 7 0 3 6 0 0
0 0 0 4 0 0 10 0 0 5 0 0 0

```

```

0 0 8 0 5 3 2 4 0 9 0 0
0 0 0 9 0 6 0 8 0 0 0
0 0 0 0 0 0 0 0 0 0
0 0 0 0 0 0 0 0 0 0

```

end fill

end arrays

E.3.2: VVER 1000 Test Model

VVER1000_fullcore_all reflectors

read parameter

*****Assumptions and References*****

'Created by Margaret Kurtts

'REF1. Lotsch, T., V. Khalimonchuk, and A. Kuchin, Proposal of a Benchmark for Core Burnup Calculations for a VVER-1000 Reactor Core, 2009

'REF2. Lotsch, T., V. Khalimonchuk, and A. Kuchin. Corrections and additions to the proposal of a benchmark for core burnup calculations for a WVER-1000 reactor, 2010.

'REF3. Wolfram Alpha Computational Knowledge Engine. [Online Database and Computational Tool] [cited 2016 May 24]; Available from: <http://www.wolframalpha.com/>.

'REF4. Nuclear Power: Convert/Calculator-Boric Acid. [Web page] [cited 2016 May 25]; Available from: <http://www.nuclear-power.net/glossary/boron-10/convertcalculator-boric-acid/>.

'Table 4 [1]-materials for fuel, guide tube, spacer.

'Table 3 [1]-materials for control rods, burnable absorbers

'Table 5 [1]-materials for stiffing plate

'Table 1 [1]-reactor temperature data

'Tab 1 [2]-Moderator Boron Concentration and fuel temperature

'Burndata comes from [2] for power (42.5 MW/MTU) and the core was shut down after 311.74 EFPD [1,2]

'Full core using 5 fuels, radial reflector

'Testing Burndata

*****Assumptions and References*****

xsecfile=FUEL621.XSEC

outputfile=VVER1000_test621_BU.out

output_format=new

*****Power Density Calculation*****

'power density calculated is based on average fuel power density provided in benchmark, not thermal power/core V

'Methodology used to ensure agreement with Triton models used to generate cross sections

'average fuel power density 42.5 W/gU ([1],table 1)

'U/UO2 fraction = 0.881475

'fuel fraction=0.282572 (calculated using mixture vf ratios from Newt, and %fuel mixture that is fuel

'fuel density (UO2)=10.55

'power den=42.5*10.55*0.282572*0.881475=111.68

'power den=111.68

powerden=111.68

prcnt=100.0

t2n=yes

diffusionmethod=nem

thfeedback=yes

thsolver=hem

accel=cheby

problemtyp=evp

sym=full

printscreen=yes

geometry=hexa

end parameter

read edit

power dim=2 dist=avg scale=yes plot=yes end plot

power visit=123 geom=full coreline=solid

flux visit=456 geom=full coreline=solid

BU visit=789 geom=full coreline=solid

end edit

read plot

visit=123 gap=0.2 0.2 .5 scale=yes center=xyz color_scale=rel

```

        colors=0.0 "blue" 0.25 "cyan" 0.5 "green" 0.75 "yellow" 1.0 "red" endcolors end visit
visit=456 gap=0.2 0.2 0.5 scale=yes center=xyz color_scale=rel

        colors=0.0 "blue" 0.25 "cyan" 0.5 "green" 0.75 "yellow" 1.0 "red" endcolors end visit
visit=789 gap=0.2 0.2 0.5 scale=yes center=xyz color_scale=rel

        colors=0.0 "blue" 0.25 "cyan" 0.5 "green" 0.75 "yellow" 1.0 "red" endcolors end visit
end plot

read heattransfer

*****Heat Transfer Information and Calculations*****

' All steam table data, properties of water generated from Wolfram Alpha at www.wolframalpha.com
' Coolant Pressure at Core Outlet = 15.7 MPa [2, Table 3]
' Coolant Temperature at core Outlet = 592.75 K [2, Table 3] = 607.28 F
' Coolant Density at core outlet: Temp 592.75 K, Pres 15.7 MPa, dens=683.8 kg/m^3 [3]
' Coolant Temp at Core inlet = 563.15 K [2, Table 3] = 554 F
' Coolant Density at Core inlet: Temp 563.15 K, Pres 15.7 MPa, dens=746.5 kg/m^3 [3]
' Average coolant temp = 578 K [2, Table 3] = 580.73 F
' Coolant Density Average: Temp 578 K Pres 15.7 MPa, dens=716.7 kg/m^3 [3]
' Coolant flow rate = 88000 m^3/hr [2, Table 3]
' Saturation Temperature of water at 15.7 MPa is 619 K = 654.53 F [3]
' Density of water at saturation at 15.7 MPa 590.7 kg/m^3, 36.876 lbm/ft^3 [3]
' Density of steam at saturation at 15.7 MPa 104.1 kg/m^3, 6.499 lbm/ft^3 [3]
' Internal energy of water at saturation at 15.7 MPa is 1.611x10^6 J/kg = 692.6 BTU/lbm [3]
' Internal energy of steam at saturation at 15.7 MPa is 2.439x10^6 J/kg = 1048.6 BTU/lbm [3]
' Inlet Coolant Mass Flow Velocity
' Density of coolant at inlet (above)= 746.5 kg/m^3
' Mass flow rate = coolant density*coolant flow rate = 746.5 kg/m^3 * 88000 m^3/hr = 6.5692E07 kg/hr
' Mass flow rate conversion: 6.5692E07 kg/hr = 1.44826E08 lbm/hr
' Area of bundles = 163*477 =77751 cm^2 = 83.6905 ft^2
' Wet area of bundles = wtfro*area bundles = .5554*83.6905=46.4817 ft^2
' Coolant Mass Flow Velocity = Mass flow/Wet Area of bundles
' (1.44826E08 lbm/hr)/ 46.4817 ft^2 = 3.11576E06 lbm/hr-ft^2

*****

```

' Inlet Coolant Mass FlowVelocity (lb/hr-ft^2)

g=3.11576E06

' bypass region = 0 (no bypass)

bypass=0.0

' Sat temp at 15.7 MPa (F)

tsat=654.53

' Density coolant vapor at Sat at 15.7 MPa (lbm/ft^3)

rhovsat=6.499

' Internal energy of coolant vapor at sat at 15.7 MPa (BTU/lbm)

uvsat=1048.6

' Temp of coolant at inlet (F)

tinlet=554

*****Coolant Fit Generation at 15.7 MPa [3]*****

'Temperature (K) (lbm/ft^3)	Temperature (F)	Internal Energy (J/kg)	Internal Energy (BTU/Lbm)	Density (kg/m^3)	Density
'550		530.33 770	1.196E+06	48.070	514.28
'560		548.33 752.4	1.247E+06	46.971	536.21
'570		566.33 733.3	1.299E+06	45.778	558.57
'580		584.33 712.3	1.354E+06	44.467	582.22
'590		602.33 688.8	1.411E+06	43.000	606.73
'600		620.33 661.8	1.472E+06	41.315	632.96

Fits generated using MATLAB Polyfit tool

t_vs_ufit -97.1512972 1.594225239 -0.000727706 end t_vs_ufit

u_vs_tfit 362.6758597 -0.593634149 0.001658951 end u_vs_tfit

rho_vs_ufit 53.18310251 0.028116898 -7.4028469E-05 end rho_vs_ufit

end heattransfer

read fuelmech

*****Fuel Mech Calculations*****

"fuel pin

' Number of fuel pins per assembly 312

' Number of fuel assembly types (colors) in xsec file = 1

' Area of fuel assembly (from above)=477.014 cm² 0.5135 ft²

' Pin Diameter = 0.91 cm [2, table 1]

' Pin Radius =0.455 cm or 0.1791 in

' Pin Inner Clad Diam = 0.773 cm [2, table 1]

' Pin Outer fuel Diam = 0.757 cm [2, table 1] 0.2980 in

' Pin fuel rad = 0.3785 cm 0.1490 in

' Pin area = pi*(.91/2)² = 0.6504 cm²

' total area of fuel pins in assembly = 312*0.6504 = 202.9211 cm²

"Control Rod

' CR guide tube outer diam = 1.26 cm [2, table 1]

' CR guide tube inner diam = 1.09 cm [2, table 1]

' CR clad outer diam = 0.82 cm [2, table 1]

' Area of guide tube = pi*(1.26/2)² = 1.247 cm²

' Area of CR wet (RO) = pi*(1.09/2)² = 0.933 cm²

' Area of guide tube material = (pi*(1.26/2)²) -(pi*(1.09/2)²)= 0.31377 cm²

' Area of CR material = pi*(0.82/2)² = 0.5281 cm²

' Number of CR guide tubes in TVSA = 18 [2, table 1]

' Assembly CR guide tube area = 18*1.246 = 22.444 cm²

' Assembly CR guide tube material area = 18*0.31377 = 5.6478 cm²

' Assembly CR material (R/I) = 18*0.5281 = 9.5058 cm²

"Central Guide Tube

' CG tube inner diam = 1.1 cm [2, table 1]

' CG tube outer diam = 1.3 cm [2, table 1]

' CG tube material area = (pi*(1.3/2)²)-(pi*(1.1/2)²)=0.3770 cm²

"Stiffening angle plate

' thickness of stiffening plate = 0.1 cm [1, figure 10]

' Assembly side gap NOT covered by stiffening plate = side - 7.65 cm = 13.55-7.65=5.9 cm [1, figure 10]

' Area of single stiffening plate corner = 5.9*0.1 =0.59 cm^2

' Number of Stiffening plates per assembly = 6 [1, Table 5]

' Assembly area with stiffening material = 6*0.59 = 3.54 cm^2

' Fuel fraction (single assembly) =202.9211/477.014 = 0.4254

'''Wet Fraction Rods Out

' Material (not water) area / assembly area = (fuel pin+CR guide tubes+CG guide tube+stiffangle)/area

' wmaterialNOTwetRO=(202.9211+5.6478+0.377+3.54)/477.014=0.44545

' wtfro=1-wmaterialNOTwetRO=0.55455

'''Wet Fraction Rods In

' Material (not water)area/assembly =(fuelpins+CRguidetubes+CRmaterial+CGguidetube+stiffangle)/area

' wmaterialNOTwetRI=(202.9211+5.6478+9.506+0.377+3.54)/477.014=0.46534

' wtfri=1-wmaterialNOTwetRI=0.53462

'''wtfro and wtfri calculation for reflector region

' Wet fraction for the reflector region is the same RI and RO

'-----Reflector Region Wet Fraction Calcs (VF from Newt)-----

Mixture ID	Name	VF total	VF Colors	VF material/color	V mixture Wet	Fraction Wet
	WTFRO/WTFRI					
'303	Fuel(2) 0.00E+00	0.53802	3.17E-01	6.85E-01 4.62E-01		0
'304	Mod(2) 1		3.69E-01 5.38E-01		5.38E-01	
'100	Steel(1) 0.00E+00	0.47557	1.84E-02	3.15E-01 5.84E-02		0
'200	Stel/Mod(1) 7.51E-02	5.19E-02			1.65E-01	0.455761
'300	mod(1) 1		4.59E-03 1.46E-02		1.46E-02	
'400	steel(1) 0.00E+00	2.76E-02			8.75E-02	0
'500	mod(1) 1		1.21E-01 3.86E-01		3.86E-01	
'600	Steel(1) 0.00E+00	9.09E-02			2.89E-01	0

' Wet Fraction of Radial Reflector Region: 0.47557

' Wet Fraction of Bottom Reflector Region: 0.61461 (calcs similar to above, not listed here)

```

' Wet Fraction of Top Reflector Region: 0.80741 (calcs similar to above, not listed here)

' fuel density = 10.55 g/cc [1, table 4 average of values, consistant with scale files]

' fuel density = 658.6 lbm/ft^3

*****

fiss_frac=1.0

fuelden=658.6

numfrods 3r0.0 5r312 end numfrods

bunarea 3r0.0 5r0.5135 end bunarea

frodrad 3r0.0 5r0.1490 end frodrad

'Fuel fraction calculations use single assembly fuel material VF from NEWT calcs

fuelfrac 3r0.0 2r0.282562 0.282585 0.282584 0.282577 end fuelfrac

wtfro 0.47557 0.61461 0.80741 5r0.55455 end wtfro

wtfri 0.47557 0.61461 0.80741 5r0.53462 end wtfri

'The following fits were pulled out of the regression test file NESTLE.XSC.MACRO.PWR

wc=1.00

wp=0.85

heff_vs_t 0.78363116E-01 -0.19203380E-04 0.73696720E-08 end heff_vs_t

tavg_vs_lpd 0.56955571E+3 0.16964059E+03 -0.2916911E+1 end tavg_vs_lpd

tsurf_vs_lpd 0.56955571E+3 0.924990E+2 0.432861000 -0.377884E-1 end tsurf_vs_lpd

cp_vs_tfit 0.8110000193E-01 end cp_vs_tfit

'lattice ID below

lattice_ids 1 2 3 4 5 6 7 8 end lattice_ids

end fuelmech

read burndata

pres=2277.092

*****Burnup Calculations*****

'BOC burn data

'Coolant inlet temp = 563.15 K=554.0 F

*****

```

```

burnup=0.00      sm=no  xe=no  pctpwr=99.0    crod_id=1  pctflow=100.00  tinlet=549.00 search=boronppm
end

burnup=250      sm=eq  xe=eq  pctpwr=99.0    crod_id=2  pctflow=100.00  tinlet=549.00
search=boronppm end

burnup=500      sm=eq  xe=eq  pctpwr=99.0    crod_id=3  pctflow=100.00  tinlet=549.00
search=boronppm end

burnup=1000     sm=eq  xe=eq  pctpwr=99.0    crod_id=4  pctflow=100.00  tinlet=549.00
search=boronppm end

burnup=2000     sm=eq  xe=eq  pctpwr=99.0    crod_id=5  pctflow=100.00  tinlet=549.00
search=boronppm end

burnup=3000     sm=eq  xe=eq  pctpwr=99.0    crod_id=6  pctflow=100.00  tinlet=549.00
search=boronppm end

burnup=4000     sm=eq  xe=eq  pctpwr=99.0    crod_id=7  pctflow=100.00  tinlet=549.00
search=boronppm end

burnup=5000     sm=eq  xe=eq  pctpwr=99.0    crod_id=8  pctflow=100.00  tinlet=549.00
search=boronppm end

burnup=6000     sm=eq  xe=eq  pctpwr=99.0    crod_id=9  pctflow=100.00  tinlet=549.00
search=boronppm end

burnup=7000     sm=eq  xe=eq  pctpwr=99.0    crod_id=10  pctflow=100.00
tinlet=549.00 search=boronppm end

burnup=8000     sm=eq  xe=eq  pctpwr=99.0    crod_id=11  pctflow=100.00
tinlet=549.00 search=boronppm end

burnup=9000     sm=eq  xe=eq  pctpwr=99.0    crod_id=12  pctflow=100.00
tinlet=549.00 search=boronppm end

burnup=10000    sm=eq  xe=eq  pctpwr=99.0    crod_id=13  pctflow=100.00  tinlet=549.00
search=boronppm end

burnup=11000    sm=eq  xe=eq  pctpwr=99.0    crod_id=14  pctflow=100.00  tinlet=549.00
search=boronppm end

burnup=12000    sm=eq  xe=eq  pctpwr=99.0    crod_id=15  pctflow=100.00  tinlet=549.00
search=boronppm end

burnup=13000    sm=eq  xe=eq  pctpwr=50.0    crod_id=16  pctflow=100.00  tinlet=549.00
search=boronppm end

end burndata

read geom

"reflection

down=noentry

up=noentry

outer=noentry

inner=cyclic

```

```

numrings=8

"xy mesh

' bundle pitch = 23.48 cm = 9.2441 in

' half pitch = 4.62205

' side length 13.55 cm = 5.3346 in

' 6-14 x assemblies

' 15 y assemblies

bpitch=9.2441

deltax 6r4.2205 end deltax

deltay 15r5.334 end deltax

' # nodes

"z direction calculations

' Core active fuel height 353 cm = 138.98 in

' 12 axial nodes. 1 bottom Refl, 10 fuel, 1 top refl

' deltax= 138.98/10 = 13.898

deltaz 12r13.898 end deltax

figure 2 10r1 3 end figure

bottomfuelnode=2

topfuelnode=11

*****Control Rod Bank Information*****

' Working control rod group = 10 [2, para 3.1.1, pg 6]

' All Control Rods in groups 1-9 assumed to be fully OUT. Not specified.

' Model Z dimension 12*13.898 = 166.776, CR fallout = 166.776

' CRG 1-9 are at 166.776 (fully out), WG10 will be inserted 2 nodes (27.796 in, or 138.98)

*****

crload= topdown

crbank 1 100 9r166.776 138.98 end crbank

crbank 2 100 9r166.776 138.98 end crbank

crbank 3 100 9r166.776 138.98 end crbank

crbank 4 100 9r166.776 138.98 end crbank

crbank 5 100 9r166.776 138.98 end crbank

```

```

crbank 6      100      9r166.776 138.98  end crbank
crbank 7      100      9r166.776 138.98  end crbank
crbank 8      100      9r166.776 138.98  end crbank
crbank 9      100      9r166.776 138.98  end crbank
crbank 10     100      9r166.776 138.98  end crbank
crbank 11     100      9r166.776 138.98  end crbank
crbank 12     100      9r166.776 138.98  end crbank
crbank 13     100      9r166.776 138.98  end crbank
crbank 14     100      9r166.776 138.98  end crbank
crbank 15     100      9r166.776 138.98  end crbank
crbank 16     100      9r166.776 138.98  end crbank

```

```
end geom
```

```
read arrays
```

```
*****TVSA Fuel Bundle Information*****
```

```

' Color Cross Section # 235U Pins   Gd Absorber Pins
' TVSA 235U Enrichment # UPins   %Gd   %235U # Pins
' 2    13AU    1.30    312
' 3    22AU    2.2     312
' 4    30AV5   3.00    303  5.00  2.40  9
' 5    39AWU   4.00    243  5.00  3.30  9
'          3.60    60
' 6    390GO   4.00    240  5.00  3.30  6
'          3.60    66

```

```
'1 Radial Reflector
```

```
'2 Bottom Reflector
```

```
'3 Top Reflector
```

```
*****
```

```
' Core loading map for fuel [1, Figure 16]
```

```
ara=1 nux=33 nuy=17 fill
```

```
0 1 1 1 1 1 1 1 0
```

```

1 1 8 7 7 7 7 8 1 1
1 8 6 5 6 5 6 5 6 8 1
1 7 5 5 4 4 4 4 5 5 7 1
1 7 6 4 4 6 5 6 4 4 6 7 1
1 7 5 4 6 5 4 4 5 6 4 5 7 1
1 7 6 4 5 4 6 5 6 4 5 4 6 7 1
1 8 5 4 6 4 5 4 4 5 4 6 4 5 8 1
0 1 6 5 4 5 6 4 6 4 6 5 4 5 6 1 0
1 8 5 4 6 4 5 4 4 5 4 6 4 5 8 1
1 7 6 4 5 4 6 5 6 4 5 4 6 7 1
1 7 5 4 6 5 4 4 5 6 4 5 7 1
1 7 6 4 4 6 5 6 4 4 6 7 1
1 7 5 5 4 4 4 4 5 5 7 1
1 8 6 5 6 5 6 5 6 8 1
1 1 8 7 7 7 7 8 1 1
0 1 1 1 1 1 1 1 0

```

end fill

'Bottom Reflector Array

ara=2 nux=33 nuy=17 fill

```

0 2 2 2 2 2 2 2 0
2 2 2 2 2 2 2 2 2
2 2 2 2 2 2 2 2 2 2
2 2 2 2 2 2 2 2 2 2 2
2 2 2 2 2 2 2 2 2 2 2 2
2 2 2 2 2 2 2 2 2 2 2 2 2
2 2 2 2 2 2 2 2 2 2 2 2 2 2
2 2 2 2 2 2 2 2 2 2 2 2 2 2 2
0 2 2 2 2 2 2 2 2 2 2 2 2 2 2 2 0
2 2 2 2 2 2 2 2 2 2 2 2 2 2 2 2
2 2 2 2 2 2 2 2 2 2 2 2 2 2 2
2 2 2 2 2 2 2 2 2 2 2 2 2

```

```

2 2 2 2 2 2 2 2 2 2 2 2 2
2 2 2 2 2 2 2 2 2 2 2 2
2 2 2 2 2 2 2 2 2 2 2
2 2 2 2 2 2 2 2 2 2
0 2 2 2 2 2 2 2 0

end fill

'Top Reflector Array
ara=3 nux=33 nuy=17 fill

0 3 3 3 3 3 3 3 0
3 3 3 3 3 3 3 3 3
3 3 3 3 3 3 3 3 3 3
3 3 3 3 3 3 3 3 3 3 3
3 3 3 3 3 3 3 3 3 3 3 3
3 3 3 3 3 3 3 3 3 3 3 3 3
3 3 3 3 3 3 3 3 3 3 3 3 3 3
0 3 3 3 3 3 3 3 3 3 3 3 3 3 0
3 3 3 3 3 3 3 3 3 3 3 3 3 3
3 3 3 3 3 3 3 3 3 3 3 3 3
3 3 3 3 3 3 3 3 3 3 3 3
3 3 3 3 3 3 3 3 3 3 3
3 3 3 3 3 3 3 3 3 3
3 3 3 3 3 3 3 3 3
3 3 3 3 3 3 3 3
0 3 3 3 3 3 3 0

end fill

'Control Rod Map Banks 1-10 [2, Fig 11]
ara=100 nux=33 nuy=17 fill

0 0 0 0 0 0 0 0 0
0 0 0 0 0 0 0 0 0
0 0 0 8 0 6 0 9 0 0 0

```

```

0 0 9 0 4 2 3 5 0 8 0 0
0 0 0 5 0 0 10 0 0 4 0 0 0
0 0 6 3 0 7 0 0 7 0 2 6 0 0
0 0 0 2 10 0 0 8 0 0 10 3 0 0 0
0 0 8 4 0 0 1 0 0 1 0 0 5 9 0 0
0 0 0 0 0 7 0 0 9 0 0 7 0 0 0 0 0
0 0 9 5 0 0 8 0 0 8 0 0 4 8 0 0
0 0 0 3 10 0 0 1 0 0 10 2 0 0 0
0 0 6 2 0 7 0 0 7 0 3 6 0 0
0 0 0 4 0 0 10 0 0 5 0 0 0
0 0 8 0 5 3 2 4 0 9 0 0
0 0 0 9 0 6 0 8 0 0 0
0 0 0 0 0 0 0 0 0 0
0 0 0 0 0 0 0 0 0

```

end fill

end arrays

E.3.3: NESTLE VVER-1000 Control Rod Insertion Node Depth 4

VVER1000_CR testing_Node4

read parameter

*****Assumptions and References*****

'Created by Margaret Kurttis

' REF1. Lotsch, T., V. Khalimonchuk, and A. Kuchin, Proposal of a Benchmark for Core Burnup Calculations for a VVER-1000 Reactor Core, 2009

' REF2. Lotsch, T., V. Khalimonchuk, and A. Kuchin. Corrections and additions to the proposal of a benchmark for core burnup calculations for a WVER-1000 reactor, 2010.

' REF3. Wolfram Alpha Computational Knowledge Engine. [Online Database and Computational Tool] [cited 2016 May 24]; Available from: <http://www.wolframalpha.com/>.

' REF4. Nuclear Power: Convert/Calculator-Boric Acid. [Web page] [cited 2016 May 25]; Available from: <http://www.nuclear-power.net/glossary/boron-10/convertcalculator-boric-acid/>.

'Table 4 [1]-materials for fuel, guide tube, spacer.

'Table 3 [1]-materials for control rods, burnable absorbers

'Table 5 [1]-materials for stiffing plate

'Table 1 [1]-reactor temperature data

'Tab 1 [2]-Moderator Boron Concentration and fuel temperature

'Burndata comes from [2] for power (42.5 MW/MTU) and the core was shut down after 311.74 EFPD [1,2]

'Full core using 5 fuels, radial reflector

'CR insertion testing. inserted 4 nodes..actually rests at top of node 8 or bottom of node 9)

*****Assumptions and References*****

xsecfile=FUEL621.XSEC

outputfile=VVER1000_CRnode4.out

output_format=new

*****Power Density Calculation*****

'power density calculated is based on average fuel power density provided in benchmark, not thermal power/core V

'Methodology used to ensure agreement with Triton models used to generate cross sections

'average fuel power density 42.5 W/gU ([1],table 1)

'U/UO2 fraction = 0.881475

'fuel fraction=0.282572 (calculated using mixture vf ratios from Newt, and %fuel mixture that is fuel

'fuel density (UO2)=10.55

'power den=42.5*10.55*0.282572*0.881475=111.68

'power den=111.68

powerden=111.68

prcnt=100.0

t2n=yes

diffusionmethod=nem

thfeedback=yes

thsolver=hem

accel=cheby

problemtyp=evp

sym=full

printscreen=yes

geometry=hexa

end parameter

```

read edit

power dim=2 dist=avg scale=yes plot=yes end plot

power visit=123 geom=full coreline=solid

flux visit=456 geom=full coreline=solid

BU visit=789 geom=full coreline=solid

end edit

```

```

read plot

visit=123 gap=0.2 0.2 .5 scale=yes center=xyz color_scale=rel

        colors=0.0 "blue" 0.25 "cyan" 0.5 "green" 0.75 "yellow" 1.0 "red" endcolors end visit

visit=456 gap=0.2 0.2 0.5 scale=yes center=xyz color_scale=rel

        colors=0.0 "blue" 0.25 "cyan" 0.5 "green" 0.75 "yellow" 1.0 "red" endcolors end visit

visit=789 gap=0.2 0.2 0.5 scale=yes center=xyz color_scale=rel

        colors=0.0 "blue" 0.25 "cyan" 0.5 "green" 0.75 "yellow" 1.0 "red" endcolors end visit

end plot

```

```
read heattransfer
```

```
*****Heat Transfer Information and Calculations*****
```

```
' All steam table data, properties of water generated from Wolfram Alpha at www.wolframalpha.com
```

```
' Coolant Pressure at Core Outlet = 15.7 MPa [2, Table 3]
```

```
' Coolant Temperature at core Outlet = 592.75 K [2, Table 3] = 607.28 F
```

```
' Coolant Density at core outlet: Temp 592.75 K, Pres 15.7 MPa, dens=683.8 kg/m^3 [3]
```

```
' Coolant Temp at Core inlet = 563.15 K [2, Table 3] = 554 F
```

```
' Coolant Density at Core inlet: Temp 563.15 K, Pres 15.7 MPa, dens=746.5 kg/m^3 [3]
```

```
' Average coolant temp = 578 K [2, Table 3] = 580.73 F
```

```
' Coolant Density Average: Temp 578 K Pres 15.7 MPa, dens=716.7 kg/m^3 [3]
```

```
' Coolant flow rate = 88000 m^3/hr [2, Table 3]
```

```
' Saturation Temperature of water at 15.7 MPa is 619 K = 654.53 F [3]
```

```
' Density of water at saturation at 15.7 MPa 590.7 kg/m^3, 36.876 lbm/ft^3 [3]
```

```
' Density of steam at saturation at 15.7 MPa 104.1 kg/m^3, 6.499 lbm/ft^3 [3]
```

```
' Internal energy of water at saturation at 15.7 MPa is 1.611x10^6 J/kg = 692.6 BTU/lbm [3]
```

' Internal energy of steam at saturation at 15.7 MPa is 2.439×10^6 J/kg = 1048.6 BTU/lbm [3]

' Inlet Coolant Mass Flow Velocity

' Density of coolant at inlet (above)= 746.5 kg/m^3

' Mass flow rate = coolant density*coolant flow rate = $746.5 \text{ kg/m}^3 * 88000 \text{ m}^3/\text{hr} = 6.5692 \text{E}07 \text{ kg/hr}$

' Mass flow rate conversion: $6.5692 \text{E}07 \text{ kg/hr} = 1.44826 \text{E}08 \text{ lbm/hr}$

' Area of bundles = $163 * 477 = 77751 \text{ cm}^2 = 83.6905 \text{ ft}^2$

' Wet area of bundles = $w\text{tfro} * \text{area bundles} = .5554 * 83.6905 = 46.4817 \text{ ft}^2$

' Coolant Mass Flow Velocity = Mass flow/Wet Area of bundles

' $(1.44826 \text{E}08 \text{ lbm/hr}) / 46.4817 \text{ ft}^2 = 3.11576 \text{E}06 \text{ lbm/hr-ft}^2$

' Inlet Coolant Mass FlowVelocity (lb/hr-ft²)

g=3.11576E06

' bypass region = 0 (no bypass)

bypass=0.0

' Sat temp at 15.7 MPa (F)

tsat=654.53

' Density coolant vapor at Sat at 15.7 MPa (lbm/ft³)

rhovsat=6.499

' Internal energy of coolant vapor at sat at 15.7 MPa (BTU/lbm)

uvsat=1048.6

' Temp of coolant at inlet (F)

tinlet=554

*****Coolant Fit Generation at 15.7 MPa [3]*****

'Temperature (K) (lbm/ft ³)	Temperature (F)	Internal Energy (J/kg)	Internal Energy (BTU/Lbm)	Density (kg/m ³)	Density
'550		530.33 770	1.196E+06	48.070	514.28
'560		548.33 752.4	1.247E+06	46.971	536.21
'570		566.33 733.3	1.299E+06	45.778	558.57
'580		584.33 712.3	1.354E+06	44.467	582.22

'590	602.33	688.8	1.411E+06	43.000	606.73
'600	620.33	661.8	1.472E+06	41.315	632.96

'Fits generated using MATLAB Polyfit tool

```
t_vs_ufit -97.1512972      1.594225239      -0.000727706 end t_vs_ufit
u_vs_tfit 362.6758597     -0.593634149     0.001658951 end u_vs_tfit
rho_vs_ufit 53.18310251   0.028116898     -7.4028469E-05 end rho_vs_ufit
```

end heattransfer

read fuelmech

*****Fuel Mech Calculations*****

'''fuel pin

' Number of fuel pins per assembly 312

' Number of fuel assembly types (colors) in xsec file = 1

' Area of fuel assembly (from above)=477.014 cm² 0.5135 ft²

' Pin Diameter = 0.91 cm [2, table 1]

' Pin Radius =0.455 cm or 0.1791 in

' Pin Inner Clad Diam = 0.773 cm [2, table 1]

' Pin Outer fuel Diam = 0.757 cm [2, table 1] 0.2980 in

' Pin fuel rad = 0.3785 cm 0.1490 in

' Pin area = pi*(.91/2)² = 0.6504 cm²

' total area of fuel pins in assembly = 312*0.6504 = 202.9211 cm²

'''Control Rod

' CR guide tube outer diam = 1.26 cm [2, table 1]

' CR guide tube inner diam = 1.09 cm [2, table 1]

' CR clad outer diam = 0.82 cm [2, table 1]

' Area of guide tube = pi*(1.26/2)² = 1.247 cm²

' Area of CR wet (RO) = pi*(1.09/2)² = 0.933 cm²

' Area of guide tube material = (pi*(1.26/2)²) -(pi*(1.09/2)²)= 0.31377 cm²

' Area of CR material = pi*(0.82/2)² = 0.5281 cm²

' Number of CR guide tubes in TVSA = 18 [2, table 1]

' Assembly CR guide tube area = $18 \times 1.246 = 22.444 \text{ cm}^2$

' Assembly CR guide tube material area = $18 \times 0.31377 = 5.6478 \text{ cm}^2$

' Assembly CR material (R/I) = $18 \times 0.5281 = 9.5058 \text{ cm}^2$

'''Central Guide Tube

' CG tube inner diam = 1.1 cm [2, table 1]

' CG tube outer diam = 1.3 cm [2, table 1]

' CG tube material area = $(\pi \times (1.3/2)^2) - (\pi \times (1.1/2)^2) = 0.3770 \text{ cm}^2$

'''Stiffening angle plate

' thickness of stiffening plate = 0.1 cm [1, figure 10]

' Assembly side gap NOT covered by stiffening plate = side - 7.65 cm = $13.55 - 7.65 = 5.9 \text{ cm}$ [1, figure 10]

' Area of single stiffening plate corner = $5.9 \times 0.1 = 0.59 \text{ cm}^2$

' Number of Stiffening plates per assembly = 6 [1, Table 5]

' Assembly area with stiffening material = $6 \times 0.59 = 3.54 \text{ cm}^2$

' Fuel fraction (single assembly) = $202.9211 / 477.014 = 0.4254$

'''Wet Fraction Rods Out

' Material (not water) area / assembly area = (fuel pin+CR guide tubes+CG guide tube+stiffangle)/area

' wtmaterialNOTwetRO = $(202.9211 + 5.6478 + 0.377 + 3.54) / 477.014 = 0.44545$

' wtfro = $1 - \text{wtmaterialNOTwetRO} = 0.55455$

'''Wet Fraction Rods In

' Material (not water) area / assembly = (fuel pins+CR guidetubes+CR material+CG guidetube+stiffangle)/area

' wtmaterialNOTwetRI = $(202.9211 + 5.6478 + 9.506 + 0.377 + 3.54) / 477.014 = 0.46534$

' wtfri = $1 - \text{wtmaterialNOTwetRI} = 0.53462$

'''wtfro and wtfri calculation for reflector region

' Wet fraction for the reflector region is the same RI and RO

'-----Reflector Region Wet Fraction Calcs (VF from Newt)-----

Mixture ID	Name	VF total	VF Colors	VF material/color	V mixture Wet	Fraction Wet
	WTFRO/WTFRI					
'303	Fuel(2) 0.00E+00	0.53802	3.17E-01	6.85E-01 4.62E-01		0
'304	Mod(2) 1		3.69E-01 5.38E-01		5.38E-01	
'100	Steel(1) 0.00E+00	0.47557	1.84E-02	3.15E-01 5.84E-02		0

'200	7.51E-02	Stel/Mod(1)	5.19E-02	1.65E-01	0.455761
'300	1	mod(1)	4.59E-03 1.46E-02	1.46E-02	
'400		steel(1)	2.76E-02 0.00E+00	8.75E-02	0
'500	1	mod(1)	1.21E-01 3.86E-01	3.86E-01	
'600		Steel(1)	9.09E-02 0.00E+00	2.89E-01	0

' Wet Fraction of Radial Reflector Region: 0.47557

' Wet Fraction of Bottom Reflector Region: 0.61461 (calcs similar to above, not listed here)

' Wet Fraction of Top Reflector Region: 0.80741 (calcs similar to above, not listed here)

' fuel density = 10.55 g/cc [1, table 4 average of values, consistant with scale files]

' fuel density = 658.6 lbm/ft^3

fiss_frac=1.0

fuelden=658.6

numfrods 3r0.0 5r312 end numfrods

bunarea 3r0.0 5r0.5135 end bunarea

frodrad 3r0.0 5r0.1490 end frodrad

'Fuel fraction calculations use single assembly fuel material VF from NEWT calcs

fuelfrac 3r0.0 2r0.282562 0.282585 0.282584 0.282577 end fuelfrac

wtfro 0.47557 0.61461 0.80741 5r0.55455 end wtfro

wtfri 0.47557 0.61461 0.80741 5r0.53462 end wtfri

'The following fits were pulled out of the regression test file NESTLE.XSC.MACRO.PWR

wc=1.00

wp=0.85

heff_vs_t 0.78363116E-01 -0.19203380E-04 0.73696720E-08 end heff_vs_t

tavg_vs_lpd 0.56955571E+3 0.16964059E+03 -0.2916911E+1 end tavg_vs_lpd

tsurf_vs_lpd 0.56955571E+3 0.924990E+2 0.432861000 -0.377884E-1 end tsurf_vs_lpd

cp_vs_tfit 0.8110000193E-01 end cp_vs_tfit

'lattice ID below

lattice_ids 1 2 3 4 5 6 7 8 end lattice_ids

end fuelmech

read burndata

pres=2277.092

*****Burnup Calculations*****

'BOC burn data

'Coolant inlet temp = 563.15 K=554.0 F

burnup=0.00 end	sm=no	xe=no	pctpwr=99.0	cro_d_id=1	pctflow=100.00	tinlet=549.00	search=boronppm
burnup=250 search=boronppm end	sm=eq	xe=eq	pctpwr=99.0	cro_d_id=2	pctflow=100.00	tinlet=549.00	
burnup=500 search=boronppm end	sm=eq	xe=eq	pctpwr=99.0	cro_d_id=3	pctflow=100.00	tinlet=549.00	
burnup=1000 search=boronppm end	sm=eq	xe=eq	pctpwr=99.0	cro_d_id=4	pctflow=100.00	tinlet=549.00	
burnup=2000 search=boronppm end	sm=eq	xe=eq	pctpwr=99.0	cro_d_id=5	pctflow=100.00	tinlet=549.00	
burnup=3000 search=boronppm end	sm=eq	xe=eq	pctpwr=99.0	cro_d_id=6	pctflow=100.00	tinlet=549.00	
burnup=4000 search=boronppm end	sm=eq	xe=eq	pctpwr=99.0	cro_d_id=7	pctflow=100.00	tinlet=549.00	
burnup=5000 search=boronppm end	sm=eq	xe=eq	pctpwr=99.0	cro_d_id=8	pctflow=100.00	tinlet=549.00	
burnup=6000 search=boronppm end	sm=eq	xe=eq	pctpwr=99.0	cro_d_id=9	pctflow=100.00	tinlet=549.00	
burnup=7000 tinlet=549.00 search=boronppm end	sm=eq	xe=eq	pctpwr=99.0	cro_d_id=10	pctflow=100.00		
burnup=8000 tinlet=549.00 search=boronppm end	sm=eq	xe=eq	pctpwr=99.0	cro_d_id=11	pctflow=100.00		
burnup=9000 tinlet=549.00 search=boronppm end	sm=eq	xe=eq	pctpwr=99.0	cro_d_id=12	pctflow=100.00		
burnup=10000 search=boronppm end	sm=eq	xe=eq	pctpwr=99.0	cro_d_id=13	pctflow=100.00	tinlet=549.00	
burnup=11000 search=boronppm end	sm=eq	xe=eq	pctpwr=99.0	cro_d_id=14	pctflow=100.00	tinlet=549.00	
burnup=12000 search=boronppm end	sm=eq	xe=eq	pctpwr=99.0	cro_d_id=15	pctflow=100.00	tinlet=549.00	

```

burnup=13000      sm=eq   xe=eq   pctpwr=50.0      crod_id=16      pctflow=100.00      tinlet=549.00
search=boronppm end

end burndata

read geom

"reflection

down=noentry

up=noentry

outer=noentry

inner=cyclic

numrings=8

"xy mesh

' bundle pitch = 23.48 cm = 9.2441 in

' half pitch = 4.62205

' side length 13.55 cm = 5.3346 in

' 6-14 x assemblies

' 15 y assemblies

bpitch=9.2441

deltax 6r4.2205 end deltax

deltay 15r5.334 end deltax

' # nodes

"z direction calculations

' Core active fuel height 353 cm = 138.98 in

' 12 axial nodes. 1 bottom Refl, 10 fuel, 1 top refl

' deltaz= 138.98/10 = 13.898

deltaz 12r13.898 end deltaz

figure 2 10r1 3 end figure

bottomfuelnode=2

topfuelnode=11

*****Control Rod Bank Information*****

' Working control rod group = 10 [2, para 3.1.1, pg 6]

```

' All Control Rods in groups 1-9 assumed to be fully OUT. Not specified.

' Model Z dimension $12 * 13.898 = 166.776$, CR fallout = 166.776

' CRG 1-9 are at 166.776 (fully out), WG10 will be inserted 2 nodes (27.796 in, or 138.98)

' CR 11 is the test rod, it is "inserted" into assembly 139 at node 4 (111.184)

crload= topdown

crbank	1	100	9r166.776	138.98	111.184	end crbank
crbank	2	100	9r166.776	138.98	111.184	end crbank
crbank	3	100	9r166.776	138.98	111.184	end crbank
crbank	4	100	9r166.776	138.98	111.184	end crbank
crbank	5	100	9r166.776	138.98	111.184	end crbank
crbank	6	100	9r166.776	138.98	111.184	end crbank
crbank	7	100	9r166.776	138.98	111.184	end crbank
crbank	8	100	9r166.776	138.98	111.184	end crbank
crbank	9	100	9r166.776	138.98	111.184	end crbank
crbank	10	100	9r166.776	138.98	111.184	end crbank
crbank	11	100	9r166.776	138.98	111.184	end crbank
crbank	12	100	9r166.776	138.98	111.184	end crbank
crbank	13	100	9r166.776	138.98	111.184	end crbank
crbank	14	100	9r166.776	138.98	111.184	end crbank
crbank	15	100	9r166.776	138.98	111.184	end crbank
crbank	16	100	9r166.776	138.98	111.184	end crbank

end geom

read arrays

*****TVSA Fuel Bundle Information*****

' Color Cross Section # ^{235}U Pins Gd Absorber Pins

' TVSA ^{235}U Enrichment # UPins %Gd % ^{235}U # Pins

'4 13AU 1.30 312

```
'5      22AU      2.2      312
'6      30AV5     3.00     303  5.00   2.40   9
'7      39AWU     4.00     243  5.00   3.30   9
'          3.60     60
'8      390GO     4.00     240  5.00   3.30   6
'          3.60     66
```

```
'1 Radial Reflector
```

```
'2 Bottom Reflector
```

```
'3 Top Reflector
```

```
*****
```

```
' Core loading map for fuel [1, Figure 16]
```

```
ara=1 nux=33 nuy=17 fill
```

```
    0 1 1 1 1 1 1 1 0
    1 1 8 7 7 7 7 8 1 1
    1 8 6 5 6 5 6 5 6 8 1
    1 7 5 5 4 4 4 4 5 5 7 1
    1 7 6 4 4 6 5 6 4 4 6 7 1
    1 7 5 4 6 5 4 4 5 6 4 5 7 1
    1 7 6 4 5 4 6 5 6 4 5 4 6 7 1
    1 8 5 4 6 4 5 4 4 5 4 6 4 5 8 1
0 1 6 5 4 5 6 4 6 4 6 5 4 5 6 1 0
    1 8 5 4 6 4 5 4 4 5 4 6 4 5 8 1
    1 7 6 4 5 4 6 5 6 4 5 4 6 7 1
    1 7 5 4 6 5 4 4 5 6 4 5 7 1
    1 7 6 4 4 6 5 6 4 4 6 7 1
    1 7 5 5 4 4 4 4 5 5 7 1
    1 8 6 5 6 5 6 5 6 8 1
    1 1 8 7 7 7 7 8 1 1
    0 1 1 1 1 1 1 1 0
```

```
end fill
```

```
' Bottom Reflector Array
```

ara=2 nux=33 nuy=17 fill

```
0 2 2 2 2 2 2 2 0
2 2 2 2 2 2 2 2 2
2 2 2 2 2 2 2 2 2
2 2 2 2 2 2 2 2 2
2 2 2 2 2 2 2 2 2
2 2 2 2 2 2 2 2 2
2 2 2 2 2 2 2 2 2
2 2 2 2 2 2 2 2 2
2 2 2 2 2 2 2 2 2
0 2 2 2 2 2 2 2 2 2 2 2 2 2 2 2 0
2 2 2 2 2 2 2 2 2 2 2 2 2 2 2
2 2 2 2 2 2 2 2 2 2 2 2 2 2
2 2 2 2 2 2 2 2 2 2 2 2
2 2 2 2 2 2 2 2 2 2 2
2 2 2 2 2 2 2 2 2 2
2 2 2 2 2 2 2 2 2
2 2 2 2 2 2 2 2 2
0 2 2 2 2 2 2 2 0
```

end fill

'Top Reflector Array

ara=3 nux=33 nuy=17 fill

```
0 3 3 3 3 3 3 3 0
3 3 3 3 3 3 3 3 3
3 3 3 3 3 3 3 3 3
3 3 3 3 3 3 3 3 3
3 3 3 3 3 3 3 3 3
3 3 3 3 3 3 3 3 3
3 3 3 3 3 3 3 3 3
3 3 3 3 3 3 3 3 3
3 3 3 3 3 3 3 3 3
0 3 3 3 3 3 3 3 3 3 3 3 3 3 3 3 0
3 3 3 3 3 3 3 3 3 3 3 3 3 3 3
```

```

3 3 3 3 3 3 3 3 3 3 3 3 3 3 3
3 3 3 3 3 3 3 3 3 3 3 3 3 3
3 3 3 3 3 3 3 3 3 3 3 3 3
3 3 3 3 3 3 3 3 3 3 3 3
3 3 3 3 3 3 3 3 3 3 3
3 3 3 3 3 3 3 3 3 3
0 3 3 3 3 3 3 3 0

```

end fill

'Control Rod Map Banks 1-10 [2, Fig 11]

ara=100 nux=33 nuy=17 fill

```

0 0 0 0 0 0 0 0 0 0
0 0 0 0 0 0 0 0 0 0
0 0 0 8 0 6 0 9 0 0 0
0 0 9 0 4 2 3 5 0 8 0 0
0 0 0 5 0 0 10 0 0 4 0 0 0
0 0 6 3 0 7 0 11 7 0 2 6 0 0
0 0 0 2 10 0 0 8 0 0 10 3 0 0 0
0 0 8 4 0 0 1 0 0 1 0 0 5 9 0 0
0 0 0 0 0 7 0 0 9 0 0 7 0 0 0 0 0
0 0 9 5 0 0 8 0 0 8 0 0 4 8 0 0
0 0 0 3 10 0 0 1 0 0 10 2 0 0 0
0 0 6 2 0 7 0 0 7 0 3 6 0 0
0 0 0 4 0 0 10 0 0 5 0 0 0
0 0 8 0 5 3 2 4 0 9 0 0
0 0 0 9 0 6 0 8 0 0 0
0 0 0 0 0 0 0 0 0 0
0 0 0 0 0 0 0 0 0 0

```

end fill

end arrays

E.3.4: VVER-1000 SS316 Model

VVER1000_fullcore_all_reflectors

read parameter

*****Assumptions and References*****

'Created by Margaret Kurttis

'REF1. Lotsch, T., V. Khalimonchuk, and A. Kuchin, Proposal of a Benchmark for Core Burnup Calculations for a VVER-1000 Reactor Core, 2009

'REF2. Lotsch, T., V. Khalimonchuk, and A. Kuchin. Corrections and additions to the proposal of a benchmark for core burnup calculations for a VVER-1000 reactor, 2010.

'REF3. Wolfram Alpha Computational Knowledge Engine. [Online Database and Computational Tool] [cited 2016 May 24]; Available from: <http://www.wolframalpha.com/>.

'REF4. Nuclear Power: Convert/Calculator-Boric Acid. [Web page] [cited 2016 May 25]; Available from: <http://www.nuclear-power.net/glossary/boron-10/convertcalculator-boric-acid/>.

'Table 4 [1]-materials for fuel, guide tube, spacer.

'Table 3 [1]-materials for control rods, burnable absorbers

'Table 5 [1]-materials for stiffing plate

'Table 1 [1]-reactor temperature data

'Tab 1 [2]-Moderator Boron Concentration and fuel temperature

'Burndata comes from [2] for power (42.5 MW/MTU) and the core was shut down after 311.74 EFPD [1,2]

'Full core using 5 fuels, radial reflector, upper and lower reflector

'Replace moderator in control rod guide tubes with SS for 1 assembly (139)

*****Assumptions and References*****

xsecfile=FUEL621_SS.XSEC

outputfile=VVER1000_SS.out

output_format=new

*****Power Density Calculation*****

'power density calculated is based on average fuel power density provided in benchmark, not thermal power/core V

'Methodology used to ensure agreement with Triton models used to generate cross sections

'average fuel power density 42.5 W/gU ([1],table 1)

'U/UO2 fraction = 0.881475

'fuel fraction=0.282572 (calculated using mixture vf ratios from Newt, and %fuel mixture that is fuel

'fuel density (UO2)=10.55

'power den=42.5*10.55*0.282572*0.881475=111.68

'power den=111.68

powerden=111.68

prcnt=100.0

t2n=yes

diffusionmethod=nem

thfeedback=yes

thsolver=hem

accel=cheby

problemtyp=evp

sym=full

printscreen=yes

geometry=hexa

end parameter

read edit

power dim=2 dist=avg scale=yes plot=yes end plot

power visit=123 geom=full coreline=solid

flux visit=456 geom=full coreline=solid

BU visit=789 geom=full coreline=solid

end edit

read plot

visit=123 gap=0.2 0.2 .5 scale=yes center=xyz color_scale=rel

colors=0.0 "blue" 0.25 "cyan" 0.5 "green" 0.75 "yellow" 1.0 "red" endcolors end visit

visit=456 gap=0.2 0.2 0.5 scale=yes center=xyz color_scale=rel

colors=0.0 "blue" 0.25 "cyan" 0.5 "green" 0.75 "yellow" 1.0 "red" endcolors end visit

visit=789 gap=0.2 0.2 0.5 scale=yes center=xyz color_scale=rel

colors=0.0 "blue" 0.25 "cyan" 0.5 "green" 0.75 "yellow" 1.0 "red" endcolors end visit

end plot

read heattransfer

*****Heat Transfer Information and Calculations*****

' All steam table data, properties of water generated from Wolfram Alpha at www.wolframalpha.com

' Coolant Pressure at Core Outlet = 15.7 MPa [2, Table 3]

' Coolant Temperature at core Outlet = 592.75 K [2, Table 3] = 607.28 F

' Coolant Density at core outlet: Temp 592.75 K, Pres 15.7 MPa, dens=683.8 kg/m³ [3]

' Coolant Temp at Core inlet = 563.15 K [2, Table 3] = 554 F

' Coolant Density at Core inlet: Temp 563.15 K, Pres 15.7 MPa, dens=746.5 kg/m³ [3]

' Average coolant temp = 578 K [2, Table 3] = 580.73 F

' Coolant Density Average: Temp 578 K Pres 15.7 MPa, dens=716.7 kg/m³ [3]

' Coolant flow rate = 88000 m³/hr [2, Table 3]

' Saturation Temperature of water at 15.7 MPa is 619 K = 654.53 F [3]

' Density of water at saturation at 15.7 MPa 590.7 kg/m³, 36.876 lbm/ft³ [3]

' Density of steam at saturation at 15.7 MPa 104.1 kg/m³, 6.499 lbm/ft³ [3]

' Internal energy of water at saturation at 15.7 MPa is 1.611x10⁶ J/kg = 692.6 BTU/lbm [3]

' Internal energy of steam at saturation at 15.7 MPa is 2.439x10⁶ J/kg = 1048.6 BTU/lbm [3]

' Inlet Coolant Mass Flow Velocity

' Density of coolant at inlet (above)= 746.5 kg/m³

' Mass flow rate = coolant density*coolant flow rate = 746.5 kg/m³ * 88000 m³/hr = 6.5692E07 kg/hr

' Mass flow rate conversion: 6.5692E07 kg/hr = 1.44826E08 lbm/hr

' Area of bundles = 163*477 = 77751 cm² = 83.6905 ft²

' Wet area of bundles = wtfro*area bundles = .5554*83.6905=46.4817 ft²

' Coolant Mass Flow Velocity = Mass flow/Wet Area of bundles

' (1.44826E08 lbm/hr)/ 46.4817 ft² = 3.11576E06 lbm/hr-ft²

' Inlet Coolant Mass FlowVelocity (lb/hr-ft²)

g=3.11576E06

' bypass region = 0 (no bypass)

bypass=0.0

' Sat temp at 15.7 MPa (F)

tsat=654.53

' Density coolant vapor at Sat at 15.7 MPa (lbm/ft^3)

rhovsat=6.499

' Internal energy of coolant vapor at sat at 15.7 MPa (BTU/lbm)

uvsat=1048.6

' Temp of coolant at inlet (F)

tinlet=554

*****Coolant Fit Generation at 15.7 MPa [3]*****

'Temperature (K) (lbm/ft^3)	Temperature (F)	Internal Energy (J/kg)	Internal Energy (BTU/Lbm)	Density (kg/m^3)	Density
'550	530.33	770	1.196E+06	48.070	514.28
'560	548.33	752.4	1.247E+06	46.971	536.21
'570	566.33	733.3	1.299E+06	45.778	558.57
'580	584.33	712.3	1.354E+06	44.467	582.22
'590	602.33	688.8	1.411E+06	43.000	606.73
'600	620.33	661.8	1.472E+06	41.315	632.96

'Fits generated using MATLAB Polyfit tool

t_vs_ufit -97.1512972 1.594225239 -0.000727706 end t_vs_ufit

u_vs_tfit 362.6758597 -0.593634149 0.001658951 end u_vs_tfit

rho_vs_ufit 53.18310251 0.028116898 -7.4028469E-05 end rho_vs_ufit

end heattransfer

read fuelmech

*****Fuel Mech Calculations*****

'''fuel pin

' Number of fuel pins per assembly 312

' Number of fuel assembly types (colors) in xsec file = 1

' Area of fuel assembly (from above)=477.014 cm² 0.5135 ft²

' Pin Diameter = 0.91 cm [2, table 1]

' Pin Radius =0.455 cm or 0.1791 in

' Pin Inner Clad Diam = 0.773 cm [2, table 1]

' Pin Outer fuel Diam = 0.757 cm [2, table 1] 0.2980 in

' Pin fuel rad = 0.3785 cm 0.1490 in

' Pin area = $\pi \cdot (.91/2)^2 = 0.6504 \text{ cm}^2$

' total area of fuel pins in assembly = $312 \cdot 0.6504 = 202.9211 \text{ cm}^2$

'''Control Rod

' CR guide tube outer diam = 1.26 cm [2, table 1]

' CR guide tube inner diam = 1.09 cm [2, table 1]

' CR clad outer diam = 0.82 cm [2, table 1]

' Area of guide tube = $\pi \cdot (1.26/2)^2 = 1.247 \text{ cm}^2$

' Area of CR wet (RO) = $\pi \cdot (1.09/2)^2 = 0.933 \text{ cm}^2$

' Area of guide tube material = $(\pi \cdot (1.26/2)^2) - (\pi \cdot (1.09/2)^2) = 0.31377 \text{ cm}^2$

' Area of CR material = $\pi \cdot (0.82/2)^2 = 0.5281 \text{ cm}^2$

' Number of CR guide tubes in TVSA = 18 [2, table 1]

' Assembly CR guide tube area = $18 \cdot 1.246 = 22.444 \text{ cm}^2$

' Assembly CR guide tube material area = $18 \cdot 0.31377 = 5.6478 \text{ cm}^2$

' Assembly CR material (R/I) = $18 \cdot 0.5281 = 9.5058 \text{ cm}^2$

'''Central Guide Tube

' CG tube inner diam = 1.1 cm [2, table 1]

' CG tube outer diam = 1.3 cm [2, table 1]

' CG tube material area = $(\pi \cdot (1.3/2)^2) - (\pi \cdot (1.1/2)^2) = 0.3770 \text{ cm}^2$

'''Stiffening angle plate

' thickness of stiffening plate = 0.1 cm [1, figure 10]

' Assembly side gap NOT covered by stiffening plate = side - 7.65 cm = $13.55 - 7.65 = 5.9 \text{ cm}$ [1, figure 10]

' Area of single stiffening plate corner = $5.9 \cdot 0.1 = 0.59 \text{ cm}^2$

' Number of Stiffening plates per assembly = 6 [1, Table 5]

' Assembly area with stiffening material = $6 \cdot 0.59 = 3.54 \text{ cm}^2$

' Fuel fraction (single assembly) = $202.9211 / 477.014 = 0.4254$

'''Wet Fraction Rods Out

' Material (not water) area / assembly area = (fuel pin+CR guide tubes+CG guide tube+stiffangle)/area

' wmaterialNOTwetRO=(202.9211+5.6478+0.377+3.54)/477.014=0.44545

' wtfro=1-wmaterialNOTwetRO=0.55455

'''Wet Fraction Rods In

' Material (not water)area/assembly =(fuelpins+CRguidetubes+CRmaterial+CGguidetube+stiffangle)/area

' wmaterialNOTwetRI=(202.9211+5.6478+9.506+0.377+3.54)/477.014=0.46534

' wtfri=1-wmaterialNOTwetRI=0.53462

'''wtfro and wtfri calculation for reflector region

' Wet fraction for the reflector region is the same RI and RO

'-----Reflector Region Wet Fraction Calcs (VF from Newt)-----

Mixture ID	Name WTFRO/WTFRI	VF total	VF Colors	VF material/color	V mixture Wet	Fraction Wet
'303	0.00E+00	Fuel(2) 0.53802	3.17E-01	6.85E-01 4.62E-01		0
'304	1	Mod(2)	3.69E-01 5.38E-01		5.38E-01	
'100	0.00E+00	Steel(1) 0.47557	1.84E-02	3.15E-01 5.84E-02		0
'200	7.51E-02	Stel/Mod(1)	5.19E-02		1.65E-01	0.455761
'300	1	mod(1)	4.59E-03 1.46E-02		1.46E-02	
'400		steel(1) 0.00E+00	2.76E-02		8.75E-02	0
'500	1	mod(1)	1.21E-01 3.86E-01		3.86E-01	
'600		Steel(1) 0.00E+00	9.09E-02		2.89E-01	0

' Wet Fraction of Radial Reflector Region: 0.47557

' Wet Fraction of Bottom Reflector Region: 0.61461 (calcs similar to above, not listed here)

' Wet Fraction of Top Reflector Region: 0.80741 (calcs similar to above, not listed here)

' fuel density = 10.55 g/cc [1, table 4 average of values, consistant with scale files]

' fuel density = 658.6 lbm/ft^3

fiss_frac=1.0

```

fuelden=658.6

numfrods 3r0.0 6r312 end numfrods

bunarea 3r0.0 6r0.5135 end bunarea

frodrad 3r0.0 6r0.1490 end frodrad

'Fuel fraction calculations use single assembly fuel material VF from NEWT calcs

fuelfrac 3r0.0 2r0.282562 0.282585 0.282584 0.282577 0.282562 end fuelfrac

wtfro 0.47557 0.61461 0.80741 5r0.55455 0.53462 end wtfro

wtfri 0.47557 0.61461 0.80741 6r0.53462 end wtfri

'The following fits were pulled out of the regression test file NESTLE.XSC.MACRO.PWR

wc=1.00

wp=0.85

heff_vs_t 0.78363116E-01 -0.19203380E-04 0.73696720E-08 end heff_vs_t

tavg_vs_lpd 0.56955571E+3 0.16964059E+03 -0.2916911E+1 end tavg_vs_lpd

tsurf_vs_lpd 0.56955571E+3 0.924990E+2 0.432861000 -0.377884E-1 end tsurf_vs_lpd

cp_vs_tfit 0.8110000193E-01 end cp_vs_tfit

'lattice ID below

lattice_ids 1 2 3 4 5 6 7 8 9 end lattice_ids

end fuelmech

read burndata

pres=2277.092

*****Burnup Calculations*****

'BOC burn data

'Coolant inlet temp = 563.15 K=554.0 F

*****

burnup=0.00          sm=no  xe=no  pctpwr=99.0          crod_id=1  pctflow=100.00      tinlet=549.00 search=boronppm
end

burnup=250          sm=eq  xe=eq  pctpwr=99.0          crod_id=2  pctflow=100.00      tinlet=549.00
search=boronppm end

burnup=500          sm=eq  xe=eq  pctpwr=99.0          crod_id=3  pctflow=100.00      tinlet=549.00
search=boronppm end

burnup=1000         sm=eq  xe=eq  pctpwr=99.0          crod_id=4  pctflow=100.00      tinlet=549.00
search=boronppm end

```

burnup=2000 search=boronppm end	sm=eq	xe=eq	pctpwr=99.0	cro_d_id=5	pctflow=100.00	tinlet=549.00
burnup=3000 search=boronppm end	sm=eq	xe=eq	pctpwr=99.0	cro_d_id=6	pctflow=100.00	tinlet=549.00
burnup=4000 search=boronppm end	sm=eq	xe=eq	pctpwr=99.0	cro_d_id=7	pctflow=100.00	tinlet=549.00
burnup=5000 search=boronppm end	sm=eq	xe=eq	pctpwr=99.0	cro_d_id=8	pctflow=100.00	tinlet=549.00
burnup=6000 search=boronppm end	sm=eq	xe=eq	pctpwr=99.0	cro_d_id=9	pctflow=100.00	tinlet=549.00
burnup=7000 tinlet=549.00 search=boronppm end	sm=eq	xe=eq	pctpwr=99.0	cro_d_id=10	pctflow=100.00	
burnup=8000 tinlet=549.00 search=boronppm end	sm=eq	xe=eq	pctpwr=99.0	cro_d_id=11	pctflow=100.00	
burnup=9000 tinlet=549.00 search=boronppm end	sm=eq	xe=eq	pctpwr=99.0	cro_d_id=12	pctflow=100.00	
burnup=10000 search=boronppm end	sm=eq	xe=eq	pctpwr=99.0	cro_d_id=13	pctflow=100.00	tinlet=549.00
burnup=11000 search=boronppm end	sm=eq	xe=eq	pctpwr=99.0	cro_d_id=14	pctflow=100.00	tinlet=549.00
burnup=12000 search=boronppm end	sm=eq	xe=eq	pctpwr=99.0	cro_d_id=15	pctflow=100.00	tinlet=549.00
burnup=13000 search=boronppm end	sm=eq	xe=eq	pctpwr=50.0	cro_d_id=16	pctflow=100.00	tinlet=549.00

end burndata

read geom

""reflection

down=noentry

up=noentry

outer=noentry

inner=cyclic

numrings=8

""xy mesh

' bundle pitch = 23.48 cm = 9.2441 in

' half pitch = 4.62205

' side length 13.55 cm = 5.3346 in

```

'6-14 x assemblies

' 15 y assemblies

bpitch=9.2441

deltax 6r4.2205 end deltax

deltay 15r5.334 end deltax

'# nodes

"z direction calculations

' Core active fuel height 353 cm = 138.98 in

' 12 axial nodes. 1 bottom Refl, 10 fuel, 1 top refl

' deltax= 138.98/10 = 13.898

deltaz 12r13.898 end deltax

figure 2 10r1 3 end figure

bottomfuelnode=2

topfuelnode=11

*****Control Rod Bank Information*****

' Working control rod group = 10 [2, para 3.1.1, pg 6]

' All Control Rods in groups 1-9 assumed to be fully OUT. Not specified.

' Model Z dimension 12*13.898 = 166.776, CR fullout = 166.776

' CRG 1-9 are at 166.776 (fully out), WG10 will be inserted 2 nodes (27.796 in, or 138.98)

*****

crload= topdown

crbank  1      100      9r166.776 138.98  end crbank

crbank  2      100      9r166.776 138.98  end crbank

crbank  3      100      9r166.776 138.98  end crbank

crbank  4      100      9r166.776 138.98  end crbank

crbank  5      100      9r166.776 138.98  end crbank

crbank  6      100      9r166.776 138.98  end crbank

crbank  7      100      9r166.776 138.98  end crbank

crbank  8      100      9r166.776 138.98  end crbank

crbank  9      100      9r166.776 138.98  end crbank

crbank 10      100      9r166.776 138.98  end crbank

```

```

crbank 11 100 9r166.776 138.98 end crbank
crbank 12 100 9r166.776 138.98 end crbank
crbank 13 100 9r166.776 138.98 end crbank
crbank 14 100 9r166.776 138.98 end crbank
crbank 15 100 9r166.776 138.98 end crbank
crbank 16 100 9r166.776 138.98 end crbank

```

end geom

read arrays

*****TVSA Fuel Bundle Information*****

```

' Color Cross Section # 235U Pins Gd Absorber Pins
' TVSA 235U Enrichment # UPins %Gd %235U # Pins
'4 13AU 1.30 312
'5 22AU 2.2 312
'6 30AV5 3.00 303 5.00 2.40 9
'7 39AWU 4.00 243 5.00 3.30 9
' 3.60 60
'8 390GO 4.00 240 5.00 3.30 6
' 3.60 66

```

'1 Radial Reflector

'2 Bottom Reflector

'3 Top Reflector

'9 13AU with SS assembly 139 only

' Core loading map for fuel [1, Figure 16]

ara=1 nux=33 nuy=17 fill

```

0 1 1 1 1 1 1 1 0
1 1 8 7 7 7 7 8 1 1
1 8 6 5 6 5 6 5 6 8 1
1 7 5 5 4 4 4 4 5 5 7 1
1 7 6 4 4 6 5 6 4 4 6 7 1

```

```

1 7 5 4 6 5 4 9 5 6 4 5 7 1
1 7 6 4 5 4 6 5 6 4 5 4 6 7 1
1 8 5 4 6 4 5 4 4 5 4 6 4 5 8 1
0 1 6 5 4 5 6 4 6 4 6 5 4 5 6 1 0
1 8 5 4 6 4 5 4 4 5 4 6 4 5 8 1
1 7 6 4 5 4 6 5 6 4 5 4 6 7 1
1 7 5 4 6 5 4 4 5 6 4 5 7 1
1 7 6 4 4 6 5 6 4 4 6 7 1
1 7 5 5 4 4 4 4 5 5 7 1
1 8 6 5 6 5 6 5 6 8 1
1 1 8 7 7 7 7 8 1 1
0 1 1 1 1 1 1 1 0

```

end fill

'Bottom Reflector Array

ara=2 nux=33 nuy=17 fill

```

0 2 2 2 2 2 2 2 0
2 2 2 2 2 2 2 2 2
2 2 2 2 2 2 2 2 2
2 2 2 2 2 2 2 2 2
2 2 2 2 2 2 2 2 2
2 2 2 2 2 2 2 2 2
2 2 2 2 2 2 2 2 2
2 2 2 2 2 2 2 2 2
2 2 2 2 2 2 2 2 2
2 2 2 2 2 2 2 2 2
2 2 2 2 2 2 2 2 2
2 2 2 2 2 2 2 2 2
2 2 2 2 2 2 2 2 2
2 2 2 2 2 2 2 2 2
2 2 2 2 2 2 2 2 2
2 2 2 2 2 2 2 2 2
2 2 2 2 2 2 2 2 2
2 2 2 2 2 2 2 2 2
2 2 2 2 2 2 2 2 2

```

```

    0 2 2 2 2 2 2 2 0
end fill
'Top Reflector Array
ara=3 nux=33 nuy=17 fill
    0 3 3 3 3 3 3 3 0
    3 3 3 3 3 3 3 3 3
    3 3 3 3 3 3 3 3 3
    3 3 3 3 3 3 3 3 3
    3 3 3 3 3 3 3 3 3
    3 3 3 3 3 3 3 3 3
    3 3 3 3 3 3 3 3 3
    3 3 3 3 3 3 3 3 3
    3 3 3 3 3 3 3 3 3
    0 3 3 3 3 3 3 3 3 3 3 3 3 3 3 3 3 0
    3 3 3 3 3 3 3 3 3 3 3 3 3 3 3
    3 3 3 3 3 3 3 3 3 3 3 3 3 3
    3 3 3 3 3 3 3 3 3 3 3 3
    3 3 3 3 3 3 3 3 3 3 3
    3 3 3 3 3 3 3 3 3 3
    3 3 3 3 3 3 3 3 3
    3 3 3 3 3 3 3 3 3
    0 3 3 3 3 3 3 3 0
end fill
'Control Rod Map Banks 1-10 [2, Fig 11]
ara=100 nux=33 nuy=17 fill
    0 0 0 0 0 0 0 0 0
    0 0 0 0 0 0 0 0 0
    0 0 0 8 0 6 0 9 0 0
    0 0 9 0 4 2 3 5 0 8 0 0
    0 0 0 5 0 0 10 0 0 4 0 0 0
    0 0 6 3 0 7 0 0 7 0 2 6 0 0
    0 0 0 2 10 0 0 8 0 0 10 3 0 0 0

```

```

0 0 8 4 0 0 1 0 0 1 0 0 5 9 0 0
0 0 0 0 0 7 0 0 9 0 0 7 0 0 0 0 0
0 0 9 5 0 0 8 0 0 8 0 0 4 8 0 0
0 0 0 3 10 0 0 1 0 0 10 2 0 0 0
0 0 6 2 0 7 0 0 7 0 3 6 0 0
0 0 0 4 0 0 10 0 0 5 0 0 0
0 0 8 0 5 3 2 4 0 9 0 0
0 0 0 9 0 6 0 8 0 0 0
0 0 0 0 0 0 0 0 0 0
0 0 0 0 0 0 0 0 0 0

```

end fill

end arrays

E.4: Origami Input Files

E.4.1: FA13AU Assembly #139 from VVER-1000 Test Model

=origami

%FA13 with PREL from VVER1000 TEST. VVER1000 PREL extracted at intervals between 0 and 12000 MWD/MTHM (285 EFPD), PREL weighted by core averaged BU

title="VVERTEST_139wt"

prefix=whole

asmid=1

%Parameter Options

options{ mtu=.4914 %mtu: mass of UO2 in pin is 1.575 kg, 312 pins in FA13AU, dont worry about O because uo2 special defined in origami

ft71=all

pitch=23.48

nburn=10 %10 is default

% offsetz=9 for use only with CR insertion

relnorm=yes

}

%Fuel Comps

fuelcomp{

```

stdcomp(fuel1){

base=uo2

iso [92234=0.0054 92235=1.3 92236=0.0 92238=98.6946]

dens=10.55}

%mixtures

mix(1) {comps [fuel1=100.0]}

}

%Array of libs

libs=[ FA13AUCROfull ]

%Map of comps

modz=[ 0.7167 0.7167 0.7167 0.7167 0.7167 0.7167 0.7167 0.7167 0.7167 0.7167 ]

% Z is only active fuel, power distribution from Nestle takes into account reflectors

% PREL comes from assembly #139 with weighting from assembly BU

pz=[0.56631 0.91979 1.01381 1.02920 1.02281 1.00992 0.99199 0.95543 0.84410 0.51343 ]

meshz=[0.0 35.301 70.602 105.903 141.204 176.505 211.806 247.106 282.407 317.708 353.009]

% burn history to reflect the assembly level burnup from nestle of 10560.22

% Origami Burn history is 10582.5

hist[

cycle{ power=42.5 burn=4 nlib=5 }

cycle{ power=42.5 burn=245 nlib=5 }

]

end

```

E.4.2: FA13AU Control Rod Insertion Depth Node 4

```

origami

%CRXY testing

%CRO CRO CRO CRO CRO CRO CRO CRO CRI CRI CRI

title="VVERTEST_139CR4XY"

prefix=CRXY

asmid=1

%Parameter Options

```

```

options{ mtu=.4914

%mtu: mass of UO2 in pin is 1.575 kg, 312 pins in FA13AU, dont worry about O because uo2 special defined in origami

ft71=all

% pitch=23.48

nburn=10 %10 is default

relnorm=yes

}

%Fuel Comps

fuelcomp{

stdcomp(fuel1){

base=uo2

iso [92234=0.0054 92235=1.3 92236=0.0 92238=98.6946]

dens=10.55}

%mixtures

mix(1) {comps [fuel1=100.0]}

}

%Array of libs

libs=[ FA13AUCROfull FA13AUCRIfull ]

libmap=[ 1 1 1 1 1 1 1 2 2 2

0 0 0 0 0 0 0 0 0 0

0 0 0 0 0 0 0 0 0 0

0 0 0 0 0 0 0 0 0 0

0 0 0 0 0 0 0 0 0 0

0 0 0 0 0 0 0 0 0 0

0 0 0 0 0 0 0 0 0 0

0 0 0 0 0 0 0 0 0 0

0 0 0 0 0 0 0 0 0 0

0 0 0 0 0 0 0 0 0 0]

%pinpowermap

pxy=[ 0.5668 0.9211 1.0158 1.0315 1.0251 1.0112 0.9904 0.9140 0.5527 0.3275

```

```
0000000000
    0000000000
    0000000000
    0000000000
    0000000000
    0000000000
    0000000000
    0000000000
    0000000000]
```

```
%Map of comps
```

```
% modz=[0.7167]
```

```
% burn history to reflect the assembly level burnup from nestle of 9878.87
```

```
hist[
```

```
  cycle{ power=42.5 burn=4 nlib=5 }
```

```
  cycle{ power=42.5 burn=228 nlib=5 }
```

```
]
```

```
end
```

Appendix F Linux and Python Scripts

F.1: Introduction

The following Appendix contains the Linux and python scripts used to scrape the NESTLE output file for flux, burnup, and relative power. These scripts then calculated the flux ratios and burnup weighted relative power and output values into a useable file format for user post processing.

F.2: NESTLE VVER-1000 Benchmark Flux Extraction and Calculation

F.2.1: Linux

```
#!/bin/bash

#####NESTLE OUTPUT FILE PROCESSING#####

#pull 2D flux map for last burn up step from output file.

#define burnup

b=12961.12

#define number of nodes

n=1

while [ $n -le 9 ]

do

#makes one file for every node map, input the burnup value

#GROUP 1 FLUX

    grep -A36 "FLUX , Node Map, for Energy Group 1 at Axial Node $n" VVER1000OP_6.2.1rodfix63.out | grep -A36
"Average Burnup = $b (MWD/MTHM)" > fluxloops$n.out

    echo "Average Burnup = $b (MWD/MTHM)" > G1flux$n.txt

    echo "Group 1, Node $n" >> G1flux$n.txt

#pull only the scientific numbers (flux values)

grep --color=auto -oE '[- +]?[0-9]+\.[0-9]*(?:[Ee]-?[0-9]+)' fluxloops$n.out >> G1flux$n.txt

    n=$((n+1))

done

i=10

while [ $i -le 12 ]
```

```

do

#makes one file for every node map, input the burnup value

#GROUP 1 FLUX

    grep -A36 "FLUX , Node Map, for Energy Group 1 at Axial Node $i" VVER1000OP_6.2.1rodfix63.out | grep -A36
"Average Burnup = $b (MWD/MTHM)" > fluxloops$i.out

    echo "Average Burnup = $b (MWD/MTHM)" > G1flux$i.txt

    echo "Group 1, Node $i" >> G1flux$i.txt

#pull only the scientific numbers (flux values)

grep --color=auto -oE '[- +]?[0-9]+\.[0-9]*(?:[Ee]-?[0-9]+)' fluxloops$i.out >> G1flux$i.txt

i=$((i+1))

done

#GROUP 2 FLUX

###PUT GROUP 2 GREPS HERE

j=1

while [ $j -le 9 ]

do

#makes one file for every node map, input the burnup value

#GROUP 2 FLUX

    grep -A36 "FLUX , Node Map, for Energy Group 2 at Axial Node $j" VVER1000OP_6.2.1rodfix63.out | grep -A36
"Average Burnup = $b (MWD/MTHM)" > 2fluxloops$j.out

    echo "Average Burnup = $b (MWD/MTHM)" > G2flux$j.txt

    echo "Group 2, Node $j" >> G2flux$j.txt

#pull only the scientific numbers (flux values)

grep --color=auto -oE '[- +]?[0-9]+\.[0-9]*(?:[Ee]-?[0-9]+)' 2fluxloops$j.out >> G2flux$j.txt

j=$((j+1))

done

k=10

while [ $k -le 12 ]

do

#makes one file for every node map, input the burnup value

#GROUP 2 FLUX

```

```

    grep -A36 "FLUX , Node Map, for Energy Group 2 at Axial Node $k" VVER1000OP_6.2.1rodfix63.out | grep -A36
"Average Burnup = $b (MWD/MTHM)" > 2fluxloops$k.out

    echo "Average Burnup = $b (MWD/MTHM)" > G2flux$k.txt

    echo "Group 2, Node $k" >> G2flux$k.txt

    #pull only the scientific numbers (flux values)

    grep --color=auto -oE '[- +]?[0-9]+\.[0-9]*(?:[Ee]-?[0-9]+)' 2fluxloops$k.out >> G2flux$k.txt

    k=$((k+1))

done

#Call the python script for generation of flux ratio

#!/bin/sh

python fluxcalcs.py

#clean up the file mess

#!/bin/bash

x=1

while [ $x -le 12 ]

do

#clean up files into plotting folder

    mv fluxloops$x.out ./greps

    mv 2fluxloops$x.out greps

    mv G1flux$x.txt greps

    mv G2flux$x.txt greps

    mv Ratio$x.txt plotting/Ratios

    mv FA13AU$x.txt plotting/FA13AU

    x=$((x+1))

done

mv NodesMaxFluxRatio.txt plotting/Ratios

mv GlobalMaxFluxRatio.txt plotting/Ratios

mv FA13AUNodesMaxFluxRatio.txt plotting/FA13AU

mv FA13AUGlobalMaxFluxRatio.txt plotting/FA13AU

```

F.2.2: Python

```
#Data processing for Nestle Flux Ratio

#Import necessary methods

import matplotlib

import matplotlib.pyplot as plt

import numpy as np

import math

import scipy as sp

#####Pull Data from Nestle files#####

#import data flux 1 for all nodes

G1flux1=np.genfromtxt('G1flux1.txt', skiprows=2, usecols=(0,), unpack=True)

G1flux2=np.genfromtxt('G1flux2.txt', skiprows=2, usecols=(0,), unpack=True)

G1flux3=np.genfromtxt('G1flux3.txt', skiprows=2, usecols=(0,), unpack=True)

G1flux4=np.genfromtxt('G1flux4.txt', skiprows=2, usecols=(0,), unpack=True)

G1flux5=np.genfromtxt('G1flux5.txt', skiprows=2, usecols=(0,), unpack=True)

G1flux6=np.genfromtxt('G1flux6.txt', skiprows=2, usecols=(0,), unpack=True)

G1flux7=np.genfromtxt('G1flux7.txt', skiprows=2, usecols=(0,), unpack=True)

G1flux8=np.genfromtxt('G1flux8.txt', skiprows=2, usecols=(0,), unpack=True)

G1flux9=np.genfromtxt('G1flux9.txt', skiprows=2, usecols=(0,), unpack=True)

G1flux10=np.genfromtxt('G1flux10.txt', skiprows=2, usecols=(0,), unpack=True)

G1flux11=np.genfromtxt('G1flux11.txt', skiprows=2, usecols=(0,), unpack=True)

G1flux12=np.genfromtxt('G1flux12.txt', skiprows=2, usecols=(0,), unpack=True)

#import data flux 2 for all nodes

G2flux1=np.genfromtxt('G2flux1.txt', skiprows=2, usecols=(0,), unpack=True)

G2flux2=np.genfromtxt('G2flux2.txt', skiprows=2, usecols=(0,), unpack=True)

G2flux3=np.genfromtxt('G2flux3.txt', skiprows=2, usecols=(0,), unpack=True)

G2flux4=np.genfromtxt('G2flux4.txt', skiprows=2, usecols=(0,), unpack=True)

G2flux5=np.genfromtxt('G2flux5.txt', skiprows=2, usecols=(0,), unpack=True)
```

```

G2flux6=np.genfromtxt('G2flux6.txt', skiprows=2, usecols=(0,), unpack=True)
G2flux7=np.genfromtxt('G2flux7.txt', skiprows=2, usecols=(0,), unpack=True)
G2flux8=np.genfromtxt('G2flux8.txt', skiprows=2, usecols=(0,), unpack=True)
G2flux9=np.genfromtxt('G2flux9.txt', skiprows=2, usecols=(0,), unpack=True)
G2flux10=np.genfromtxt('G2flux10.txt', skiprows=2, usecols=(0,), unpack=True)
G2flux11=np.genfromtxt('G2flux11.txt', skiprows=2, usecols=(0,), unpack=True)
G2flux12=np.genfromtxt('G2flux12.txt', skiprows=2, usecols=(0,), unpack=True)

#####Calculate and Save Flux Ratios#####

#calculate flux ratios for each node

FluxRatio1=G1flux1/G2flux1
FluxRatio2=G1flux2/G2flux2
FluxRatio3=G1flux3/G2flux3
FluxRatio4=G1flux4/G2flux4
FluxRatio5=G1flux5/G2flux5
FluxRatio6=G1flux6/G2flux6
FluxRatio7=G1flux7/G2flux7
FluxRatio8=G1flux8/G2flux8
FluxRatio9=G1flux9/G2flux9
FluxRatio10=G1flux10/G2flux10
FluxRatio11=G1flux11/G2flux11
FluxRatio12=G1flux12/G2flux12

#save flux ratios to output files

np.savetxt('Ratio1.txt',FluxRatio1)
np.savetxt('Ratio2.txt',FluxRatio2)
np.savetxt('Ratio3.txt',FluxRatio3)
np.savetxt('Ratio4.txt',FluxRatio4)
np.savetxt('Ratio5.txt',FluxRatio5)
np.savetxt('Ratio6.txt',FluxRatio6)
np.savetxt('Ratio7.txt',FluxRatio7)

```

```

np.savetxt('Ratio8.txt',FluxRatio8)

np.savetxt('Ratio9.txt',FluxRatio9)

np.savetxt('Ratio10.txt',FluxRatio10)

np.savetxt('Ratio11.txt',FluxRatio11)

np.savetxt('Ratio12.txt',FluxRatio12)

#####Find Max Flux Ratios and Save#####

#find max flux ratio for each node

MaxRatio=np.arange(12,dtype=np.float)

MaxRatio[0]=max(FluxRatio1)

MaxRatio[1]=max(FluxRatio2)

MaxRatio[2]=max(FluxRatio3)

MaxRatio[3]=max(FluxRatio4)

MaxRatio[4]=max(FluxRatio5)

MaxRatio[5]=max(FluxRatio6)

MaxRatio[6]=max(FluxRatio7)

MaxRatio[7]=max(FluxRatio8)

MaxRatio[8]=max(FluxRatio9)

MaxRatio[9]=max(FluxRatio10)

MaxRatio[10]=max(FluxRatio11)

MaxRatio[11]=max(FluxRatio12)

Max=np.arange(1,dtype=np.float)

Max[0]=max(MaxRatio)

#export max flux ratio for each node to file

np.savetxt("NodesMaxFluxRatio.txt",MaxRatio)

np.savetxt("GlobalMaxFluxRatio.txt",Max)

#####Pull FA13 AU Flux Ratios#####

#pull the core map for 13 AU

```

```

Map13AU=np.genfromtxt('13AUmap.csv', delimiter=',', usecols=(4), unpack=True)

np.savetxt("FA13AUmap",Map13AU)

#####Make FA13AU files for each node, fill with ratio, save#####

#node1

FA13AU1=np.arange(len(Map13AU),dtype=np.float)

for i in range (0,48):

    index=i

    FA13AU1[index]=FluxRatio1[Map13AU[index]-1]

    np.savetxt("FA13AU1.txt",FA13AU1)

#node2

FA13AU2=np.arange(len(Map13AU),dtype=np.float)

for i in range (0,48):

    index=i

    FA13AU2[index]=FluxRatio2[Map13AU[index]-1]

    np.savetxt("FA13AU2.txt",FA13AU2)

#node3

FA13AU3=np.arange(len(Map13AU),dtype=np.float)

for i in range (0,48):

    index=i

    FA13AU3[index]=FluxRatio3[Map13AU[index]-1]

    np.savetxt("FA13AU3.txt",FA13AU3)

#node4

FA13AU4=np.arange(len(Map13AU),dtype=np.float)

for i in range (0,48):

    index=i

    FA13AU4[index]=FluxRatio4[Map13AU[index]-1]

    np.savetxt("FA13AU4.txt",FA13AU4)

#node5

FA13AU5=np.arange(len(Map13AU),dtype=np.float)

for i in range (0,48):

    index=i

```

```

FA13AU5[index]=FluxRatio5[Map13AU[index]-1]

np.savetxt("FA13AU5.txt",FA13AU5)

#node6

FA13AU6=np.arange(len(Map13AU),dtype=np.float)

for i in range (0,48):

    index=i

    FA13AU6[index]=FluxRatio6[Map13AU[index]-1]

    np.savetxt("FA13AU6.txt",FA13AU6)

#node7

FA13AU7=np.arange(len(Map13AU),dtype=np.float)

for i in range (0,48):

    index=i

    FA13AU7[index]=FluxRatio7[Map13AU[index]-1]

    np.savetxt("FA13AU7.txt",FA13AU7)

#node8

FA13AU8=np.arange(len(Map13AU),dtype=np.float)

for i in range (0,48):

    index=i

    FA13AU8[index]=FluxRatio8[Map13AU[index]-1]

    np.savetxt("FA13AU8.txt",FA13AU8)

#node9

FA13AU9=np.arange(len(Map13AU),dtype=np.float)

for i in range (0,48):

    index=i

    FA13AU9[index]=FluxRatio9[Map13AU[index]-1]

    np.savetxt("FA13AU9.txt",FA13AU9)

#node10

FA13AU10=np.arange(len(Map13AU),dtype=np.float)

for i in range (0,48):

    index=i

    FA13AU10[index]=FluxRatio10[Map13AU[index]-1]

```

```

    np.savetxt("FA13AU10.txt",FA13AU10)

#node11

FA13AU11=np.arange(len(Map13AU),dtype=np.float)

for i in range (0,48):

    index=i

    FA13AU11[index]=FluxRatio11[Map13AU[index]-1]

    np.savetxt("FA13AU11.txt",FA13AU11)

#node12

FA13AU12=np.arange(len(Map13AU),dtype=np.float)

for i in range (0,48):

    index=i

    FA13AU12[index]=FluxRatio12[Map13AU[index]-1]

    np.savetxt("FA13AU12.txt",FA13AU12)

#####Find Max FA13AU Ratio for Each Node#####

FA13AUMaxRatio=np.arange(12,dtype=np.float)

FA13AUMaxRatio[0]=max(FA13AU1)

FA13AUMaxRatio[1]=max(FA13AU2)

FA13AUMaxRatio[2]=max(FA13AU3)

FA13AUMaxRatio[3]=max(FA13AU4)

FA13AUMaxRatio[4]=max(FA13AU5)

FA13AUMaxRatio[5]=max(FA13AU6)

FA13AUMaxRatio[6]=max(FA13AU7)

FA13AUMaxRatio[7]=max(FA13AU8)

FA13AUMaxRatio[8]=max(FA13AU9)

FA13AUMaxRatio[9]=max(FA13AU10)

FA13AUMaxRatio[10]=max(FA13AU11)

FA13AUMaxRatio[11]=max(FA13AU12)

FA13AUMax=np.arange(1,dtype=np.float)

FA13AUMax[0]=max(FA13AUMaxRatio)

#export max flux ratio for each node to file

np.savetxt("FA13AUNodesMaxFluxRatio.txt",FA13AUMaxRatio)

```

```
np.savetxt("FA13AUGlobalMaxFluxRatio.txt",FA13AUMax)
```

F.3: NESTLE VVER-1000 Benchmark PREL Linux

```
#!/bin/bash
```

```
##### Grep all the PREL Data: For each BU Step, Each Node#####
```

```
Burn=12961.12          #initial BU step (zero)
```

```
BU=LAST
```

```
numnodes=12          #number of nodes (include reflector)
```

```
n=1
```

```
while [ $n -le $numnodes ]
```

```
do
```

```
    if [ $n -le 9 ]; then      #numnodes has to be less than 10 for grep spacing between "Node  
$n"
```

```
        grep -A36 "PREL , Node Map, at Axial Node $n,"  
VVER1000OP_6.2.1rodfix63.out | grep -A36 "Average Burnup = $Burn (MWD/MTHM)" > preloops$BU$n.out
```

```
    else
```

```
        grep -A36 "PREL , Node Map, at Axial Node $n,"  
VVER1000OP_6.2.1rodfix63.out | grep -A36 "Average Burnup = $Burn (MWD/MTHM)" > preloops$BU$n.out
```

```
    fi
```

```
    echo "Average Burnup = $Burn (MWD/MTHM)" > PREL$BU$n.txt
```

```
    echo "Node $n" >> PREL$BU$n.txt
```

```
    #pull only the scientific numbers (flux values)
```

```
    grep --color=auto -oE "[- +]?[0-9]+\.[0-9]*" preloops$BU$n.out >> PREL$BU$n.txt
```

```
    n=$((n+1))
```

```
done
```

```
#####Ask User for Line to Pull#####
```

```
read -p "Enter Line to Pull: " line
```

```
echo $line
```

```
line=$((line+4))  
the files are grepped above
```

```
#have to add 4 lines due to how
```

```

#####Pull Line for Each BU Step, Each Node

step=1000      #BU step size

BU=LAST

numnodes=12    #number of nodes (include reflector)

n=1

        while [ $n -le $numnodes ]

        do

                head -n$line PREL$BU$n.txt | tail -1 >> power$BU.txt

                n=$((n+1))

        done

#clean up the mess

burn=LAST

mv power$burn.txt ./plot

n=1

        while [ $n -le $numnodes ]

        do

                mv PREL$burn$n.txt ./greps

                mv preloops$burn$n.out ./greps

                n=$((n+1))

        done

```

F.4: NESTLE VVER-1000 Test Flux Extraction and Calculation

F.4.1: Linux

```
#!/bin/bash
```

```
#####NESTLE OUTPUT FILE PROCESSING#####
```

```

#pull 2D flux map for last burn up step from output file.

#define burnup

b=12000.00

#define number of nodes

n=1

while [ $n -le 9 ]

do

#makes one file for every node map, input the burnup value

#GROUP 1 FLUX

    grep -A36 "FLUX , Node Map, for Energy Group 1 at Axial Node $n" VVER1000_test621.out | grep -A36 "Average
Burnup = $b (MWD/MTHM)" > fluxloops$n.out

    echo "Average Burnup = $b (MWD/MTHM)" > G1flux$n.txt

    echo "Group 1, Node $n" >> G1flux$n.txt

    #pull only the scientific numbers (flux values)

    grep --color=auto -oE '[- +]?[0-9]+\.[0-9]*(?:[Ee]-?[0-9]+)' fluxloops$n.out >> G1flux$n.txt

    n=$((n+1))

done

i=10

while [ $i -le 12 ]

do

#makes one file for every node map, input the burnup value

#GROUP 1 FLUX

    grep -A36 "FLUX , Node Map, for Energy Group 1 at Axial Node $i" VVER1000_test621.out | grep -A36 "Average
Burnup = $b (MWD/MTHM)" > fluxloops$i.out

    echo "Average Burnup = $b (MWD/MTHM)" > G1flux$i.txt

    echo "Group 1, Node $i" >> G1flux$i.txt

    #pull only the scientific numbers (flux values)

    grep --color=auto -oE '[- +]?[0-9]+\.[0-9]*(?:[Ee]-?[0-9]+)' fluxloops$i.out >> G1flux$i.txt

    i=$((i+1))

done

#GROUP 2 FLUX

###PUT GROUP 2 GREPS HERE

```

```

j=1

while [ $j -le 9 ]

do

#makes one file for every node map, input the burnup value

#GROUP 2 FLUX

    grep -A36 "FLUX , Node Map, for Energy Group 2 at Axial Node $j" VVER1000_test621.out | grep -A36 "Average
Burnup = $b (MWD/MTHM)" > 2fluxloops$j.out

    echo "Average Burnup = $b (MWD/MTHM)" > G2flux$j.txt

    echo "Group 2, Node $j" >> G2flux$j.txt

    #pull only the scientific numbers (flux values)

    grep --color=auto -oE '[- +]?[0-9]+\.[0-9]*(?:[Ee]-?[0-9]+)' 2fluxloops$j.out >> G2flux$j.txt

    j=$((j+1))

done

k=10

while [ $k -le 12 ]

do

#makes one file for every node map, input the burnup value

#GROUP 2 FLUX

    grep -A36 "FLUX , Node Map, for Energy Group 2 at Axial Node $k" VVER1000_test621.out | grep -A36 "Average
Burnup = $b (MWD/MTHM)" > 2fluxloops$k.out

    echo "Average Burnup = $b (MWD/MTHM)" > G2flux$k.txt

    echo "Group 2, Node $k" >> G2flux$k.txt

    #pull only the scientific numbers (flux values)

    grep --color=auto -oE '[- +]?[0-9]+\.[0-9]*(?:[Ee]-?[0-9]+)' 2fluxloops$k.out >> G2flux$k.txt

    k=$((k+1))

done

#Call the python script for generation of flux ratio

#!/bin/sh

python fluxcalcs.py

#clean up the file mess

```

```

#!/bin/bash

x=1

while [ $x -le 12 ]

do

#clean up files into plotting folder

    mv fluxloops$x.out ./greps

    mv 2fluxloops$x.out greps

    mv G1flux$x.txt greps

    mv G2flux$x.txt greps

    mv Ratio$x.txt plotting/Ratios

    mv FA13AU$x.txt plotting/FA13AU

    x=$((x+1))

done

mv NodesMaxFluxRatio.txt plotting/Ratios

mv GlobalMaxFluxRatio.txt plotting/Ratios

mv FA13AUNodesMaxFluxRatio.txt plotting/FA13AU

mv FA13AUGlobalMaxFluxRatio.txt plotting/FA13AU

```

F.4.2: Python

```

#Data processing for Nestle Flux Ratio

#Import necessary methods

import matplotlib

import matplotlib.pyplot as plt

import numpy as np

import math

import scipy as sp

#####Pull Data from Nestle files#####

#import data flux 1 for all nodes

G1flux1=np.genfromtxt('G1flux1.txt', skiprows=2, usecols=(0,), unpack=True)

G1flux2=np.genfromtxt('G1flux2.txt', skiprows=2, usecols=(0,), unpack=True)

G1flux3=np.genfromtxt('G1flux3.txt', skiprows=2, usecols=(0,), unpack=True)

```

```

G1flux4=np.genfromtxt('G1flux4.txt', skiprows=2, usecols=(0,), unpack=True)
G1flux5=np.genfromtxt('G1flux5.txt', skiprows=2, usecols=(0,), unpack=True)
G1flux6=np.genfromtxt('G1flux6.txt', skiprows=2, usecols=(0,), unpack=True)
G1flux7=np.genfromtxt('G1flux7.txt', skiprows=2, usecols=(0,), unpack=True)
G1flux8=np.genfromtxt('G1flux8.txt', skiprows=2, usecols=(0,), unpack=True)
G1flux9=np.genfromtxt('G1flux9.txt', skiprows=2, usecols=(0,), unpack=True)
G1flux10=np.genfromtxt('G1flux10.txt', skiprows=2, usecols=(0,), unpack=True)
G1flux11=np.genfromtxt('G1flux11.txt', skiprows=2, usecols=(0,), unpack=True)
G1flux12=np.genfromtxt('G1flux12.txt', skiprows=2, usecols=(0,), unpack=True)

#import data flux 2 for all nodes

G2flux1=np.genfromtxt('G2flux1.txt', skiprows=2, usecols=(0,), unpack=True)
G2flux2=np.genfromtxt('G2flux2.txt', skiprows=2, usecols=(0,), unpack=True)
G2flux3=np.genfromtxt('G2flux3.txt', skiprows=2, usecols=(0,), unpack=True)
G2flux4=np.genfromtxt('G2flux4.txt', skiprows=2, usecols=(0,), unpack=True)
G2flux5=np.genfromtxt('G2flux5.txt', skiprows=2, usecols=(0,), unpack=True)
G2flux6=np.genfromtxt('G2flux6.txt', skiprows=2, usecols=(0,), unpack=True)
G2flux7=np.genfromtxt('G2flux7.txt', skiprows=2, usecols=(0,), unpack=True)
G2flux8=np.genfromtxt('G2flux8.txt', skiprows=2, usecols=(0,), unpack=True)
G2flux9=np.genfromtxt('G2flux9.txt', skiprows=2, usecols=(0,), unpack=True)
G2flux10=np.genfromtxt('G2flux10.txt', skiprows=2, usecols=(0,), unpack=True)
G2flux11=np.genfromtxt('G2flux11.txt', skiprows=2, usecols=(0,), unpack=True)
G2flux12=np.genfromtxt('G2flux12.txt', skiprows=2, usecols=(0,), unpack=True)

#####Calculate and Save Flux Ratios#####

#calculate flux ratios for each node

FluxRatio1=G1flux1/G2flux1
FluxRatio2=G1flux2/G2flux2
FluxRatio3=G1flux3/G2flux3
FluxRatio4=G1flux4/G2flux4
FluxRatio5=G1flux5/G2flux5

```

FluxRatio6=G1flux6/G2flux6

FluxRatio7=G1flux7/G2flux7

FluxRatio8=G1flux8/G2flux8

FluxRatio9=G1flux9/G2flux9

FluxRatio10=G1flux10/G2flux10

FluxRatio11=G1flux11/G2flux11

FluxRatio12=G1flux12/G2flux12

#save flux ratios to output files

np.savetxt('Ratio1.txt',FluxRatio1)

np.savetxt('Ratio2.txt',FluxRatio2)

np.savetxt('Ratio3.txt',FluxRatio3)

np.savetxt('Ratio4.txt',FluxRatio4)

np.savetxt('Ratio5.txt',FluxRatio5)

np.savetxt('Ratio6.txt',FluxRatio6)

np.savetxt('Ratio7.txt',FluxRatio7)

np.savetxt('Ratio8.txt',FluxRatio8)

np.savetxt('Ratio9.txt',FluxRatio9)

np.savetxt('Ratio10.txt',FluxRatio10)

np.savetxt('Ratio11.txt',FluxRatio11)

np.savetxt('Ratio12.txt',FluxRatio12)

#####Find Max Flux Ratios and Save#####

#find max flux ratio for each node

MaxRatio=np.arange(12,dtype=np.float)

MaxRatio[0]=max(FluxRatio1)

MaxRatio[1]=max(FluxRatio2)

MaxRatio[2]=max(FluxRatio3)

MaxRatio[3]=max(FluxRatio4)

MaxRatio[4]=max(FluxRatio5)

MaxRatio[5]=max(FluxRatio6)

```

MaxRatio[6]=max(FluxRatio7)

MaxRatio[7]=max(FluxRatio8)

MaxRatio[8]=max(FluxRatio9)

MaxRatio[9]=max(FluxRatio10)

MaxRatio[10]=max(FluxRatio11)

MaxRatio[11]=max(FluxRatio12)

Max=np.arange(1,dtype=np.float)

Max[0]=max(MaxRatio)

#export max flux ratio for each node to file

np.savetxt("NodesMaxFluxRatio.txt",MaxRatio)

np.savetxt("GlobalMaxFluxRatio.txt",Max)

#####Pull FA13 AU Flux Ratios#####

#pull the core map for 13 AU

Map13AU=np.genfromtxt('13AUmap.csv', delimiter=',', usecols=(4), unpack=True)

np.savetxt("FA13AUmap",Map13AU)

####Make FA13AU files for each node, fill with ratio, save#####

#node1

FA13AU1=np.arange(len(Map13AU),dtype=np.float)

for i in range (0,48):

    index=i

    FA13AU1[index]=FluxRatio1[Map13AU[index]-1]

    np.savetxt("FA13AU1.txt",FA13AU1)

#node2

FA13AU2=np.arange(len(Map13AU),dtype=np.float)

for i in range (0,48):

    index=i

    FA13AU2[index]=FluxRatio2[Map13AU[index]-1]

    np.savetxt("FA13AU2.txt",FA13AU2)

```

```

#node3

FA13AU3=np.arange(len(Map13AU),dtype=np.float)

for i in range (0,48):

    index=i

    FA13AU3[index]=FluxRatio3[Map13AU[index]-1]

    np.savetxt("FA13AU3.txt",FA13AU3)

#node4

FA13AU4=np.arange(len(Map13AU),dtype=np.float)

for i in range (0,48):

    index=i

    FA13AU4[index]=FluxRatio4[Map13AU[index]-1]

    np.savetxt("FA13AU4.txt",FA13AU4)

#node5

FA13AU5=np.arange(len(Map13AU),dtype=np.float)

for i in range (0,48):

    index=i

    FA13AU5[index]=FluxRatio5[Map13AU[index]-1]

    np.savetxt("FA13AU5.txt",FA13AU5)

#node6

FA13AU6=np.arange(len(Map13AU),dtype=np.float)

for i in range (0,48):

    index=i

    FA13AU6[index]=FluxRatio6[Map13AU[index]-1]

    np.savetxt("FA13AU6.txt",FA13AU6)

#node7

FA13AU7=np.arange(len(Map13AU),dtype=np.float)

for i in range (0,48):

    index=i

    FA13AU7[index]=FluxRatio7[Map13AU[index]-1]

    np.savetxt("FA13AU7.txt",FA13AU7)

#node8

```

```

FA13AU8=np.arange(len(Map13AU),dtype=np.float)

for i in range (0,48):

    index=i

    FA13AU8[index]=FluxRatio8[Map13AU[index]-1]

    np.savetxt("FA13AU8.txt",FA13AU8)

#node9

FA13AU9=np.arange(len(Map13AU),dtype=np.float)

for i in range (0,48):

    index=i

    FA13AU9[index]=FluxRatio9[Map13AU[index]-1]

    np.savetxt("FA13AU9.txt",FA13AU9)

#node10

FA13AU10=np.arange(len(Map13AU),dtype=np.float)

for i in range (0,48):

    index=i

    FA13AU10[index]=FluxRatio10[Map13AU[index]-1]

    np.savetxt("FA13AU10.txt",FA13AU10)

#node11

FA13AU11=np.arange(len(Map13AU),dtype=np.float)

for i in range (0,48):

    index=i

    FA13AU11[index]=FluxRatio11[Map13AU[index]-1]

    np.savetxt("FA13AU11.txt",FA13AU11)

#node12

FA13AU12=np.arange(len(Map13AU),dtype=np.float)

for i in range (0,48):

    index=i

    FA13AU12[index]=FluxRatio12[Map13AU[index]-1]

    np.savetxt("FA13AU12.txt",FA13AU12)

#####Find Max FA13AU Ratio for Each Node#####

FA13AUMaxRatio=np.arange(12,dtype=np.float)

```

```

FA13AUMaxRatio[0]=max(FA13AU1)
FA13AUMaxRatio[1]=max(FA13AU2)
FA13AUMaxRatio[2]=max(FA13AU3)
FA13AUMaxRatio[3]=max(FA13AU4)
FA13AUMaxRatio[4]=max(FA13AU5)
FA13AUMaxRatio[5]=max(FA13AU6)
FA13AUMaxRatio[6]=max(FA13AU7)
FA13AUMaxRatio[7]=max(FA13AU8)
FA13AUMaxRatio[8]=max(FA13AU9)
FA13AUMaxRatio[9]=max(FA13AU10)
FA13AUMaxRatio[10]=max(FA13AU11)
FA13AUMaxRatio[11]=max(FA13AU12)
FA13AUMax=np.arange(1,dtype=np.float)
FA13AUMax[0]=max(FA13AUMaxRatio)

#export max flux ratio for each node to file

np.savetxt("FA13AUNodesMaxFluxRatio.txt",FA13AUMaxRatio)
np.savetxt("FA13AUGlobalMaxFluxRatio.txt",FA13AUMax)

```

F.5: NESTLE VVER-1000 Test PREL No Weighting

F.5.1: Linux

```

#!/bin/bash

##### Grep all the PREL Data: For each BU Step, Each Node#####

step=1000          #BU step size

stepburn=1000.00

Burn=0.00          #initial BU step (zero)

BU=0

numnodes=12       #number of nodes (include reflector)

maxBU=12000       #max burnup

n=1

```

```

while [ $BU -le $maxBU ]
do
#BU 0
    if [ $BU -eq 0 ]; then
        # BU 0, Grep spacing for 6 spaces between "=" $Burn"
        while [ $n -le $numnodes ]
        do
            if [ $n -le 9 ]; then
                #numnodes has to be less than 10 for grep
                spacing between "Node $n"
                grep -A36 "PREL , Node Map, at Axial Node $n," VVER1000_test621.out |
                grep -A36 "Average Burnup = $Burn (MWD/MTHM)" > preloops$BU$n.out
            else
                grep -A36 "PREL , Node Map, at Axial Node $n," VVER1000_test621.out |
                grep -A36 "Average Burnup = $Burn (MWD/MTHM)" > preloops$BU$n.out
            fi
            echo "Average Burnup = $Burn (MWD/MTHM)" > PREL$BU$n.txt
            echo "Node $n" >> PREL$BU$n.txt
            #pull only the scientific numbers (flux values)
            grep --color=auto -oE '[- +]?[0-9]+\.[0-9]*' preloops$BU$n.out >> PREL$BU$n.txt
            n=$((n+1))
        done
#BU 10-999
    elif [ $BU -le 999 ]; then
        # BU 0, Grep spacing for 4 spaces between "=" $Burn"
        while [ $n -le $numnodes ]
        do
            if [ $n -le 9 ]; then
                #numnodes has to be less than 10 for grep
                spacing between "Node $n"
                grep -A36 "PREL , Node Map, at Axial Node $n," VVER1000_test621.out |
                grep -A36 "Average Burnup = $Burn (MWD/MTHM)" > preloops$BU$n.out
            else
                grep -A36 "PREL , Node Map, at Axial Node $n," VVER1000_test621.out |
                grep -A36 "Average Burnup = $Burn (MWD/MTHM)" > preloops$BU$n.out
            fi
            echo "Average Burnup = $Burn (MWD/MTHM)" > PREL$BU$n.txt
            echo "Node $n" >> PREL$BU$n.txt
        done
    fi
done

```

```

#pull only the scientific numbers (flux values)

grep --color=auto -oE '[- +]?[0-9]+\.[0-9]*' preloops$BU$n.out >> PREL$BU$n.txt

n=$((n+1))

done

#BU 1000-9999

$Burn"      elif [ $BU -le 9999 ]; then      # BU 0, Grep spacing for 3 spaces between "="

while [ $n -le $Numnodes ]

do

$n"          if [ $n -le 9 ]; then      #numnodes has to be less than 10 for grep spacing between "Node

grep -A36 "Average Burnup = $Burn (MWD/MTHM)" > preloops$BU$n.out |      grep -A36 "PREL , Node Map, at Axial Node $n," VVER1000_test621.out |

else

grep -A36 "Average Burnup = $Burn (MWD/MTHM)" > preloops$BU$n.out |      grep -A36 "PREL , Node Map, at Axial Node $n," VVER1000_test621.out |

fi

echo "Average Burnup = $Burn (MWD/MTHM)" > PREL$BU$n.txt

echo "Node $n" >> PREL$BU$n.txt

#pull only the scientific numbers (flux values)

grep --color=auto -oE '[- +]?[0-9]+\.[0-9]*' preloops$BU$n.out >> PREL$BU$n.txt

n=$((n+1))

done

#BU for 10000-99999

else [ $BU -le 99999 ]      # BU 0, Grep spacing for 2 spaces between "=" $Burn"

while [ $n -le $Numnodes ]

do

$n"          if [ $n -le 9 ]; then      #numnodes has to be less than 10 for grep spacing between "Node

grep -A36 "Average Burnup = $Burn (MWD/MTHM)" > preloops$BU$n.out |      grep -A36 "PREL , Node Map, at Axial Node $n," VVER1000_test621.out |

else

grep -A36 "Average Burnup = $Burn (MWD/MTHM)" > preloops$BU$n.out |      grep -A36 "PREL , Node Map, at Axial Node $n," VVER1000_test621.out |

fi

```

```

echo "Average Burnup = $Burn (MWD/MTHM)" > PREL$BU$n.txt

echo "Node $n" >> PREL$BU$n.txt

#pull only the scientific numbers (flux values)

grep --color=auto -oE '[- +]?[0-9]+\.[0-9]*' preloops$BU$.out >> PREL$BU$n.txt

n=$((n+1))

done

fi

newburn=$(echo "$Burn + $stepburn" | bc) #have to use this strange step to add floats, need the float for GREP

Burn=$newburn #modify $Burn
variable for grep

BU=$((BU+step)) #BU must be an
integer for loops

n=1
#reset n to 1 for each pass through the BU loop

done

#####Ask User for Line to Pull#####

read -p "Enter Line to Pull: " line

echo $line

line=$((line+4)) #have to add 4 lines due to how
the files are grepped above

#####Pull Line for Each BU Step, Each Node

step=1000 #BU step size

BU=0

numnodes=12 #number of nodes (include reflector)

n=1

while [ $BU -le $maxBU ]

do

while [ $n -le $numnodes ]

```

```

do
    head -n$line PREL$BU$n.txt | tail -1 >> power$BU.txt
    n=$((n+1))
done
BU=$((BU+step)) #BU must be an
integer for loops
n=1
done
#clean up the mess
burn=0
while [ $burn -le $maxBU ]
do
    mv power$burn.txt ./plot
    burn=$((burn+step))
done
burn=0
n=1
while [ $burn -le $maxBU ]
do
    while [ $n -le $numnodes ]
    do
        mv PREL$burn$n.txt ./greps
        mv preloops$burn$n.out ./greps
        n=$((n+1))
    done
    burn=$((burn+step))
    n=1
done

```

F.6: NESTLE VVER-1000 Test PREL Weighting Linux

```
#!/bin/bash
```

```

##### Grep all the PREL Data: For each BU Step, Each Node
#####

step=1000          #BU step size

stepburn=1000.00

Burn=0.00          #initial BU step (zero)

BU=0

numnodes=12       #number of nodes (include reflector)

maxBU=12000       #max burnup

n=1

while [ $BU -le $maxBU ]

do

#BU 0

    if [ $BU -eq 0 ]; then                # BU 0, Grep spacing for 6 spaces between "=" $Burn"

        while [ $n -le $numnodes ]

        do

            if [ $n -le 9 ]; then          #numnodes has to be less than 10 for grep

spacing between "Node $n"

                grep -A36 "PREL , Node Map, at Axial Node $n,"
VVER1000_test621_BU.out | grep -A36 "Average Burnup = $Burn (MWD/MTHM)" > preloops$BU$n.out

            else

                grep -A36 "PREL , Node Map, at Axial Node $n,"
VVER1000_test621_BU.out | grep -A36 "Average Burnup = $Burn (MWD/MTHM)" > preloops$BU$n.out

            fi

            echo "Average Burnup = $Burn (MWD/MTHM)" > PREL$BU$n.txt

            echo "Node $n" >> PREL$BU$n.txt

            #pull only the scientific numbers (flux values)

            grep --color=auto -oE '[- +]?[0-9]+\.[0-9]*' preloops$BU$n.out >> PREL$BU$n.txt

            n=$((n+1))

        done

#BU 10-999

    elif [ $BU -le 999 ]; then            # BU 0, Grep spacing for 4 spaces between "=" $Burn"

        while [ $n -le $numnodes ]

```

```

do
    if [ $n -le 9 ]; then
        #numnodes has to be less than 10 for grep
        spacing between "Node $n"
        grep -A36 "PREL , Node Map, at Axial Node $n,"
        VVER1000_test621_BU.out | grep -A36 "Average Burnup = $Burn (MWD/MTHM)" > preloops$BU$n.out
    else
        grep -A36 "PREL , Node Map, at Axial Node $n,"
        VVER1000_test621_BU.out | grep -A36 "Average Burnup = $Burn (MWD/MTHM)" > preloops$BU$n.out
    fi
    echo "Average Burnup = $Burn (MWD/MTHM)" > PREL$BU$n.txt
    echo "Node $n" >> PREL$BU$n.txt
    #pull only the scientific numbers (flux values)
    grep --color=auto -oE '[- +]?[0-9]+\.[0-9]*' preloops$BU$n.out >> PREL$BU$n.txt
    n=$((n+1))
done
#BU 1000-9999
    elif [ $BU -le 9999 ]; then
        # BU 0, Grep spacing for 3 spaces between "="
        $Burn"
        while [ $n -le $numnodes ]
        do
            if [ $n -le 9 ]; then
                #numnodes has to be less than 10 for grep spacing between "Node
                $n"
                grep -A36 "PREL , Node Map, at Axial Node $n,"
                VVER1000_test621_BU.out | grep -A36 "Average Burnup = $Burn (MWD/MTHM)" > preloops$BU$n.out
            else
                grep -A36 "PREL , Node Map, at Axial Node $n,"
                VVER1000_test621_BU.out | grep -A36 "Average Burnup = $Burn (MWD/MTHM)" > preloops$BU$n.out
            fi
            echo "Average Burnup = $Burn (MWD/MTHM)" > PREL$BU$n.txt
            echo "Node $n" >> PREL$BU$n.txt
            #pull only the scientific numbers (flux values)
            grep --color=auto -oE '[- +]?[0-9]+\.[0-9]*' preloops$BU$n.out >> PREL$BU$n.txt
            n=$((n+1))
        done
#BU for 10000-99999

```

```

else [ $BU -le 99999 ]                # BU 0, Grep spacing for 2 spaces between "=" $Burn"

    while [ $n -le $numnodes ]

    do

        if [ $n -le 9 ]; then        #numnodes has to be less than 10 for grep spacing between "Node
$n"

            grep -A36 "PREL , Node Map, at Axial Node $n,"
VVER1000_test621_BU.out | grep -A36 "Average Burnup = $Burn (MWD/MTHM)" > preloops$BU$n.out

        else

            grep -A36 "PREL , Node Map, at Axial Node $n,"
VVER1000_test621_BU.out | grep -A36 "Average Burnup = $Burn (MWD/MTHM)" > preloops$BU$n.out

        fi

        echo "Average Burnup = $Burn (MWD/MTHM)" > PREL$BU$n.txt

        echo "Node $n" >> PREL$BU$n.txt

        #pull only the scientific numbers (flux values)

        grep --color=auto -oE '[- +]?[0-9]+\.[0-9]*' preloops$BU$n.out >> PREL$BU$n.txt

        n=$((n+1))

    done

fi

newburn=$(echo "$Burn + $stepburn" | bc) #have to use this strange step to add floats, need the float for GREP

Burn=$newburn                            #modify $Burn
variable for grep

BU=$((BU+step))                            #BU must be an
integer for loops

n=1
#reset n to 1 for each pass through the BU loop

done

##### Grep all the nodal BU Data: For each BU Step, Each Node
#####

step=1000                #BU step size

stepburn=1000.00

Burn=0.00                #initial BU step (zero)

BU=0

numnodes=12                #number of nodes (include reflector)

maxBU=12000                #max burnup

```

```

n=1

while [ $BU -le $maxBU ]

do

#BU 0

    if [ $BU -eq 0 ]; then                                     # BU 0, Grep spacing for 6 spaces between "=" $Burn"

        while [ $n -le $numnodes ]

            do

                if [ $n -le 9 ]; then                           #numnodes has to be less than 10 for grep
spacing between "Node $n"

                    grep -A36 "BU (MWD/MTHM), Node Map, at Axial Node $n,"
VVER1000_test621_BU.out | grep -A36 "Average Burnup = $Burn (MWD/MTHM)" > BUloops$BU$n.out

                else

                    grep -A36 "BU (MWD/MTHM), Node Map, at Axial Node $n,"
VVER1000_test621_BU.out | grep -A36 "Average Burnup = $Burn (MWD/MTHM)" > BUloops$BU$n.out

                fi

                echo "Average Burnup = $Burn (MWD/MTHM)" > BU$BU$n.txt

                echo "Node $n" >> BU$BU$n.txt

                #pull only the scientific numbers (flux values)

                grep --color=auto -oE '[- +]?[0-9]+\.[0-9]*' BUloops$BU$n.out >> BU$BU$n.txt

                n=$((n+1))

            done

#BU 10-999

    elif [ $BU -le 999 ]; then                                 # BU 0, Grep spacing for 4 spaces between "=" $Burn"

        while [ $n -le $numnodes ]

            do

                if [ $n -le 9 ]; then                           #numnodes has to be less than 10 for grep
spacing between "Node $n"

                    grep -A36 "BU (MWD/MTHM), Node Map, at Axial Node $n,"
VVER1000_test621_BU.out | grep -A36 "Average Burnup = $Burn (MWD/MTHM)" > BUloops$BU$n.out

                else

                    grep -A36 "BU (MWD/MTHM), Node Map, at Axial Node $n,"
VVER1000_test621_BU.out | grep -A36 "Average Burnup = $Burn (MWD/MTHM)" > BUloops$BU$n.out

                fi

```

```

echo "Average Burnup = $Burn (MWD/MTHM)" > BU$BU$n.txt

echo "Node $n" >> BU$BU$n.txt

#pull only the scientific numbers (flux values)

grep --color=auto -oE '[- +]?[0-9]+\.[0-9]*' BUloops$BU$n.out >> BU$BU$n.txt

n=$((n+1))

done

#BU 1000-9999

$Burn"          elif [ $BU -le 9999 ]; then          # BU 0, Grep spacing for 3 spaces between "="

while [ $n -le $numnodes ]

do

$Burn"          if [ $n -le 9 ]; then          #numnodes has to be less than 10 for grep spacing between "Node

          grep -A36 "BU (MWD/MTHM), Node Map, at Axial Node $n,"
VVER1000_test621_BU.out | grep -A36 "Average Burnup = $Burn (MWD/MTHM)" > BUloops$BU$n.out

          else

          grep -A36 "BU (MWD/MTHM), Node Map, at Axial Node $n,"
VVER1000_test621_BU.out | grep -A36 "Average Burnup = $Burn (MWD/MTHM)" > BUloops$BU$n.out

          fi

echo "Average Burnup = $Burn (MWD/MTHM)" > BU$BU$n.txt

echo "Node $n" >> BU$BU$n.txt

#pull only the scientific numbers (flux values)

grep --color=auto -oE '[- +]?[0-9]+\.[0-9]*' BUloops$BU$n.out >> BU$BU$n.txt

n=$((n+1))

done

#BU for 10000-99999

$Burn"          else [ $BU -le 99999 ]          # BU 0, Grep spacing for 2 spaces between "=" $Burn"

while [ $n -le $numnodes ]

do

$Burn"          if [ $n -le 9 ]; then          #numnodes has to be less than 10 for grep spacing between "Node

          grep -A36 "BU (MWD/MTHM), Node Map, at Axial Node $n,"
VVER1000_test621_BU.out | grep -A36 "Average Burnup = $Burn (MWD/MTHM)" > BUloops$BU$n.out

          else

```

```

grep -A36 "BU (MWD/MTHM), Node Map, at Axial Node $n,"
VVER1000_test621_BU.out | grep -A36 "Average Burnup = $Burn (MWD/MTHM)" > BUloops$BU$.out

fi

echo "Average Burnup = $Burn (MWD/MTHM)" > BU$BU$.txt

echo "Node $n" >> BU$BU$.txt

#pull only the scientific numbers (flux values)

grep --color=auto -oE '[- +]?[0-9]+\.[0-9]*' BUloops$BU$.out >> BU$BU$.txt

n=$((n+1))

done

fi

newburn=$(echo "$Burn + $stepburn" | bc) #have to use this strange step to add floats, need the float for GREP

Burn=$newburn #modify $Burn
variable for grep

BU=$((BU+step)) #BU must be an
integer for loops

n=1
#reset n to 1 for each pass through the BU loop

done

#####Ask User for Line to Pull#####

read -p "Enter Line to Pull: " line

echo $line

line=$((line+4)) #have to add 4 lines due to how
the files are grepped above

#####Pull Line PREL and BU for Each BU Step, Each Node#####

step=1000 #BU step size

BU=0

numnodes=12 #number of nodes (include reflector)

n=1

```

```

while [ $BU -le $maxBU ]
do
    while [ $n -le $numnodes ]
    do
        head -n$line PREL$BU$n.txt | tail -1 >> power$BU.txt
        head -n$line BU$BU$n.txt | tail -1 >> burnup$BU.txt
        n=$((n+1))
    done
    BU=$((BU+step))
integer for loops
    n=1
done
#####execute python weighting script
#!/bin/sh
python PRELwtBU.py
#####clean up the mess#####
burn=0
while [ $burn -le $maxBU ]
do
    mv power$burn.txt ./plot
    mv burnup$burn.txt ./plot
    burn=$((burn+step))
done
mv PRELZ_BU.txt ./plot

burn=0
n=1
while [ $burn -le $maxBU ]
do
    while [ $n -le $numnodes ]
    do

```

```

mv PREL$burn$n.txt ./greps
mv preloops$burn$n.out ./greps
mv BU$burn$n.txt ./greps
mv BUloops$burn$n.out ./greps

n=$((n+1))

done

burn=$((burn+step))

n=1

done

```

F.7: NESTLE VVER-1000 Test PREL Python Calculations

```

#Data processing for Nestle Flux Ratio

#Import necessary methods

import matplotlib

import matplotlib.pyplot as plt

import numpy as np

import math

import scipy as sp

#####Pull Data from PREL files#####

#import data PREL for each BU Step

PREL0=np.genfromtxt('power0.txt', unpack=True)

PREL1000=np.genfromtxt('power1000.txt', unpack=True)

PREL2000=np.genfromtxt('power2000.txt', unpack=True)

PREL3000=np.genfromtxt('power3000.txt', unpack=True)

PREL4000=np.genfromtxt('power4000.txt', unpack=True)

PREL5000=np.genfromtxt('power5000.txt', unpack=True)

PREL6000=np.genfromtxt('power6000.txt', unpack=True)

PREL7000=np.genfromtxt('power7000.txt', unpack=True)

PREL8000=np.genfromtxt('power8000.txt', unpack=True)

PREL9000=np.genfromtxt('power9000.txt', unpack=True)

PREL10000=np.genfromtxt('power10000.txt', unpack=True)

```

```

PREL11000=np.genfromtxt('power11000.txt', unpack=True)

PREL12000=np.genfromtxt('power12000.txt', unpack=True)

#####Pull Data from BU files#####

#import data nodal BU for each BU Step

BU0=np.genfromtxt('burnup0.txt', unpack=True)

BU1000=np.genfromtxt('burnup1000.txt', unpack=True)

BU2000=np.genfromtxt('burnup2000.txt', unpack=True)

BU3000=np.genfromtxt('burnup3000.txt', unpack=True)

BU4000=np.genfromtxt('burnup4000.txt', unpack=True)

BU5000=np.genfromtxt('burnup5000.txt', unpack=True)

BU6000=np.genfromtxt('burnup6000.txt', unpack=True)

BU7000=np.genfromtxt('burnup7000.txt', unpack=True)

BU8000=np.genfromtxt('burnup8000.txt', unpack=True)

BU9000=np.genfromtxt('burnup9000.txt', unpack=True)

BU10000=np.genfromtxt('burnup10000.txt', unpack=True)

BU11000=np.genfromtxt('burnup11000.txt', unpack=True)

BU12000=np.genfromtxt('burnup12000.txt', unpack=True)

#####Define variables#####

stepsize=1000.00

n=1

numnodes=12

BU=0

maxBU=12000.00

#####Define Arrays#####

fullPREL=np.arange(12,dtype=np.float)

MaxBU=np.arange(12,dtype=np.float)

PRELZ=np.arange(12,dtype=np.float)

#####Make WT Arrays for each BU step#####

WT0=(BU1000-BU0)

WT1=(BU2000-BU1000)

```

WT2=(BU3000-BU2000)

WT3=(BU4000-BU3000)

WT4=(BU5000-BU4000)

WT5=(BU6000-BU5000)

WT6=(BU7000-BU6000)

WT7=(BU8000-BU7000)

WT8=(BU9000-BU8000)

WT9=(BU10000-BU9000)

WT10=(BU11000-BU10000)

WT11=(BU12000-BU11000)

#####Fill Average PREL Arrays#####

AVGPREL0=(PREL0+PREL1000)/2

AVGPREL1=(PREL1000+PREL2000)/2

AVGPREL2=(PREL2000+PREL3000)/2

AVGPREL3=(PREL3000+PREL4000)/2

AVGPREL4=(PREL4000+PREL5000)/2

AVGPREL5=(PREL5000+PREL6000)/2

AVGPREL6=(PREL6000+PREL7000)/2

AVGPREL7=(PREL7000+PREL8000)/2

AVGPREL8=(PREL8000+PREL9000)/2

AVGPREL9=(PREL9000+PREL10000)/2

AVGPREL10=(PREL10000+PREL11000)/2

AVGPREL11=(PREL11000+PREL12000)/2

#####Muiltly Average PREL Arrays by weight function

WTPREL0=WT0*AVGPREL0

WTPREL1=WT1*AVGPREL1

WTPREL2=WT2*AVGPREL2

WTPREL3=WT3*AVGPREL3

WTPREL4=WT4*AVGPREL4

WTPREL5=WT5*AVGPREL5

WTPREL6=WT6*AVGPREL6

WTPREL7=WT7*AVGPREL7

WTPREL8=WT8*AVGPREL8

WTPREL9=WT9*AVGPREL9

WTPREL10=WT10*AVGPREL10

WTPREL11=WT11*AVGPREL11

fullPREL[0]=np.sum([WTPREL0[0],WTPREL1[0],WTPREL2[0],WTPREL3[0],WTPREL4[0],WTPREL5[0],WTPREL6[0],WTPREL7[0],WTPREL8[0],WTPREL9[0],WTPREL10[0],WTPREL11[0]],axis=0)

fullPREL[1]=np.sum([WTPREL0[1],WTPREL1[1],WTPREL2[1],WTPREL3[1],WTPREL4[1],WTPREL5[1],WTPREL6[1],WTPREL7[1],WTPREL8[1],WTPREL9[1],WTPREL10[1],WTPREL11[1]],axis=0)

fullPREL[2]=np.sum([WTPREL0[2],WTPREL1[2],WTPREL2[2],WTPREL3[2],WTPREL4[2],WTPREL5[2],WTPREL6[2],WTPREL7[2],WTPREL8[2],WTPREL9[2],WTPREL10[2],WTPREL11[2]],axis=0)

fullPREL[3]=np.sum([WTPREL0[3],WTPREL1[3],WTPREL2[3],WTPREL3[3],WTPREL4[3],WTPREL5[3],WTPREL6[3],WTPREL7[3],WTPREL8[3],WTPREL9[3],WTPREL10[3],WTPREL11[3]],axis=0)

fullPREL[4]=np.sum([WTPREL0[4],WTPREL1[4],WTPREL2[4],WTPREL3[4],WTPREL4[4],WTPREL5[4],WTPREL6[4],WTPREL7[4],WTPREL8[4],WTPREL9[4],WTPREL10[4],WTPREL11[4]],axis=0)

fullPREL[5]=np.sum([WTPREL0[5],WTPREL1[5],WTPREL2[5],WTPREL3[5],WTPREL4[5],WTPREL5[5],WTPREL6[5],WTPREL7[5],WTPREL8[5],WTPREL9[5],WTPREL10[5],WTPREL11[5]],axis=0)

fullPREL[6]=np.sum([WTPREL0[6],WTPREL1[6],WTPREL2[6],WTPREL3[6],WTPREL4[6],WTPREL5[6],WTPREL6[6],WTPREL7[6],WTPREL8[6],WTPREL9[6],WTPREL10[6],WTPREL11[6]],axis=0)

fullPREL[7]=np.sum([WTPREL0[7],WTPREL1[7],WTPREL2[7],WTPREL3[7],WTPREL4[7],WTPREL5[7],WTPREL6[7],WTPREL7[7],WTPREL8[7],WTPREL9[7],WTPREL10[7],WTPREL11[7]],axis=0)

fullPREL[8]=np.sum([WTPREL0[8],WTPREL1[8],WTPREL2[8],WTPREL3[8],WTPREL4[8],WTPREL5[8],WTPREL6[8],WTPREL7[8],WTPREL8[8],WTPREL9[8],WTPREL10[8],WTPREL11[8]],axis=0)

fullPREL[9]=np.sum([WTPREL0[9],WTPREL1[9],WTPREL2[9],WTPREL3[9],WTPREL4[9],WTPREL5[9],WTPREL6[9],WTPREL7[9],WTPREL8[9],WTPREL9[9],WTPREL10[9],WTPREL11[9]],axis=0)

fullPREL[10]=np.sum([WTPREL0[10],WTPREL1[10],WTPREL2[10],WTPREL3[10],WTPREL4[10],WTPREL5[10],WTPREL6[10],WTPREL7[10],WTPREL8[10],WTPREL9[10],WTPREL10[10],WTPREL11[10]],axis=0)

fullPREL[11]=np.sum([WTPREL0[11],WTPREL1[11],WTPREL2[11],WTPREL3[11],WTPREL4[11],WTPREL5[11],WTPREL6[11],WTPREL7[11],WTPREL8[11],WTPREL9[11],WTPREL10[11],WTPREL11[11]],axis=0)

MaxBU[0]=np.sum([WT0[0],WT1[0],WT2[0],WT3[0],WT4[0],WT5[0],WT6[0],WT7[0],WT8[0],WT9[0],WT10[0],WT11[0]],axis=0)

MaxBU[1]=np.sum([WT0[1],WT1[1],WT2[1],WT3[1],WT4[1],WT5[1],WT6[1],WT7[1],WT8[1],WT9[1],WT10[1],WT11[1]],axis=0)

MaxBU[2]=np.sum([WT0[2],WT1[2],WT2[2],WT3[2],WT4[2],WT5[2],WT6[2],WT7[2],WT8[2],WT9[2],WT10[2],WT11[2]],axis=0)

MaxBU[3]=np.sum([WT0[3],WT1[3],WT2[3],WT3[3],WT4[3],WT5[3],WT6[3],WT7[3],WT8[3],WT9[3],WT10[3],WT11[3]],axis=0)

MaxBU[4]=np.sum([WT0[4],WT1[4],WT2[4],WT3[4],WT4[4],WT5[4],WT6[4],WT7[4],WT8[4],WT9[4],WT10[4],WT11[4]],axis=0)

MaxBU[5]=np.sum([WT0[5],WT1[5],WT2[5],WT3[5],WT4[5],WT5[5],WT6[5],WT7[5],WT8[5],WT9[5],WT10[5],WT11[5]],axis=0)

```

MaxBU[6]=np.sum([WT0[6],WT1[6],WT2[6],WT3[6],WT4[6],WT5[6],WT6[6],WT7[6],WT8[6],WT9[6],WT10[6],WT11[6]],axis=
0)

MaxBU[7]=np.sum([WT0[7],WT1[7],WT2[7],WT3[7],WT4[7],WT5[7],WT6[7],WT7[7],WT8[7],WT9[7],WT10[7],WT11[7]],axis=
0)

MaxBU[8]=np.sum([WT0[8],WT1[8],WT2[8],WT3[8],WT4[8],WT5[8],WT6[8],WT7[8],WT8[8],WT9[8],WT10[8],WT11[8]],axis=
0)

MaxBU[9]=np.sum([WT0[9],WT1[9],WT2[9],WT3[9],WT4[9],WT5[9],WT6[9],WT7[9],WT8[9],WT9[9],WT10[9],WT11[9]],axis=
0)

MaxBU[10]=np.sum([WT0[10],WT1[10],WT2[10],WT3[10],WT4[10],WT5[10],WT6[10],WT7[10],WT8[10],WT9[10],WT10[10],
WT11[10]],axis=0)

MaxBU[11]=np.sum([WT0[11],WT1[11],WT2[11],WT3[11],WT4[11],WT5[11],WT6[11],WT7[11],WT8[11],WT9[11],WT10[11],
WT11[11]],axis=0)

PRELZ[0]=fullPREL[0]/MaxBU[0]

PRELZ[1]=fullPREL[1]/MaxBU[1]

PRELZ[2]=fullPREL[2]/MaxBU[2]

PRELZ[3]=fullPREL[3]/MaxBU[3]

PRELZ[4]=fullPREL[4]/MaxBU[4]

PRELZ[5]=fullPREL[5]/MaxBU[5]

PRELZ[6]=fullPREL[6]/MaxBU[6]

PRELZ[7]=fullPREL[7]/MaxBU[7]

PRELZ[8]=fullPREL[8]/MaxBU[8]

PRELZ[9]=fullPREL[9]/MaxBU[9]

PRELZ[10]=fullPREL[10]/MaxBU[10]

PRELZ[11]=fullPREL[11]/MaxBU[11]

np.savetxt('PRELZ_BU.txt',PRELZ)

```

Vita

Margaret Kurtts is a veteran of the US Army and former Blackhawk helicopter pilot. She graduated from the United States Military Academy in 2004 with a Bachelors of Science in Physics Engineering. In 2014, she earned a Master's of Science from the University of Tennessee in Nuclear Engineering. Margaret is a committed non-proliferation professional dedicated to ensuring the peaceful use of nuclear technology.